

University of Nottingham
UK | CHINA | MALAYSIA

THE EFFECTS OF PHYTOCANNABINOIDS IN STROKE AND PHARMACOLOGY OF CBD AND TMP CO-APPLICATION IN CELLULAR MODELS

Ryan F Maguire

BSc (Hons)

Submitted to the University of Nottingham in pursuit of the degree of Doctor of Philosophy

August 2021

Statement of authenticity

I declare that this thesis has been completed by myself under the supervision of Professor Saoirse O'Sullivan, Professor, and Dr Timothy England, Clinical Associate Professor, from the school of graduate-entry medicine, University of Nottingham, Royal Derby Hospital. This thesis is a record of work that has not been submitted previously for a higher degree.

Ryan F Maguire August 2021

Acknowledgements

I would like to dedicate this thesis to my late Grandfather, John Clarke. Although you are no longer with us, I know you would be incredibly proud.

Firstly I'd like to thank my fantastic supervisors, Professor Saoirse O'Sullivan and Dr Timothy England whose mentorship and guidance enabled the completion of this thesis.

I would also like to thank my girlfriend Emily Clark; without your love and support, none of this would have been possible. My Mom, Anthony, Tayla and Poppy for their unwavering support. My dad for his beer. Dr Mark McBride, Dr Benjamin White, and Artur Kocon for the insightful and less insightful chats in the pub. My friends Dr Sophie Millar and Dr Nicole Stone for endless cups of very, very strong tea. Finally my friends from home, Ashley Worley, Channie, Danny McBride Lewis McAndrew, and Tom Hopcroft. As well as my University friends Brad Stevenson, Jamie Charlton-Little, Tom Howell and George Barrett, whose friendship provided much-needed laughter throughout my studies.

Lastly, I would like to pay tribute to the 72 mice sacrificed for the *in vivo* chapter of this thesis.

Poster and oral presentations arising from this thesis

Poster presentation:
Ryan F Maguire, Timothy J England and Saoirse O'Sullivan
The effects of phytocannabinoids in astrocytes exposed to OGD/R injury
International Cannabinoid Research Society conference. Montreal, 2018

Poster presentation:
RF Maguire, Timothy J England and Saoirse O'Sullivan
The pharmacological effects of synthetic and plant-derived cannabidiol are similar in a range of human cell lines
International Cannabinoid Research Society conference. Washington, 2019.

Oral presentation:
Ryan F Maguire, Saoirse O'Sullivan Timothy J England
A meta-analysis of *in vivo* focal ischemic studies
UK stroke forum. Telford, 2019.

Publications arising from this thesis

Published peer-reviewed articles:

Ryan F Maguire, Daniel J Wilkinson, Timothy J England and Saoirse O'Sullivan
The Pharmacological Effects of Plant-Derived versus Synthetic Cannabidiol in Human Cell Lines
Medical Cannabis and Cannabinoids. 2021. //doi.org/10.1159/000517120

Manuscripts under review:

Ryan F Maguire, Ronangh Lee, Saoirse O'Sullivan and Timothy J England
Cannabidiol and acute ischemic stroke: A meta-analysis of in vivo focal ischemic studies
Stroke. 2021

Table of Contents

1 INTRODUCTION 22

1.1 STROKE 22
1.1.1 PATHOPHYSIOLOGY OF CEREBRAL REPERFUSION INJURY 22
1.1.2 ASTROCYTES 30
1.1.3 PERICYTES 38
1.2 CURRENT TREATMENTS FOR CEREBRAL ISCHEMIC INJURY 40
1.3 ENDOCANNABINOID SYSTEM 41
1.3.1 RECEPTORS 42
1.3.2 LIGANDS AND ENZYMES 47
1.3.3 THE ENDOCANNABINOID SYSTEM AND STROKE 49
1.4 PHYTOCANNABINOIDS 51
1.4.1 CANNABIDIOL (CBD) 52
1.4.2 CANNABIDIOLIC ACID (CBDA) 53
1.4.3 CANNABIDIVARIN (CBDV) 53
1.4.4 CANNABIGEROL (CBGV) 54
1.4.5 CANNABICHROMENE (CBC) 54
1.5 PHYTOCANNABINOIDS AND STROKE 56
1.6 PHARMACODYNAMICS AND KINETICS 58
1.7 IMPROVING BIOAVAILABILITY OF PHYTOCANNABINOIDS 61
1.8 AIMS OF THESIS 63

2 CANNABIDIOL IN ACUTE ISCHEMIC STROKE: A META-ANALYSIS OF IN VIVO FOCAL ISCHEMIC STUDIES 65

2.1 INTRODUCTION 65
2.2 METHODS 67
2.2.1 SEARCH CRITERIA 67
2.2.2 QUALITY AND RISK OF BIAS 67
2.2.3 DATA ANALYSIS 68
2.3 RESULTS 69
2.3.1 DOSE-RESPONSE EFFECTS OF CBD ON INFARCT VOLUME 70
2.3.2 TIME WINDOW OF ADMINISTRATION 72
2.3.3 ROUTE OF ADMINISTRATION AND INFARCT VOLUME 72
2.3.1 NEUROLOGICAL SCORE 72
2.3.2 ROTAROD TEST 74
2.3.3 STUDY QUALITY AND RISK OF BIAS 75
2.3.4 PUBLICATION BIAS 75
2.4 DISCUSSION 76

3 THE EFFECTS OF IV CBD OR CBDA IN MICE EXPOSED TO ELECTROCOAGULATION OF THE MIDDLE CEREBRAL ARTERY 80

3.1 INTRODUCTION 80
3.2 METHODS 82
3.2.1 EXPERIMENTAL SET-UP 82
3.2.2 PERMENANT OCCLUSON OF MCA 83

3.2.3 Data analysis 83
3.3 Results 85
3.3.1 Infarct volume 85
3.3.2 Infarct volumes corrected for oedema 86
3.3.3 Space occupying effect 87
3.4 Discussion 88

4 THE EFFECTS OF CBD, CBGV, CBC AND CBDV IN ASTROCYTES EXPOSED TO OXYGEN-GLUCOSE DEPRIVATION AND REPERFUSION INJURY 91

4.1 Introduction 91
4.2 Methods 94
4.2.1 Cell culture and oxygen-glucose deprivation/reperfusion (OGD/R) conditions 94
4.2.2 Drugs 94
4.2.3 Lactate dehydrogenase (LDH) assay 94
4.2.4 Multiplex analysis of mitochondrial complex proteins 95
4.2.5 MTS assay 95
4.2.6 Enzyme-linked immunosorbent assay of IL-6 95
4.2.7 BCA 96
4.2.8 Experimental procedures for investigating the effects of CBD, CBGV, CBC and CBDV in astrocytes exposed to 4 h OGD 97
4.2.9 The effects of a 4 h and 8 h OGD protocol on astrocytes 98
4.2.10 The effects of phytocannabinoids on human astrocytes exposed to OGD using prophylactic and therapeutic strategies 98
4.2.11 Data analysis 99
4.3 Results 100
4.3.1 The effects of CBD, CBGV, CBC or CBDV in astrocytes exposed to 4 h OGD or normoxic conditions 100
4.3.2 The effects of a 4 and 8 h OGD protocol on total protein, LDH, IL-6, total protein, and mitochondrial complex protein 107
4.3.3 The effects of phytocannabinoids on human astrocytes exposed to 8h OGD using prophylactic and therapeutic application strategies 111
4.3.4 Cell damage (LDH) 112
4.3.5 Inflammation (IL-6) 117
4.3.6 The effects of CBD, CBGV, CBC, and CBDV on IL6 in astrocyte exposed to 8 h OGD 118
4.4 Discussion 121
4.4.1 The effects of CBD, CBGV, CBC and CBDV on cell death, markers of mitochondrial function and cellular metabolism in human astrocytes in normoxic and 4 h oxygen-glucose deprivation conditions 121
4.4.2 The effects of a 4 and 8 h OGD protocol on human astrocytes 123
4.4.3 Examination of the effects of phytocannabinoid on human astrocytes exposed to 8 h OGD using prophylactic and therapeutic strategies 125
4.4.4 Conclusion 126

5 THE PHARMACOLOGICAL EFFECTS OF PLANT-DERIVED VERSUS SYNTHETIC CANNABIDIOL (CBD) IN HUMAN CELL LINES 128

5.1 Introduction 128
5.2 Methods 131

5.2.1 Materials....131
5.2.2 Cell culture....131
5.2.3 Gas chromatography-mass spectrometry....132
5.2.4 Anti-cancer effects of CBD in SKOV-3 cells....132
5.2.5 Oxygen-glucose deprivation experiments in pericytes....133
5.2.6 Inflammation and permeability experiments in Caco2 cells....133
5.2.7 Data analysis....134
5.3 Results.... !Unexpected End of Formula
5.3.1 Gas chromatography/Mass spectrometry....134
5.3.2 Anti-cancer effects of plant-derived and synthetic CBD in SKOV-3 cell line....136
5.3.3 The effects of CBD in pericytes exposed to OGD....137
5.3.4 CBD effects on CaCo2 barrier integrity following inflammation....139
5.4 Discussion....140

6 THE EFFECTS OF CBD AND TMP COADMINISTRATION IN HUMAN CELL LINES....143

6.1 Introduction....143
6.2 Methods....145
6.2.1 General methods....145
6.2.2 Experimental procedures....146
6.3 Results....149
6.3.1 Effects of CBD and TMP in proliferating cancer cell lines....149
6.3.2 Effects of CBD and TMP in fully confluent cancer cell lines....150
6.3.3 Effects of CBD and TMP in fully confluent cancer cell lines over moderate exposure times (144h)....152
6.3.4 Effects of CBD and TMP in fully confluent cancer cell lines over prolonged exposure times (240h)....154
6.3.5 Effects of CBD and TMP on scratch wound closure in cancer cell lines....154
6.3.6 Effects of CBD and TMP on resazurin metabolism in Astrocytes 32h following the initiation of OGD/R....157
6.3.7 Effects of CBD and TMP on IL-6 and LDH concentrations in Astrocytes exposed to OGD/R 158
6.3.8 Effects of CBD and TMP on resazurin metabolism in Pericytes 24h following the initiation of OGD/R....159
6.3.9 Effects of CBD and TMP on IL-6 and LDH concentrations in Pericytes exposed to OGD/R 160
6.4 Discussion....162

7 GRAND DISCUSSION....167

8 BIBLIOGRAPHY....172

9 APPENDICES....206

List of figures

Figure 1.1 Depicts the boundaries of the ischemic core (10-25%) and penumbra regions as percentage reductions in cerebral blood flow (CBF) following mild cerebral artery occlusion (MCAO) in the baboon brain. As the duration of ischemia extends, the core begins to spread into the surrounding penumbra, leading to a progressively larger infarction. Reproduced from Moustafa RR and Baron J-C, 'Pathophysiology of ischemic stroke: Insights from imaging and implications for therapy and drug discovery' British Journal of Pharmacology 2008 23
Figure 1.2 Damage caused following ischemia follows a temporal pattern. At the onset of ischemia, cells experience rapid damage from excitotoxicity, leading to the initiation of Per-infarct depolarisations, inflammation and subsequent apoptosis. Reproduced from Dirnagl U, 'Pathobiology of ischemic stroke: an integrated view' Trends in Neuroscience 1999. 24
Figure 1.3 glial fibrillary acidic protein stained astrocytes from mouse cerebral cortex (A-C) (A) Non-reactive astrocytes have little overlap between their processes and appear to occupy a distinct territory (B) Intracerebral injection of lipopolysaccharide induces moderate reactive gliosis. Although astrocytes have become more arborised, their processes remain in distinct domains and barely overlap (C). Severe reactive gliosis is induced by severe traumatic brain injury, leading to glial scar formation and inflammation. This intensity of gliosis is characterised by the obvious overlapping and thickening of processes and elevations of glial fibrillary acidic protein expression. Scale bar = 8μm. Image adapted from Sofroniew, Michael V.' Molecular dissection of reactive astrogliosis and glial scar formation' Trends in Neurosciences 2009. 35
Figure 1.4 the numerous pathways activated or inhibited following CB_2 receptor activation by tetrahydrocannabinol or Anandamide. + = activation of a pathway in the presence of an agonist, - = Inhibition of a pathway following agonist activation, and +/- = A variable outcome following agonist binding. Reproduced from Dhopeshwarkar, A.' CB_2 Cannabinoid Receptors as a Therapeutic Target--What Does the Future Hold?' Molecular pharmacology 2014. 44
Figure 1.5 The molecular structure of various phytocannabinoids used throughout this thesis and Δ-9-THC for comparison. 55
Figure 2.1 Publication identification process 69
Figure 2.2 Forest plot of the effect of CBD in rats and mice on infarct volume (mm3) in an MCAO model of transient focal ischemia. Pre = administered before stroke onset; post = administered after stroke onset; h = hours. 70
Figure 2.3 Dose-response curve displaying % mean ± SD change in infarct volume of total CBD dose relative to vehicle from all studies. A) Wistar rats receiving CBD via ICV injection 30 minutes prior to MCAO. B) ddY Mice receiving two doses of CBD immediately before and 3 h after MCAO via IP injection. 71
Figure 2.4 Forest plot of the effect of CBD on neurological score at different points of evaluation in models of focal ischemia. Pre = administered before stroke onset; post = administered after stroke onset; h = hours. 73
Figure 2.5 Forest plot of the effect of CBD on neurological score at different points of evaluation in models of focal ischaemia. Pre = administered before stroke onset; post = administered after stroke onset; h = hours. 73

Figure 2.6 Forest plot of the effect of CBD on time spent on Rotarod. Pre = administered before stroke onset; post = administered after stroke onset; h = hours 74
Figure 2.7 Funnel plot for infarct volume data. Standard error of the mean difference (SE - MD) for each study is plotted against its effect size (MD). 76
Figure 3.1 Schematic diagram of the experimental time course. pMCAO = permanent middle cerebral artery occlusion, iv = intravenous, MRI = Magnetic Resonance Imaging. 83
Figure 3.2 The effect of CBD or CBDA on infarct volume 24 h following the initiation of pMCAO. Data is presented as raw mean infarct volume (mm^3) with standard deviation (SD). Numbers inside bars display sample size for each experimental group, and numbers above bars display the mean result for each condition. Data was compared against vehicle for statistical significance against vehicle using a one-way ANOVA. 85
Figure 3.3 The effect of CBD (A) or CBDA (B) on infarct volume corrected for oedema 24 h following pMCAO. Data are presented as % of the hemisphere with standard deviation. Numbers inside bars display sample size for each experimental group, and numbers above bars display the mean result for each condition. Data was compared against vehicle for statistical significance against vehicle using a one-way ANOVA. * p≤0.05 86
Figure 3.4 The effect of CBD (A) or CBDA (B)on the space-occupying effect 24 h following pMCAO. Data is presented as % volume increase of hemisphere with standard deviation. Numbers inside bars display sample size for each experimental group, and numbers above bars display the mean result for each condition. Data was compared against vehicle for statistical significance against vehicle using a one-way ANOVA. * p≤0.05. 87
Figure 4.1 schematic diagram of experimental procedure for astrocytes exposed to 4 h OGD and CBD, CBGV, CBC and CBDV 97
Figure 4.2 schematic diagram of experimental procedure for astrocytes exposed to 4 h OGD and 8 h OGD. 98
Figure 4.3 Schematic diagram of the experimental protocol. Baseline samples were taken 24h before the OGD protocol. “Pre” and “post” depict where drugs were administered. Media was changed again at 16 h (see arrow) to ensure cells were exposed to the drugs for an even period of time (because in the POST-treatment protocol, the drugs were removed after 8 h to match the PRE-treatment drug exposure time). Total length of experiment = 160h. 99
Figure 4.4 Histograms representing the change in LDH levels from vehicle control in either normoxic or 4 h OGD conditions following 24-hour treatment with CBD (A), CBGV (B), CBC (C) or CBDV (D). Data are presented as mean ± SEM (n=6-7). Data were analysed by two-way ANOVAs with multiple comparisons **p<0.01, ***p<0.001, ****p<0.0001 vs their respective vehicle, or as indicated by connecting lines. 101
Figure 4.5 The effects of a 4 h OGD protocol on mitochondrial complex proteins normalised to NNT protein levels. Mitochondrial complex proteins complex I (A), complex II (B), complex III (C), complex IV (D), complex V (E) Data are presented as mean SEM and analysed using Mann-Whitney tests within each mitochondrial complex. *p<0.05, ***p<0.001, ****p<0.0001 vs normoxia. 102
Figure 4.6 Histograms representing the effects of CBD in normoxic (A) or 4 h OGD (B) conditions in astrocytes. Astrocytes (p6) were exposed to CBD for 24 hours, following which mitochondrial complex proteins levels were assessed. Astrocytes. Data are presented as mean SEM (n = 6 per group, from two separate

experiments) and are normalised to NNT. Data were analysed by two-way ANOVAs and multiple comparisons between groups. 103
Figure 4.7 Histograms representing the effects of CB in normoxic (A) or 4 h OGD (B) conditions in astrocytes. Astrocytes (p6) were exposed to CBGV for 24 hours, following which mitochondrial complex proteins levels were assessed. Astrocytes. Data are presented as mean fluorescent intensity SEM (n = 6 per group, from two experiments). Data were analysed by two-way ANOVAs and multiple comparisons between groups. 104
Figure 4.8 Histograms representing the effects of CBC in normoxic (A) or 4 h OGD (B) conditions in astrocytes. Astrocytes (p6) were exposed to CBC for 24 hours, following which mitochondrial complex proteins levels were assessed. Astrocytes. Data are presented as mean SEM (n = 6 per group, from two separate experiments) and are normalised to NNT. Data were analysed by two-way ANOVAs and multiple comparisons between groups. 104
Figure 4.9 Histograms representing the effects of CBDV in normoxic (A) or 4 h OGD (B) conditions in astrocytes. Astrocytes (p6) were exposed to CBDV for 24 hours, following which mitochondrial complex proteins levels were assessed. Astrocytes. Data are presented as mean SEM (n = 6 per group, from two separate experiments) and are normalised to NNT. Data were analysed by two-way ANOVAs and multiple comparisons between groups. 105
Figure 4.10 Data are presented as mean SEM (n = 22 - 24 per condition, from two separate experiments). Data were analysed for statistical significance by unpaired t-test. 106
Figure 4.11 Histograms representing the effects of CBD (A), CBGV (B), CBC (C), or CBDV (D) 24-hour exposure on cellular metabolism in astrocytes (p6) following either normoxic or 4 h OGD protocol. Data are presented as mean SEM (n = 6-12, from two separate experiments). Data were analysed by two-way ANOVAs and multiple comparison between concentrations and conditions. .. 107
Figure 4.12 The effect of a 4 h or 8 h OGD protocol on the total protein of fully confluent human astrocytes (P5), as measured 72h post-OGD. Data are presented as mean ± SEM (n=10), from two separate experiments. Data were analysed by Student's t-test with multiple comparisons between the groups. **p<0.01, ****p<0.0001 vs. normoxia, or as indicated by connecting lines 108
Figure 4.13 Histograms showing the effect a 4 h or 8 h OGD protocol has on fully confluent human astrocyte (P5-7) LDH concentrations at 24hr intervals and immediately post OGD (4 h or 8 h). Data are presented as mean ± SEM (n=4, from two separate experiments). Data were analysed by a two way ANOVA followed by multiple comparisons between corresponding time-points between conditions. *p<0.05, ***p<0.001, ****p<0.0001 vs their respective baseline groups. 109
Figure 4.14 Histograms showing the effect a 4h or 8h OGD protocol has on fully confluent human astrocyte (P5-7) IL-6 concentrations at 24hr intervals and immediately post OGD (4h or 8h). Concentrations were interpolated from a standard curve and compared to baseline to test for statistical significance using two-way repeated-measures ANOVA and Dunnett's post-hoc. The Shapiro-Wilk test determined that the data were normally distributed. Data are presented as mean ± SEM (n=5, from two separate experiments). *p<0.05, **p<0.01, ****p<0.0001 vs their respective baseline groups. 110
Figure 4.15 Histograms representing mitochondrial complex protein expression in fully confluent astrocytes (p5-7), represented as the net mean absorbance ± SEM (n=5, from two separate experiments). The Shapiro-Wilk test determined that the

data were normally distributed. Data were analysed using a two-way repeated measures ANOVA and Dunnett's post-hoc. **p<0.01, ****p<0.0001 as indicated by connecting lines. 111
Figure 4.16 The effect of phytocannabinoid treatment on total protein levels/well 144 h following 8 h OGD in fully confluent astrocytes. Data are represented as mean ± SEM (n=9-12, from two separate experiments). The Shapiro-Wilk test determined that the data were normally distributed. Data were analysed using a two-way repeated measures ANOVA and Tukey's post-hoc. *p<0.05 as indicated by connecting lines. 112
Figure 4.17 The effect of CBD treatment on LDH levels over time in fully confluent astrocytes, represented as percentage change from baseline for pre-treated (A) or post-treated (B) cells after an 8-hour OGD protocol. The Shapiro-Wilk test determined that the data were normally distributed. Data are presented as mean ± SEM and analysed using two-way repeated measures ANOVA and Dunnett's post-hoc comparison to vehicle. CBD pre-treated (vehicle N=9, CBD N=10), CBD post-treated (Vehicle N=12, CBD N=12) from 3 separate experiments. *p<0.05, ***p<0.001, ****p<0.0001 vs their respective vehicle. 113
Figure 4.18 The effect of CBD treatment on LDH levels over time in fully confluent astrocytes, represented as percentage change from baseline for pre-treated (A) or post-treated (B) cells after an 8-hour OGD protocol. The Shapiro-Wilk test determined that the data were normally distributed. Data are presented as mean ± SEM and analysed using a two-way repeated measures ANOVA and Dunnett's post-hoc comparison to vehicle. CBD pre-treated (vehicle N=9, CBD N=10), CBD post-treated (Vehicle N=12, CBD N=12) from three separate experiments. *p<0.05, ***p<0.001, ****p<0.0001 vs their respective vehicle. 114
Figure 4.19 The effect of CBC treatment on LDH levels over time in fully confluent astrocytes, represented as percentage change from baseline for pre-treated (A) or post-treated (B) cells after an 8-hour OGD protocol. The Shapiro-Wilk test determined that the data were normally distributed. Data are presented as mean ± SEM and analysed using a two-way repeated measures ANOVA and Dunnett's post-hoc comparison to vehicle. CBC pre-treated (vehicle N=12, CBC N=12), CBC post-treated (Vehicle N=12, CBC N=9) from three separate experiments. *p<0.05, **p<0.01, ***p<0.001, ****p<0.0001 vs vehicle. 115
Figure 4.20 The effect of CBDV treatment on LDH levels over time in fully confluent astrocytes, represented as percentage change from baseline for pre-treated (A) or post-treated (B) cells after an 8 h OGD protocol. The Shapiro-Wilk test determined that the data were normally distributed. Data are presented as mean ± SEM and analysed using a two-way repeated measures ANOVA and Dunnett's post-hoc comparison to vehicle. CBDV pre-treated (vehicle N=12, CBC N=12), CBC post-treated (Vehicle N=12, CBC N=9) from three separate experiments. *p<0.05, **p<0.01, ***p<0.001, ****p<0.0001 vs vehicle. 116
Figure 4.21 IL-6 percentage change from baseline in vehicle-treated cells (N=23, from two separate experiments). Concentrations were interpolated from a standard curve. Data are presented as mean ± SEM. Data were analysed using a repeated measures one-way ANOVA, with Dunnett's post-hoc comparison to baseline, **p<0.01. 117
Figure 4.22 Histograms showing the effects of CBD (A), CBGV (B), CBC (C) and CBDV (D) on IL-6 area under the curve for 16 hours of reperfusion following an 8-hour OGD protocol. N= 6–9, from three separate experiments. Data are represented as mean ± SEM. Data were analysed using a one-way ANOVA for each phytocannabinoid. 118

Figure 5.1 Effects of various CBD samples on SKOV-3 cellular metabolism using resazurin assays. CBD (10 or 50 µM) was applied to proliferating SKOV-3 cells for 24 (**a**) and 48 h (**b**) (n = 15 from 3 separate experiments). Effects of CBD (10 and 50 µM) on confluent SKOV-3 cells applied for 24 (**c**) and 48 h (**d**) (n = 10 from two separate experiments). Data are displayed as mean ± SEM % change from vehicle and were compared for statistical significance against vehicle using a one-way ANOVA. *p ≤ 0.05; ****p ≤ 0.0001. CBD, cannabidiol..... 136
Figure 5.2 Effects of CBD (THC Pharm) 25 µM on proliferating SKOV-3 cells after 24 or 48 h in the presence of WAY-100635, AM251, AM630, GW9662, O1918, SB366791 GW6471, or CID16020046 (n = 7 from two separate experiments). Data are displayed as mean ± SEM absorbance, and CBD + antagonist data were compared against CBD 25 µM alone using a one-way ANOVA. *p ≤ 0.05; ****p ≤ 0.0001. CBD, cannabidiol. 137
Figure 5.3 Effects of CBD in pericytes (p4–6) exposed to 4-h OGD. **a** Effect of CBD (10 or 100 nM) on LDH concentrations 24 h following initiation of OGD (n = 6, from two separate experiments). Effect of various CBD samples (10 or 100 nM) on media IL-6 concentrations immediately after OGD (**b**), or 24 h following the initiation of OGD (**c**) (n = 6, from 2 separate experiments). Data are displayed as mean ± SEM % change from normoxic control and were compared for statistical significance against the normoxic control (#) or OGD vehicle (*) using a one-way ANOVA. *p ≤ 0.05, **p ≤ 0.01, and ***p ≤ 0.001. CBD, cannabidiol; OGD, oxygen-glucose deprivation. 138
Figure 5.4 Effects of natural and synthetic CBD (100 nM) on LDH and IL-6 concentrations in pericytes exposed to 4 h OGD in the presence or absence of the 5HT1A antagonist WAY-100635 (300 nM). **a** IL-6 concentrations 24 h following the initiation of OGD (n = 11–13, from three separate experiments). **b** LDH concentrations in media from 24 h following initiation of OGD (n = 12–13, from 3 separate experiments). Data are expressed as mean ± SEM % change from normoxic and were compared to normoxic control (#) or OGD vehicle (*) using a one-way ANOVA with a multiple comparison. *p ≤ 0.05, **p ≤ 0.01, ***p ≤ 0.001, and ****p ≤ 0.0001. M, Medropharm; F, Flora Fusion; C, CBDepot; A, Ai Lab; L, Logical; T, THC Pharm; CBD, cannabidiol; OGD, oxygen-glucose deprivation. 138
Figure 5.5 Effects of natural (**a–d**) and synthetic CBD (**e**, **f**) on intestinal permeability following a 24 h inflammatory protocol (IFNγ and TNFα, shown as the solid bar) in differentiated Caco-2 cells. Data are displayed as mean ± SEM % change from baseline inserts (n = 5–6, from three separate experiments). Time course data are displayed as AUC and analyzed using a one-way ANOVA. CBD samples were compared to vehicle or each other using a multiple comparison *p ≤ 0.05, **p ≤ 0.01, and ***p ≤ 0.001. AUC, area under the curve; CBD, cannabidiol. 139
Figure 5.6 Effects of natural (**a–d**) and synthetic (**e**, **f**) CBD on intestinal permeability following a 24-h inflammatory protocol (IFNγ and TNFα, shown as the solid bar) in differentiated Caco-2 cells in the presence or absence of the CB_1 receptor antagonist AM251 (---). Time course data are displayed as AUC and analyzed using a one-way ANOVA. CBD samples were compared to vehicle or each other using a multiple comparison **p ≤ 0.01, ***p ≤ 0.001, and ****p ≤ 0.0001. AUC, area under the curve; CBD, cannabidiol. 140
Figure 6.1 The effects of CBD, TMP and CBD + TMP (1-30 µM) on cellular viability in proliferating cancer cell lines using resazurin assays. A) Effects of CBD, TMP and CBD + TMP on proliferating CaCo2 cells (p49-50) 48 and 72 h following drug application. B) Effects of CBD, TMP and CBD + TMP on proliferating DU-145 cells

(p12-13) 48 and 72 h following drug application. C) Effects of CBD, TMP and CBD + TMP on proliferating SKOV-3 cells (p36-37) 48 and 72h following drug application. In all cell types n= 8, from two separate experiments. Data are presented as percentage change from vehicle S.E.M and was compared for statistical significance against vehicle (*) or between CBD and CBD + TMP (#) at their respective concentrations and time-points using a one way ANOVA.*/# P ≤ 0.05, **/## P ≤ 0.01, ***/### P ≤ 0.001, ****/#### P ≤ 0.0001. 150
Figure 6.2 The effects of CBD, TMP and CBD + TMP (1-30 µM) on cellular viability in fully confluent cancer cell lines using resazurin assays. A) Effects of CBD, TMP and CBD + TMP on fully confluent CaCo2 cells (p49-50) 48 and 72 h following drug application. B) Effects of CBD, TMP and CBD + TMP on fully confluent DU-145 cells (p12-13) 48 and 72h following drug application. C) Effects of CBD, TMP and CBD + TMP on fully confluent SKOV-3 cells (p36-37) 48 and 72 h following drug application. In all cell types n= 8, from two separate experiments. Data are presented as percentage change from vehicle S.E.M and was compared for statistical significance against vehicle (*) or between CBD and CBD + TMP at their respective concentrations and time-points (#) using a one way ANOVA.*/# P ≤ 0.05, **/## P ≤ 0.01, ***/### P ≤ 0.001, ****/#### P ≤ 0.0001. 152
Figure 6.3 The effects of CBD, TMP and CBD + TMP (10,15 and 20 µM) on cellular viability using moderate concentrations over moderate exposure times in three fully confluent cancer cell lines using resazurin assays. Fresh media containing drugs or vehicle was applied at 0h and then again at 72 h. A) The effects of CBD, TMP and CBD + TMP in fully confluent CaCo2 (p45-47) cells 144h following the initial application of drugs. B) The effects of CBD, TMP and CBD + TMP in fully confluent DU-145 (p35-38) cells 144 h following the initial application of drugs. C) The effects of CBD, TMP and CBD + TMP in fully confluent SKOV-3 (p23-24) cells 144 h following the initial application of drugs. In all cell types n=6, from two separate experiments. Data are presented as percentage change from vehicle S.E.M and was compared for statistical significance against vehicle (*) or between CBD and CBD + TMP at their respective concentrations and time-points (#) using a one way ANOVA.*/# P ≤ 0.05, **/## P ≤ 0.01, ***/### P ≤ 0.001, ****/#### P ≤ 0.0001. 153
Figure 6.4 The effects of CBD, TMP and CBD + TMP (100nM, 1µM and 5µM) on cellular viability using low concentrations over extended exposure times in three fully confluent cancer cell lines using resazurin assays. Fresh media containing drugs or vehicle was applied at 0h and then every 48h until 240h. A) The effects of CBD, TMP and CBD + TMP in fully confluent CaCo2 (p21-27) cells 240h following the initial application of drugs. B) The effects of CBD, TMP and CBD + TMP in fully confluent DU-145 (p12-13) cells 240h following the initial application of drugs. C) The effects of CBD, TMP and CBD + TMP in fully confluent SKOV-3 (p36) cells 240h following the initial application of drugs. In all cell types n=8, from two separate experiments. Data are presented as percentage change from vehicle S.E.M and was compared for statistical significance against vehicle (*) or between CBD and CBD + TMP at their respective concentrations and time-points (#) using a one way ANOVA.*/# P ≤ 0.05, **/## P ≤ 0.01, ***/### P ≤ 0.001, ****/#### P ≤ 0.0001. 154
Figure 6.5 The effects of CBD, TMP and CBD + TMP (10 or 20 µM) on serum-starved DU-145 cells (p27-28) in a scratch wound assay. Effects of CBD, TMP and CBD + TMP on wound closure rate at A) 24 h or B) 48 h. In all experiments n= 6, from two separate experiments. C) Light microscope images 48h following scratch wound procedure correspond with figure 6.5B**.** Data are presented as mean percentage closure from baseline S.E.M and was compared for statistical significance against vehicle or between CBD and CBD + TMP at their respective

concentrations and time-points using a one way ANOVA.* P ≤ 0.05, ** P ≤ 0.01, *** P ≤ 0.001, **** P ≤ 0.0001..... 155
Figure 6.6 The effects of CBD, TMP and CBD + TMP (10 or 20 µM) on serum-starved SKOV-3 cells (p27) in a scratch wound assay. CBD, TMP and CBD + TMP effects on wound closure rate at A) 24h or B) 48h. In all experiments n= 6, from two separate experiments. C) Light microscope images 48 h following scratch wound procedure correspond with figure 6.6B**.** Data are presented as mean percentage closure from baseline S.E.M and was compared for statistical significance against vehicle or between CBD and CBD + TMP at their respective concentrations and time-points using a one way ANOVA.* P ≤ 0.05, ** P ≤ 0.01, *** P ≤ 0.001, **** P ≤ 0.0001. 157
Figure 6.7 The effects of CBD, TMP and CBD + TMP (1 or 10 µM) in astrocytes exposed to 8 h OGD and 24 h reperfusion. Drugs were applied immediately before and after OGD. The effects of CBD, TMP and CBD + TMP on LDH media concentrations A) immediately post-OGD (8 h) and B) 32 h following the initiation of OGD. C) The effect of CBD, TMP and CBD + TMP on cellular viability 32 h following the initiation of OGD using resazurin assays. D) The effects of CBD, TMP and CBD + TMP on IL-6 media concentrations 32 h following the initiation of OGD. In all assays n= 6-8, from two separate experiments. Data are presented as percentage change from normoxic S.E.M and was compared for statistical significance against vehicle (*) or between CBD and CBD + TMP at their respective concentrations and time-points (#) using a one way ANOVA.*/# P ≤ 0.05, **/## P ≤ 0.01, ***/### P ≤ 0.001, ****/#### P ≤ 0.0001. 159
Figure 6.8 The effects of CBD, TMP and CBD + TMP (100 nM or 1 µM) in Pericytes exposed to 4 h OGD and 20 h reperfusion. Drugs were applied immediately before and after OGD. The effects of CBD, TMP and CBD + TMP on LDH media concentrations A) immediately post-OGD (4 h) and) 24 h following the initiation of OGD. C) The effect of CBD, TMP and CBD + TMP on cellular viability 24 h following the initiation of OGD using resazurin assays. D) The effects of CBD, TMP and CBD + TMP on IL-6 media concentrations 24 h following the initiation of OGD. In all assays n= 6, from two separate experiments. Data are presented as percentage change from normoxic S.E.M and was compared for statistical significance against vehicle (*) or between CBD and CBD + TMP at their respective concentrations and time-points (#) using a one way ANOVA.*/# P ≤ 0.05, **/## P ≤ 0.01, ***/### P ≤ 0.001, ****/#### P ≤ 0.0001. 161

List of tables

Table 1 List of phytocannabinoids and their activity at various receptors. Data of activity at receptors was adapted from (De Petrocellis et al., 2011; Morales, Hurst and Reggio, 2017). NAM = Negative allosteric modulator, PAM = Positive allosteric modulator, OPR = opioid receptors. 56
Table 2 Logp values of phytocannabinoids generated by QikProp 3.5 integrated in Maestro (Schrödinger, LLC, New York, USA). 59
Table 3 Pharmacokinetic data from two separate studies assessing brain content of phytocannabinoids in mice and rats after receiving ip or po doses of phytocannabinoids (Deiana et al., 2011; Anderson, Low, et al., 2019). Cmax expressed as a percentage of the total dose was calculated as dose * average body weight = total dose administered. C_{max} * average brain weight = amount of drug in the brain. (amount of drug in brain/total dose administered)*100 = % of total dose in brain. RoA = route of administration, C_{max} = maximum concentration measured, T_{max} = Time until maximum concentration was measured, Ip = intraperitoneal, po = oral administration, BDL = below detectable limit, N/A = not available. 61
Table 4 Summary of results from each experiment in chapter 4. 120
Table 5 where appropriate data were collated between similar experiments. All data are displayed as a percentage—all data displayed as percentage change relative to vehicle (±SEM). CBD samples were compared to vehicle or each other using a one-way ANOVA alongside multiple comparisons. CBD = cannabidiol, NA = not available, ND = not detectable, CBDV = cannabidivarin, THC = delta-9-tetrahydrocannabinol, CBG = cannabigerol, GC/MS = gas chromatography/mass spectrometry, HPLC = high performance liquid chromatography, CC = convergence chromatography. 135

Abbreviations

2-AG – 2-Arachidonoylglycerol

7-OH-CBD – 7-Hydroxy-Cannabidiol

AA – Arachidonic acid

AEA – Anandamide

AMPA – α-amino-3-hydroxy-5-methyl-4-isoxazolepropionic acid

Apaf-1 – Apoptosis protease activating factor 1

AQP4 – Aquaporin-4

ATP – Adenosine triphosphate

AUC – Area under the curve

BBB – Blood-brain barrier

BCS – Biopharmaceutical Classification System

BM – Basement membrane

cAMP – Cyclic adenosine monophosphate

CB_1 – Cannabinoid receptor 1

CB_2 – Cannabinoid receptor 2

CBC – Cannabichromene

CBD – Cannabidiol

CBDA – Cannabidiolic acid

CBDV – Cannabidivarin

CBDVA – Cannabidivarinic acid

CBF – Cerebral blood flow

CBG – Cannabigerol

CBGA – Cannabigerolic acid

CBGV – Cannabigerol

CBGVA – Cannabigerovarinic acid

CBN – Cannabinol

CNS – Central nervous system

COX – Cyclooxygenase

COX-2 – Cyclooxygenase 2

DAG – Diacylglycerol

DAGL – Diacylglycerol lipase

DNA – Deoxyribonucleic acid

EAAT 1 – Excitatory amino acid transporter 1

EAAT 2 – Excitatory amino acid transporter 2

ECS – Endocannabinoid system

EGFR – Epidermal growth factor receptor

FAAH – Fatty-acid amide hydrolase

FABP – Fatty acid-binding protein

FATP – Fatty acid transport protein

GFAP – Glial fibrillary acidic protein

GI – Gastrointestinal

GPCR – G protein-coupled receptors

GPP – Geranyl diphosphate

GPR18 – G protein-coupled receptor 18

GPR55 – G protein-coupled receptor 55

ICAM-1 – Intracellular adhesion molecule 1

IFNγ – Interferon-gamma

IL-1 – Interleukin-1

IL-10 – Interleukin-10

IL-13 – Interleukin-13

IL-2 – Interleukin-2

IL-4 – Interleukin-4

IL-6 – Interleukin-6

INF-γ – Interferon-gamma

iNOS – Inducible nitric oxide synthase

LDH – Lactate dehydrogenase

LPS – Lipopolysaccharides

MAGL – Monoacylglycerol lipase

MAPR – Mitogen-activated protein kinase

MCAO – Middle cerebral artery occlusion

mGluR – Metabotropic glutamate receptors

MMP – Matrix metalloproteases

NAGly – N-arachidonoylglycine

NArPE – N-arachidonoyl-phosphatidylethanolamine

NBC – Sodium bicarbonate cotransporter

NCX – Na^{+}-Ca^{++} exchanger

NHS – National health service

NMDA – N-methyl-D-aspartate

NO – Nitric oxide

NOS – Nitric oxide synthase

OGD – Oxygen-glucose deprivation

OGD/R – Oxygen-glucose deprivation/reperfusion

PARP-1 – Poly-adenosine diphosphate-ribose polymerase-1
PFK-1 – Phosphofructokinase 1
PK – Pharmacokinetic
PKA – Protein kinase A
pMCAO – Permanent middle cerebral artery occlusion
PPAR – Peroxisome proliferator-activated receptor
PPRE – Peroxisome-proliferator response elements
ROS – Reactive oxygen species
SOD – Superoxide dismutase
STAT – Signal transducer and activator of transcription
TGF-β – Transforming growth factor-beta
THC – Tetrahydrocannabinol
THCA – Tetrahydrocannabinolic acid
TJ – Tight junction
TMP – Tetramethylpyrazine
TNFα – Tumor necrosis factor-alpha
tPA – Tissue plasminogen activator
TRP – Transient receptor potential
TRPA – Transient receptor potential ankyrin
TRPA1 – Transient receptor potential ankyrin 1
TRPM – Transient receptor potential melastatin
TRPM8 – Transient receptor potential melastatin 8
TRPV – Transient receptor potential vanilloid
TRPV1 – Transient receptor potential vanilloid 1
TRPV1 – Transient receptor potential vanilloid 1
TRPV2 – Transient receptor potential vanilloid 2
TRPV3 – Transient receptor potential vanilloid 3
TRPV4 – Transient receptor potential vanilloid 4
VCAM-1 – Vascular cell adhesion molecule 1
VEGF – Vascular endothelial growth factor
WHO – World health organisation

Abstract

In an ever ageing population, stroke represents a growing burden on society. After the age of 55, the likelihood of experiencing a stroke increases two-fold. People in this age group are also at a substantially higher risk of developing a disability following a stroke. Numerous studies have demonstrated the involvement of the endocannabinoid system in modulating molecular disturbances associated with stroke. Thus phytocannabinoids that modulate the endocannabinoid system may represent a novel strategy for treating a stroke.

A Meta-analysis was conducted to collate the data of relevant studies in the area of cannabidiol (CBD) mediated protection in animal models of stroke. A search of existing literature identified two separate laboratories both using focal ischemic-reperfusion injury (8 articles) induced by middle cerebral artery occlusion, to assess the efficacy of CBD. CBD administered intraperitoneally in male ddY mice (n: control 70, CBD 68) reduced infarct volume by a mean difference of 29.60 mm3 (Cl [34.94, 24.26], $p<0.00001$) and CBD administered via intracerebroventricular injections in adult male Wistar rats (n: control 81, CBD 81) reduced infarct volume by a mean of 88.62 mm3 (Cl [101.98, 75.26], $p<0.0001$). Publication bias was evident ($p=0.004$), and median study quality was 2 (range 0-4/10). Eggers statistic suggested publication bias was evident and negative studies were missing. The results of the meta-analysis indicated more robust evidence was needed to form any meaningful conclusions surrounding the efficacy of CBD in animal models of stroke.

The results from the previous chapter prompted an *in vivo* investigation into the effects of CBD and cannabidiolic acid (CBDA) in a mouse model of stroke. CBD and CBDA had no significant effect on infarct volume 24 h following permanent middle carotid artery occlusion (pMCAO). An indirect measurement of vasogenic swelling was made, which showed CBD at 1 mg/kg increased brain water content by 7.6% ± 2.6, 95% CI [-5.9, 8.1] ($p<0.05$) relative to control mice. These results suggest that without adequate reperfusion CBD or CBDA do not reduce infarct volume 24 h following pMCAO. If this is indeed the case, future studies should aim to directly assess whether reperfusion is a necessary perquisite for CBD and CBDA to display efficacy.

Astrocytes are implicated in maintaining neuronal homeostasis and therefore preserving their viability during or following a stroke could represent a novel therapeutic strategy. Using an *in vitro* model of human astrocytes exposed to oxygen glucose deprivation (OGD), these experiments aimed to identify whether less researched minor phytocannabinoids could influence several endpoints associated with OGD damage, such as; lactate dehydrogenase (LDH) for cellular damage, interleukin-6 (IL-6) for inflammation and mitochondrial complex proteins for impaired energy production. The efficacy of each phytocannabinoid was assessed by being applied before or after OGD injury. These experiments identified that CBD is only effective at protecting against OGD induced damage when applied following the insult. In contrast, CBGV provided the greatest extent of protection, reducing cellular damage when administered before or after OGD, indicating this phytocannabinoid might address molecular disturbances at both the ischemic and reperfusion period. Further studies should look to assess the co-application of these phytocannabinoids and assess their effects in more complex cellular models.

The next set of *in vitro* experiments aimed to distil the belief held by the non-scientific community that naturally sourced CBD is superior to CBD produced by synthetic means using empirical evidence. To do so, the pharmacological activity of CBD from two different sources (synthetic vs. naturally occurring) was compared in three human cellular models; cancer, stroke and irritable bowel syndrome (IBD). The results from these experiments demonstrated no pharmacological difference exist in the anti-proliferative, anti-inflammatory, or permeability effects of purified natural versus synthetic CBD. Indicating the reliability and formulations of CBD should be considered above the starting source in the development of medicines.

Using two human cellular models of disease, cancer and stroke, a series of *in vitro* experiments aimed to assess the pharmacological properties of CBD and tetramethylpyrazine (TMP). These experiments would specifically aim to assess whether co-application at a 1:1 ratio produces synergistic, additive, neutral or compromised efficacy. Co-applied CBD and TMP produces an additive effect on anti-proliferative properties, particularly in ovarian cancer cell line SKOV3. The anti-migratory effects of CBD were attenuated when applied alongside TMP in DU145 and SKOV-3 cells. TMP applied alongside CBD in cellular models of OGD/R injury had no effect on or antagonised CBD's effects. Mechanism of action studies are required to understand why the combination of CBD and TMP produces additive or compromising effects in certain anti-cancer endpoints.

1 Introduction

1.1 Stroke

A stroke is defined by the World Health Organisation (WHO) as a sudden loss of brain function due to a disruption in cerebral blood flow (CBF), in which symptoms persist for at least 24 h or subsequently lead to death (Hatano, 1976). The National Health Service (NHS) and social care costs for stroke in 2005 were estimated at £2.8 billion a year, and in an ever ageing population, this figure is likely to grow (Saka, McGuire and Wolfe, 2005). Data from over 8600 stroke survivors found that 65% of people reported developing a severe disability following a stroke. The authors also noted that a stroke could cause a broader range of disabilities than any other disease (Adamson, Beswick and Ebrahim, 2004). Around every ten years after the age of 55, the likelihood of experiencing a stroke increases two-fold. People in this age group who suffer a stroke are also at more risk of developing a chronic disability (Kelly-Hayes *et al.*, 2003; Chong and Sacco, 2005). Given the socio-economic challenges stroke presents, it is highly desirable to develop novel treatments that can prevent the underlying cause or address the series of harmful events that occur during and following a stroke.

1.1.1 Pathophysiology of cerebral reperfusion injury

A stroke occurs for one of two reasons; a cerebral artery cannot deliver blood to the brain's tissues (ischemic), or a cerebral blood vessel that would otherwise supply blood to the brain bursts (haemorrhagic). By some estimates, ischemic stroke accounts for 87% of all strokes and are typically the result of an occluded blood vessel (Hatano, 1976; Beal, 2010). An interruption in blood flow prevents sufficient oxygen (ischemia) and glucose (hypoglycemia) from reaching the brain's tissues, forcing cells to switch from oxidative phosphorylation to glycolysis. Metabolism of glucose by anaerobic means produces 36 less adenosine triphosphate (ATP) relative to oxidative phosphorylation, thus drastically reducing net ATP production (Silver, Deas and Erecińska, 1997). Depletion of ATP quickly results in tissue damage, the severity of which depends not only on the duration of ischemia but the location of the blockage and the capacity of collateral blood flow to buffer the effects (Doyle, Simon and Stenzel-Poore, 2008; Sims and Muyderman,

2009). The most significant reduction in blood supply occurs in the ischemic core, where blood flow has dropped to 10-25% of its average capacity. Here, cells are at risk from irreversible damage if blood flow is not restored within minutes (Sims and Anderson, 2002). Encapsulating the ischemic core is a region defined as the ischemic penumbra (Figure 1.1); blood flow here still operates at 40-60% of the regular blood supply. Whilst cells in this region will eventually suffer the same fate as cells within the core, they do so at a much slower rate and represent a region of salvageable tissue (Astrup *et al.*, 1977; Hossmann, 1994). Indeed cells presenting characteristics of apoptosis are more numerous in the ischemia penumbra and peak in number around 24 h following stroke (figure 1.2) (Sims and Muyderman, 2009). Despite some functional deficits in this region, experiments in primates have shown that neurons in this area can produce enough ATP to sustain a resting membrane potential. With timely reperfusion, regular electrical activity returns (Bretón, César and Rodríguez, 2012).

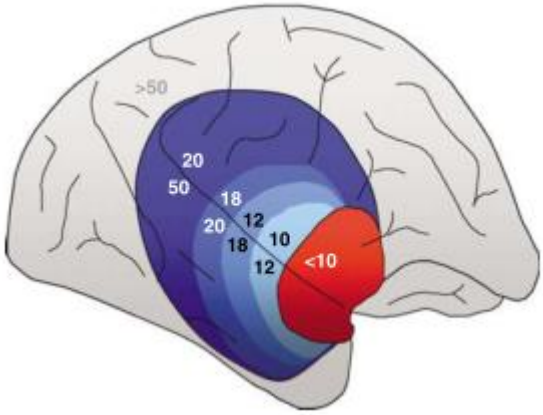


Figure 1.1 Depicts the boundaries of the ischemic core (10-25%) and penumbra regions as percentage reductions in cerebral blood flow (CBF) following mild cerebral artery occlusion (MCAO) in the baboon brain. As the duration of ischemia extends, the core begins to spread into the surrounding penumbra, leading to a progressively larger infarction. Reproduced from Moustafa RR and Baron J-C, 'Pathophysiology of ischemic stroke: Insights from imaging and implications for therapy and drug discovery' British Journal of Pharmacology, 2008

As the duration of ischemia increases, the ischemic core continues to grow into the penumbral region. The mechanisms for spreading damage appear to be multifactorial and correlate well with spreading depolarisation and tissue acidification (Hossmann, 1994). In rats exposed to mild carotid artery occlusion (MCAO), restoring blood flow within the first 30-60 minutes dramatically reduces the infarct size that develops (Memezawa, Smith and Siesjo, 1992). This indicates that the mechanisms responsible for spreading

damage require more extended periods of ischemia to manifest. Studies in rodent models have demonstrated that 50% reductions in infarct size can be achieved, providing neuroprotective treatments are administered early into the reperfusion period, emphasising the effectiveness of timely treatments (Memezawa, Smith and Siesjo, 1992; Yoshimoto and Siesjö, 1999).

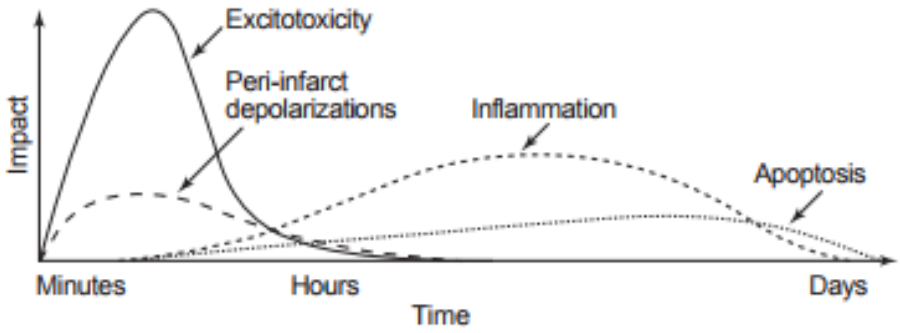


Figure 1.2 Damage caused following ischemia follows a temporal pattern. At the onset of ischemia, cells experience rapid damage from excitotoxicity, leading to the initiation of peri-infarct depolarisations, inflammation and subsequent apoptosis. Reproduced from Dirnagl U, 'Pathobiology of ischemic stroke: an integrated view' Trends in Neuroscience 1999.

Molecular consequences of cerebral ischemia

The brain represents 2% of total body weight yet is responsible for 20% of total oxygen consumption and 25% of total glucose consumption (Zauner *et al.*, 2002; Heiss, 2014). Sufficient oxygen levels enable the oxidative phosphorylation of glucose, allowing cells to generate 13 times more ATP than anaerobic producing pathways, allowing neuronal cells to meet enormous energy demands (Alberts *et al.*, 2002). Estimates suggest that 70% of this energy is required for the regular operation of sodium-potassium adenosine triphosphatase (Na^+/K^+-ATPase) pumps responsible for maintaining high intracellular K^+ and low intracellular Na^+ concentrations (Edvinsson and Krause, 2002). As the maintenance of this gradient is heavily dependent upon sufficient ATP levels, sustained interruption in ATP synthesis, such as those seen in ischemic stroke, lead to a rapid redistribution of ions across the cell membrane. Notably, significant increases in extracellular K^+ and intracellular Na^+ (Doyle, Simon and Stenzel-Poore, 2008). In neurons, this redistribution of ions causes a 100-fold increase in intracellular Ca^{++}, mainly through the opening of voltage-

sensitive Ca^{++} channels and subsequent liberation of Ca^{++} from intracellular stores, resulting in neurotransmitter release (Ulrich Dirnagl, 1999; Südhof, 2012).

60-70% of the synapses in the human brain utilise the excitatory transmitter glutamate. One principal problem arising from uncontrolled neurotransmitter release is excitotoxicity (Victor Nadler, 2010). Glutamate release leads to the activation and opening of ionotropic N-methyl-D-aspartate (NMDA) receptors, causing an influx of Ca^{++}. The propagation of this phenomenon is thought to be important in the generation of peri-infarct depolarisations (Olney, 1969; Mehta, Manhas and Raghubir, 2007). Other glutamate receptors, such as metabotropic glutamate receptors (mGluR), contribute somewhat to excitotoxicity; however, the NMDA receptor is considered to play the largest role (Waxman and Lynch, 2005). In contrast to receptor mediated excitotoxicity, another group demonstrated that the reversed operation of glutamate transporters is the most significant contributor to glutamate release. Under normal physiological conditions, glutamate transporters utilise the electrochemical gradient of Na^{+} to power the transport of glutamate into the cell. However, during an ischemic episode, the redistribution of ions reduces extracellular Na^{+} levels and induces the reverse operation of this transporter. Allowing glutamate to exit the cell along its concentration gradient (Rossi, Oshima and Attwell, 2000). This mechanism provides a method for significant intracellular Ca^{++} increases by glutamate and causes activation of many calcium-dependent proteases and lipases, leading to uncontrolled cellular catabolism (Edvinsson and Krause, 2002). Indeed, neuroprotection is observed following the application of NMDA antagonists in experimental models; however, their use in a clinical setting is limited by the importance of NMDA receptors in physiological functions, e.g. memory formation, respiration and cardiovascular regulation (Ulrich Dirnagl, 1999; Lipton, 2004).

Another consequence of uncontrolled intracellular Ca^{++} is the activation of intrinsic apoptotic pathways, caused by a loss of mitochondrial membrane potential (Celsi *et al.*, 2009). Inability to control the electrochemical gradient across the mitochondrial membrane causes the liberation of cytochrome C (Sattler and Tymianski, 2000). Cytochrome C then binds apoptosis protease activating factor 1 (Apaf-1) and procaspase-9 present in the cytosol, the latter of which produces activated caspase -9 (Zou *et al.*, 1997; Li *et al.*,

1998). Caspase-9 then activates downstream caspases such as Caspase-3, -6 and -7, leading to chromatin condensation, deoxyribonucleic acid (DNA) fragmentation and membrane blebbing (Porter and Jänicke, 1999; Kuida, 2000). Interestingly, compounds that restrict the mitochondrial pore from opening are neuroprotective and could represent a target for future therapeutics (Halestrap *et al.*, 1997; Schinzel *et al.*, 2005).

During ischemia, low oxygen levels ensure any remaining energy substrates are metabolised via anaerobic metabolism, resulting in lactate production. Lactate levels in the ischemic brain can increase 10-fold relative to homeostatic levels. As well as anaerobic metabolism, reduced blood flow limits lactate buffering capacity, causing a localised build up in the extracellular fluid (Welsh, Marcy and Sims, 1991; Paschen, Oláh and Mies, 2002). Significant increases in lactate cause acidification of the intracellular environment, and decreased pH levels can cause the dysfunction of many enzymes. Phosphofructokinase 1 (PFK-1), a critical enzyme in the glycolytic pathway, is inhibited by an acidic microenvironment (Näveri, Näveri and Härkönen, 2001). This subsequently reduces the effectiveness of glycolytic pathways, reducing net ATP production and exacerbating the intensity of ischemia. Acidosis also increases the production of reactive oxygen species (ROS) due to rising intracellular H^+ concentrations, allowing for protonation of various ions, e.g. superoxide anion (O^{-2}) conversion into hydrogen peroxide (H_2O_2) (Saeed *et al.*, 2007).

Relative to other organs, the brain possesses small quantities of antioxidants, leaving the brain particularly vulnerable to the damage caused by ROS production (Coyle and Puttfarcken, 1993). High levels of intracellular Ca^{++} and Na^+ cause mitochondria to produce high levels of free radicals (Doyle, Simon and Stenzel-Poore, 2008). Increased intracellular Ca^{++} activates nitric oxide synthase (NOS) and increases the generation of nitric oxide (NO). NO then combines with superoxide to produce peroxynitrite, resulting in severe damage to proteins, lipids and DNA. The production of NO also activates poly-adenosine diphosphate-ribose polymerase-1 (PARP-1), an enzyme involved in the repair of DNA (Doyle, Simon and Stenzel-Poore, 2008). The PARP-1 enzyme is estimated to be one of the largest consumers of nicotinamide adenine dinucleotide (NAD^+) which can rapidly deplete ATP levels during times of increased free radical production (Suh *et al.*, 2003). While a stable blood flow is needed to increase energy

production, in somewhat of a double edged sword, ROS production is further amplified by the return of oxygen.

Molecular consequences of reperfusion

Reperfusion represents an event required for long-term functional recovery of tissue; however, it also represents a period of further tissue damage. The source of this damage is partly attributed to increased ROS production due to the return of oxygen, which leads to the depletion of already low antioxidant levels (Metodiewa and Kośka, 2000). ROSs are mainly produced by complex proteins I and II in the mitochondrial respiratory chain, and considerable damage is only caused when the net production outweighs the ability to scavenge them (Boveris and Chance, 1973).

The oxidation of xanthine and hypoxanthine produces highly reactive oxygen causing the peroxidation of lipid membranes (Nishino, 1994). The subsequent production of toxic aldehydes damages functional proteins such as; ion channels, transporters, and cytoskeletal proteins (Nishino, 1994; Beetsch *et al.*, 1998). This event is particularly damaging to the brain due to its high lipid content (Mehta, Manhas and Raghubir, 2007). Therefore, it is somewhat unsurprising anti-oxidant therapies produce neuroprotection in experimental models of ischemia-reperfusion injury. One such study demonstrated the antioxidant enzyme superoxide dismutase (SOD) reduces infarct volume when administered 3 h after MCAO in rats (Baker *et al.*, 1998). Suggesting ROS-mediated damage plays a significant role during the reperfusion period and represents a target for future therapeutics.

Another aspect of damage caused by reperfusion involves the blood-brain barrier (BBB). The BBB is composed of microvascular endothelial cells and the basement membrane (BM). Astrocytes and pericytes play a vital role in influencing the barrier's integrity and would therefore represent a potential target for manipulating the BBB (Ballabh, Braun and Nedergaard, 2004; Muoio, Persson and Sendeski, 2014). The BBB exists to restrict the transfer of contents from the blood into the brain, allowing the brain to maintain an extracellular fluid without blood plasma influencing its contents (Abbott, Rönnbäck and Hansson, 2006). However, during reperfusion, a surge in free radical production activates matrix metalloproteases (MMPs) leading to significant BBB degradation (Doyle, Simon and Stenzel-Poore, 2008). MMPs

are secreted in a pro-enzymatic form; however, upon activation by plasminogen activator or the pro-hormone convertase, furin they begin to degrade tight junction (TJ) proteins (e.g. occludin and claudin) and basal lamina proteins (e.g. fibronectin, laminin and collagen) (Lakhan *et al.*, 2013). These proteins are integral structures of the BBB and provide barrier integrity by tightly connecting neighbouring endothelial cells (Wolburg and Lippoldt, 2002). Interestingly the activity of MMPs is also modulated via inhibition by a group of proteins called tissue inhibitor metalloproteinases (TIMPs) (Malemud, 2006). One in vivo study demonstrated deletion of the TIMP-1 gene results in increased MMP-9 activity and increased BBB leakiness relative to wild-type mice (Fujimoto *et al.*, 2008). Furthermore, the over expression of the TIMP-1 gene in mice provided greater protection against increased BBB permeability by decreasing MMP-9 activation and expression (Tejima *et al.*, 2009). Uninterrupted degradation of tight junction and lamina proteins increases BBB permeability, facilitating the entry of large molecules and immune cells (neutrophils, lymphocytes and monocytes) through transcellular paths into the central nervous system (CNS) (Cunningham, Wetzel and Rosenberg, 2005; Adibhatla and Hatcher, 2008). All of which can promote the entry of damaging molecules and uncontrolled inflammation.

Molecular consequences of inflammation

Immune response

Following an insult to the brain, the inflammatory response is initially started by microglia, the brain's resident immune cells (Graeber and Streit, 2010). Microglia become activated by many factors, including; internal contents of necrotic cells, neurotransmitters, plasma constitutes, and abnormal proteins (Codolo *et al.*, 2013). Once activated, microglia can transform into macrophages, remove cell debris, and contribute to the release of pro-inflammatory signals (Hanisch and Kettenmann, 2007). Microglia can exert pro-inflammatory and anti-inflammatory effects following an insult to the CNS, dictated by the type of activated state assumed (M1= Pro-inflammatory, M2= Anti-inflammatory). In microglia cell culture, the addition of bacterial lipopolysaccharides (LPS), Tumor necrosis factor-alpha (TNF-α), Interferon-gamma (IFNγ), or necrotic neurons can induce an M1 phenotype.

In this state, microglia can be characterised by the up-regulation of mitogen-activated protein kinase (MAPK), secretion of TNF-α, Interleukin-6 (IL-6), expression of cyclooxygenase 2 (COX-2) and inducible nitric oxide synthase (iNOS) and the production of ROSs (Fernandes, Miller-Fleming and Pais, 2014). The M2 phenotype is induced in microglia cultures by administrating interleukin-13 (IL-13) and interleukin-4 (IL-4). This state can be characterised by the expression of cysteine-rich protein, FIZZ-1, Heparin-binding lectin, Ym1 and Arginase 1 (Freilich, Woodbury and Ikezu, 2013). *In vivo* experiments assessing the anti-inflammatory properties of M2 activated microglia indicates that the release of IL-4 decreases iNOS and TNF-α activity (Chao, Molitor and Hu, 1993). Interestingly, the inhibition of microglia using minocycline in an MCAO model of ischemia increased CA1 pyramidal neuronal survival by 77%. However, when minocycline was given 30 minutes into the reperfusion period, neuronal survival was decreased by 6% (Yrjänheikki *et al.*, 1998). These results indicate a temporal pattern in switching to the M1 or M2 phenotype following ischemia, underscoring the importance of timely interventions. It is now postulated that various intermediate forms between M1 and M2 exist; however, the exact mechanism that controls this spectrum remains to be elucidated (David and Kroner, 2011). Given the ability of microglia to perform these contrasting roles, careful consideration is required when developing drugs that they interact with. A deeper understanding of what causes intermediate activation states during ischemia/reperfusion injury will aid in drug development.

Other immune cells derived from general circulation, such as; neutrophils, lymphocytes and monocytes, transmigrate across a leaky BBB in a process mediated by intracellular adhesion molecule 1 (ICAM-1) and vascular cell adhesion molecule 1 (VCAM-1) (Greenwood *et al.*, 2011). The invasion of immune cells increases the inflammatory response by producing cytokines, chemokines, free radicals, proteolytic enzymes, and adhesion molecules, leading to uncontrolled inflammation and subsequent tissue damage (Huang, Upadhyay and Tamargo, 2006). Immune cell infiltration's initial function may exacerbate tissue damage and worsen neurological outcomes; however, other parts act to clear cell debris, release anti-inflammatory molecules, and aid in glial scar formation (Doyle, Simon and Stenzel-Poore, 2008). Providing evidence any manipulation of the immune response must be in line with the temporal pattern of protection vs. damage exacerbation.

Cytokines

Following an increase of cerebral immune cell infiltration, cytokines such as IL-6, interleukin 1 (IL-1), and TNF-α in the brain are dramatically elevated 24 h following experimental stroke (Hill *et al.*, 1999; Simi *et al.*, 2007). In rats subjected to MCAO, IL-6 becomes elevated within 3–3.5 h of stroke, with peak expression at 12 h (Wang *et al.*, 1995). Indeed, elevated intrathecal levels of IL-6 correlate with larger infarct size and worse outcomes in stroke patients (Tarkowski *et al.*, 1995). However, IL-6 signalling is required at later stages for tissue remodelling/recovery by activating transcription factor signal transducer and activator of transcription (STAT) (Hakkoum, Stoppini and Muller, 2007). Other studies have also demonstrated that intrathecal TNF-α levels correlate well with the degree of ischemic damage (Zaremba, Skrobanski and Losy, 2001). TNF-α promotes neutrophil infiltration into the brain by inducing the expression of adhesion molecules and the production of other inflammatory mediators (Khoshnam *et al.*, 2017). In experimental models of stroke, the administration of anti-TNF-α antibodies decrease infarct volume and improves neurological outcomes (Lavine, Hofman and Zlokovic, 1998).

The natural production of endogenous anti-inflammatory cytokines can attenuate the release of pro-inflammatory cytokines and chemokines (Ooboshi *et al.*, 2005). For example, interleukin-10 (IL-10) can reduce the pro-inflammatory actions of TNF-α by neutralising the activation of downstream signalling pathways (Liesz *et al.*, 2009). It has also been shown that the exogenous administration of the anti-inflammatory molecule transforming growth factor-beta (TGF-β) can reduce the number of circulating neutrophils, reducing tissue damage following cerebral ischemia in primates (Mori *et al.*, 1992)

1.1.2 Astrocytes

Astrocytes were initially assumed to be merely structural support cells, providing scaffolding for neurons. However, as research into these cells has

advanced, so have their roles in physiology. Astrocytes are now considered to play pivotal roles in synaptic plasticity, ion buffering, ROS scavenging, water transport, BBB maintenance, glutamate uptake, and controlling highly localised CBF (Abbott, Rönnbäck and Hansson, 2006; Rossi, Brady and Mohr, 2007; Koehler, Roman and Harder, 2009; Sofroniew and Vinters, 2010; Becerra-Calixto and Cardona-Gómez, 2017). The ever-expanding roles of astrocytes have begun to implicate them in more and more pathologies. However, it is unclear whether they act like innocent bystanders, perpetrators or supporters of neurological outcomes following cerebral ischemia.

Astrocytes are the most abundant type of cell found in the human brain and are typically divided into two sub-types. Protoplasmic astrocytes are thoroughly distributed throughout the grey matter and possess many fine processes contacting as many as 2,000,000 synapses (Bushong *et al.*, 2002). They form a tripartite synapse at these sites, allowing astrocytes to modulate neurotransmission (Perea, Navarrete and Araque, 2009). The second sub-type, fibrous astrocytes, are mainly localised to white matter tracts. Relative to their grey matter counterpart, the processes are thicker and less arborised; they generally project greater distances and terminate at nodes of Ranvier along neuronal axons (Sofroniew and Vinters, 2010). Astrocytes in white and grey matter borders can display an intermediate morphology between the two types (Chen and Swanson, 2003). Both sub-types also possess specialised terminal contacts called 'endfeet', making direct contact and enveloping the endothelial cells surrounding blood vessels, allowing for highly localised control of CBF (Sofroniew and Vinters, 2010; Ding, 2014). It is estimated that every cerebral blood vessel is contacted by at least one astrocyte end foot, underscoring the importance of astrocyte modulation of CBF (MacVicar and Newman, 2015).

Unlike neurons, astrocytes are unable to propagate an electrical signal throughout a network. Instead, the rapid transmission of signals throughout a network is performed by spreading waves of Ca^{++} (Scemes and Giaume, 2006). This phenomenon requires the presence of gap junctions that connect neighbouring astrocytes and facilitate the transfer of ions and small molecules between them (Finkbeiner, 1992; Scemes and Giaume, 2006). In response to increases in intracellular $Ca^{++,}$ astrocytes can then release

chemical messengers which modulate blood vessels and neuronal activity (Sofroniew and Vinters, 2010).

Astrocytes and stroke

Like neurons, astrocytes are also vulnerable to the effects of ischemia; however, they are not as sensitive. The reversal of MCAO in rodents within the first hour of ischemia often results in the selective loss of neurons (Du et al., 1996; Endres et al., 1998). Some of this resistance has been attributed to the exclusive presence of glycogen within astrocytes, providing an alternative energy source when glucose delivery is impaired (Brown, 2004). However, the anaerobic utilisation of glycogen produces lactate, meaning any net benefit gained may be hindered by the acidic microenvironment (Giffard, Monyer and Choi, 1990; Rossi, Brady and Mohr, 2007). Another possible reason for their increased resistance to ischemia is the low expression of NMDA receptors. These channels are proposed to significantly contribute to Ca^{++} influx during excitotoxicity (Matute *et al.*, 2002). Instead, astrocytes predominately utilise the α-amino-3-hydroxy-5-methyl-4-isoxazolepropionic acid (AMPA) and kainite receptors to transduce glutamate signals. The desensitisation of AMPA receptors during ischemia allow astrocytes to endure dramatically elevated extracellular glutamate (David *et al.*, 1996).

Interestingly, astrocytes from different brain regions respond differently to glutamate excitotoxicity when induced in dissected brain slices. Those derived from the hippocampus appear unaffected by the application of exogenous glutamate; however, astrocytes derived from the neocortex are readily damaged by a similar protocol (David *et al.*, 1996; Prieto and Alonso, 1999). Additional work in this area has shown protoplasmic astrocytes are more vulnerable to ischemic/reperfusion injury than their fibrous counterparts, potentially reflecting different roles following stroke (Lukaszevicz *et al.*, 2002). Understanding what causes differences in sensitivity to ischemia may identify a distinct set of pharmacological targets that increase the survival of susceptible astrocyte subtypes. Unlike neurons, astrocytes are generally more resistant to the types of damage induced by ischemia. However, acidosis is one example of an exemption to this rule (Giffard, Monyer and Choi, 1990). Enhanced sensitivity could result from the preferential expression of electrogenic sodium bicarbonate cotransporters 1

(NBCe1) in astrocytes. Experiments in cortical astrocytes have shown that these transporters produce an inward flux of Na^+ during acidosis and cause a collapse of ionic gradients (Theparambil *et al.*, 2020). If pH levels fall below pH6.6, astrocytes cannot have energy, and a complete cessation of energy production occurs (Swanson, Farrell and Stein, 1997). Furthermore, inducing the expression of NBC in 3t3 cells, otherwise unaffected by acidosis, becomes vulnerable to these conditions (Giffard *et al.*, 2000).

Ischemic/reperfusion injury also causes astrocytes to undergo a process termed reactive gliosis, conforming to one of two states, m1 being pro-inflammatory and m2 anti-inflammatory (Swanson, Ying and Kauppinen, 2004). Research however indicates this is not a binary concept, and astrocytes can display a spectrum of reactive phenotypes. To what degree cells become 'reactive' depends on the extent of damage, nature of the injury, and the markers used to define gliosis (Sofroniew, 2009). The upregulation of glial fibrillary acidic protein (GFAP) is often used to quantify the extent of reactive gliosis, as its expression correlates well with the intensity of gliosis (Eddleston, M. P. Mucke, 1993). Morphologically, reactive astrocytes appear to possess more primary processes, and their appearance becomes thickened with more overlap between individual astrocyte processes (figure 1.4).

It should be noted that GFAP staining does not reveal the entire structure of the astrocyte. Like Lucifer yellow, stains that fill the whole astrocyte can confirm this (Wilhelmsson *et al.*, 2006). Another characteristic of reactive gliosis is the expression of epidermal growth factor receptor (EGFR), detected in reactive astrocytes and activated microglia/macrophages following an insult, and EGFR activation has been implicated in astrocyte transition from nonreactive to the reactive state (Pekny and Pekna, 2014). Exogenously applied IL-6, IL-10 TNF-α, and interferon-gamma (INF-γ) appear to induce and potentiate reactive gliosis, suggesting their importance in mediating this effect *in vivo* (John, Lee and Brosnan, 2003).

In severe cases of gliosis, a scar formation can occur. The formation of a glial scar is associated with the proliferation of astrocytes, where newly formed processes intermingle and intertwine extensively, creating a physical barrier to seal off the injury from surrounding tissue (Wanner *et al.*, 2013). More recent work has also implicated pericytes in the progression of glial

scar formation (Goritz *et al.*, 2011). The roles of a glial scar following injury appear to have contrasting roles that manifest at different time points following cerebral ischemia. In the acute phase, gliosis can reduce ecotoxicity, buffer ions and scavenge free radicals. However, in the later stages of injury, reactive gliosis appears to inhibit axonal sprouting (Sofroniew and Vinters, 2010; Pekny, Wilhelmsson and Pekna, 2014).

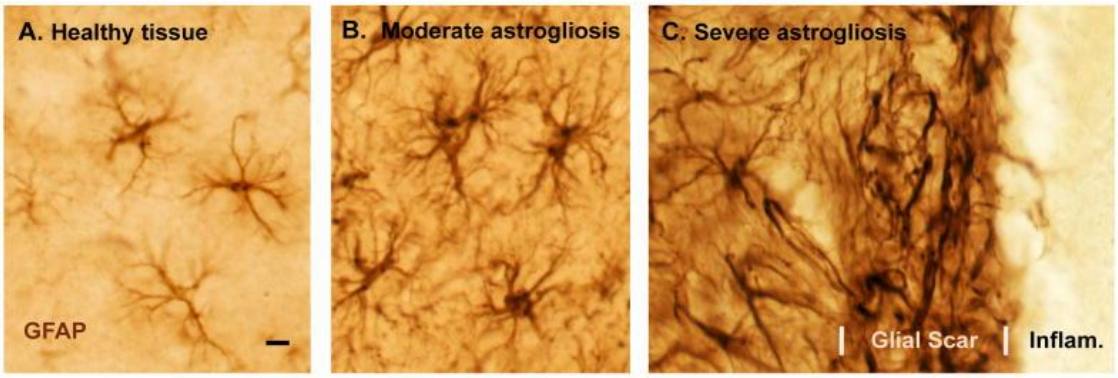


Figure 1.3 glial fibrillary acidic protein stained astrocytes from mouse cerebral cortex (A-C) (A) Non-reactive astrocytes have little overlap between their processes and appear to occupy a distinct territory (B) Intracerebral injection of lipopolysaccharide induces moderate reactive gliosis. Although astrocytes have become more arborised, their processes remain in distinct domains and barely overlap (C). Severe reactive gliosis is induced by severe traumatic brain injury, leading to glial scar formation and inflammation. This intensity of gliosis is characterised by the obvious overlapping and thickening of processes and elevations of glial fibrillary acidic protein expression. Scale bar = 8μm. Image adapted from Sofroniew, Michael V.' Molecular dissection of reactive astrogliosis and glial scar formation' Trends in Neurosciences 2009.

Reactive oxygen species (ROS) scavenging

The main antioxidant in the brain, glutathione, is predominately produced by astrocytes, and in experimental models where glutathione content has been sequestered, the brain's sensitivity to ischemic injury increases (Mizui, Kinouchi and Chan, 1992; Scheiber, Mercer and Dringen, 2014). This puts astrocytes in an ideal position to protect neurons from ROS production if their survival could be promoted. Indeed astrocytes co-cultured with neurons increase the resistance of neurons to free radicals, and astrocytes depleted of glutathione increase neurons susceptibility to damage (Chen and Swanson, 2003). As previously mentioned, increased H^+ ions result in acidification of the extracellular space, and astrocytes can actively sequester H^+ ions. However, whether these mechanisms can persist during ischemia is uncertain (Deitmer and Rose, 1996).

Excitotoxicity

Astrocytes play a prominent role in maintaining low extracellular glutamate concentrations, sequestering released glutamate from the extracellular space via Na^+ dependent excitatory amino acid transporters 1 and 2 (EAAT1-2) (Chen and Swanson, 2003). Upon uptake into astrocytes, glutamate is converted to glutamine by glutamine synthase and recycled

back into neurons (Schousboe *et al.*, 2014). Increased levels of glutamate during excitotoxicity saturate the ability of astrocytes to metabolise glutamate (Sibson *et al.*, 1998). The accumulation of glutamine has been associated with cytotoxic swelling in astrocytes; however, whether glutamine contributes more than glutamate to cellular swelling is unclear (Norenberg, Rama Rao and Jayakumar, 2005).

The extent to which astrocytes protect neurons during excitotoxicity can be demonstrated in cell cultures devoid of astrocytes. In this setting, neuronal vulnerability to glutamate-induced excitotoxicity is 100 times greater than co-cultures (Rosenberg and Aizenman, 1989). Further reinforcing the importance of astrocyte glutamate uptake comes from experiments utilising knockout gene studies. The knockdown of glutamate transporter genes expressed by astrocytes, but not neurons, produce excitotoxicity and exacerbates ischemic damage in models of stroke (Rothstein *et al.*, 1996; Rao *et al.*, 2001). As the acidification of the intracellular environment produces glutamate release in rodent brain slices, ischemia-induced acidosis could represent another mechanism for excitotoxicity (Beppu *et al.*, 2014). In contrast, acidic conditions reduce the activity of NMDA receptors in neurons, raising the possibility that this event could reduce excitotoxicity depending on the cumulative net benefit (Giffard *et al.*, 1990; Traynelis and Cull-Candy, 1990). Multiple mechanisms likely contribute to glutamate excitotoxicity, and the complex interplay between the magnitude of these mechanisms determines any overall positive or negative net gain.

Ion buffering

Astrocytes are highly permeable to K^+, allowing K^+ to freely move in and out of the cell along its concentration gradient. Local increases in extracellular K^+, like those caused by an action potential, cause increases in intracellular astrocytic K^+. This increase results in a K^+ current that diffuse throughout the astrocytic syncytium, thereby enabling the redistribution of K^+. This phenomenon is referred to as spatial buffering (Kuffler, Nicholls and Orkand, 1966). In ischemic conditions, increased extracellular K^+ contributes to excitotoxicity, peri-infarct depolarisations and astrocyte swelling. Indeed, more dramatic elevations in extracellular K^+ trigger the activation of astrocytic Na+/K+ ATPase, which boosts astrocyte spatial buffering capacity (Walz and Hertz, 1982). Depleted astrocyte populations significantly

increase extracellular K^+, initiating neuronal depolarisations (Sykova et al., 1992). Despite this, the effect of astrocyte K^+ buffering in ischemia is difficult to predict due to the variety of complications that ischemia induces. Sequestering extracellular K^+ should prevent or reduce neuronal depolarisation and subsequent glutamate release. In contrast, the activity of astrocyte spatial buffering may be a key player in the involvement of spreading depression (Nedergaard and Hansen, 1993), a phenomenon shown to extend the area of the ischemic core during ischemia (Mies et al., 1993; Busch et al., 1996).

Cerebral oedema

Brain oedema is classified as the pathological swelling of brain tissue due to increased brain water content. Increases in water volume cause the brain to expand and compress against the skull. Increases in intracranial pressure subsequently reduce CBF and cause mechanical damage that leads to cerebral herniation (Manley *et al.*, 2009).

Brain oedema is mediated by two distinct mechanisms, vasogenic or cytotoxic swelling. Vasogenic swelling is concerned with the movement of water and solutes across a leaky BBB, thereby increasing the water content of the extracellular fluid. On the other hand, cytotoxic swelling is due to water uptake into the cell from the extracellular fluid (Klatzo, 1967). The degree to which each mechanism contributes to swelling is highly dependent upon the time following the insult. In ischemic stroke, cytotoxic swelling appears to be more predominant in the early stages of cerebral oedema, and vasogenic swelling becomes more prominent in the later stages (Manley *et al.*, 2009). Indeed MACO models of stroke first cause cytoplasmic swelling, followed by BBB breakdown and subsequent Vasogenic swelling (Simard *et al.*, 2007).

Cytotoxic swelling is the result of osmotically active molecules moving into the cell from the extracellular fluid. In the CNS, the expression of the water membrane channel aquaporin-4 (AQP4) is restricted to astrocytes and the ependymal cells that line the cerebral ventricles (Nielsen *et al.*, 1997). These channels are densely expressed in astrocyte processes that contact blood vessels and allow for the bi-directional flow of water along its concentration gradient (Sofroniew and Vinters, 2010). Rodent genetic studies in which rats had the AQP4 gene knocked out showed reduced water permeability and

brain swelling following cerebral ischemia (Manley *et al.*, 2004). Ultrastructural imaging of gerbil astrocytes has demonstrated that astrocyte end-feet in contact with capillaries are the first cellular elements to swell following brain ischemia, indicating channels located in this area are important in initiating cytotoxic swelling (Dodson *et al.*, 1977). A net movement of water causes vasogenic swelling due to increased permeability of the BBB. Contributing mechanisms for the breakdown of BBB include the release of chemokines, cytokines and vascular growth factors from astrocytes, migrating leukocytes and microglia (Michinaga and Koyama, 2015). Reactive astrocytes secrete nitric oxide, TNF-α and MMPs that exacerbate brain oedema by upregulating the expression of AQP4 on astrocyte end-feet and increasing BBB permeability (Pekny and Nilsson, 2005). The latter significantly contributes to vasogenic swelling and appears to be aggravated by AQP4 channel knockout (Papadopoulos *et al.*, 2004).

1.1.3 Pericytes

Pericytes are perivascular mural cells located on the abluminal side of capillaries. Alongside neurons and astrocytes, they comprise the neurovascular unit. Here pericytes significantly contribute to the development and maintenance of the BBB (Sweeney, Ayyadurai and Zlokovic, 2016). Pericytes control the expression of endothelial tight (ZO-1 and claudin 5) and adherens (VE-cadherin) junction proteins, the alignment of tight junction proteins and paracellular transfer of vesicles across the BBB (Armulik *et al.*, 2010). Tight and adherens junctions maintain the integrity of the BBB by restricting the paracellular movement of large molecules (peptides and proteins), pathogens and cells into the brain. Pericytes communicate with astrocytes and neurons at the neurovascular unit (Sweeney, Ayyadurai and Zlokovic, 2016). It has been demonstrated that tight junctions form before astrocyte endfeet contact endothelial cells and pericytes (Bonkowski *et al.*, 2011), suggesting astrocytes are not essential for tight junction formation at the BBB. However, following the formation of endfeet connections by astrocytes, they can regulate tight junction integrity via Wnt and hedgehog signalling pathways (Correale and Villa, 2009). As seen in stroke, the degradation of the BBB by MMPs creates several problems. Namely the entry of otherwise peripherally restricted immune

cells, vasogenic swelling (oedema) and demyelination of neurons (Moretti *et al.*, 2015).

Cerebral Blood Flow (CBF)

During a stroke, the contraction of pericytes entraps erythrocytes at the capillaries, which reduces microcirculation (Yemisci *et al.*, 2009). Indeed *in vitro* studies have shown pericytes constrict in response to increased intracellular Ca^{++}, such a those seen with excitotoxicity (Kamouchi *et al.*, 2004). Another study demonstrated that necrosis of pericytes following ischemic injury in cerebral cortical slices produced a long-lasting constriction of the capillaries, which persists even when reperfusion is initiated (Hall *et al.*, 2014). In a rat model of cerebral ischemia, if the death of pericytes is prevented using the free radical scavenger, edaravone, infarct volume is reduced via the prevention of pericyte contraction and proliferation (Deguchi *et al.*, 2014). These results indicate that pericytes play a protective effect in ischemic-reperfusion injury. By promoting CBF, pericytes reduce the effects of ischemia and glycemia, suggesting treatments that protect pericytes would reduce damage caused by stroke.

Blood-brain barrier (BBB)

The BBB represents an interface between the CNS and systemic circulation. The BBB maintains CNS homeostasis by regulating the diffusion of substances between these two organs (Zlokovic, 2008). The breakdown of the BBB happens as a consequence of stroke, and biochemical markers that correlate with BBB breakdown also correlate with the severity of stroke (Argaw *et al.*, 2012a).

Current evidence suggests pericytes modulate BBB integrity and thus ischemic injury through vascular endothelial growth factor (VEGF) in ischemic stroke. Indeed VEGF is upregulated in the ischemic brain and has been found to induce BBB leakage (Lennmyr *et al.*, 1998; Zhang *et al.*, 2000). A substantial portion of VEGF production has been localised to astrocytes; in an elegant study showing if VEGF production is prevented in astrocytes, BBB breakdown is significantly reduced (Argaw *et al.*, 2012b). In contrast, some evidence suggests that prolonged exposure to VEGF enhances post-ischemic BBB integrity; however, this could be due to splice variants of VEGF protein (Zechariah *et al.*, 2013; Bowler and Oltean, 2019).

In addition, pericytes can affect the progression of ischemia through ROS production. One study demonstrated that pericytes are a primary source of NOX4. Its expression in pericytes is greatly enhanced following MCAO in rats, which induces the breakdown of the BBB by increasing MMP-9 production (Nishimura *et al.*, 2016).

1.2 Current treatments for cerebral ischemic injury

The most commonly used intervention for acute stage cerebral ischemic injury is tissue plasminogen activator (tPA). TPA belongs to the family of serine proteases and acts as a thrombolytic agent by catalysing plasminogen to its active form plasmin (Jilani and Siddiqui, 2021). Proteolytic activity of plasmin breaks down blood clots by cleaving peptide bonds on the carboxyl group in fibrins, thus breaking the clot into smaller pieces and recanalising the vessel (Chapin and Hajjar, 2015). Unfortunately, several prerequisites are required before a patient can receive tPA, and it is estimated that only 3-5% of stroke patients in the US meet the criteria to receive this treatment (Roth, 2011). The small number of patients who meet

the requirements for tPA is mainly the result of its limited time window for administration, recommended being three hours following the onset of stroke symptoms. In other patients who meet a distinct set of criteria, this is extended to 4.5 h (Jilani and Siddiqui, 2021).

Further hindering timely treatment is the need to establish the cause of the stroke. Treatment with tPA in haemorrhagic stroke cases will increase bleeding through the burst vessel, making any damage significantly worse. Whilst appropriate use of tPA reduces rates of disability by at least 30% based on recurring assessments in stroke survivors for three months; its use is greatly limited by the criteria mentioned earlier (Marler, 1995). The lack of any other option for treatment during and following stroke is of great concern in an ever-ageing population. Currently, no neuroprotective drugs are used to aid in post-stroke function recovery, highlighting the need for a new generation of stroke treatments.

1.3 Endocannabinoid system

The term endocannabinoid was coined in the mid-'90s and is now widely used to refer to the molecular components primarily responsible for controlling this lipid signalling system (Di Marzo *et al.*, 1994; Di Marzo and Fontana, 1995). The endocannabinoid system represents a complex signalling system consisting of endogenous ligands, receptors, enzymes responsible for synthesis and degradation, and transporters (Di Marzo, Bisogno and De Petrocellis, 2005). The existence and homology of this system are preserved throughout vertebrate evolution, with human CB_1 receptors sharing 98% homology with their rat counterparts (de Fonseca *et al.*, 2005; Elphick and Egertová, 2005). However, there are differences with regards to the distribution of the receptor throughout tissues between species. For example, the CB_1 receptor expression in the cerebellum is much lower than its rodent counterpart, highlighting the need for careful interpretation when extrapolating results from animal models (Herkenham *et al.*, 1991).

1.3.1 Receptors

Cannabinoid receptor 1 (CB_1)

CB_1 receptors are estimated to be one of the most abundantly expressed G protein-coupled receptors (GPCR) in the CNS (Kendall and Yudowski, 2017). They are highly expressed in the basal ganglia, cerebellum, frontal cortex, amygdala, and hippocampus (Herkenham *et al.*, 1990; Glass, Dragunow and Faull, 1997; Tsou *et al.*, 1998; Mackie, 2005). Studies assessing the distribution of CB_1 in the forebrain found greater expression in inhibitory synapses relative to excitatory ones, and their distribution is highly localised to presynaptic terminals and axons (Bodor *et al.*, 2005; Nyíri *et al.*, 2005; Katona *et al.*, 2006). CB_1 receptors are also found in several peripheral tissues, such as; adipose tissue, liver, pancreas, skeletal muscle and the gastrointestinal tract (Croci *et al.*, 1998; Cota *et al.*, 2003; Osei-Hyiaman *et al.*, 2005; Cavuoto *et al.*, 2007; Cota, 2007).

CB_1 is a member of the rhodopsin subfamily of GPCRs and was found to inhibit adenylyl cyclase through the involvement of $G_{i/o}$-coupled receptors (Howlett and Fleming, 1984; Howlett, Qualy and Khachatrian, 1986). Through $G_{i/o}$-coupled CB_1 receptors located on presynaptic neurons, activation reduces the release of neurotransmitters via retrograde signalling (Howlett, 2005). Because GABAergic neurons predominantly express CB_1 receptors, its activation predominantly modulates inhibitory signalling in the brain. A phenomenon referred to as depolarisation-induced suppression of inhibition (Wilson and Nicoll, 2001). Through $G_{i/o}$ proteins, CB_1 receptors can also modulate the activity of inward rectifying and A-type outward K^+ channels, D-type outward K^+ channels, as well as N-type and P/Q type calcium channels (Pertwee, 2006). The interactions with ion channels put the CB_1 receptor in an ideal position to control neuronal excitability.

More recently, the CB_1 receptor was shown to couple with G_s-coupled receptors, stimulating adenylate cyclase activity and increasing cyclic adenosine monophosphate (cAMP) (Glass and Felder, 1997; Glass and Northup, 1999). CB_1 receptors also display constitutive activity, demonstrated by the activity of the G-protein effector in the absence of

agonists and the attenuation of this activity in the presence of a CB_1 inverse agonist (Nie and Lewis, 2001; Kendall and Yudowski, 2017).

Cannabinoid receptor 2 (CB_2)

The CB_2 receptor shares a 44% protein identity with CB_1, but its distribution and pharmacology vary (Munro, Thomas and Abu-Shaar, 1993; Glass and Northup, 1999). Early studies localised the expression of CB_2 to only immune cells; however, more recently in microglia, neurons of the hippocampus and the gastrointestinal tract (Ameri, 1999; Ashton *et al.*, 2006; Gong *et al.*, 2006; Brusco *et al.*, 2008; Wright, Duncan and Sharkey, 2008). Contrasting roles have been found regarding the involvement of CB_2 in the inflammatory response; however, some of this can be explained by agonist bias at the receptor (Wotherspoon *et al.*, 2005; Stella, 2010). For example, endocannabinoids, 2-AG and Anandamide, have opposing effects on immune cell migration (Turcotte *et al.*, 2016).

CB_2 receptors are primarily coupled to $G_{i/o}$ effector proteins, where activation reduces cAMP and decreases protein kinase A (PKA) (Pertwee, 1997). CB_2 activation can also modulate K^+ and Ca^{++} channels (Figure 1.5) (Ho *et al.*, 1999; McAllister *et al.*, 1999; Atwood *et al.*, 2012). Some discrepancies exist in the literature regarding whether CB_2 receptors can modulate ion channels (Ibsen, Connor and Glass, 2017). CB_2 receptors expressed by immune cells modulate cytokine/chemokine release, representing one of the inflammatory aspects of the endocannabinoid system that could be targeted (Pertwee, 2006). CB_2 receptors outside of the immune system have been suggested to be involved in the modulation of synaptic plasticity and drug addiction; however, the exact mechanism by which CB_2 influences these is unclear (Xi *et al.*, 2011; Stempel *et al.*, 2016).

The well-distributed presence of cannabinoid receptors throughout the body allows this system to modulate many physiological functions, making it an appealing target for pharmacological interventions in multiple diseases.

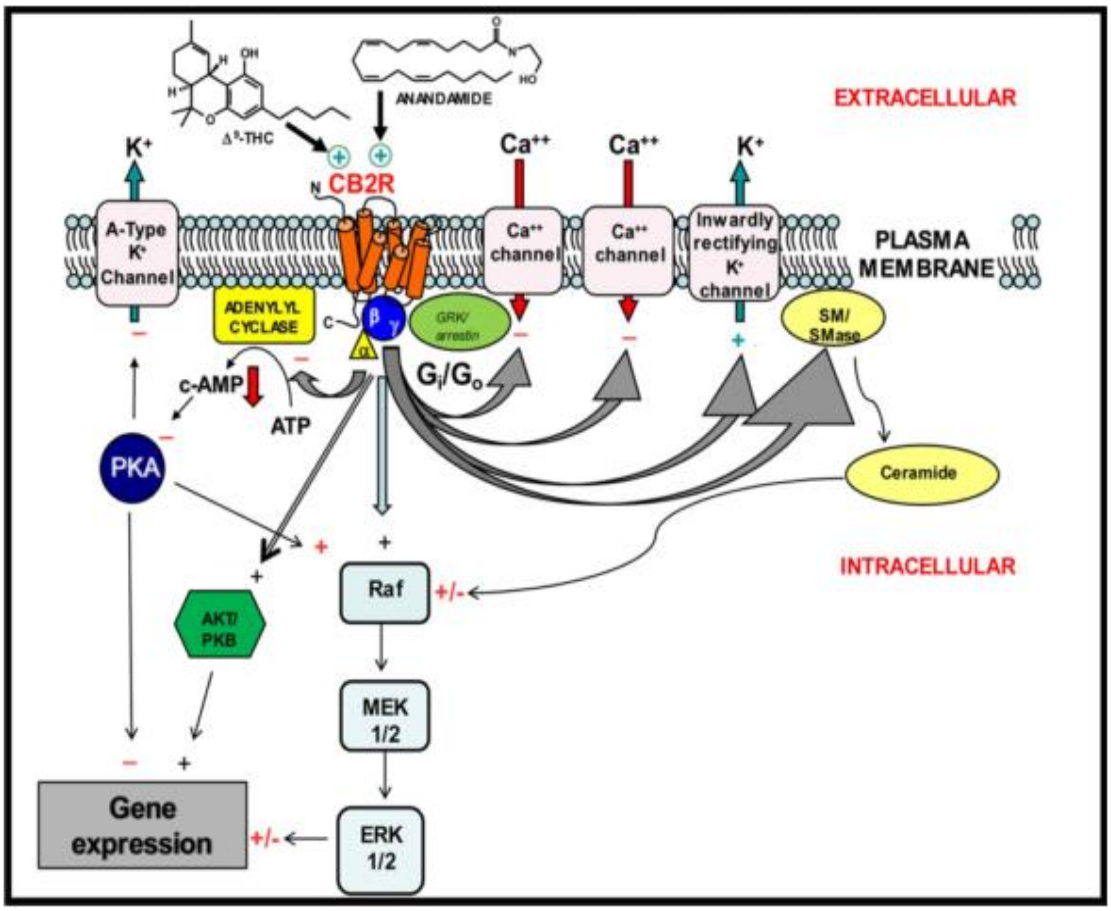


Figure 1.4 the numerous pathways activated or inhibited following CB_2 receptor activation by tetrahydrocannabinol or Anandamide. + = activation of a pathway in the presence of an agonist, - = Inhibition of a pathway following agonist activation, and +/- = A variable outcome following agonist binding. Reproduced from Dhopeshwarkar, A.' CB_2 Cannabinoid Receptors as a Therapeutic Target--What Does the Future Hold?' Molecular pharmacology 2014.

Non-classical and novel cannabinoid receptors

The term endocannabinoid receptors are generally restricted to the classical receptors CB_1 and CB_2. However, it is now recognised that endocannabinoids bind to other receptors outside of this system. For example, anandamide has an affinity for transient receptor potential vanilloid 1 (TRPV1), transient receptor potential melastatin 8 (TRPM8), transient receptor potential ankyrin 1 (TRPA1) and g protein-coupled receptor 55 (GPR55) in the low micromolar range (De Petrocellis and Di Marzo, 2010).

Transient receptor potential (TRP) channel

The transient receptor potential (TRP) superfamily encompasses a wide range of receptors such as; transient receptor potential vanilloid (TRPV), transient receptor potential melastatin (TRPM) and transient receptor potential ankyrin (TRPA) (Nilius and Owsianik, 2011). TRPV1 is a non-selective ligand-gated ion channel primarily expressed on C-type sensory afferent nerves, the dorsal root ganglion and to a lesser extent in the CNS (Du *et al.*, 2019). The predominance of TRPV1 in sensory nerve pathways highlights its importance in the transduction of sensory and noxious signals. Indeed, TRPV1 is most notably known for transducing the sensation of heat upon activation by capsaicin, the active ingredient in chilli powder (Brown and Iadarola, 2015). Other mechanisms also activate TRP channels, including heat above 42^{o}C or pH levels below 5.5 (Johnson and Greenwood-Van Meerveld, 2016). The first endogenous ligand identified for the TRPV1 was the endocannabinoid anandamide (Zygmunt *et al.*, 1999). Likewise, the channel also interacts with multiple phytocannabinoids (Muller *et al.*, 2020). Activation of this receptor leads to rapid desensitisation, meaning for some time, the receptor no longer responds to stimulation (Iannotti et al., 2014)

Other less studied TRP channels activated by cannabinoids are TRPM8 and TRPA1 channels. Like TRPV1, the first endogenous ligand found to bind to the TRPM8 receptor was anandamide (Petrocellis *et al.*, 2008). TRPM8 channels are expressed by primary afferent neurons and activate in response to temperatures below 27^{o}C and the 'cooling' agent menthol (McKemy, 2007). Finally, TRPA1 often co-localised with TRPV1 channels on sensory neurons and activates in response to noxious stimuli, temperatures below 17^{o}C, as well as the endocannabinoid anandamide (Vay, Gu and McNaughton, 2012; Muller, Morales and Reggio, 2018).

G-protein-coupled receptors (GPR)

GPR55 is a novel cannabinoid receptor that shares 14% homology with the CB_2 receptor and 13% homology with the CB_1 receptor (Elbegdorj, Westkaemper and Zhang, 2013). The GPR55 receptor is expressed in multiple human brain areas, such as the hypothalamus, striatum, putamen, nucleus accumbens and caudate nucleus (Sawzdargo *et al.*, 1999). There is also evidence that GPR55 is expressed by large-diameter dorsal root

ganglia neurons, which positively modulates sensory neurons' excitability (Lauckner *et al.*, 2008). GPR55 couples to G_{α} 11-13 and G_{q} proteins and was thought initially to be the receptor responsible for the vasodilator properties of cannabinoids (Johns *et al.*, 2007; Ross, 2009). Whether traditional endocannabinoids activate GPR55 is a controversial matter; however, the receptor does unequivocally respond to tetrahydrocannabinol (THC), rimonabant and CP55-940 (Rempel *et al.*, 2013)

G protein-coupled receptor 18 (GPR18) is another novel cannabinoid receptor; it shares 21% homology with GPR55, 13% with CB_1 and 8% with CB_2 (Lauckner *et al.*, 2008; Morales *et al.*, 2020). The highest levels of GPR18 expression are found within the cerebellum, testes and spleen; however, lower expression levels are also found in white blood cells, thymus and small intestine (Alexander, 2012; Morales *et al.*, 2020). This receptor couples to $G_{\alpha i/o}$, $G_{\alpha q}$/11 and $G_{\alpha s}$ proteins (Kohno *et al.*, 2006; Takenouchi *et al.*, 2012; L *et al.*, 2014), and has been shown to activate in response to the endogenous anandamide (AEA) metabolite N-arachidonoylglycine (NAGly) and resolvin D2 (Kohno *et al.*, 2006; N *et al.*, 2015). Indicating that GPR18 may have a significant role in the resolution of inflammation. The pro-resolving effects of GPR18 activation have been demonstrated in a rat periodontitis model where resolvin D2 reduced inflammation, as well as upregulating GPR18 expression (Siddiqui *et al.*, 2019)

Peroxisome proliferator-activated receptor (PPAR)

Three isoforms of the peroxisome proliferator-activated receptor (PPAR) exist; PPARα, PPARγ, PPARδ, which are all expressed in the adult human brain (Auwerx *et al.*, 1999; Warden *et al.*, 2016). PPARs regulate gene expression by binding peroxisome-proliferator response elements (PPREs) within the promoter regions of genes (Corbett, Gonzalez and Pahan, 2015). Because these receptors reside in the nucleus of the cell, lipid ligands require chaperones, such as fatty acid-binding protein (FABP) and fatty acid transport protein (FATP), to carry the ligand to the receptor (Martin *et al.*, 1997; Armstrong *et al.*, 2014)

PPARα is predominantly expressed by highly metabolically active tissues, such as muscle and heart (Stienstra *et al.*, 2007). PPARα regulates fatty acid uptake and metabolism, mitochondrial metabolism, glucose

metabolism, and glutamatergic, cholinergic, and dopaminergic signalling (Wójtowicz *et al.*, 2020). Interestingly PPARα is involved in the degradation of Aβ plaques associated with various neurodegenerative disorders (Luo *et al.*, 2020).

PPARγ exists in three versions; PPARγ1 is expressed by almost all cells, whereas PPARγ2 is primarily found in adipose tissue, and PPARγ3 in immune cells (Feige *et al.*, 2006). The proteins transcribed by PPARγ1 and PPARγ3 are identical; however, PPARγ2 contains an extra NH2-terminal composed of 30 amino acids (Janani and Ranjitha Kumari, 2015). Both forms of PPARγ1 and PPARγ2 are required to develop adipose tissue and modulate insulin sensitivity (Janani and Ranjitha Kumari, 2015). This well-defined role of PPARy in modulating adipogenesis could represent an important target for the treatment of diabetes and obesity (Corrales, Vidal-Puig and Medina-Gómez, 2018). The endocannabinoids anandamide and 2-arachidonoylgycerol (2-AG) have been shown to possess activity at this receptor, representing a strategy for manipulating this system (O'Sullivan, 2016).

1.3.2 Ligands and enzymes

Upon discovering the cannabinoid receptors, it was hypothesised that where receptors exist, so should endogenous ligands. This theory led to the discovery of two small lipid molecules, AEA and 2-AG (Devane *et al.*, 1992; Mechoulam *et al.*, 1995; Sugiura and Waku, 2000).

These endogenous signalling molecules are derived from membrane-bound phospholipids that contain arachidonic acid (AA)—being rapidly produced on demand by increases in intracellular Ca^{++} or the activation of GPCRs (Di Marzo, Bisogno and De Petrocellis, 2005).

2-Arachidonoylglycerol (2-AG)

2-AG was first was isolated from rat brains by Sugiura and colleagues in 1995 (Sugiura *et al.*, 1995). 2-AG is synthesised by two isoforms of diacylglycerol lipase (DAGLα and DAGLβ) that hydrolyse arachidonoyl-containing diacylglycerols (DAGs) (Bisogno *et al.*, 2003). DAGLs are mainly localised to post-synaptic neurons, allowing 2-AG to partake in retrograde neuronal signalling (Bisogno *et al.*, 2003). In the production of 2-AG, the

inositol triphosphate is first removed from arachidonoyl-containing phosphatidylinositol bisphosphate (PIP2), then the acyl group by either isoform of DAG lipase. The metabolism of 2-AG is primarily carried out by Monoacylglycerol lipase (MAGL), which breaks 2-AG into AA and glycerol (Deutsch and Chin, 1993). Of the two classic cannabinoid receptors, 2-AG displays a greater affinity for CB_2, but unlike AEA, behaves as a full agonist at CB_1 (Hillard, 2000).

2-AG also modulates receptors outside of CB_1 and CB_2, such as adenosine A_3, GPR55, PPARγ and TRPV1 (Bouaboula *et al.*, 2005; Ryberg *et al.*, 2007; Lane *et al.*, 2010). 2-AG acts as a negative allosteric modulator of the human adenosine A_3 receptor, which modulates inflammatory responses mediated by adenosine signalling (Kurabayashi *et al.*, 2005). Through activation of PPARγ 2-AG reduces the expression of interleukin 2 (IL-2) in splenocytes (Rockwell *et al.*, 2006). 2-AG has also been shown to act as an agonist at the TRPV1 receptor, indicating a potential role in mediating noxious stimuli and inflammatory pain responses (McVey *et al.*, 2003)

1.3.3 The endocannabinoid system and stroke

Various studies have implicated the endocannabinoid system in regulating responses to stroke. For example, endocannabinoid levels are raised in ischemic tissue, and CB_1 and CB_2 are upregulated following ischemia-reperfusion injury (Hillard, 2008; Greco *et al.*, 2020). Activation of CB_1 receptors regulates post-synaptic neurotransmitter release and reduces excitotoxicity caused by spreading depolarisations (Zoppi *et al.*, 2011). Outside of presynaptic modulation of glutamate release, neuronal CB_1 activation may increase glutamate glial uptake through regulation of PPARγ activity in astrocytes (Zoppi *et al.*, 2011). Indeed, the EAAT-2 is a target gene of PPARγ activation and proves protective in models of ischemic reperfusion injury (Romera *et al.*, 2007)

Genetic studies using knockout mice have also implicated CB_1 in providing protective effects following an ischemic insult, with knock out animals showing larger infarcts, reduced CBF and increased excitotoxicity (Parmentier-Batteur *et al.*, 2002). Surprisingly a similar study using CB_1 and CB_2 knockout mice showed the deletion of both receptors was neuroprotective (Ward *et al.*, 2018).

On the other hand, CB_2's activation minimises the production of pro-inflammatory signals, immune cell recruitment, disruption to BBB permeability, subsequently reducing infarct volume (Zhang *et al.*, 2007; Ramirez *et al.*, 2012). Pazos' and colleagues showed in piglet models of neonatal hypoxia, CB_2 activation was associated with the protective effects of cannabidiol (CBD) (Pazos *et al.*, 2013).

In contrast, a study using longer follow up times, as most animal studies only monitor animals for short periods (<7days) (Casals *et al.*, 2011). Rivers-Auty and colleagues showed that when outcomes were followed for 15-days, CB_2 activation by GW405833 had no significant effect on cognitive ability, demonstrated using a morris water maze (Rivers-Auty, Smith and Ashton, 2014). Highlighting the need for longer follow up times to increase the translational value of animal studies.

The exact role of endocannabinoids following a stroke is unclear; in an observational study of 23 stroke patients aged 60-81 years old, elevated 2-AG levels 12 h following stroke correlated with smaller infarct volumes,

however at 24 h, increased 2-AG levels were associated with larger infarcts (Buciuc, Conte and Scharf, 2021). Suggesting a dual role for 2-AG depending on the time relative to the insult. Another study assessing the effects of 2-AG 4 h following rat pMCAO in rats showed 6 mg/kg significantly further reduced CBF associated with pMCAO (Shearer, Coker and Carswell, 2018). Increases in CBF could be beneficial in the initial stage of stroke; however, increases in blood flow during reperfusion may exacerbate tissue damage by increasing ROS production.

TRPV1 has been demonstrated to be protective following ischemic reperfusion injury by inducing a state of mild hypothermia. In a mouse model of ischemic-reperfusion injury TRPV agonism, Cao and colleagues showed that dihydrocapsaicin (1.25mg/kg) reduced body temperature to 32.8 ± 0.5°C and subsequently reduced infarct volume (Cao, Balasubramanian and Marrelli, 2014). Additionally, this effect was not present in TRPV1 knockout mice. Other studies have demonstrated CB_1 agonists possess a similar effect, and hypothermia mediated reductions in infarct volume were ablated when the animal was warmed (Hayakawa *et al.*, 2004).

The GPR55 receptor has received less attention in the setting of ischemic reperfusion injury. However, one study demonstrated GPR55 activation reduced the activity of AMPA receptors, which may have implications in reducing excitotoxicity (Whalley *et al.*, 2018). The extent to which a reduction in AMPA activity could provide protection is debatable. The AMPA receptor contributes considerably less to excitotoxicity than other glutamatergic pathways, such as reversal of glutamate transporters (Veldhuis *et al.*, 2003).

FABP3, 5 and 7 expression has been shown to increase in mice and monkeys exposed to ischemic episodes (Guo *et al.*, 2021). In monkeys, this expression peaks 15 days following the insult (Boneva *et al.*, 2010). As previously mentioned, levels of 2-AG and AEA are increased in the ischemic brain (Naccarato *et al.*, 2010; Buciuc, Conte and Scharf, 2021), all of which possess an affinity for FABPs (Haj-Dahmane *et al.*, 2018). FABPs act to chaperone lipid-like signalling molecules through the intracellular space to the nucleus, where they can interact with PPARs that regulate the transcriptional activity of genes (Yu *et al.*, 2014). Interestingly FABP inhibition is protective following MCAO in mice, but counterintuitively PPARy activation is neuroprotective also (Hind, England and O'Sullivan, 2016; Guo

et al., 2021). However, inhibition of FABP reduces the ability of cells to shuttle lipid-like ligands to the nucleus, meaning extracellular receptors are exposed to endogenous or exogenous ligands for longer, thus creating a greater net benefit or deficit depending on the nature of the ligand.

These changes in the endocannabinoid system following ischemic reperfusion injury indicate therapeutic strategies targeting this system may provide a method to treat stroke.

Anandamide (AEA)

AEA was first isolated from pig brains in 1992 by Devane and colleagues (Devane *et al.*, 1992). It is formed from the precursor *N*-arachidonoyl-phosphatidylethanolamine (NAPE), which is itself derived from AA. NAPE is then cleaved into AEA and by phospholipase D (NAPE–PLD, where it immediately leaves the cell as a chemical messenger (Di Marzo *et al.*, 1994; Okamoto *et al.*, 2004). After the release, AEA rapidly diffuses into the cell and is chaperoned by fatty acid-binding protein (FABP) 5/7 across the intracellular space to metabolic enzymes (Fowler, 2012). AEA is then primarily hydrolysed by fatty-acid amide hydrolase (FAAH) into ethanolamine and arachidonic acid, which feed directly into the production of prostaglandins via the cyclooxygenase (COX) enzymes (Wang and Ueda, 2009; Nomura *et al.*, 2011). AEA is an agonist at both the CB_1 and CB_2 receptors but displays a higher affinity for CB_1 (Sido, Nagarkatti and Nagarkatti, 2015). AEA also acts as an agonist at TRPV1, PPARα and PPARγ (Ross, 2003; Bouaboula *et al.*, 2005; Romano and Lograno, 2012).

1.4 Phytocannabinoids

The use of cannabis for its therapeutic properties is not a new phenomenon, and archaeological evidence suggests it may have been used for these purposes as far back as 10,000 years ago (Okazaki *et al.*, 2011). Cannabinol (CBN) was the first phytocannabinoid successfully isolated in 1896 by Wood and colleagues (Wood, Spivey and Easterfield, 1896). It is an oxidation product produced naturally over time from the natural degradation of THC via heat and UV light, and its discovery led to the isolation of 120 structurally unique phytocannabinoids (Burstein, 2015). Delta-9-THCA and cannabidiolic acid (CBDA) are the most abundant phytocannabinoids in

Cannabis Sativa, while CBCA is predominantly found in young plants (De Meijer, Hammond and Micheler, 2009; Schurman *et al.*, 2019). All phytocannabinoids are formed from cannabigerolic acid (CBGA), which itself is produced from geranyl diphosphate (GPP) and olivtolic Acid in a reaction catalysed by the enzyme olivtolic geranyl transferase. CBGA's fate is then determined by the presence of corresponding oxide cyclase enzymes, tetrahydrocannabinolic acid (THCA) synthase for the production of THCA, and CBDA synthase for CBDA. These acidic versions are relatively unstable and naturally decarboxylate into neutral forms, e.g. THC, CBD, cannabichromene (CBC) (Gülck and Møller, 2020). Additional propyl variants also exist, that are produced from a divarinolic acid precursor of CBGA. These phytocannabinoids carry a c3 side chain rather than a c5 and are denoted as THCAV, CBDAV etc. Likewise, these propyl variants also degrade into their corresponding neutral forms via removal of acidic group (Gülck and Møller, 2020). Slight differences in molecular structure produce significant changes in pharmacology, emphasising the need to explore the properties of each phytocannabinoid.

1.4.1 Cannabidiol (CBD)

Alongside THC, CBD (Figure 1.6) is the most well-researched phytocannabinoid. Its effects are explored in many cellular and animal models, such as; stroke, cancer, irritable bowel syndrome (IBS), pain and several neurological conditions (Britch, Babalonis and Walsh, 2021). Despite the plethora of pre-clinical research, few controlled clinical trials have taken place outside of epilepsy. CBD was licensed in 2010 to treat rare forms of childhood-onset epilepsy (Dravet and Lennox-Gastat syndrome) in the form of sublingually consumed oil (Franco and Perucca, 2019). CBD displays somewhat promiscuous pharmacology and modulates over 65 known molecular targets (Ibeas Bih *et al.*, 2015) (Table 1.0). CBD exhibits no agonistic activity at CB_1 receptors and consequently lacks the psychoactive effects seen with THC consumption (Pertwee, 2008). Despite its lack of psychoactivity, CBD has been suggested to indirectly activate the CB_1 receptor through inhibition of AEA metabolism by FAAH (Watanabe *et al.*, 1996).

Further complicating the net effect of CBD at the CB_1 receptor is its activity as a negative allosteric modulator at the receptor (Laprairie *et al.*, 2015).

Indeed studies have shown CBD can reduce the psychotomimetic and memory impairments associated with THC consumption (Morgan *et al.*, 2018). However, in this study, the effect was only present in low-frequency users, and CBD had no effect in reducing the psychotomimetic effects of THC in heavy cannabis users. Relative to the CB_1 receptor, CBD possesses a greater affinity for CB_2, albeit a low enough affinity to be considered a low-affinity agonist and, given the constitutive activity of the CB_2 receptors, an inverse agonist (Pertwee, 2008; Mancini *et al.*, 2009; McPartland *et al.*, 2015).

Outside of the classic endocannabinoid receptors, CBD acts as an agonist at 5-HT_{1A}, $PPAR_{\gamma}$ and TRPV1 receptors, all of which have been implicated in many cellular models (Peres *et al.*, 2018). In contrast to its agonistic activity, CBD acts as an antagonist at GPR55, GPR18, $5HT3_A$

1.4.2 Cannabidiolic acid (CBDA)

CBDA (figure 1.6) is the acidic precursor to CBD and is less well explored than its neutral counterpart. Like CBD, CBDA also displays anti-inflammatory action through COX-2 and prostaglandin production inhibition (Takeda *et al.*, 2014). Further evidence of its anti-inflammatory effects comes from studies showing interactions with PPARγ. In this study, CBDA possessed 1.5 times more affinity for the PPARγ in transfected cells than CBD (Nadal *et al.*, 2017). CBDA also activates TRPV1 and TRPA1 and behaves as an antagonist at TRPM8, albeit less potently than CBD (Petrocellis *et al.*, 2008).

CBDA appears to reduce vomiting behaviour in rats in response to conditioned gaping effects more potently than CBD, through 5HT1A activation (Bolognini *et al.*, 2013).

1.4.3 Cannabidivarin (CBDV)

For most phytocannabinoids a propyl analogue exists. In the case of CBD, this is cannabidivarin (CBDV) (Figure 1.6). CBDV has no psychotropic effects, making it an attractive candidate for drug development (Izzo *et al.*, 2009). CBDV possesses a weak affinity at CB_1 and CB_2 receptors but has a higher affinity for molecular targets outside of the traditional endocannabinoid system (ECS) (Morales, Reggio and Jagerovic, 2017). The

anti-convulsive effects of CBDV have been associated with the activation of TRPV1 channels as this effect is abolished by co-application of CBDV and the TRPV1 antagonist capsazepine in the cellular model of epilepsy (Iannotti *et al.*, 2014). CBDV also significantly inhibits the orphan endogenous GPR55 receptor activation in the micromolar range (Anavi-Goffer *et al.*, 2012). More recent work has also demonstrated the efficacy of CBDV in a mouse model of colitis and ulcerative colitis tissue explants; these effects were mediated by the TRPA1 receptors (Pagano *et al.*, 2019). Other work in a multi-cellular model of ischemic reperfusion injury of the BBB and reductions in cellular damage was partially mediated by GPR55 (Stone, England and O'Sullivan, 2021).

1.4.4 Cannabigerol (CBGV)

Another minor phytocannabinoid lacking the psychotropic effects of THC is cannabigerolvarin (CBGV) (Figure 1.6) (Morales, Reggio and Jagerovic, 2017). There is currently no data on the effects of CBGV in cellular or animal disease models; however, some data exist for its activity at several TRP receptors. CBGV behaves as an agonist at TRPA1, transient receptor potential vanilloid 3 (TRPV3), TRPV1, and transient receptor potential vanilloid 2 (TRPV2) receptors (De Petrocellis *et al.*, 2011).

1.4.5 Cannabichromene (CBC)

Cannabichromene (CBC) (Figure 1.6) is a minor component of the Cannabis plant, which behaves as a partial agonist at CB_1 and CB_2 receptors (Zagzoog *et al.*, 2020). Like other phytocannabinoids, CBC possesses an affinity for TRP receptors. De Petrocellis and colleagues showed that of the aforementioned phytocannabinoids, CBC is the most potent agonist of the TRPA1 channels (De Petrocellis *et al.*, 2011). CBC also activates TRPV3 and transient receptor potential vanilloid 4 (TRPV4) channels with a lower potency relative to TRPA1 and inhibits TRPM8 receptors (De Petrocellis *et al.*, 2011). CBCs relatively high potency at TRPA1 has been shown to mediate its reductions in inflammation and hypermobility in a mouse model of gut inflammation (Izzo *et al.*, 2012).

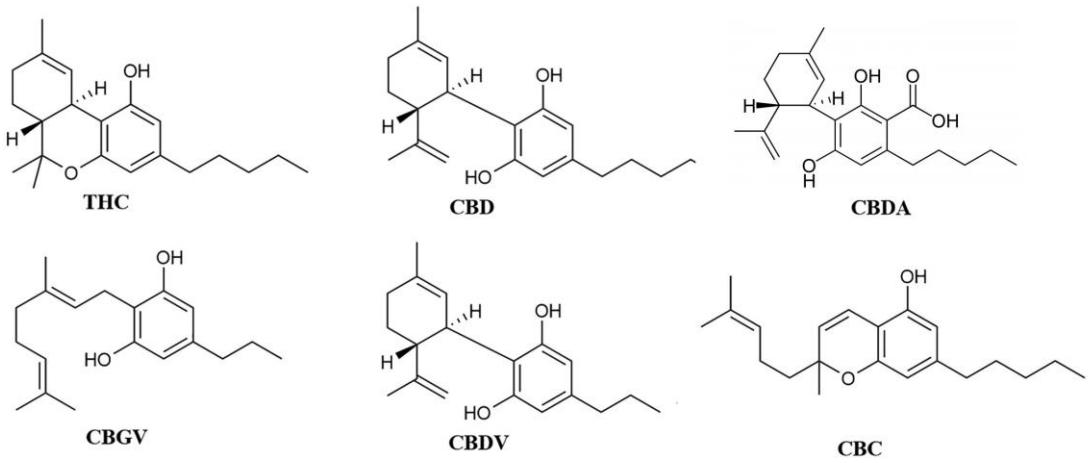


Figure 1.5 The molecular structure of various phytocannabinoids used throughout this thesis and Δ-9-THC for comparison.

Compound	Functionality	Target
CBC	Agonist (weak)	CB_1
CBC	Agonist (weak)	CB_2
CBC	Agonist	TRPA1
CBC	Antagonist	TRPM8
CBC	Agonist	TRPV3
CBC	Agonist	TRPV4
CBD	Agonist	5HT1A
CBD	Partial agonist	5HT2A
CBD	Antagonist	5HT3A
CBD	Agonist	A1A
CBD	Antagonist (weak)	CB_1
CBD	NAM	CB_1
CBD	Antagonist (weak)	CB_2
CBD	PAM	GABAa
CBD	PAM	GlyRa1
CBD	PAM	GlyRa3
CBD	Antagonist	GPR18
CBD	Antagonist	GPR55
CBD	Agonist	PPARγ
CBD	Agonist	TRPA1
CBD	Agonist	TRPV1
CBD	Agonist	TRPV2
CBD	Agonist	TRPV3
CBD	Allosteric	δ-OPR
CBD	Allosteric	μ-OPR
CBDV	Agonist	TRPA1
CBDV	Agonist	TRPV1
CBDV	Agonist	TRPV2
CBDV	Agonist	TRPV3
CBGV	Agonist	TRPV4
CBGV	Agonist	TRPA1
CBGV	Agonist	TRPV3
CBGV	Agonist	TRPV1
CBGV	Agonist	TRPV2

Table 1 List of phytocannabinoids and their activity at various receptors. Data of activity at receptors was adapted from (De Petrocellis et al., 2011; Morales, Hurst and Reggio, 2017). NAM = Negative allosteric modulator, PAM = Positive allosteric modulator, OPR = opioid receptors.

1.5 Phytocannabinoids and stroke

Various evidence suggests CBD may prove beneficial in stroke, suggesting that other phytocannabinoids may behave the same. CBD has been shown to modulate intracellular Ca^{++} by modulating the mitochondrial Na^{+}-Ca^{++}

exchanger (NCX). Interestingly, CBD raises intracellular Ca^{++} in homeostatic conditions; however, during high excitability conditions, CBD reduces intracellular Ca^{++}. Appropriately modulating intracellular Ca^{++} could provide protection against several molecular events associated with stroke, i.e. opening of the permeability transition pore, increases in Ca^{++} mediated by glutamate uptake, and activation of Ca^{++} dependent inflammatory pathways (Ryan, Alison J Drysdale, *et al.*, 2009; Furman and Norris, 2014; O'Donnell, Jackson and Robinson, 2016).

Another group investigated how CBD interacts with mitochondria in an oxygen-glucose deprivation/reperfusion (OGD/R) model using hippocampal neurons. In this study, OGD/R caused a significant decline in basal mitochondrial respiration, ATP linked oxygen consumption rate, maximum respiration and spare respiratory capacity. CBD attenuated these changes and increased the activity of the pentose-phosphate pathway, a branch of glycolysis associated with enhancing antioxidant defences. Using the same endpoints, the authors of this study examined the effects of CBD in a normoxic setting. In this setting, CBD significantly increases basal mitochondrial respiration, ATP linked oxygen consumption rate, maximum respiration and spare respiratory capacity. However, the pentose-phosphate pathway remained unchanged (Sun *et al.*, 2017). From this work, it is clear CBD partially mediates its neuroprotective effects through interactions with mitochondria, raising the possibility that other phytocannabinoids could behave the same.

CBD has also been shown to modulate BBB permeability; in these experiments, the addition of CBD to a co-culture of astrocytes and brain endothelial cells increased the permeability of the BBB, as measured by transepithelial resistance. However, where an OGD protocol has increased BBB permeability, CBD was able to attenuate these increases. This possibly indicates that the endocannabinoid system is altered during an OGD insult, which affects the responses transduced by receptors. Interestingly the ascribed effects were attributed to receptors outside the classic endocannabinoid system, mainly 5-HT1a and PPAR- γ (Hind, England and O'Sullivan, 2016).

Other phytocannabinoids are less well explored in the setting of cerebral ischemic reperfusion injury. However, some pre-clinical research using

cellular models of stroke has shown CBDV and cannabigerol (CBG) can reduce IL-6 secretion and lactate dehydrogenase (LDH) levels following an OGD protocol. CBDV could also reduce levels of VEGF, while CBG could lessen the intensity of DNA damage (Stone, England and O'Sullivan, 2021). In the same study, the effect of CBDV was shown to be partially mediated by GPR55 and GPR18.

One factor preventing the successful development of phytocannabinoid medications is their undesirable pharmacokinetic profiles (Millar *et al.*, 2018). The lipophilic nature of phytocannabinoids places them in class II of the Biopharmaceutical Classification System (BCS) of drugs (Franco *et al.*, 2020). Meaning the drug is highly permeable at membranes but possesses low aqueous solubility, giving them poor characteristics for absorption. However, strategies to overcome this hurdle are becoming more investigated (Millar *et al.*, 2020).

1.6 Pharmacodynamics and kinetics

Phytocannabinoids generally possess characteristics undesirable for drug delivery in oral form, namely, low aqueous solubility. High logP values (low aqueous solubility) predict a drug will precipitate in the gastrointestinal environment, creating an elimination rate faster than absorption (Chan and Stewart, 1996). (Table 2.0). This ultimately leads to reduced efficacy and high inter-individual variability in pharmacokinetics (Chan and Stewart, 1996; Hellriegel, Bjornsson and Hauck, 1996). In this context, the bioavailability of phytocannabinoids varies by route and mode of administration (Huestis, 2007; Martin *et al.*, 2018). To assess these parameter measurement such as peak plasma concentration (Cmax) and time till peak concentration are used (Tmax) by temporally sampling blood.

Phytocannabinoid	logP
CBDA	7.9
CBGV	6.4
CBC	6.0
Δ9-THC	5.6
CBD	5.4
CBDV	4.6

Table 2 Logp values of phytocannabinoids generated by QikProp 3.5 integrated in Maestro (Schrödinger, LLC, New York, USA).

Most consumed forms of CBD are supplied in an oil or alcoholic solution, either soft-gel capsules, liquid solutions, sublingual drops, or an oromucosal spray (Thomas, Compton and Martin, 1990). Delivery of oral and oromucosal CBD and THC at equal ratios in humans show high inter/intrasubject variability (Guy and Robson, 2003a). Upon oral consumption in a soft-gel capsule, the bioavailability of CBD is estimated at 6%; however, limited data in this area prevents any meaningful conclusion from a population-based perspective (Millar *et al.*, 2018). CBD delivered in an oil solution or spray is the most common form of delivery for current cannabinoid-based medications. Epidiolex® is delivered orally in an oil solution, and Sativex is an oromucosal spray. The oromucosal route circumvents some of the problems associated with the oral route and produces lower T_{max} values. However, Itin and colleagues suggest that a substantial proportion of oromucosally delivered doses may ultimately be absorbed by the gastrointestinal (GI) tract (Itin, Domb and Hoffman, 2019). The authors of this study noted that the pharmacokinetics (PK) of Sativex was different when administered in a fasting state relative to a fed state. However, pharmacokinetic profiles should only be influenced in a fed-state when consumed orally.

Furthermore, in work published by Guy and colleagues, the PK parameters of Sativex were similar between oromucosal and oral routes of administration (Guy and Robson, 2003b). These observations are in agreement with further work by Itin and colleagues, demonstrating that the lipophilic nature of CBD causes it to accumulate in the oral mucosal lining or enter the GI tract upon swallowing (Itin *et al.*, 2020). However, the authors suggest this route of administration remains viable, so long as exposure

times to the oral mucosal lining are adequate and a method of preventing washout of the drug by saliva is present.

Methods to increase oral bioavailability include administering CBD alongside a high-fat/high-calorie meal (Itin, Domb and Hoffman, 2019). Studies have demonstrated that CBD and THC delivered in an oromucosal spray or CBD delivered in oral capsules produces a four-fold increase in bioavailability relative to the fasted state (Birnbaum *et al.*, 2019). Adult patients with refractory epilepsy have four- to fourteen-fold increases in area under the curve (AUC) and Cmax, respectively, in the fed state, compared to fasted (Stott *et al.*, 2013). Perhaps a consequence of increased micelle and chylomicron formation making more drugs available for lymphatic transport or increasing the dissolution rate of the drug in the GI tract (Porter, Trevaskis and Charman, 2007; Zgair *et al.*, 2016). High-fat meals also inhibit drug efflux transporters' activity on the apical membranes of enterocytes (Ingels *et al.*, 2004). This inhibition stimulates the release of biliary secretion, which further inhibits efflux transporter activity and increases the dissolution of lipophilic drugs (Wu and Benet, 2005).

Although lymphatic transport bypasses the liver into the systemic circulation, evidence suggests CBD delivered orally is still subject to first-pass metabolism. One study showed that the AUC of 7-hydroxy-cannabidiol (7-OH-CBD) is about 40% the level of orally delivered CBD; however, participants were also receiving concomitant treatment with epileptic drugs Clobazam, Valproate, or Stripentol (Morrison *et al.*, 2019). In human subjects with severely impaired hepatic metabolism, the Cmax of CBD was increased over 2.5-fold relative to subjects with unimpaired hepatic function (Taylor *et al.*, 2019). Therefore even with increased absorption of CBD, first-pass metabolism ultimately presents another barrier in increasing bioavailability. Further complicating the pharmacokinetics of CBD is the ability to inhibit the cytochrome liver enzymes responsible for its metabolism (Stout and Cimino, 2014)

Pharmacokinetic data for other phytocannabinoids in humans are limited. One study has investigated the effects of several acidic phytocannabinoids in mice (Anderson, Low, *et al.*, 2019). This study concluded that 5mg/kg of cannabidivarinic acid (CBDVA), cannabigerovarinic acid (CBGVA) and

CBDA produced peak brain concentrations of 0.8 µg/g, 3.8 µg/g, and 2 µg/g, respectively (Table 3.0). In contrast, another study assessing neutral forms of phytocannabinoids in rats showed the peak brain concentration of CBDV and CBD to be 3.57 µg/g and 6.9 µg/g, respectively (table 3.0) (Deiana *et al.*, 2012). Careful consideration should be used when comparing these values across studies, as different vehicle were used. When authors used a ttween-80 to assess acidic phytocannabinoids, this resulted in different pharmacokinetic profiles relative to an ethanol based vehicle. These results indicate that the vehicle used to transport cannabinoids into the body needs to be optimised for effective absorption.

Phyto	Species	RoA	Dose (mg/kg)	C_{max} (µg/g)	T_{max} (min)	Total dose (mg)	% of total dose in brain
CBCA	C57BL/6J mice	ip	5	BDL	N/A	0.175	N/A
CBDA	C57BL/6J mice	ip	5	2	45	0.175	0.457
CBDVA	C57BL/6J mice	ip	5	0.8	30	0.175	0.183
CBGA	C57BL/6J mice	ip	5	2.3	30	0.175	0.526
CBGVA	C57BL/6J mice	ip	5	3.8	90	0.175	0.869
THCA	C57BL/6J mice	ip	5	BDL	N/A	0.175	N/A
CBD	Wistar rats	ip	120	6.9	60	27	0.051
CBDV	Wistar rats	ip	60	3.57	30	13.5	0.053
CBG	Wistar rats	ip	120	3.48	120	27	0.026
THCV	Wistar rats	ip	30	1.69	30	6.75	0.050
CBD	Wistar rats	po	120	1.3	360	27	0.010
CBDV	Wistar rats	po	60	0.94	60	13.5	0.014
CBG	Wistar rats	po	120	0.42	60	27	0.003
THCV	Wistar rats	po	30	0.43	30	6.75	0.013

Table 3 Pharmacokinetic data from two separate studies assessing brain content of phytocannabinoids in mice and rats after receiving ip or po doses of phytocannabinoids (Deiana et al., 2011; Anderson, Low, et al., 2019). Cmax expressed as a percentage of the total dose was calculated as dose * average body weight = total dose administered. C_{max} * average brain weight = amount of drug in the brain. (amount of drug in brain/total dose administered)*100 = % of total dose in brain. RoA = route of administration, C_{max} = maximum concentration measured, T_{max} = Time until maximum concentration was measured, Ip = intraperitoneal, po = oral administration, BDL = below detectable limit, N/A = not available.

1.7 Improving bioavailability of Phytocannabinoids

Simple techniques to increase the bioavailability of phytocannabinoids are through smoking or vaporisation. The bioavailability in five individuals after smoking 20 mg of [^{2}H]-CBD was reported at 31 ± 13% of the total dose

(Ohlsson *et al.*, 1986). However, methods such as smoking are regarded as crude and do not represent clinically viable delivery strategies.

Preferably, strategies to overcome the inherent poor bioavailability of CBD would be consumed orally, and several viable strategies exist to do so. The use of surfactants at critical micelle concentrations enables the formation of micelles, which can promote the passage of lipophilic drugs through lymphatic absorption (Han *et al.*, 2016). The formation of micelles requires relatively large amounts of surfactant to be added to the oil formulation or a critical temperature to be reached (Krafft temperature) (Rana *et al.*, 2017). This also increases absorption by increasing the dissolution rate of the drug, increasing the available drug for absorption across the small intestine (Hörter and Dressman, 2001; Tang, Khan and Muhammad, 2001). However, the use of surfactants is limited by their safety profile, and high concentrations can irritate the gastrointestinal tract (Csáki, 2011). Naturally occurring surfactants generally possess better safety profiles but have limited emulsifying properties (Gupta, Kesarla and Omri, 2013).

Another method to increase the bioavailability of drugs with poor aqueous solubility is through co-crystallisation. Co-crystals contain two or more molecules that create a compound with superior absorption properties than its constituents. The active pharmaceutical ingredient is bound to the co-former by non-covalent interactions such as; hydrogen bonds, halogen bonding, and van der Waals forces (Lara-Ochoa and Espinosa-Pérez, 2007). The co-former is usually a pharmacological inert molecule such as saccharin. Alternatively, the co-former can possess a complementary pharmacological profile to the active pharmaceutical ingredient.

For example, a co-crystal of carbamazepine : saccharin co-crystal possessed a superior pharmacokinetic profile to existing forms of carbamazepine in its stability, dissolution rate, and oral absorption profile in dogs (Hickey *et al.*, 2007). Another study demonstrated the co-crystal, fluoxetine HCl : succinic acid displayed a two-fold increase in aqueous solubility relative to the active pharmaceutical ingredient alone (Childs *et al.*, 2004).

Another factor worth consideration in the development of new drug entities is the existence of polymorphs. Polymorphs result in differences in the

molecular arrangements of molecules within a crystal, which can result in markedly different bioavailability. For example, it has been shown that the alpha polymorph of chloramphenicol palmitate produces low bioavailability upon oral delivery. In contrast, the beta-polymorph produces significantly higher serum levels upon administering the same dose (Aguiar *et al.*, 1967). Thus co-crystals can be used to isolate a specific polymorph and ensure consistency in its pharmacokinetic parameters.

Artelo biosciences have developed a co-crystal using CBD and tetramethylpyrazine (TMP) at a 1:1 ratio to alleviate the poor physicochemical characteristics reducing the bioavailability of CBD. Unlike most other co-formers used in a co-crystal, TMP is not a pharmacologically inert substance. TMP has has been used in Chinese medicine since the 1960s to treat ischemic stroke and various cardiovascular diseases (Lin, 2009). TMP has also shown potential in pre-clinical models of stroke, cancer, and pain (Lin *et al.*, 2015; Jia *et al.*, 2016; Xiong *et al.*, 2017). Given the overlapping pharmacology, one line of thought is that the combination of both drugs could produce synergistic effects in pathologies relevant to both drugs.

1.8 **Aims of thesis**

The primary aim of the thesis was to investigate the use of phytocannabinoids in cellular and animal models of stroke. A secondary aim of this thesis was to determine the pharmacological effects of CBD co-applied with TMP at 1:1 ratio in cellular models.

Chapter 2 first aimed to assess the evidence of the efficacy of CBD in animal models of stroke by using a systematic review and meta-analysis. A strict criteria was imposed to ensure minimal differences in study design, thus appropriate collation of data. A secondary aim of the meta-analysis was to assess whether substantial publication bias was present within this area of research.

Using an in vivo model, chapter 3 aimed to assess the effects of CBD or CBDA on infarct volume using MRI images. Using a clinically relevant route, intravenously (iv), following permanent occlusion of the middle cerebral

artery (pMCAO). It was hypothesised CBD and, to a greater extent CBDA, would reduce infarct volume 24 h following pMCAO. This animal study hoped to replicate the findings of the studies used for the meta-analysis for chapter 2.

The first aim of chapter 4 was to assess the effects of a range of phytocannabinoids (CBD, CBGV, CBC and CBDV) on various markers of mitochondrial function and NAD(P)H-dependent oxidoreductase enzymes in human astrocytes in normoxic and hypoxic (after a 4 h oxygen-glucose deprivation (OGD) protocol conditions. The second aim was to assess how the duration of OGD affects the magnitude of damage produced by an OGD/R protocol in astrocytes by comparing a 4 h vs an 8 h OGD protocol. Next pre- and post-application of phytocannabinoids was used to assess the effects of these compounds during the ischemic and reperfusion phases of cell damage. It was hypothesised that where sufficient damage was induced by the OGD protocol, phytocannabinoids would display protective effects.

Chapter 5 aimed to distil the belief held by the non-scientific community that naturally sourced CBD is superior to CBD produced by synthetic means using empirical evidence. This study would also serve to identify whether the source of CBD needs to be considered when creating CBD formulations. To achieve this three human cellular models were used, stroke, cancer and IBD, to assess whether the source of CBD influenced any of the effects seen in these models. Likewise the pharmacological mechanisms of action associated with producing CBD's effect was assessed for each source of CBD.

Using two human cellular models of disease, cancer and stroke, Chapter 6 aimed to assess the individual pharmacological properties of CBD and TMP and assess whether co-application of these molecules at a 1:1 ratio produces synergistic, additive, neutral or compromised efficacy. Given some of the overlapping pharmacology, it was hypothesised TMP would work synergistically or additively with CBD by decreasing cellular viability in cancer cells and reducing markers of inflammation and cell death in cellular models of stroke.

2 Cannabidiol in acute ischemic stroke: A meta-analysis of in vivo focal ischemic studies

2.1 Introduction

Cannabidiol (CBD) is one of the most abundant phytocannabinoids produced by the plant *Cannabis Sativa L*. In the UK, CBD has been licensed to treat drug-resistant epilepsy (Epidyolex, (GW pharmaceuticals and demonstrates a good safety profile (Silvestro *et al.*, 2019). To date, no clinical trials have assessed the use of CBD in stroke patients. One randomised controlled cross-over double-blind pilot study evaluating the efficacy of Sativex (CBD and THC, 1:1 ratio) in treating post-stroke spasticity over two years started in 2017 (Marinelli *et al.*, 2017); however, the results for this study are yet to be published. A meta-analysis assessing the efficacy of cannabinoids in experimental stroke models indicated that endocannabinoids, phytocannabinoids and synthetic cannabinoids all display efficacy in improving infarct volume and neurological outcome (England *et al.*, 2015).

Several *in vivo* studies have investigated the pharmacological targets responsible for the neuroprotective effect in animal models of ischemia/reperfusion injury. In mice, the ability of CBD to reduce infarct volume was associated with interactions with the 5-hydroxytryptamine (5-HT1a) receptor. Research in a piglet model of neonatal hypoxia demonstrated a partial role for the cannabinoid receptor 2 (CB_2) (Mishima *et al.*, 2005; Pazos *et al.*, 2013). *In vitro* work has identified other mechanisms through which CBD may mediate these effects, including anti-oxidant activity against glutamate-induced excitotoxicity (Hampson *et al.*, 2000); preventing an increase in intracellular Ca^{++} by modulating the mitochondrial Na^{+}-Ca^{++} exchanger (NCX) (Ryan, Alison J. Drysdale, *et al.*, 2009); increasing basal mitochondrial respiration, ATP linked oxygen consumption rate and spare respiratory capacity (Sun *et al.*, 2017), and protect blood-brain barrier (BBB) integrity following oxygen-glucose deprivation/ reperfusion (OGD/R) in a co-culture model of the BBB (Hind, England and O'Sullivan, 2016). CBD has also been shown to influence aquaporin 4 (AQP4) expression, which may have implications on the effect of cerebral oedema in both the early (cytotoxic swelling) and late (vasogenic swelling) phase (Couch *et al.*, 2019). Given the surmounting pre-clinical evidence of the potential of CBD as a treatment for ischemic stroke, a meta-analysis collating outcome data from multiple *in vivo* studies is warranted.

The primary aim of this study is to systematically review and perform a meta-analysis on the effects of CBD in *in vivo* models of focal ischemic stroke. A secondary purpose was to determine how CBD influences neurological and functional outcomes.

2.2 Methods

2.2.1 Search criteria

Preclinical studies were identified as those using animal models to assess the effects of cannabidiol in focal ischemia. Studies were searched up to June 12th 2020, in Ovid MEDLINE(R), Embase and PubMed. The author and final year student, Ronan lee performed the search and screened articles to acquire data. Keywords searched included: (Cannabidiol OR CBD OR Epidolex OR Epidyolex) AND (Stroke OR Focal isch*mia OR Focal isch*emic stroke OR Brain isch*mia OR Cerebral isch*mia OR Cerebral infarct OR Intracranial thrombosis OR Intracranial embolism OR Brain infarction).

Articles underwent full-text screening and were included if they met five eligibility criteria; 1) experimental studies only (not humans) observing focal ischemic animal models in adults, 2) CBD as the sole administered treatment, 3) Measured at least one of the following; infarct size as volume or percentage, functional outcomes, neurological score, 4) A control group was present, 5) data was from a source that was not a review or abstract. Duplicated papers were identified and removed from the results; data was not included where only an abstract was available. No language restrictions were applied; Google Translate was used to translate papers to English.

2.2.2 Quality and risk of bias

The methodological quality and heterogeneity of each study were assessed using the SYstematic Review Centre for Laboratory animal experiments (SYRCLE) risk of bias tool. Papers were assessed for the presence of selection, performance, detection, attrition, reporting an expected bias (Hooijmans *et al.*, 2014). This tool was used to rank the studies from most prone to bias (0) to least prone to bias (+10). Publication bias was visualised using a funnel plot, and asymmetry was tested using Egger's statistic. A sensitivity analysis was also undertaken to estimate any unfounded variation and subsequently used to exclude low-quality studies. Calculations used a random-effects model; statistical heterogeneity was expressed as I^2. Data quality was further assessed using the presence or absence of physiological monitoring, including blood glucose, blood gas, cerebral blood flow, blood pressure, and temperature.

2.2.3 Data analysis

Data were analysed using Cochrane Review Manager (version 5.3, Copenhagen, The Nordic Cochrane Centre, The Cochrane Collaboration, 2014) and Stata/SE (v15.1 StataCorp TX, USA). Studies were divided into groups based on species, data was then analysed according to the type of data obtained: i) Continuous data (changes in infarct size/volume, time spent on the Rotarod, neurological score) is presented as standardised mean difference (SMD) or weighted mean difference (WMD); ii) binary data using odds ratio and 95% confidence intervals. The total dose was usually given as mg/kg. However, where this information was not available, the average weight of the animals was used to calculate the equivalent mg/kg dosage. Grab application (version 1.8 Apple Mac) was used to obtain values from graphs if not provided within the article. Where complete information was not available, attempts were made to contact authors via email. For numbers where a range was given, the lowest number in the range was used, except for control animals, where the highest number in the range was used. Information collected for analysis included animal species, age, sample size, weight, type of model, the total dose of CBD, route and time of drug administration. Dose-response curves were generated in graph pad PRISM 7. Egger's statistic and meta-regression was performed using Stata/SE (version 15.1 for Mac).

2.3 **Results**

From the initial search, 219 papers were found. After eligibility criteria were applied and duplicate studies removed, a total of 8 studies examining focal ischemia were included (Figure 2.1, See appendix Table 1) (299 animals). Two laboratories generated focal ischemic studies, using ddY mice (Hayakawa *et al.*, 2004, 2008, 2009; Mishima *et al.*, 2005; Hayakawa, Mishima, Nozako, Hazekawa, *et al.*, 2007; Hayakawa, Mishima, Nozako, Ogata, *et al.*, 2007) and Wistar rats (Khaksar and Bigdeli, 2016, 2017a, 2017b, 2017c). Only transient middle cerebral artery occlusion (MCAO) models were used in the selected studies, and occlusion times ranged from 1 to 4 hours. In all studies, CBD was administered before, during, after or in combination, either by intracerebroventricular (ICV) (n=72) or intraperitoneal (IP) injection (n=161) (Supplementary Table 1).

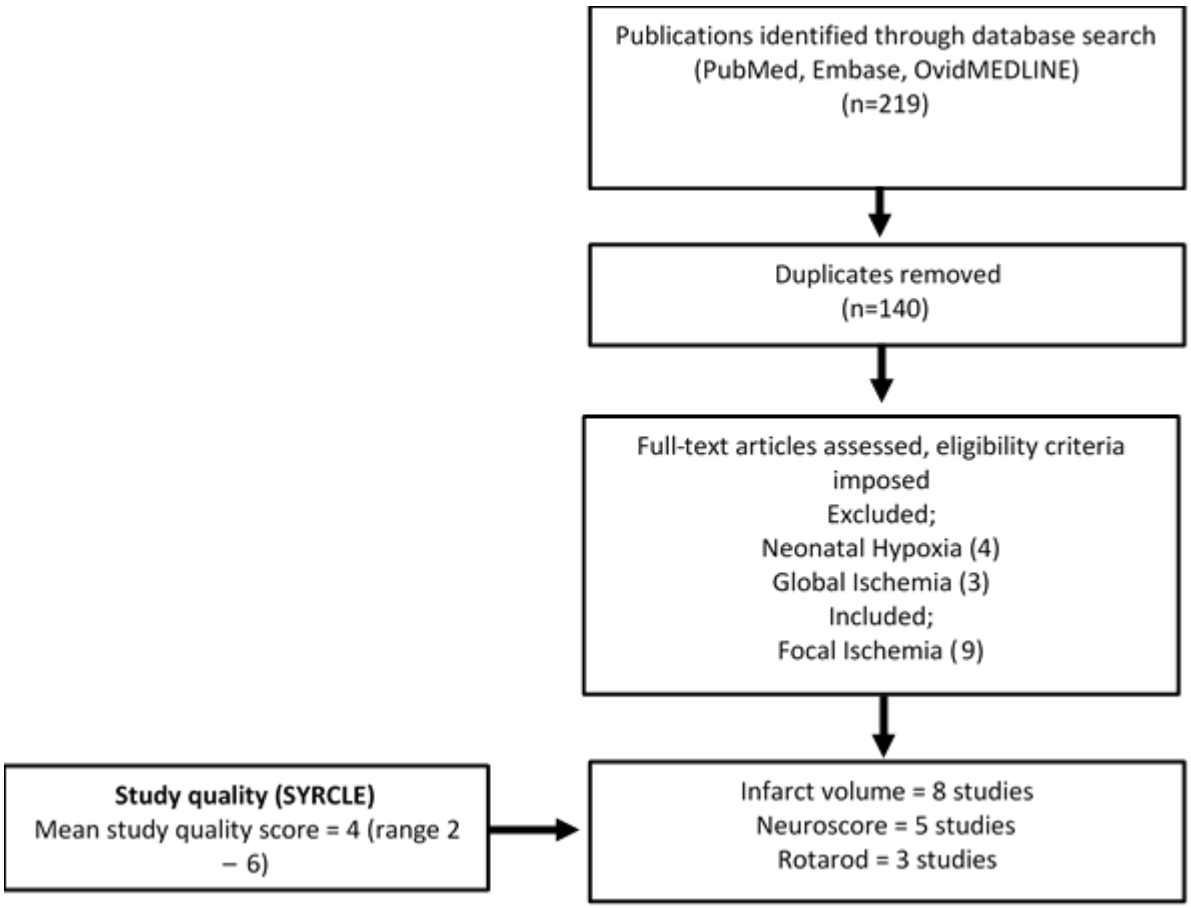


Figure 2.1 Publication identification process

Overall, CBD reduced infarct volume relative to control by a mean difference of -53.7 mm^3, 95% CI [-68.3, -39.4], P<0.0001) (Figure 2.2), equivalent to a mean percentage reduction of 50% relative to control animals.

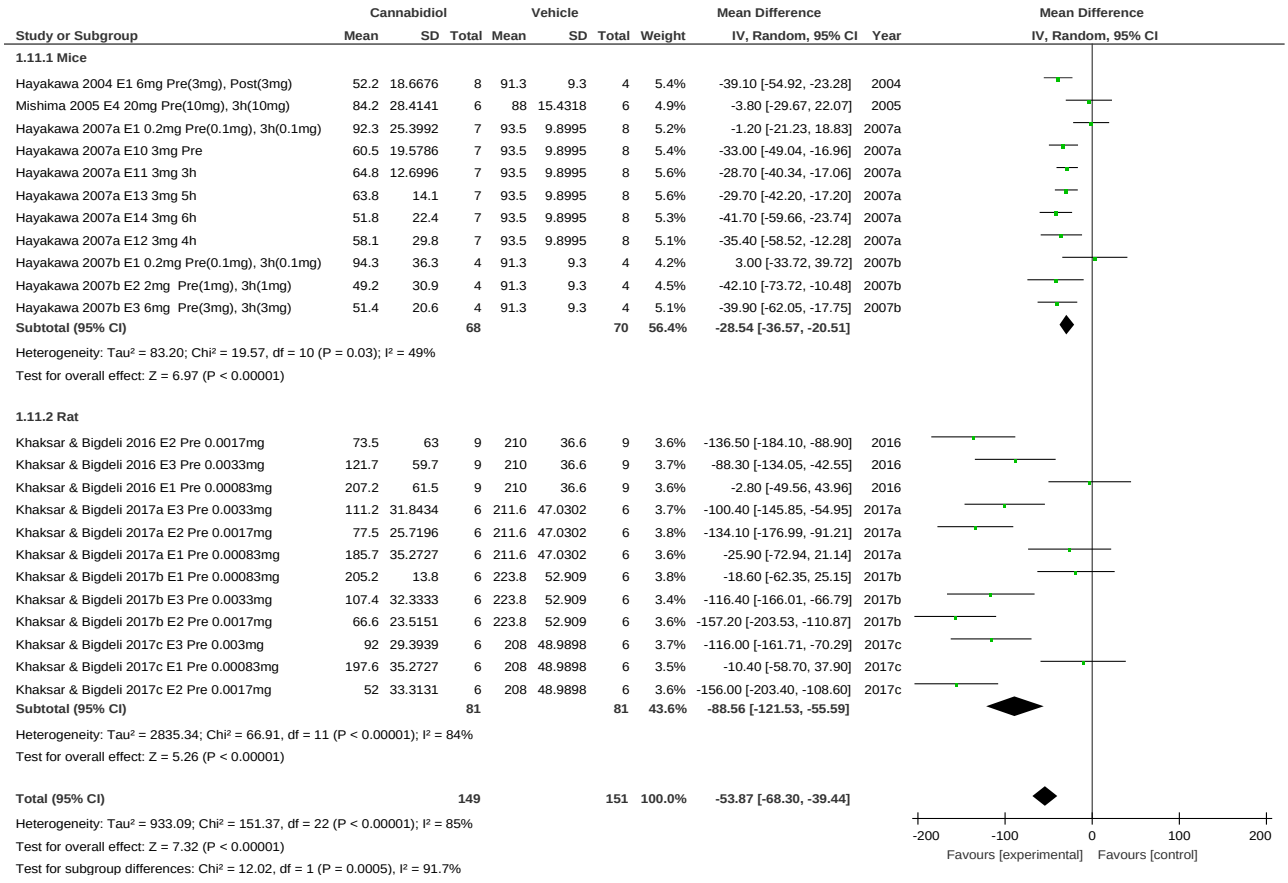


Figure 2.2 Forest plot of the effect of CBD in rats and mice on infarct volume (mm3) in an MCAO model of transient focal ischemia. Pre = administered before stroke onset; post = administered after stroke onset; h = hours.

2.3.1 Dose-response effects of CBD on infarct volume

In the four studies using rats (Khaksar and Bigdeli, 2016, 2017a, 2017c, 2017b), CBD administration (ICV) 30 min prior to MCAO reduced infarct volume, producing a bell-shaped dose-response curve. The lowest dose used 0.83 µg/kg caused a mean percentage reduction of 9% compared to control (MD -20 mm^3, 95% CI [-43.39, 3.59], P=0.0017), 1.7 µg/kg caused a mean percentage reduction of 69% (MD -153 mm^3, 95% CI [-175.3, -131], P<0.0001) and the highest dose used (3.3 µg/kg) led to a reduction of 51% (MD -113 mm^3, 95% CI[-135.5, -90], P<0.0001) (Figure 2.3A).

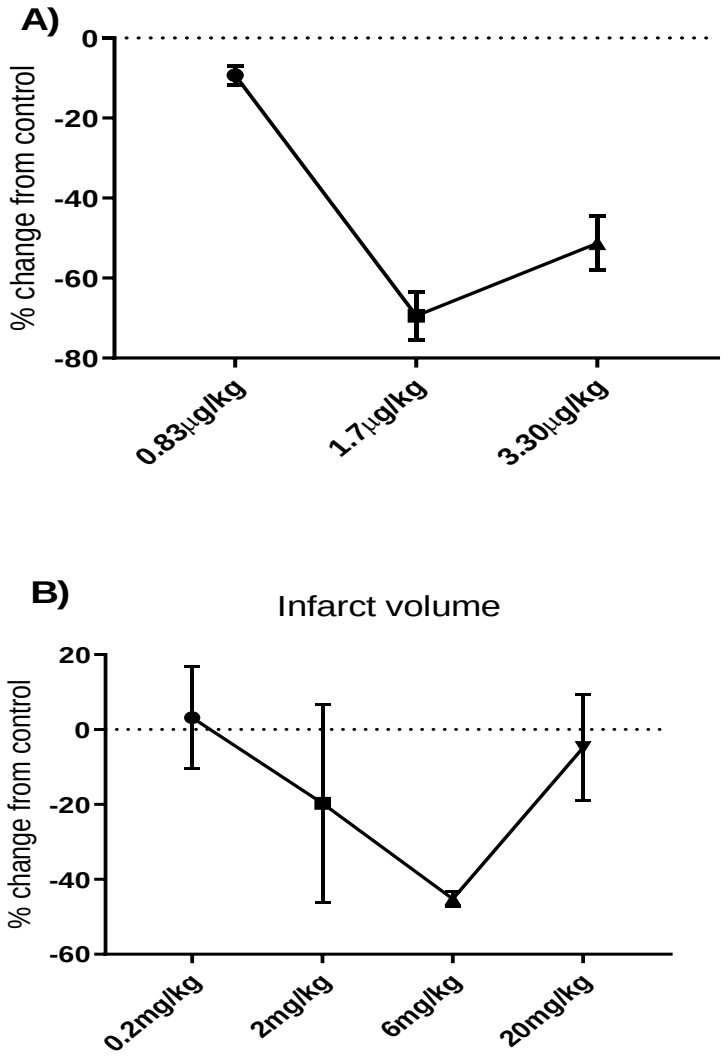


Figure 2.3 Dose-response curve displaying % mean ± SD change in infarct volume of total CBD dose relative to vehicle from all studies. A) Wistar rats receiving CBD via ICV injection 30 minutes prior to MCAO. B) ddY Mice receiving two doses of CBD immediately before and 3 h after MCAO via IP injection. Data from Khaksar and Bigdeli, 2016, 2017a, 2017c, 2017b and Hayakawa, Mishima, Nozako, Hazekawa, et al., 2007 were used to create this graph.

In the three studies that used mice (Hayakawa, Mishima, Nozako, Hazekawa, *et al.*, 2007), CBD administration (IP) also produced a similar pattern of response with higher doses associated with lower efficacy (Figure 2.3B). All but one experiment dosed before, during and after the insult; therefore, this experiment (only using post insult dosing) was excluded from dose-response analyses (Figure 2B). The lowest dose (0.2 mg/kg) demonstrated a 2% mean difference compared to control which was not significant (MD +1.7 mm^3, 95% CI [-9.47, 12.72], P = 0.978), 2 mg/kg resulted in a 46% mean reduction (MD -42.1 mm^3, 95% CI[-53.1, -31], P<0.00001),

6 mg/kg caused 45% reduction (MD -39.9 mm^3, 95% CI [-46.61, -33.38], P<0.00001) and the highest dose (20 mg/kg) showed a non-significant 4.6% reduction in infarct volume (MD -4.3 mm^3, 95% CI[-34, 25.46], P=0.78).

In studies observing infarct volume, data obtained from Wistar rats had significant statistical heterogeneity (I^2 = 84% [P<0.00001]). Data from ddY mice exhibited low heterogeneity (I^2 = 49% [P<0.00001] (Figure 2.2~~3~~).

2.3.2 Time window of administration

In the single publication assessing the effect of later drug administration (a more clinically relevant scenario) (Hayakawa, Mishima, Nozako, Hazekawa, *et al.*, 2007), CBD significantly reduced infarct volume by an SMD of -2.10 (95% CI -2.77 to -1.42, P<0.00001, 4 experiments, 60 animals, time window of administration 3-6 hours) compared to all experiments administering the first dose before the stroke, SMD -1.17 (95% CI -1.48 to -0.86, P<0.00001, 19 experiments, 240 animals). A significant effect was seen when administered at 6 hours, the latest time tested, SMD -2.33 (-95% CI 3.73 to -0.92, P=0.001).

2.3.3 Route of administration and infarct volume

The influence CBD on infarct volume was compared between different routes of administration (Figure 2.3A-B). A larger reduction in was observed when CBD was administered via ICV (SMD -2.43, 95% CI [-3.53,-1.33], P<0.00001, 4 studies, 96 animals), when compared to IP (SMD -1.15, 95% CI [-1.55, -0.75], P<0.00001, 5 studies, 203 animals).

2.3.1 Neurological score

Neurological deficits in mice were quantified using a 5 point scoring system. 0, normal motor function; 1, flexion of the torso and the contralateral forelimb upon lifting of the animal by the tail; 2, circling to the ipsilateral side, but normal posture at rest; 3, circling to the ipsilateral side; 4, rolling to the ipsilateral side; and 5, leaning to the ipsilateral side at rest (no spontaneous motor activity). In rats, a similar protocol was used using a 28-point scoring system; likewise, higher scores represent worse outcomes. Neurological score was measured in 16 experiments

(202 animals) and was separated into early and late evaluation (Figure 2.4). Early evaluation (at 24 hours) (13 experiments, 178 animals, 38 mice and 140 rats) determined a significant improvement in neurological score (SMD -1.04, 95% CI [-1.43, -0.65], P<0.0001). Late evaluation (at 336-hour, 3 experiments, 24 animals) observed no significant improvement with CBD treatment (SMD -0.92, 95% CI [-1.96, -0.11], P=0.08) (Figure 2.4). When split by species, using early measurements only, both mice and rats showed a significant improvement (SMD -0.80, 95% CI [-1.70, 0.1], I^2= 46%, P=0.08 and -1.66, 95% CI [-2.63, -0.69], I^2= 77%, P=0.0008, respectively). A comparison between mice and rats at later time points was impossible as all late data came from rats, who also received CBD through a different route of administration (IP).

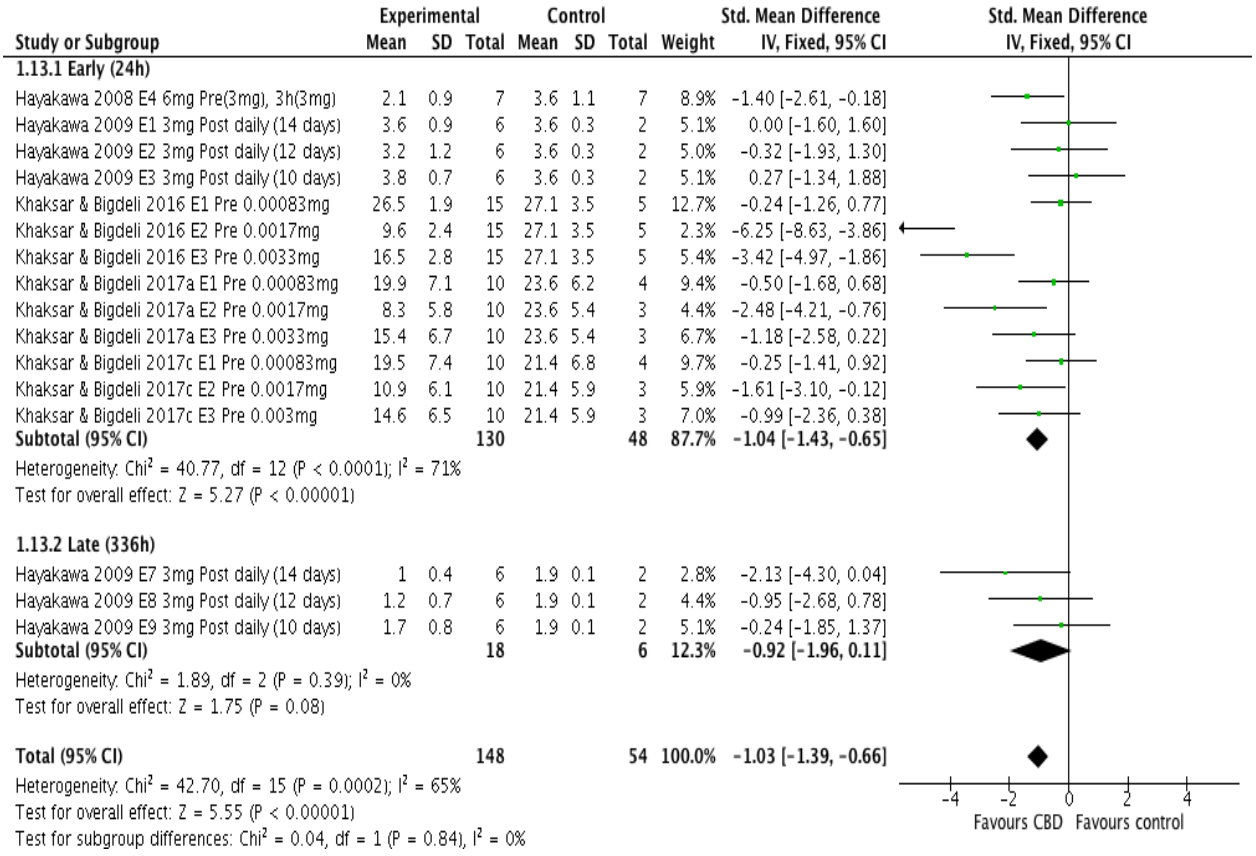


Figure 2.4 Forest plot of the effect of CBD on neurological score at different points of evaluation in models of focal ischemia. Pre = administered before stroke onset; post = administered after stroke onset; h = hours.

2.3.2 Rotarod test

Rotarod tests are used as a non-subjective means to quantify motor coordination. The longer the animal can remain on the rota-rod (seconds), the better their sensorimotor outcome. All the presented rotarod test data was generated by the same group (Hayakawa et al.) on the same species (DDY mice) (figure 2.6). 104 mice were grouped into early, 24 h, and 72 h assessment groups and a late 336 h group. Rota-rod scores at 24 h (5 experiments, n=52) saw no significant difference between CBD and control (time spent on rotarod MD -1.83 seconds, 95% CI [-7.54,3.88], P=0.53). In contrast, scores at 72 h demonstrated a significant improvement in the CBD group (2 experiments, 28 animals, MD 50.44 seconds, 95% CI [27.41,73.47], P<0.0001), as well as the scores at 336 h (3 experiments, n=24, MD 37.83 seconds, 95% CI [22.46,53.20], P<0.00001); the higher doses and repeated treatment possessed the greatest effect.

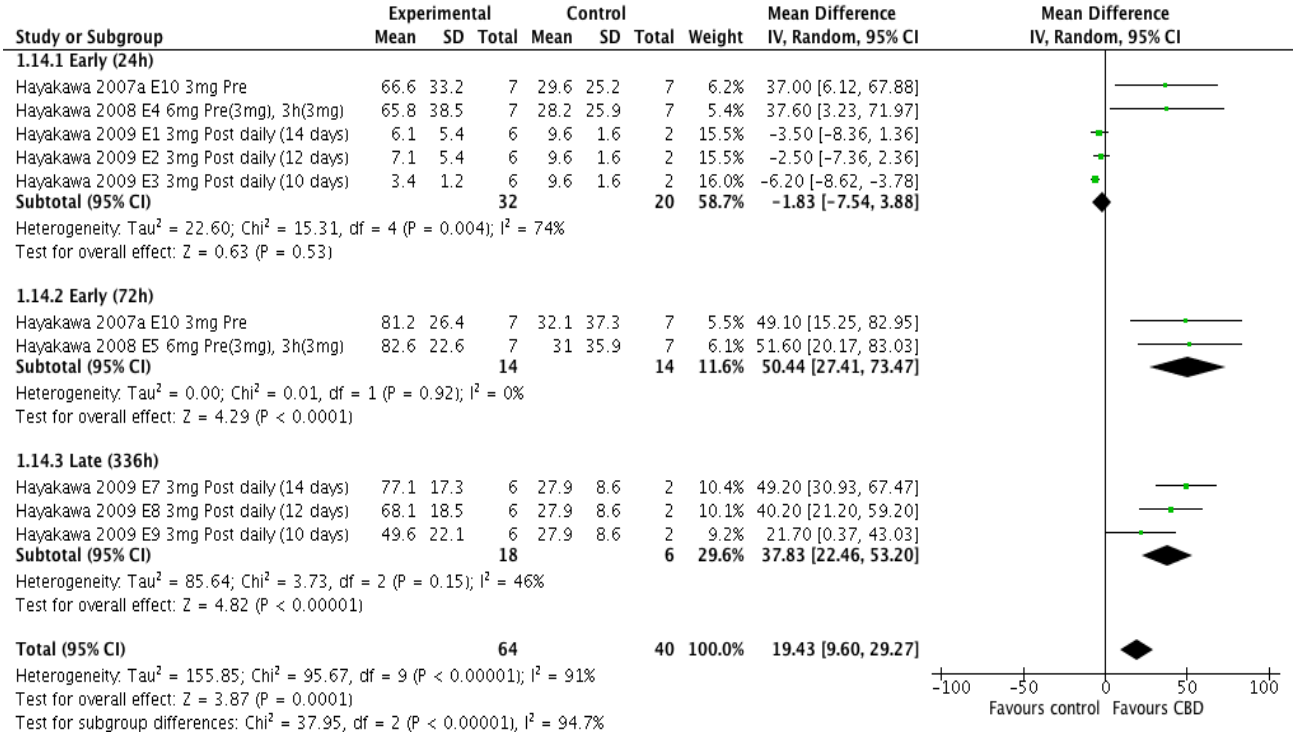


Figure 2.6 Forest plot of the effect of CBD on time spent on Rotarod. Pre = administered before stroke onset; post = administered after stroke onset; h = hours

2.3.3 Study quality and risk of bias

Quality of study median score was 5 (range, 4-7, Supplementary Tables 1 and 2). The study quality did not influence infarct volume (meta-regression, P=0.391). Median risk of bias score was 5 (range, 4-7, Supplementary Tables 1 and 3). This score also did not impact infarct volume (P=0.495). Five of ten publications used randomisation, four reported blinding of outcome assessments, six monitored temperature during surgery, and no studies provided evidence of sample size calculations. Four of ten studies had a statement on conflicts of interest (Khaksar and Bigdeli, 2016, 2017b, 2017c, 2017a). Furthermore, all ten measured outcomes at 1 to 3 days and one at day 14 (Hayakawa *et al.*, 2009). Measurements of physiological monitoring during anaesthesia were limited; only studies by Hayakawa and Mishima did so (supplementary Table 4); three of ten studies measured blood pressure, four measured blood gases, two measured glucose and four measured regional cerebral blood flow. None of the physiological parameters affected infarct volume measurements. All ten measured outcomes other than lesion size (neuroscore and Rotarod), two assessed a time window for administration (Hayakawa, Mishima, Nozako, Hazekawa, *et al.*, 2007; Hayakawa *et al.*, 2009) and 6 established dose-response effects for infarct volume (Hayakawa, Mishima, Nozako, Hazekawa, *et al.*, 2007; Hayakawa, Mishima, Nozako, Ogata, *et al.*, 2007; Khaksar and Bigdeli, 2016, 2017a, 2017b, 2017c).

2.3.4 Publication bias

Bias score was normally distributed across the studies, with the range of scores occurring between 4 and 9 and a median score of 7. Significant bias was present for all studies measuring infarct volume (Figure 2.7, Egger's statistic P<0.004).

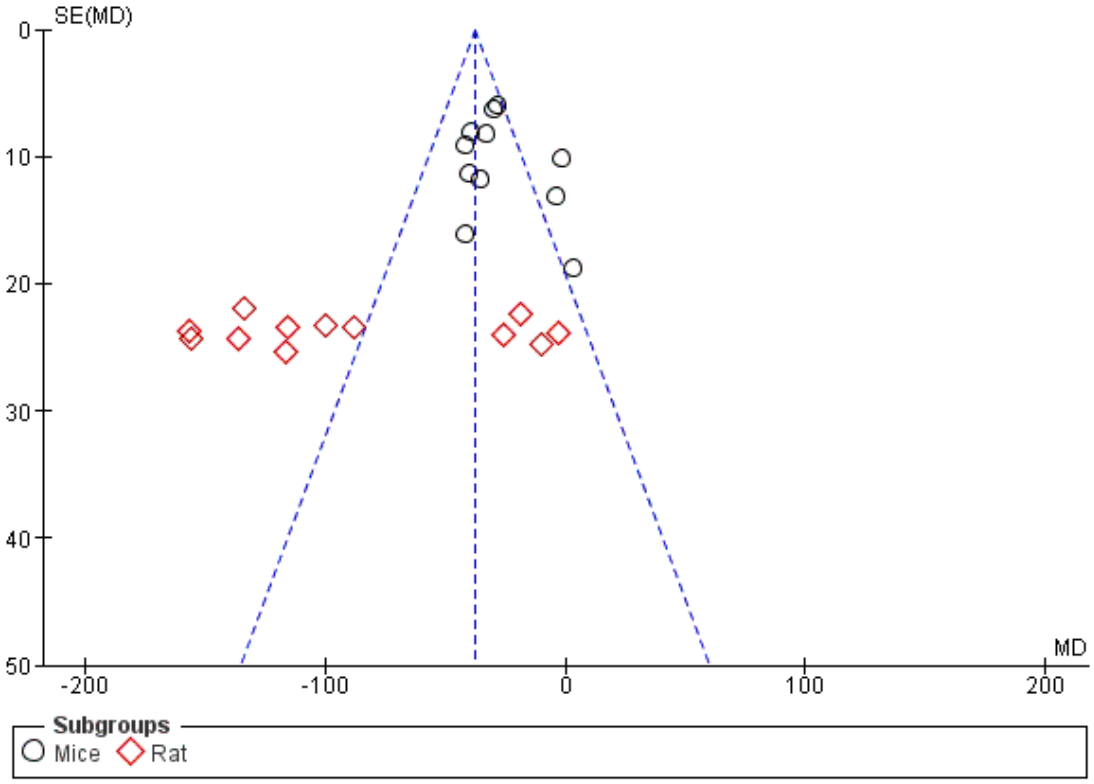


Figure 2.7 Funnel plot for infarct volume data. Standard error of the mean difference (SE - MD) for each study is plotted against its effect size (MD).

2.4 Discussion

This meta-analysis demonstrates that CBD significantly reduces infarct volume and improves motor coordination and neurological outcomes in transient models of ischemic reperfusion injury. However, the interpretation of data is confounded by publication bias and relatively few laboratories publishing work in this field. Further, only male rats and mice without co-morbidity were investigated. Nonetheless, CBD exerted a potent effect with an average stroke lesion volume reduction of 50% compared to control; further preclinical work assessing alternative stroke models, time, dose and routes of administration are warranted, especially given the favourable safety profile seen when CBD is used in other conditions (Szaflarski *et al.*, 2018).

When examining dose-response effects on infarct volume in rats, 1.7 µg/kg provided the most significant reduction in infarct volume, and in mice, the most efficacious dose was 6 mg/kg. The dose-response produced a bell-shaped curve, a typical feature of CBD pharmacology (Gallily, Yekhtin and Ondřej Hanuš, 2015). Despite lower weight-adjusted doses, the percentage of infarct volume reduction in rats was

greater than in mice (by 23%). This is likely a consequence of the different routes of administration used (icv vs ip) and species differences. Whilst rats received a considerably smaller dose, administration into the CSF bypasses first-pass metabolism. Drugs administered via this route pass back into the general circulation through the choroid plexus before re-entering the brain across the BBB (Pardridge, 2011). Therefore, this method of administration is more comparable to slow intravenous injection than a direct route into the brain.

In contrast, intraperitoneal administration does not bypass first-pass metabolism. The drug diffuses into the surrounding tissue, and absorption into circulation mainly occurs in the mesenteric arteries, which ultimately empty into the hepatic portal vein. Therefore, drugs administered via this route will encounter phase I and II metabolism, which is more comparable to an oral pathway (Lukas, Brindle and Greengard, 1971). CBD is considered to have poor bioavailability when delivered orally. Some studies in humans show as little as 6% of the bioavailability of the total dose consumed (Montagne, 2004); it is reasonable to speculate that these contrasting types of administration would influence the efficacy of CBD in these models. Optimising the CBD formulation to ensure that CBD absorption is rapid and provides sufficient plasma concentrations for human clinical trials in stroke patients must be carefully considered (Millar *et al.*, 2020).

Regardless of different routes of administration, existing literature has noted species differences and shown that with IP administration, mice achieve higher CBD plasma levels relative to rats exposed to the same weight-adjusted dose (14.3 and 2.6µg/ml, respectively) (Deiana *et al.*, 2012). Interestingly, in the same study, the authors also demonstrated that oral administration produced similar peak plasma concentrations between species; however, there was a six-fold higher peak in brain CBD concentration in rats than in mice. Thus, efficacy is not just determined by the routes of administration but by the differences in pharmacokinetic profiles between species.

CBD demonstrated efficacy on infarct volume when administered both before and up to 6 hours after the stroke. Administration in the hyperacute setting, on admission to hospital and before reperfusion therapies may be practical, either through intravenous routes in parallel with thrombolysis or intra-arterial administration during mechanical thrombectomy. Before moving into clinical trials examining the efficacy of CBD in stroke, the likelihood of drug-drug interactions in the stroke demographic (commonly older people with co-morbidities) needs careful

consideration. CBD is primarily metabolised by the liver enzymes CYP2C19 and CYP3A4, and co-administration with compounds that inhibit or are competitively metabolised by these enzymes can causes increases in the concentration of the administered drugs (Zendulka *et al.*, 2016). For example, CBD co-administered with Clobazam can cause a 3-5-fold increase in the plasma concentration it's an active metabolite, N-desmethylclozbazam (Anderson, Absalom, *et al.*, 2019). Thus, if drugs use the same pathway for metabolism, there is an increased risk of interaction and adverse events.

Treatment with CBD led to early neurological improvement at 24 h, but with no significant benefit seen in the later measurements at 336 h. Only one study observed later measurements, indicating more studies would be needed to validate these results (Hayakawa *et al.*, 2009). This raises concern that early treatment effects are not sustained, and it would be wise to investigated repeated doses that cover the inflammatory period over several days or weeks. However, the opposite was seen when Hayakawa evaluated sensorimotor coordination in mice using rota-rod tests (Hayakawa, Mishima, Nozako, Hazekawa, *et al.*, 2007; Hayakawa *et al.*, 2008, 2009). There was no improvement in the early 24-hour groups, but a significant benefit was observed in the 72 h and 336 h groups. This result stresses the importance of using a range of neurological scores and tests at early and late time points. There was also a notable absence of cognitive testing in the experiments performed.

There are a few limitations to consider in interpreting the data. First, the presence of publication bias means efficacy of CBD could be over or under-estimated due to unpublished data. Secondly, studies used only male rodents. Testing both sexes is vital due to differences in stroke pathophysiology and cannabinoid pharmacology (Craft, Marusich and Wiley, 2013). Additionally, all animals used were relatively young and had no comorbidities; further studies should use models incorporating diabetes, hypertension and age. Considering the results from assessing publication bias, it may be possible that these studies have been conducted but not published nor identified with our systematic searches.

In conclusion, preliminary *in vivo* evidence suggesting CBD may be helpful as a treatment for focal ischemic reperfusion injury. However, findings are limited since these data possess statistical heterogeneity, the potential for publication bias, and are derived from only two laboratories in male animals without comorbidities. Following STAIR guidelines (Albers *et al.*, 2011), future studies from independent

laboratories should assess the efficacy of CBD in permanent models of occlusion, including female animals, follow sensorimotor outcomes at early and late time-points, and use sample size calculations before moving into human clinical studies of CBD in hyperacute stroke. Furthermore, studies should consider assessing repeat dosing using clinically relevant time-points (post-stroke) and routes of administration.

Overall this chapter highlighted some of the promising results in this area, but a lack of data from few sources (two separate labs) may lead to overestimation of the effectiveness of CBD in animal's models of stroke. The next chapter therefore sought to affirm this body of evidence by replicating these studies whilst following Stroke Therapy Academic Industry Roundtable Preclinical Recommendations (STAIR) guidelines to increase the validity of any findings.

3 The effects of iv CBD or CBDA in mice exposed to electrocoagulation of the middle cerebral artery

3.1 Introduction

A meta-analysis assessing the efficacy of cannabinoids in experimental models of stroke has been conducted (England *et al.*, 2015). The findings from this study indicate that endocannabinoids, phytocannabinoids and synthetic cannabinoids all display efficacy in animal models of stroke. THC has shown efficacy in both *in vitro* and *vivo* models of stroke; however, its psychoactive effects hinder its use clinically. In comparison, CBD provides a similar extent of protection without the unwanted psychoactive effects. Several *in vivo* studies have investigated the pharmacological effects and targets responsible for the effects of CBD in animal models of cerebral ischemic injury.

Furthermore, in chapter one, a meta-analysis of in vivo focal ischemic studies in rodent models demonstrated CBD could reduce infarct volume and improve sensorimotor outcomes. One of the studies used in the meta-analysis shows that in mice exposed to 4 h middle cerebral artery occlusion (MCAO), the ability of CBD to reduce infarct volume was associated with activation of the 5-hydroxytryptamine (5-HT1a) receptor. Research in young piglets exposed to 16minutes Bilateral Common Carotid Artery Occlusion (BCCAO) as a model of neonatal hypoxia demonstrated a partial role for the cannabinoid receptor 2 (CB2) (Pazos *et al.*, 2013).

Only eleven *in vivo* studies have assessed the potential of CBD in treating cerebral focal ischemia. Ten of these studies have been conducted using transient models (Hayakawa *et al.*, 2004, 2008; Mishima *et al.*, 2005; Hayakawa, Mishima, Nozako, Hazekawa, *et al.*, 2007; Hayakawa, Mishima, Nozako, Ogata, *et al.*, 2007; Khaksar and Bigdeli, 2016, 2017c, 2017a, 2017b; Mori *et al.*, 2017), and one study using a permanent model (Rodríguez-Muñoz *et al.*, 2018). Subsequently, the lack of preclinical data has made it challenging to justify assessing CBD in a clinical setting. However, a randomised controlled cross-over double-blind pilot study evaluating the effects of Sativex (CBD and THC, 1:1 ratio) in treating post-stroke spasticity over two years started in 2017 (Marinelli *et al.*, 2017), but the results for this study are not yet

available. For CBD to be assessed in a clinical setting, the Stroke Therapy Academic Industry Roundtable (STAIR) guidelines recommend evaluating the neuroprotective effects of a drug in both transient and permanent models of stroke, as many stroke patient infarcts reperfuse slowly, if at all (Shuaib, 2006). Additionally, the plasma concentrations of the drug used in a transient model should reflect the plasma concentrations achieved in the permanent model, as higher concentrations are harder to accomplish in permanent models of cerebral ischemia (Shuaib, 2006). Therefore it is ideal for initial studies to use permanent occlusion and then proceed with transient models. The single study that has assessed CBD in a permanent model found 4ul of 10nmol solution delivered by intracerebroventricular (icv) injection 60 minutes post-surgery reduced infarct volume by 75% at 48 h relative to control mice (Rodríguez-Muñoz *et al.*, 2018). Unfortunately, no other concentrations were assessed, and the dose was measured in molar concentrations rather than mg/kg, making any conclusion surrounding an effective dose difficult.

Due to their lipophilic nature, cannabinoids suffer from poor bioavailability, suggesting more potent compounds with a similar mechanism of action could provide efficacy at lower circulating levels (Millar *et al.*, 2020). Cannabidiolic acid (CBDA) is one of the most abundant cannabinoids produced by Cannabis Sativa L. (Gülck and Møller, 2020). Following decarboxylation, via heat and light, cannabinoids transform into their corresponding neutral forms (Flores-Sanchez and Verpoorte, 2008). For CBDA, the removal of the carboxylic acid produces cannabidiol (CBD).

CBDA possess greater potency at the 5-HT1a receptor relative to CBD in animal's models assessing anti-vomiting and anti-nausea effects (Bolognini *et al.*, 2013). Therefore, this effect could extend to other models of disease where 5-HT1A mediates efficacy, such as *in vivo* and *in vitro* models of stroke (Mishima *et al.*, 2005; Hind, England and O'Sullivan, 2016).

An intravenous route of administration is relatively easy to administer, offering fast onset of action and reduces the extent of first-pass metabolism. Using this route of administration in a permanent model of stroke reproduces a clinically relevant situation. Furthermore the current design of the study hopes to replicate the findings of other studies, validating the in vivo design allowing further experiments to explore the same effects in females and animals with co-morbidities.

Artelo biosciences provided funding for the animal aspects of this study to be carried out by a third party research group (Experimental Stroke Research Platform,

Université de Caen Basse-Normandie, France). The raw data from these experiments was then manipulated, and statistical analysed to investigate any observations.

Overall the research aimed to assess the effects of CBD or CBDA on infarct volume when delivered via a clinically relevant route, intravenously (iv), following permanent occlusion of the middle cerebral artery (pMCAO). It was hypothesised CBD and, to a greater extent CBDA, would reduce infarct volume 24 h following pMCAO.

3.2 **Methods**

All animal procedures were carried out by the third party, Experimental Stroke Platform Research (ESPR) (Caen, France). Project supervisors Dr Saoirse O'Sullivan and Dr Timothy England were responsible for the design of the study. The author of the thesis, Ryan Maguire, carried out the data analysis, interpretation of results and wrote the chapter.

3.2.1 Experimental set-up

In vivo Experiments were performed on adult male Swiss mice (n=40, 35-40 g; CURB, Caen, France). Mice were kept under a 12h light/dark cycle at room temperature, food and water were available *ad libitum*. All experiments were conducted following directives from the European Communities Council (November 24, 1986, 86/609/EEC) and French Legislation (act no. 87-848, Ministère de l'Agriculture et de la Forêt) on animal experimentation. Mice were randomly assigned between two experimental arms; CBD (n=36) or CBDA (n=36) that consisted of four groups within each arm (Vehicle, 0.1mg/kg, 1mg/kg and 10mg/kg). Doses were chosen based on available literature investigating the effects of CBD in animal models of stroke (Mishima *et al.*, 2005). Mice were excluded from data analysis if lesions extended to sub-cortical regions.

3.2.2 Permanent occlusion of MCA

Mice were deeply anaesthetized with 5% isoflurane (in a mixture of NO_2/O_2), placed in a stereotaxic device; anaesthesia was maintained for up to 2 h with 2% isoflurane in a 70/30% mixture of NO_2/O_2. A small skin incision between the right eye and ear was made, the masseter muscle was excised, and a small craniotomy (1mm) was performed on the parietal bone to expose the right middle cerebral artery (MCA). MCA is then electrocoagulated using a bipolar electrocoagulator and cut to avoid self-reperfusion. After the initial monitoring period, the wound was sutured mice placed in their housing cage. 20 minutes following pMCAO, mice received iv injections of 0.1mg/kg, 1mg/kg or 10mg/kg of either CBD or CBDA (figure 3.1). 20 minutes was chosen as this other literature indicates that CBD provides the most protection when applied before or close to the time of insult.

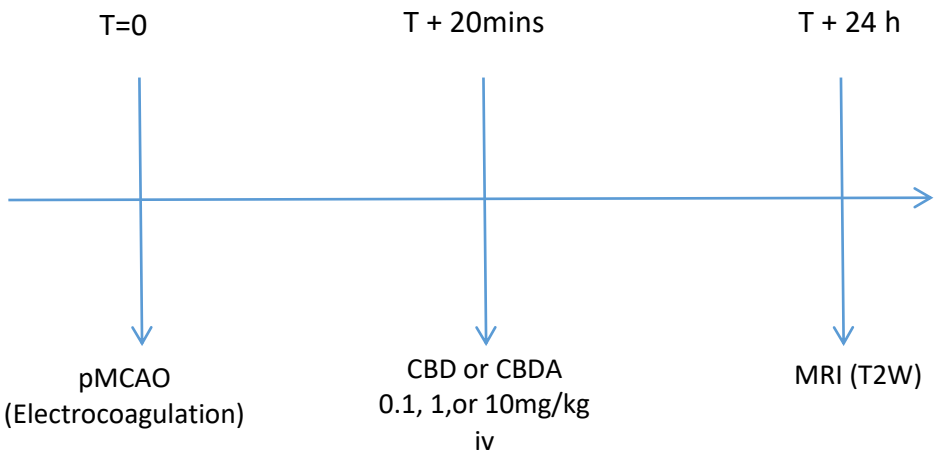


Figure 3.1 Schematic diagram of the experimental time course. pMCAO = permanent middle cerebral artery occlusion, iv = intravenous, MRI = Magnetic Resonance Imaging.

3.2.3 Data analysis

MRI analysis was carried out 24 h following pMCAO using a Pharmascan 7 T/12 cm system with surface coils (Bruker, Germany). T2-weighted images were acquired for lesion sizes measurement 24 h following pMCAO. Images were analysed using ImageJ software (v1.45r). Statistical analysis of data was performed using graphpad PRISM 7. Infarct data is presented as mean volume (mm3) and Standard Deviation (SD) and comparison of controls was done using a student's t-test and group analysis

was achieved using a one-way ANOVA. According to Gerrets and colleagues, oedema in the affected hemisphere can lead to overestimating infarct volume; therefore, a formula was used to correct lesion volume for oedema to gain more reliable data. Lesion volume corrected for oedema is expressed as % hemispheric lesion volume corrected for oedema (%HLV^e). Furthermore, Gerrets and colleagues also demonstrated that the space-occupying effect (hemispheric lesion volume corrected for oedema – lesion volume uncorrected for oedema) correlates well with brain water content. Therefore can be used to indirectly quantify vasogenic swelling (Gerriets *et al.*, 2004).

3.3 Results

3.3.1 Infarct volume

pMCAO in control animals caused a mean infarct volume of 25.6mm^3 ± 4.1, 95% CI [16.0, 35.3] in the CBD arm and 18.5 mm^3 ± 2.4 95% CI [12.4, 24.5] in the CBDA arm (figure 3.2A-B). Using an unpaired t-test, no statistical differences existed between the control groups.

The application of CBD 20minutes following pMCAO produced a mean increase in infarct volume relative to control of 13.2mm^3 ± 5.7, 95% CI [-1.38, 27.4] (NS) at 0.1mg/kg, 10.8mm^3 ± 5.4, 95% CI [-2.5, 27.1] at 1mg/kg and 6.7mm^3 ± 5.4, 95% CI [-6.7, 20.0] at 10mg/kg (figure 3.2A). Using a one way- ANOVA no statistical differences existed between CBD groups and control.

The application of CBDA 20minutes following pMCAO produced a mean decrease in infarct volume of -1.4mm^3 ± 4.4, 95% CI [-9.4, 12.8] at 0.1mg/kg, a mean increase of 1.7mm^3 ± 4.5, 95% CI [-12.8, 9.4] at 1mg/kg and 0.5mm^3 ± 4.4, 95% CI [-10.3, 11.4] at 10mg/kg (figure 3.2B). Using a one-way ANOVA, no statistical differences existed between CBDA groups and control.

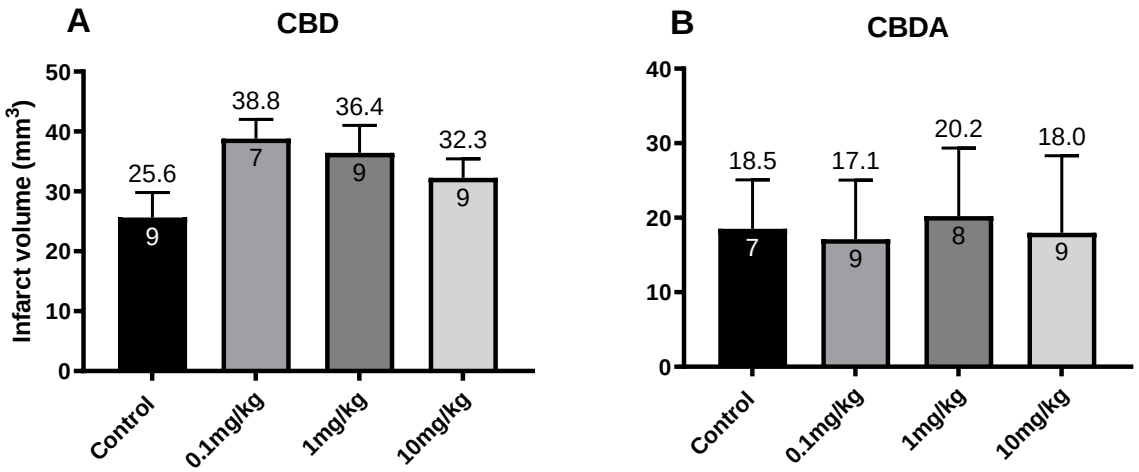


Figure 3.2 The effect of CBD or CBDA on infarct volume 24 h following the initiation of pMCAO. Data is presented as raw mean infarct volume (mm^3) with standard deviation (SD). Numbers inside bars display sample size for each experimental group, and numbers above bars display the mean result for each condition. Data was compared against vehicle for statistical significance against vehicle using a one-way ANOVA.

3.3.2 Infarct volumes corrected for oedema

Following the transformation of infarct volume (mm^3) to oedema corrected hemispheric lesion volume (%HLV[e]), CBD (figure 3.3A) at 0.1mg/kg produced a mean increase of 3.6% ± 3.0, 95% CI [-11.1, 3.9] relative to control. CBD at 1mg/kg produce a mean decrease of 1.1% ± 3.0, 95% CI [-5.9, 8.1] relative to control. CBD at 10mg/kg produced a mean decrease of 0.3% ± 2.9, 95% CI [-6.6, 7.3] relative to control.

CBDA (figure 3.3B) at 0.1mg/kg produced a mean increase of 4.7% ± 2.9, 95% CI [-14.7, 0.6] relative to control. CBDA at 1mg/kg produce a statistically significant mean increase of 7.6% ± 3.0, 95% CI [-5.9, 8.1] ($p<0.05$) relative to control using a one-way ANOVA. CBDA at 10mg/kg produced a mean increase of 2.7% ± 2.7, 95% CI [-9.6, 4.1] relative to control. Using an unpaired t-test, no statistical differences existed between the control groups.

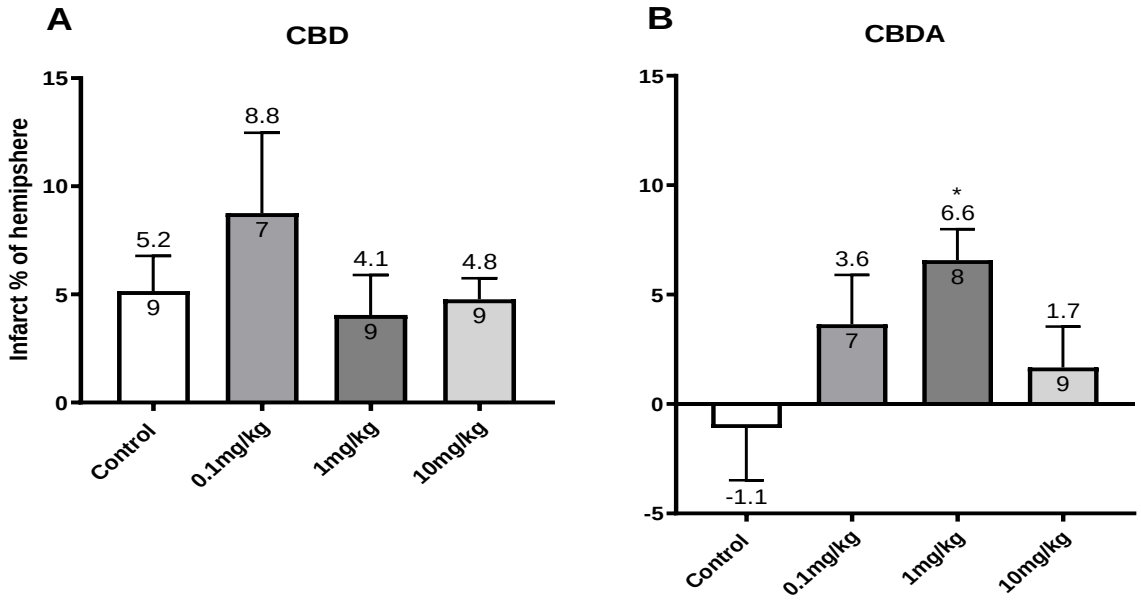


Figure 3.3 The effect of CBD (A) or CBDA (B) on infarct volume corrected for oedema 24 h following pMCAO. Data are presented as % of the hemisphere with standard deviation. Numbers inside bars display sample size for each experimental group, and numbers above bars display the mean result for each condition. Data was compared against vehicle for statistical significance using a one-way ANOVA. * p≤0.05

3.3.3 Space occupying effect

Space occupying effect (%HSE) was used to estimate brain water content, subsequently serving as an indirect measurement of oedema in the affected hemisphere. CBD (figure 3.4A) at 0.1mg/kg produced a mean increase of 4.4% ± 2.8, 95% CI [-11.3, 2.5] relative to control. CBD at 1mg/kg produce a statistically significant mean increase of 7.6% ± 2.6, 95% CI [-5.9, 8.1] ($p<0.05$) relative to control. CBD at 10mg/kg produced a mean increase of 4.9% ± 2.6, 95% CI [-14.4, -1.1] relative to control.

CBDA (figure 3.4B) at 0.1mg/kg produced a mean decrease of 4.1% ± 2.7, 95% CI [-2.6, 10.8] relative to control. CBDA at 1mg/kg produce a mean decrease of 5.4% ± 2.6, 95% CI [-1.1, 12.0] ($p<0.01$) relative to control. CBDA at 10mg/kg produced a mean decrease of 1.8% ± 2.5, 95% CI [-4.4, 8.2] relative to control. Using an unpaired t-test, no statistical differences existed between the control groups.

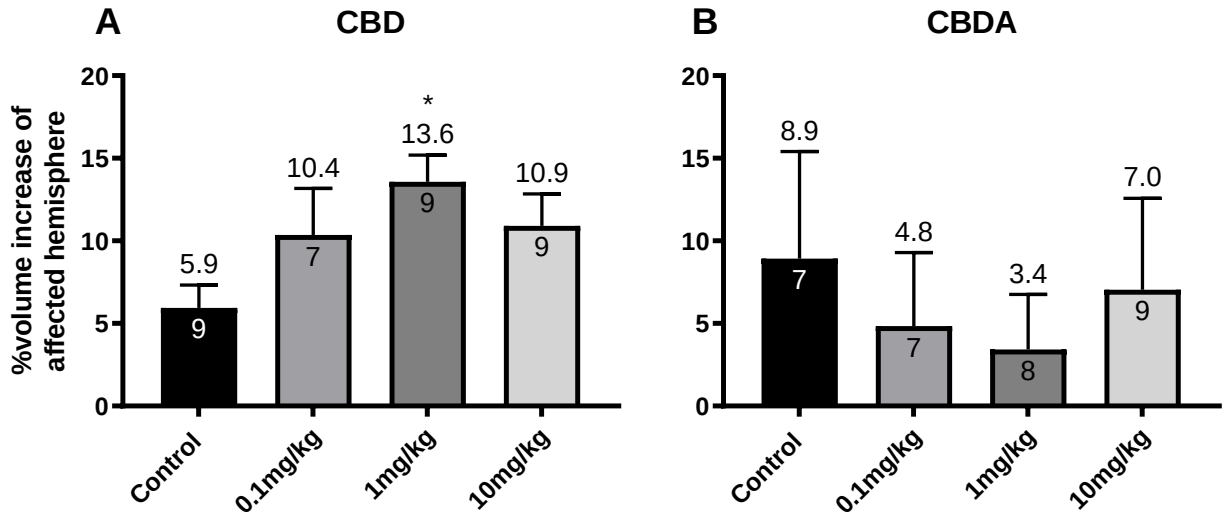


Figure 3.4 The effect of CBD (A) or CBDA (B)on the space-occupying effect 24 h following pMCAO. Data is presented as % volume increase of hemisphere with standard deviation. Numbers inside bars display sample size for each experimental group, and numbers above bars display the mean result for each condition. Data was compared against vehicle for statistical significance against vehicle using a one-way ANOVA. * $p \leq 0.05$.

3.4 **Discussion**

Current literature has indicated CBD possess efficacy in animal models of stroke, where reperfusion takes place. This study aimed to investigate the effects of CBD and CBDA in the absence of reperfusion by permanent occlusion of the MCA and to use a clinically relevant route of administration (iv). The results indicated 24 h following pMCAO CBD, or CBDA delivered intravenously 20 minutes post-insult has no effect on infarct volume in mice. The results, however, did demonstrate that CBD could increase brain water content following the insult, indicating an increase in vasogenic swelling. However, this data should be interpreted with caution as brain water content was not directly measured and indirectly assessed using the formula from Gerriets and colleagues (Gerriets *et al.*, 2004). Thus, the formula's accuracy depends on how accurately the variables used were measured and is therefore susceptible to human errors, e.g., not mounting the brain square when taking MRI images. In conclusion, this study suggests CBD and CBDA delivered intravenously are ineffective at treating stroke injuries without reperfusion.

Considering this study conflicts with existing literature, which has demonstrated a protective effect for CBD in rodent models of stroke (Hayakawa *et al.*, 2004, 2008; Mishima *et al.*, 2005; Hayakawa, Mishima, Nozako, Hazekawa, *et al.*, 2007; Hayakawa, Mishima, Nozako, Ogata, *et al.*, 2007; Khaksar and Bigdeli, 2016, 2017c, 2017a, 2017b; Mori *et al.*, 2017; Rodríguez-Muñoz *et al.*, 2018). Differences in the experimental design must be carefully considered. Most studies showing a protective effect for CBD have done so in models that temporarily occlude the MCA. Temporary occlusion allows for a period of reperfusion in which cerebral blood flow can return to the affected tissues. In permanent occlusion models, cerebral blood flow to the ischemic core is practically absent (Reichenbach *et al.*, 2016). However, neuroprotective drugs that prove protective in the penumbral region could reduce the eventual size of the infarct if assessed at later timepoints (>24 h). Indeed as time progresses, the ischemic core begins to extend into penumbral regions, which still receive moderate levels of CBF—giving neuroprotective drugs a chance to prove protective in permanent models of occlusion (Paciaroni, Caso and Agnelli, 2009).

While reperfusion represents an event required for long-term functional tissue recovery, it is also an event in which further tissue damage occurs. The source of this damage can be partially attributed to increased ROS production due to the return of oxygen, which leads to the depletion of antioxidants supplies, programmed cell death mechanisms and necrosis (Eltzschig and Eckle, 2011). Therefore, it could be CBD

and CBDA applied post-stroke predominately target molecular events associated with this period of damage, and a lack of reperfusion could cause an absence of a protective effect. Whilst there is one other experiment demonstrating protective effects of CBD following permanent occlusion of the MCA (Rodríguez-Muñoz *et al.*, 2018), this study utilised an intraperitoneal (ip) route of administration.

It is also recognised that higher concentrations are needed for a drug to achieve efficacy in a permanent model (Sydserff *et al.*, 2002). Thus, the results from our experiment could indicate the concentrations of drugs used were too low and without adequate reperfusion of the tissue; there is insufficient drug reaching the damaged tissue. In this respect, the effects of collateral blood flow must be considered, as this will ultimately affect the amount of blood and subsequently drug reaching the affected region. Collateral blood flow can restrict penumbra growth by supplying the deprived area with blood; however, collateral blood flow displays high inter-subject variability in mice and humans (Zhang *et al.*, 2010; Campbell *et al.*, 2013). In mice, the expression of two genes, Vascular Endothelial Growth Factor-A (VEGF-A) and Chloride intracellular channel-4 (Clic4), were found to influence the formation of the collateral circulation strongly, and subsequently the severity of stroke (Clayton, Chalothorn and Faber, 2008; Chalothorn *et al.*, 2009). Another study showed that the same type of mice (Swiss albino mice) used in this study had a small number of native collateral blood vessels. These mice showed poor ability to form new vessels following MCAO, associated with worse outcomes (Zhang *et al.*, 2010). Thus, differences in collateral blood flow determined by genetic variations between breeds may potentially affect drug delivery via iv in pMCAO models of stroke and should be considered when conducting studies using permanent occlusion.

No studies thus far have examined the effect of CBD or CBDA delivered via iv in animals' models of stroke, which is likely to be the most clinically relevant route of administration in the acute stage of treatment. Since CBDA is more potent at the 5HT1A receptor (Bolognini *et al.*, 2013) and the protective effects in models of stroke are primarily mediated by this receptor (Mishima *et al.*, 2005), one would expect to see a protective effect of CBDA at lower concentrations relative to CBD (Hayakawa, Mishima, Nozako, Hazekawa, *et al.*, 2007). As other studies have shown efficacy at lower concentrations, it is unlikely the concentrations of drugs were sub-efficacious. Suggesting the primary reason for an absence of effect was that the drug could not reach the target tissues due to low collateral blood flow in the species of mice used.

Future studies using iv routes of administration should use temporary occlusion models or examine a broader range of concentrations, time-points and endpoints to gain a more accurate insight into the effects of CBD and CBDA where reperfusion has not taken place. These studies should examine sensory-motor functions later and assess these same endpoints in temporary and permanent MCAO models. As it could be with increased time-points, drugs may display efficacy in reducing sensory-motor deficits even in models where reperfusion does not occur. Studies should also include aged and female animals and animals with co-morbidities to gauge the pharmacology of CBD and CBDA in a representative population.

In conclusion, this study demonstrated that without adequate reperfusion CBD and CBDA applied 20 minutes intravenously following permanent occlusion of the MCA has no effect on infarct volume.

4 The effects of CBD, CBGV, CBC and CBDV in astrocytes exposed to oxygen-glucose deprivation and reperfusion injury

4.1 Introduction

Astrocytes play several protective roles in response to ischemia-reperfusion injury, including glutamate uptake, spatial buffering of ions, scavenging free radicals and maintaining blood-brain barrier (BBB) integrity (Sofroniew and Vinters, 2010; Pekny, Wilhelmsson and Pekna, 2014). Thus, therapies that promote astrocyte survival and homeostatic function following cerebral ischemic/reperfusion injury may reduce infarct volume and improve neurological outcomes.

Correct mitochondrial function is crucial for cellular energy metabolism, signalling, and apoptosis (Friedman and Nunnari, 2014). During ischemic conditions, a dramatic reduction in oxygen and glucose reduces the cells' ability to perform oxidative phosphorylation (Gourdin and Dubois, 2013). Under these conditions, cells solely rely on glycolysis to metabolise remaining energy substrates. Leading to increased free radical production and acidification from lactate production through glycolysis (Gourdin and Dubois, 2013). Ultimately, this leads to the opening of the mitochondrial permeability transition pore (mPTP), causing a loss of mitochondrial membrane potential and liberation of cytochrome C. Cytochrome C then activates Caspase 3 & 9 leading to leading to apoptosis (Jiang and Wang, 2004). Thus therapies that prevent mitochondrial dysfunction during and following ischemic injury could improve clinical outcomes.

To date, there are limited data on the effects of phytocannabinoids other than CBD on mitochondrial function. CBD affects mitochondrial function at high micromolar concentrations leading to apoptosis (Massi et al., 2004; Rimmerman et al., 2013; Shrivastava et al., 2011; Singh et al., 2015; Rimmerman, 2013). However, many of these studies are conducted in cancer cells lines, and lower concentrations of CBD were not used. However, some studies have shown CBD to be protective of mitochondrial function. For example, CBD improved the toxic effects of Doxorubicin (DOX) on cardiac mitochondrial function (Hao et al., 2015) and normalised mitochondrial fission protein DNM1L expression levels in rats with brain iron overload (Da Silva *et al.*, 2014). Ryan and colleagues showed protective effects of 100 nM CBD against mitochondrial stress in rat hippocampal cells by reducing intracellular Ca^{++} condition in high excitability conditions (Ryan, Alison J. Drysdale, *et al.*, 2009).

Interestingly when neurons were no longer subject to high excitability conditions, CBD produced the opposite effect and slightly increased intracellular Ca^{++}. Thus, the effects of phytocannabinoids on mitochondrial function are likely to differ in pathological and physiological settings.

The ability of CBD to modulate intracellular Ca^{++} has been shown to involve interactions with the mitochondrial sodium-calcium (Na^{+}-Ca^{++}) exchanger (NCX) (Ryan, Alison J. Drysdale, *et al.*, 2009). These effects on intracellular Ca^{++} could provide protection against several molecular events associated with stroke, i.e., the opening of the permeability transition pore, increases in Ca^{++} mediated by glutamate uptake, and activation of various inflammatory pathways (Ryan, Alison J. Drysdale, *et al.*, 2009; Furman and Norris, 2014; O'Donnell, Jackson and Robinson, 2016).

Other groups have investigated the effects of CBD on mitochondria in an oxygen-glucose deprivation/reperfusion (OGD/R) model using hippocampal neurons (Sun *et al.*, 2017). In this study, OGD/R caused a significant decline in basal mitochondrial respiration, ATP linked oxygen consumption rate, maximum respiration, and spare respiratory capacity. CBD attenuated these changes and increased the activity of the pentose-phosphate pathway, a branch of glycolysis associated with enhancing antioxidant defences. Using the same endpoints, the authors of this study examined the effects of CBD in a normoxic setting and demonstrated that CBD significantly increases basal mitochondrial respiration, ATP linked oxygen consumption rate, maximum respiration, and spare respiratory capacity. However, the pentose-phosphate pathway remained unchanged. This work suggests CBD partially mediates its neuroprotective effects through interactions with mitochondria, raising the possibility that other phytocannabinoids could.

The meta-analysis conducted in chapter 2 indicated CBD possessed beneficial effects in animal models of stroke, suggesting that other phytocannabinoids could produce similar effects. In chapter 3, experiments failed to reproduce the effects of CBD established in rodent models of stroke by Hayakawa and Khaksar (Hayakawa *et al.*, 2004, 2008, 2009; Mishima *et al.*, 2005; Hayakawa, Mishima, Nozako, Ogata, *et al.*, 2007; Hayakawa, Mishima and Fujiwara, 2010; Khaksar and Bigdeli, 2016, 2017a, 2017c, 2017b). Thus the overall aim of this study was to use a cellular model of stroke to investigate whether other phytocannabinoids could be suitable for *in vivo* testing.

- The first aim of the present study was to assess the effects of a range of phytocannabinoids (CBD, CBGV, CBC and CBDV) on various markers of

mitochondrial function and NAD(P)H-dependent oxidoreductase enzymes in human astrocytes in normoxic and hypoxic (after a 4 h oxygen-glucose deprivation (OGD) protocol conditions.

- The second aim of this study was to assess how the duration of OGD affects the magnitude of damage produced by an OGD/R protocol in astrocytes by comparing a 4 h vs an 8 h OGD protocol. Additionally, extending the time points into several days post-OGD to establish the best window for assessing cell damage. Once selecting a suitable duration of OGD in human astrocytes, experiments sought to investigate the effects of a range of novel phytocannabinoids (CBDV, CBC and CBGV) compared with CBD effects.

- Experiments also compared the impact of PRE-versus POST application of the phytocannabinoids to assess the effects of these compounds during the ischemic and reperfusion phases of cell damage.

4.2 Methods

4.2.1 Cell culture and oxygen-glucose deprivation/reperfusion (OGD/R) conditions

Human brain astrocytes (ScienCell, USA) were maintained in a humidified cell culture incubator at 37^{o}C with 5% CO_2 and cultured to 70-80% confluence in a T75 flask using specialised human astrocyte medium (ScienCell, USA). Media was changed every two to three days until cells reached 70-80% confluence. At which point cells were seeded at 20,000 cells/cm^2 in a 96-well plate. Once confluent, cells were incubated for 24 h to establish baseline samples. Cells were then exposed to oxygen-glucose deprivation/reperfusion (OGD/R) for 4 or 8 h as a stroke model. For these conditions, media was replaced with RPMI glucose-free media (Invitrogen, USA), and plates were sealed into GasPak EZ Anaerobe Pouches (Beckton Dickinson, UK) and returned to the incubator. The pouches used produce an anoxic environment within 20 minutes of placing the cell plate in the bag (Hind, England and O'Sullivan, 2016).

4.2.2 Drugs

Phytocannabinoids CBD, CBDV, CBGV, and CBC were supplied by GW pharmaceuticals and stored as 10 mM stocks in ethanol at stored at -80°C.

4.2.3 Lactate dehydrogenase (LDH) assay

The LDH assay (LDH-Cytotoxicity Assay Kit, Abcam, USA) was used to assess the extent of cell damage at each time point measured. LDH is a ubiquitously expressed cytosolic oxidoreductase enzyme, that catalyses pyruvate's interconversion to lactate and NAD^+ to NADH.

Since LDH is a relatively stable enzyme, its presence outside of a cell reflects a compromised cell membrane, an event associated with cell damage. By utilising the reaction of LDH reducing NAD^+ to NADH, extracellular NADH can react with a specific probe to generate a yellow colour (λmax = 450 nm). The degree of colour change directly correlates with the amount of LDH present in each media sample and cell damage. The activity was measured according to the manufactures instructions (abcam102526) using a Thermo MultiSkan spectrum plate reader running Skanit

software 2.2.

4.2.4 Multiplex analysis of mitochondrial complex protein expression

The multiplex Oxidative Phosphorylation kit (ThermoFisher, USA) allows for the simultaneous quantification of all five mitochondrial protein complex's involved in oxidative phosphorylation; Complex I (NADH- ubiquinone oxidoreductase), Complex II (succinate ubiquinone oxidoreductase), Complex III (ubiquinone cytochrome c oxidoreductase), Complex IV (cytochrome C oxidase), Complex V (ATP synthase) and Nicotinamide nucleotide transhydrogenase (NNT), which is an integral protein of the inner mitochondrial membrane. The assay only detects intact, and therefore functionally operational complexes rather than any single subunits, meaning the expression correlates well with the functional activity (Zheng, 2012).

4.2.5 MTS assay

Cellular metabolism was measured using the CellTiter 96® AQueous One Solution Cell Proliferation Assay (Promega, UK). The reagent solution was added at the end of each respective experiment. MTS is metabolised by cells into a coloured formazan product. Dehydrogenase enzymes carry out this reaction in viable cells. Following incubation for 1 h, absorbance is read at 490nm using a Thermo MultiSkan Spectrum plate reader.

4.2.6 Enzyme-linked immunosorbent assay of IL-6

To assess the inflammatory response caused by OGD/R, the secretion of Interleukin-6 (IL-6) was measured using an ELISA IL-6 kit (R&D Systems, UK) via colourimetric measurements. Corning® 96 well EIA/RIA plates are used for this assay, as they possess high binding plastic on the bottom of each well to improve binding between the plastic and the secondary antibody. The first step involves coating the bottom of each well in a capture antibody specific for IL-6 and leaving the plate at 4^{o}C overnight. The next day each well is blocked for 1 h using 1% bovine serum albumin to reduce non-specific binding. In the next step, quality controls, standards and samples of

interest are added to wells and left for 2hours to bind with the capture antibody. A detection antibody is then added to the wells, which binds the analyte-capture antibody complex, ‘sandwiching’ the molecule of interest between two antibodies. Streptavidin horseradish peroxidase (HRP) is then added to each well; HRP binds the detection antibody and boosts the signal by increasing the binding capacity of Streptavidin. Next, TMB is added to each well; this soluble molecule forms a coloured product. The degree of colour change is directly proportional to the amount of IL-6 present in each well. Finally, 50µl of the stop solution 2N H_2SO_4 is added to each well, and absorbance is measured immediately using a Thermo MultiSkan Spectrum plate reader at 490nm. Readings obtained at 540nm were subtracted from the results to account for plate imperfections.

4.2.7 BCA

The BCA assay is a biochemical assay used to quantify the total protein concentration in each sample (Abcam, USA). Cu^{2+} ions from copper sulphate reduce to Cu^{+} ions in the presence of peptide bonds, which are present between proteins. In this reaction, two molecules of bicinchoninic acid chelate with each Cu^{+} ion, forming a purple-coloured complex that strongly absorbs light at a wavelength of 562 nm.

4.2.8 Experimental procedures for investigating the effects of CBD, CBGV, CBC and CBDV in astrocytes exposed to 4 h OGD

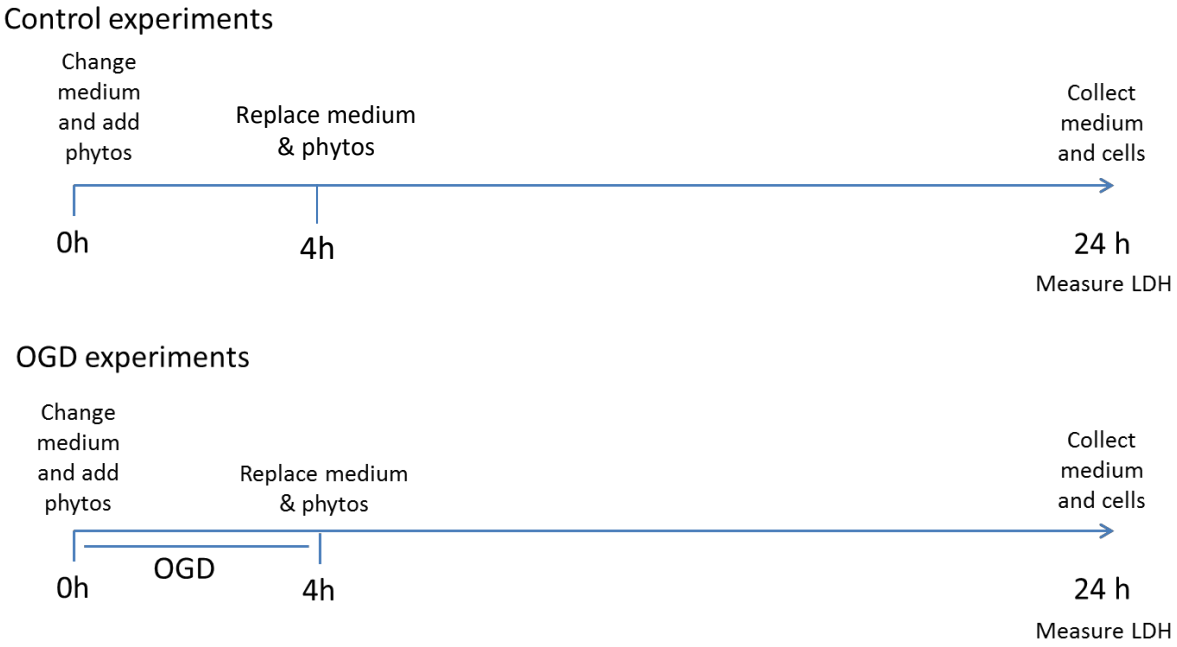


Figure 4.1 schematic diagram of experimental procedure for astrocytes exposed to 4 h OGD and CBD, CBGV, CBC and CBDV

In the control experiment (figure 4.1), fully confluent human astrocytes (P3 and P4, n=6, from two separate experiments) were treated with phytocannabinoids at 10 nM, 100 nM, 1 µM and 10 µM for 4 h. At that point, the medium was changed, and cells were incubated for a further 20 h. Following 24 h incubation, media and cell lysates were collected and frozen at -80°C for later analysis.

In OGD experiments (figure 4.1), fully confluent human astrocytes (P3 and P4, n=6, from two separate experiments) were treated with phytocannabinoids and placed in OGD conditions for 4 h. Following this cells were returned to normoxic conditions and replaced with regular astrocyte medium containing fresh phytocannabinoids. 20 h later, the medium was collected and frozen at -80°C for later analysis.

At 24 h MTS was added to wells to assess cellular metabolism. LDH assays were carried out on media samples obtained from a 24 h time-point. Cell lysates were washed in PBS, collected in RIPA buffer at the 24 h time-point, and frozen at -80°C. BCA and mitochondrial complex protein assays were carried out on cell lysates

4.2.9 The effects of a 4 h and 8 h OGD protocol on astrocytes

Fully confluent astrocytes were placed in 0% oxygen and 0% glucose conditions for 4 h or 8 h (figure 4.2). Following this, cells were returned to normoxic conditions (atmospheric O_2, 5% CO_2 + glucose) until 72 h. Baseline samples were obtained by taking media samples from cells left in media for 24 h before initiating the OGD protocol. LDH and IL-6 assay were carried out on media samples obtained from all time points measured. Cell lysates were washed in PBS, collected in RIPA buffer at the 72 h time-point, and frozen at -80°C. BCA and mitochondrial complex protein assays were carried out on cell lysates.

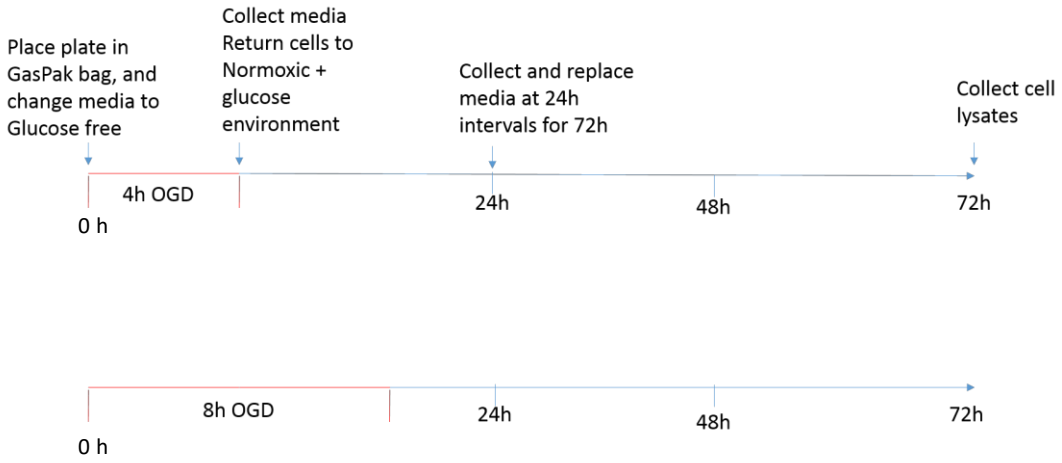
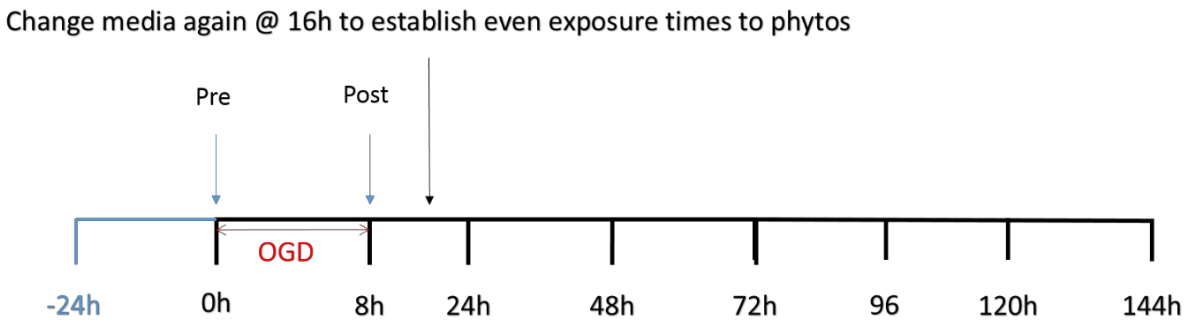


Figure 4.2 schematic diagram of experimental procedure for astrocytes exposed to 4 h OGD and 8 h OGD

4.2.10 The effects of phytocannabinoids on human astrocytes exposed to OGD using prophylactic and therapeutic strategies

Fully confluent astrocytes were placed in 0% oxygen and 0% glucose conditions for 8 h. Following this, cells were returned to normoxic conditions (atmospheric O_2, 5% CO_2 + glucose) for 144 h (figure 4.3). Baseline samples were obtained by taking media samples from cells left in media for 24 h before initiating the OGD protocol. LDH and IL-6 assays were carried out on media samples obtained from all time points



measured. Cell lysates were washed twice in PBS, collected in RIPA buffer at the 144 h time-point, and frozen at -80°C. BCA (protein assays) were performed on cell lysates collected at the end of the experiment.

Figure 4.3 Schematic diagram of the experimental protocol. Baseline samples were taken 24h before the OGD protocol. "Pre" and "post" depict where drugs were administered. Media was changed again at 16 h (see arrow) to ensure cells were exposed to the drugs for an even period of time (because in the POST-treatment protocol, the drugs were removed after 8 h to match the PRE-treatment drug exposure time). Total length of experiment = 160h.

4.2.11 Data analysis

Data were analysed using Graphpad Prism 8. Data were tested for normality using Shapiro-Wilk; normally distributed data are presented as mean ± SEM. Using one-way ANOVA with Dunnett's multiple comparison test, data were analysed to detect statistically significant changes between groups and conditions. Time-course data were analysed using a two-way ANOVA and Dunnett's multiple comparison test to see statistically significant differences between groups and conditions. A p-value less than <0.05 was considered statistically significant.

4.3 Results

4.3.1 The effects of CBD, CBGV, CBC or CBDV in astrocytes exposed to 4 h OGD or normoxic conditions

Cell damage (LDH)

OGD protocol

Comparing normoxic control and OGD vehicle demonstrated that the 4 h OGD had no significant effect on LDH levels (figure 4.4).

CBD

24 h treatment with CBD 10 μM increased LDH levels by 68% ±17.2 ($p < 0.01$) in normoxic conditions and by 401 ±15.8 ($p < 0.0001$) in OGD conditions relative to the corresponding vehicle control (figure 4.4A). When compared between conditions, CBD 10 μM significantly increased LDH levels by 333% ±16.4 ($p<0.0001$) more in OGD conditions relative to normoxic conditions (figure 3.1A).

CBGV

24 h treatment with CBGV in OGD conditions had no significant effect on LDH at any concentration tested compared to its corresponding control. In normoxic conditions, CBGV 10 μM increased LDH levels by 80% ±21 ($p<0.01$) relative to normoxic control (figure 4.4B). When CBGV was compared across conditions (normoxic vs. OGD) at corresponding concentrations LDH was increased by 88% ±21.5 ($p<0.001$) at 100 nM, 73% ±26 ($p<0.01$) at 1 μM, and 64% ±28.3 ($p<0.05$) at 10 μM (figure 3.1B).

CBC

In OGD conditions, 24 h exposure to CBC 10 μM significantly increase LDH by 122% ±23 ($p<0.0001$) (figure 4.4C). No other statistically significant effects were present.

CBDV

There was no significant interaction between concentrations or conditions on LDH levels (figure 4.4D).

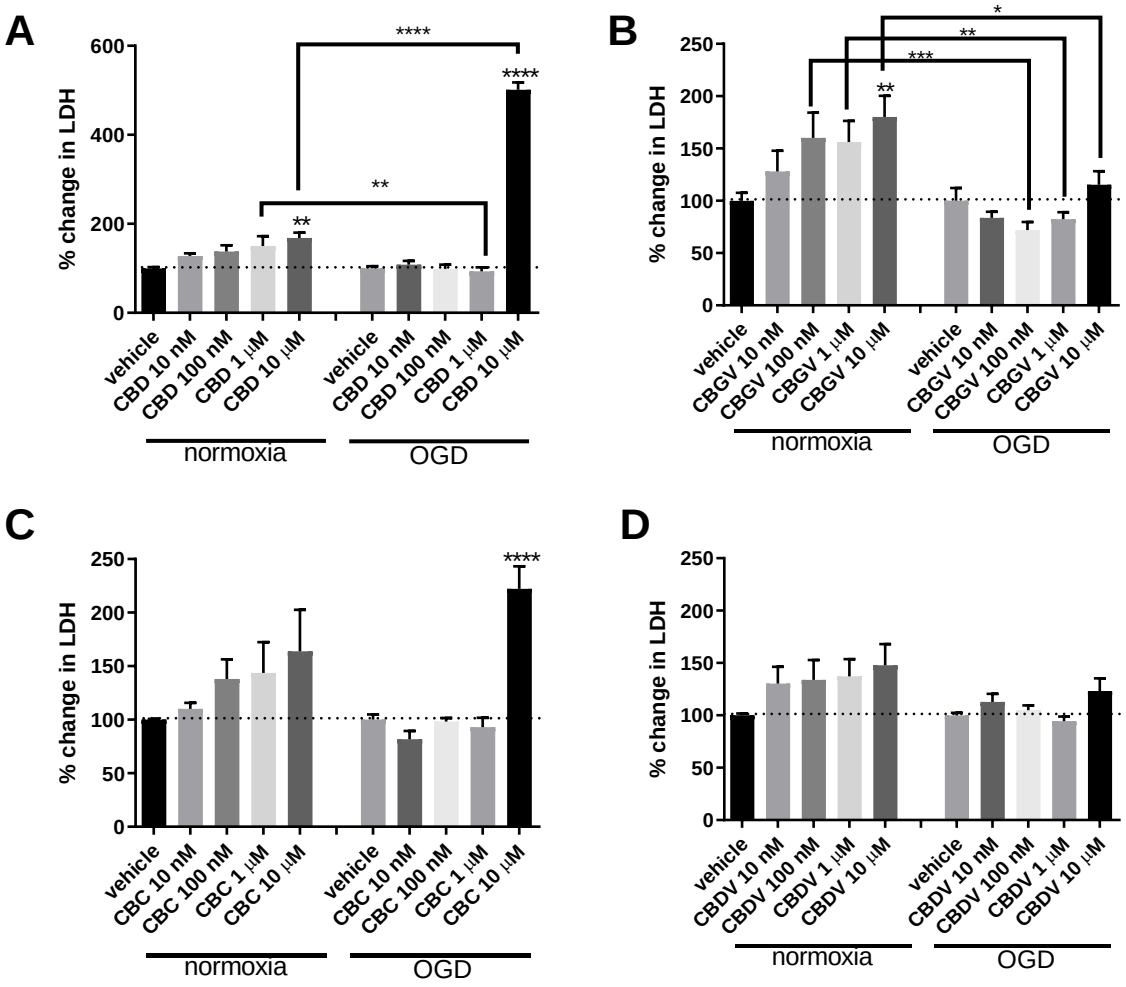


Figure 4.4 Histograms representing the change in LDH levels from vehicle control in either normoxic or 4 h OGD conditions following 24-hour treatment with CBD (A), CBGV (B), CBC (C) or CBDV (D). Data are presented as mean ± SEM (n=6-7). Data were analysed by two-way ANOVAs with multiple comparisons **p<0.01, ***p<0.001, ****p<0.0001 vs their respective vehicle, or as indicated by connecting lines

Mitochondrial complex protein levels in normoxic and 4 h OGD conditions

OGD protocol

All vehicle-treated cells (n=32) were combined to assess how OGD/R protocol affected the presence of intact mitochondrial complex expression. Data were normalised to the NNT protein levels; OGD significantly reduced the mean fluorescence intensity of mitochondrial complex I, II, III and IV ($p = 0.013$, $p = 0.0002$, $p < 0.0001$, and $p = 0.013$, respectively relative to normoxic control (figure 4.5A-E).

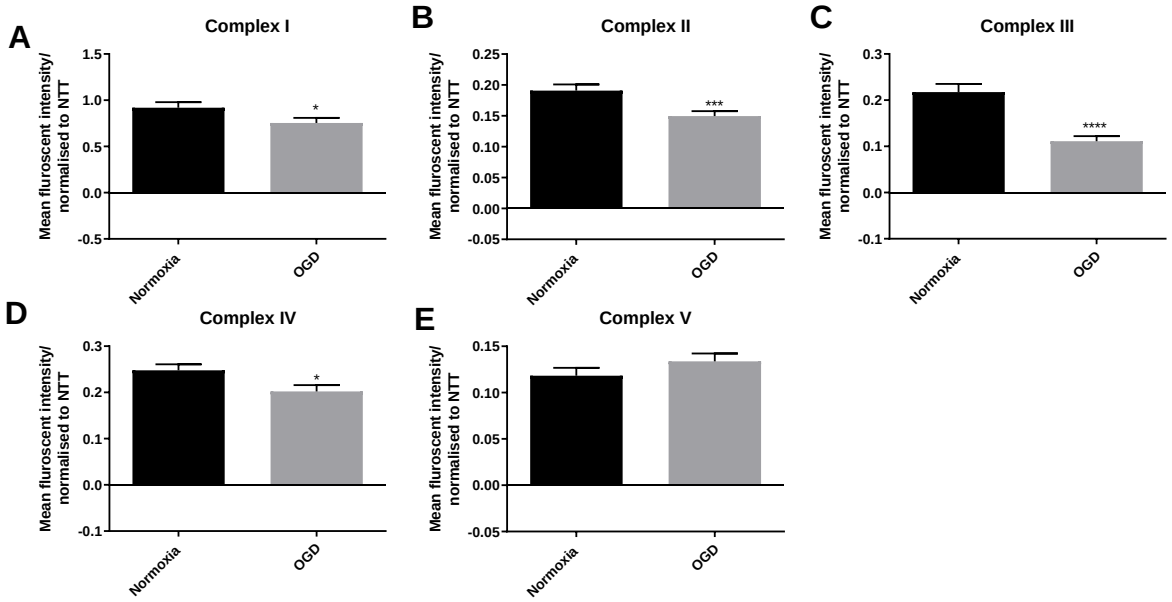


Figure 4.5 The effects of a 4 h OGD protocol on mitochondrial complex proteins normalised to NNT protein levels. Mitochondrial complex proteins complex I (A), complex II (B), complex III (C), complex IV (D), complex V (E) Data are presented as mean SEM and analysed using Mann-Whitney tests within each mitochondrial complex. *p<0.05, ***p<0.001, ****p<0.0001 vs normoxia.

CBD

In normoxic conditions CBD 100 nM and 10 μM significantly decreased the expression of mitochondrial Complex I protein levels relative to its corresponding normoxic control by 0.27 ±0.1 ($p<0.001$) and 0.73 ±0.18 ($p<0.001$) (figure 4.6A). CBD had no significant effect on the expression of any of the mitochondrial complex proteins tested in OGD conditions (figure 3.3B). There were no significant differences between CBD in normoxic and OGD conditions at any of the respective concentrations and mitochondrial complex proteins (figure 3.3A-B).

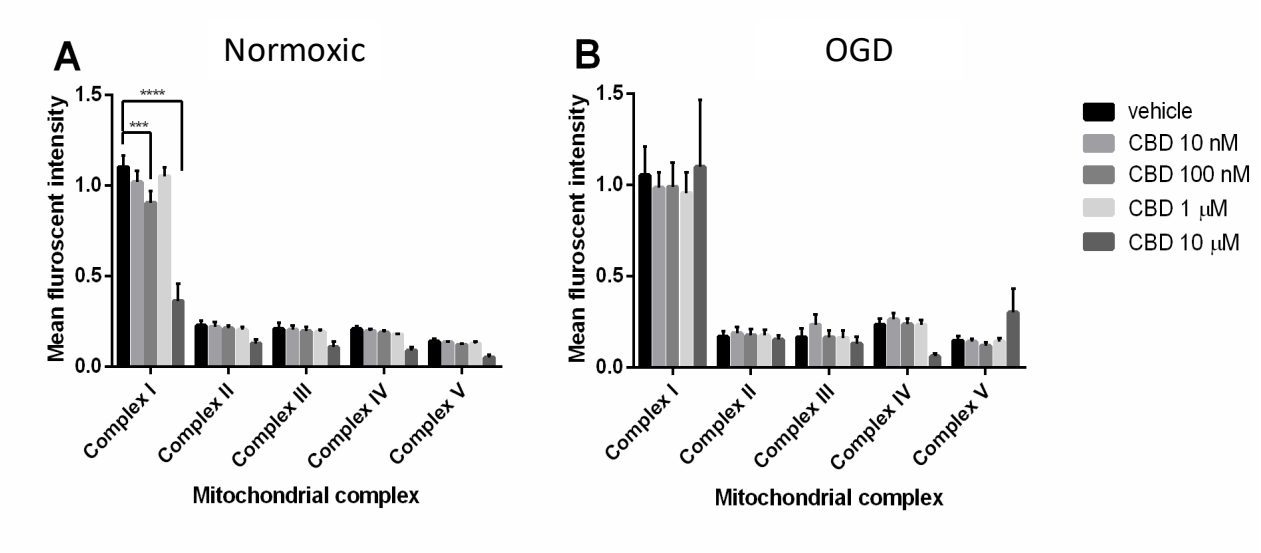


Figure 4.6 Histograms representing the effects of CBD in normoxic (A) or 4 h OGD (B) conditions. Astrocytes (p6) were exposed to CBD for 24 hours, following which mitochondrial complex proteins levels were assessed. Data are presented as mean SEM (n = 6 per group, from two separate experiments) and are normalised to NNT. Data were analysed by two-way ANOVAs and multiple comparisons between groups.

CBGV

CBGV had no significant effects in either OGD or normoxic conditions at any of the concentrations tested (figure 4.7A-B). There were no significant differences between CBGV in normoxic and OGD conditions at any of the respective concentrations and mitochondrial complex proteins (figure 4.7A-B).

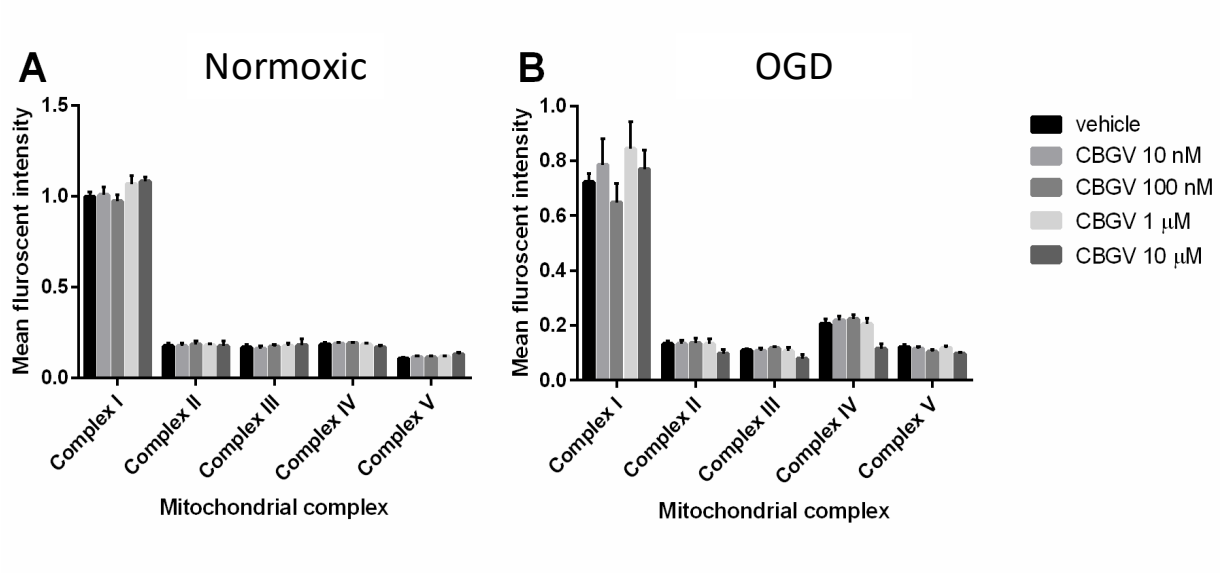


Figure 4.7 Histograms representing the effects of CB in normoxic (A) or 4 h OGD (B) conditions. Astrocytes (p6) were exposed to CBGV for 24 hours, following which mitochondrial complex proteins levels were assessed. Astrocytes. Data are presented as mean fluorescent intensity SEM (n = 6 per group, from two experiments). Data were analysed by two-way ANOVAs and multiple comparisons between groups.

CBC

CBC had no significant effects in either OGD or normoxic conditions at any concentrations tested (figure 4.8A-B). There were no significant differences between CBC in normoxic and OGD conditions at any respective concentrations and mitochondrial complex proteins (figure 4.8A-B).

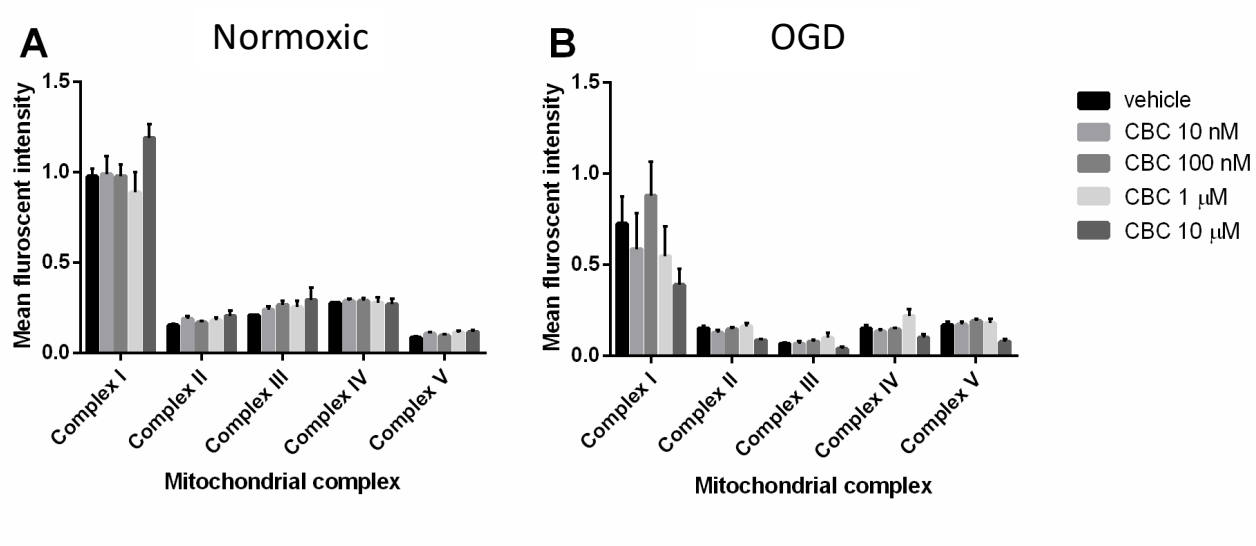


Figure 4.8 Histograms representing the effects of CBC in normoxic (A) or 4 h OGD (B) conditions. Astrocytes (p6) were exposed to CBC for 24 hours, following which mitochondrial complex proteins levels were assessed. Astrocytes. Data are presented as mean SEM (n = 6 per group, from two separate experiments) and are normalised to NNT. Data were analysed by two-way ANOVAs and multiple comparisons between groups.

CBDV

CBDV did not affect mitochondrial complex protein expression in normoxic conditions (figure 4.9B). In OGD conditions, 10 µM CBDV increased the mean fluorescent intensity of mitochondrial complex protein expression I by 0.32 ±0.14 ($p<0.001$) (figure 4.9B). There were no significant differences between CBGV in normoxic and OGD conditions at any respective concentrations or mitochondrial complex protein expression levels (figure 4.9A-B).

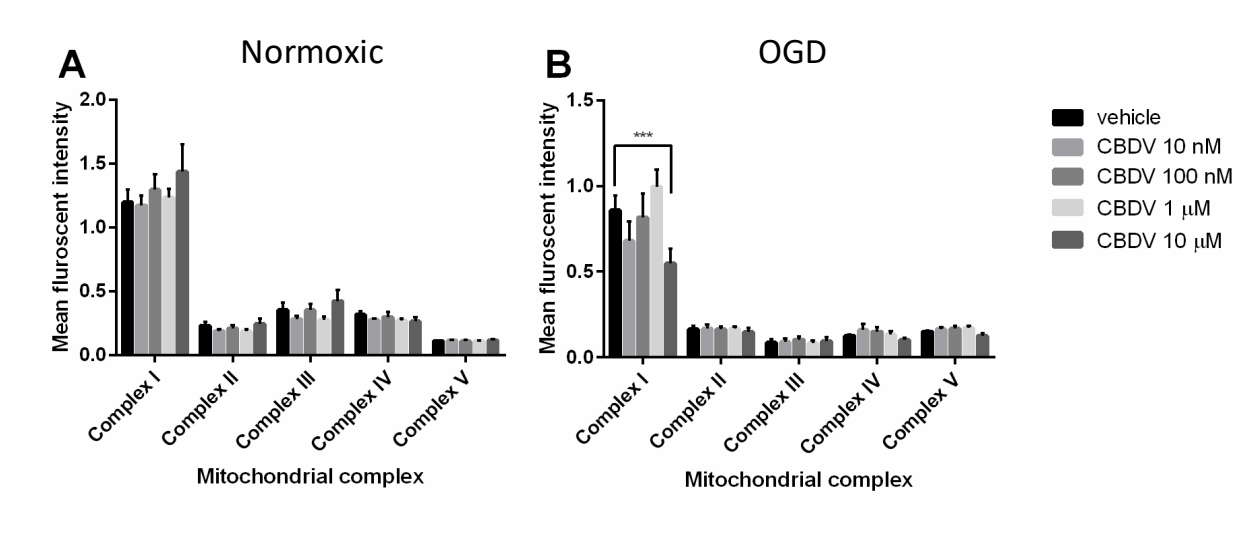


Figure 4.9 Histograms representing the effects of CBDV in normoxic (A) or 4 h OGD (B) conditions in astrocytes. Astrocytes (p6) were exposed to CBDV for 24 hours, following which mitochondrial complex proteins levels were assessed. Astrocytes. Data are presented as mean SEM (n = 6 per group, from two separate experiments) and are normalised to NNT. Data were analysed by two-way ANOVAs and multiple comparisons between groups.

Cellular metabolism (MTS)

OGD protocol

The 4 h OGD protocol caused a significant increase in cellular metabolism of 5% ±1.5 ($p<0.05$) (figure 4.10)

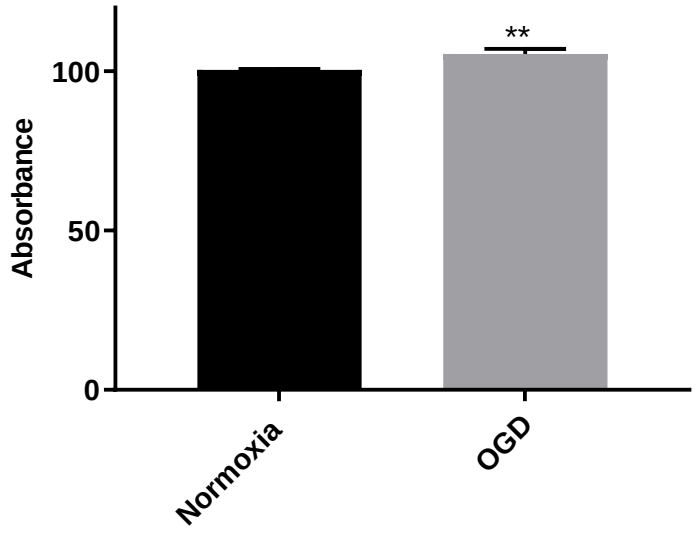


Figure 4.10 Data are presented as mean SEM (n = 22 - 24 per condition, from two separate experiments). Data were analysed for statistical significance by unpaired t-test.

CBD, CBGV, CBC and CBDV

24 h treatment with any of the phytocannabinoids at any of the concentrations tested had no significant effect on cellular metabolism. There were also no significant interactions between any of the phytocannabinoids at their corresponding concentrations when compared between conditions (normoxic vs. OGD) (figure 4.11A-D).

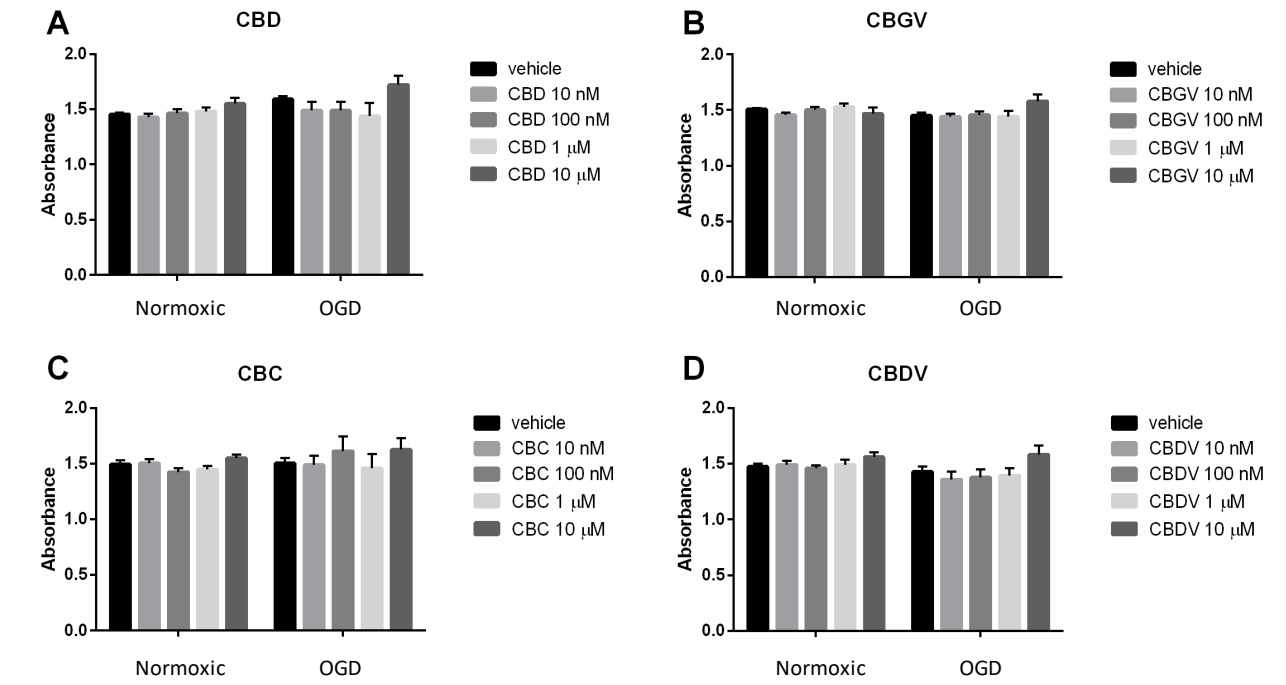


Figure 4.11 Histograms representing the effects of CBD (A), CBGV (B), CBC (C), or CBDV (D) 24-hour exposure on cellular metabolism in astrocytes (p6) following either normoxic or 4 h OGD protocol. Data are presented as mean SEM (n = 6-12, from two separate experiments). Data were analysed by two-way ANOVAs and multiple comparison between concentrations and conditions.

4.3.2 The effects of a 4 and 8 h OGD protocol on total protein, LDH, IL-6, total protein, and mitochondrial complex protein expression

Total protein content (BCA)

To better assess the extent to which phytocannabinoids protect against OGD/R injury, the duration of OGD was extended by 4 h. Both 4 and 8 h OGD protocols caused a significant reduction in total protein measured in the cell lysates at 72 h by 33% ±9.3 ($p<0.01$) in 4 h OGD and by 68% ±9 ($p<0.0001$) relative to normoxic control. When compared against each other, the 8 h OGD caused a 35% ±8.7 ($p<0.01$) reduction in total protein compared to the 4 h OG (figure 4.12).

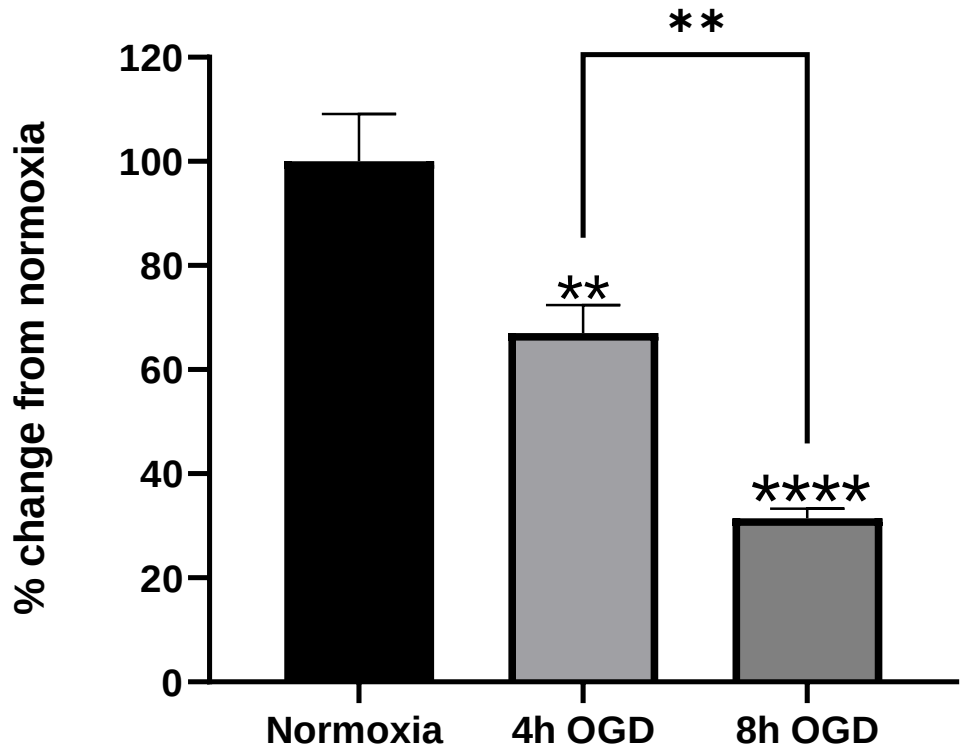


Figure 4.12 The effect of a 4 h or 8 h OGD protocol on the total protein of fully confluent human astrocytes (P5), as measured 72h post-OGD. Data are presented as mean ± SEM (n=10), from two separate experiments. Data were analysed by Student's t-test with multiple comparisons between the groups. **p<0.01, ****p<0.0001 vs. normoxia, or as indicated by connecting lines

Cell damage (LDH)

Increasing the duration of a 4 h OGD to 8 h did not significantly affect LDH levels at their respective time points between OGD conditions. Following a 4 h OGD protocol LDH levels significantly increased by 32% ±4.7 ($p<0.05$) post-OGD, 23%% ±1.4 ($p<0.01$) at 48 h and 47% ±8.6 ($p<0.05$) at 72 h relative to baseline (figure 4.13). The 8 h OGD protocol significantly increased LDH levels by 39% ±3.7 ($p<0.05$) post-OGD, 13% ±2 ($p<0.05$) at 48 h and 32% ±4.7 ($p<0.01$) at 72 h relative to baseline (figure 4.13). No significant effect was present between the two conditions at their corresponding time points.

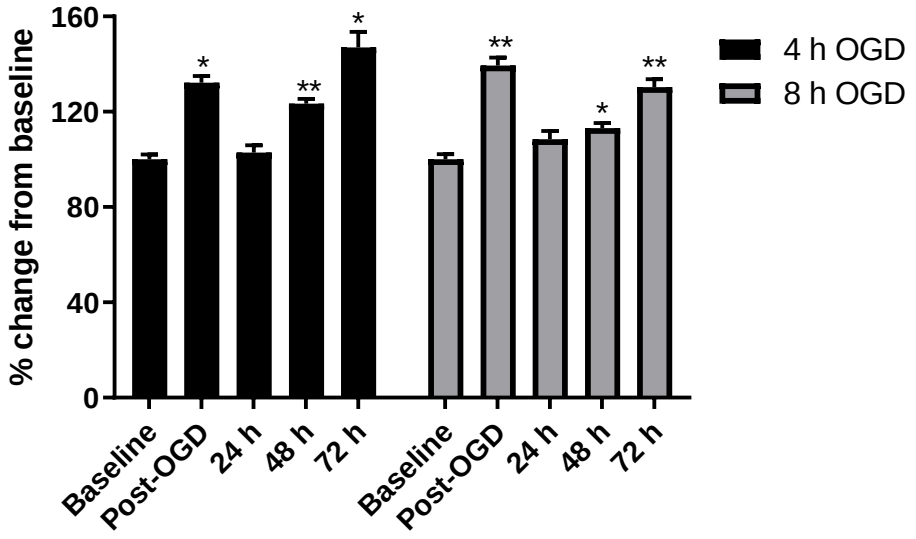


Figure 4.13 Histograms showing the effect a 4 h or 8 h OGD protocol has on fully confluent human astrocyte (P5-7) LDH concentrations at 24hr intervals and immediately post OGD (4 h or 8 h). Data are presented as mean ± SEM (n=4, from two separate experiments). Data were analysed by a two way ANOVA followed by multiple comparisons between corresponding time-points between conditions. *p<0.05, ***p<0.001, ****p<0.0001 vs their respective baseline groups.

IL-6

Following 4 h OGD, significant changes in IL-6 level were observed at all-time points, post-OGD IL-6 levels were decreased by 58% ±6 ($p<0.05$) relative to baseline (figure 4.14). At all other time points in the 4 h OGD protocol, IL-6 was increased by 53% ±7.1 ($p<0.05$) at 24 h, 110% ±7.9 ($p<0.0001$) at 48 h and 54% ±9.3 ($p<0.05$) at 72 h relative to the corresponding baseline control (figure 4.14). The 8 h OGD protocol also produced significant differences in IL-6 concentration, at all time-points except 24 h. At post-OGD IL-6 levels were decreased by 58% ±6.5 ($p<0.05$) relative to baseline (figure 4.14). At other time points in the 8 h OGD protocol, IL-6 was increased 95% ±20.9 ($p<0.0001$) at 48 h and 132% ±24.6 ($p<0.0001$) at 72 h relative to the corresponding baseline control (figure 4.14).

When time-points were compared across conditions (4 h vs 8 h), the 72h time-point in 8 h OGD protocol was significantly increased relative to the 72 h time-point in the 4 h OGD protocol by 77% ±21.9 ($p<0.01$) (figure 4.14).

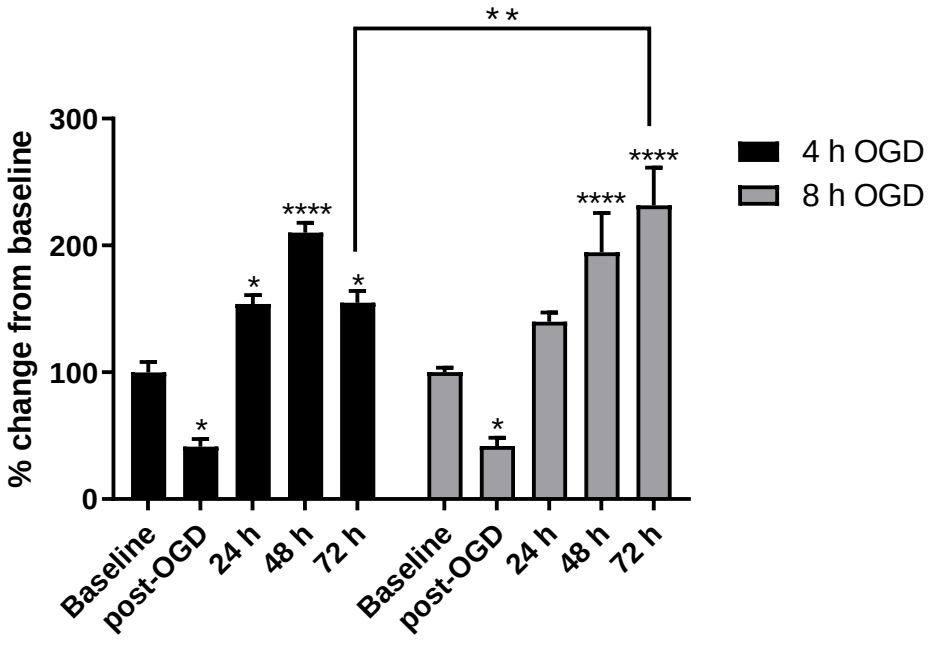


Figure 4.14 Histograms showing the effect a 4 h or 8 h OGD protocol has on fully confluent human astrocyte (P5-7) IL-6 concentrations at 24 h intervals and immediately post OGD (4 h or 8 h). Concentrations were interpolated from a standard curve and compared to baseline to test for statistical significance using two-way repeated-measures ANOVA and Dunnett's post-hoc. The Shapiro-Wilk test determined that the data were normally distributed. Data are presented as mean ± SEM (n=5, from two separate experiments). *p<0.05, **p<0.01, ****p<0.0001 vs their respective baseline groups.

Mitochondrial complex proteins expression

Unfortunately, NNT data was not usable; therefore, rather than normalising to NNT data, the data were displayed as raw absorbance. At 72 h, the 4 h OGD significantly increased the amount of mitochondrial complex protein I and V ($p<0.01$), likewise the 8 h OGD significantly increased mitochondrial complex protein I and V ($p<0.0001$) (figure 4.15). No significant differences existed in mitochondrial complex proteins between conditions.

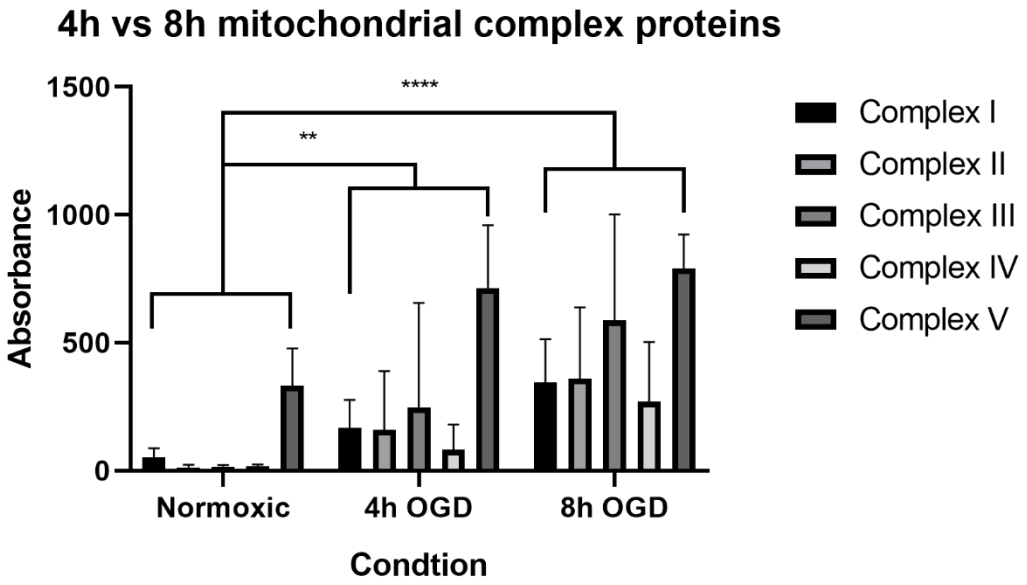


Figure 4.15 Histograms representing mitochondrial complex protein expression in fully confluent astrocytes (p5-7), represented as the net mean absorbance ± SEM (n=5, from two separate experiments). The Shapiro-Wilk test determined that the data were normally distributed. Data were analysed using a two-way repeated measures ANOVA and Dunnett's post-hoc. **p<0.01, ****p<0.0001 as indicated by connecting lines.

4.3.3 The effects of phytocannabinoids on human astrocytes exposed to 8h OGD using prophylactic and therapeutic application strategies

Total protein content (BCA)

Neither pre-or-post-treatment with CBD, CBGV, CBC or CBDV significantly affected total protein content. For each phytocannabinoid there was also no significant effect between each concentration (figure 4.16A-D).

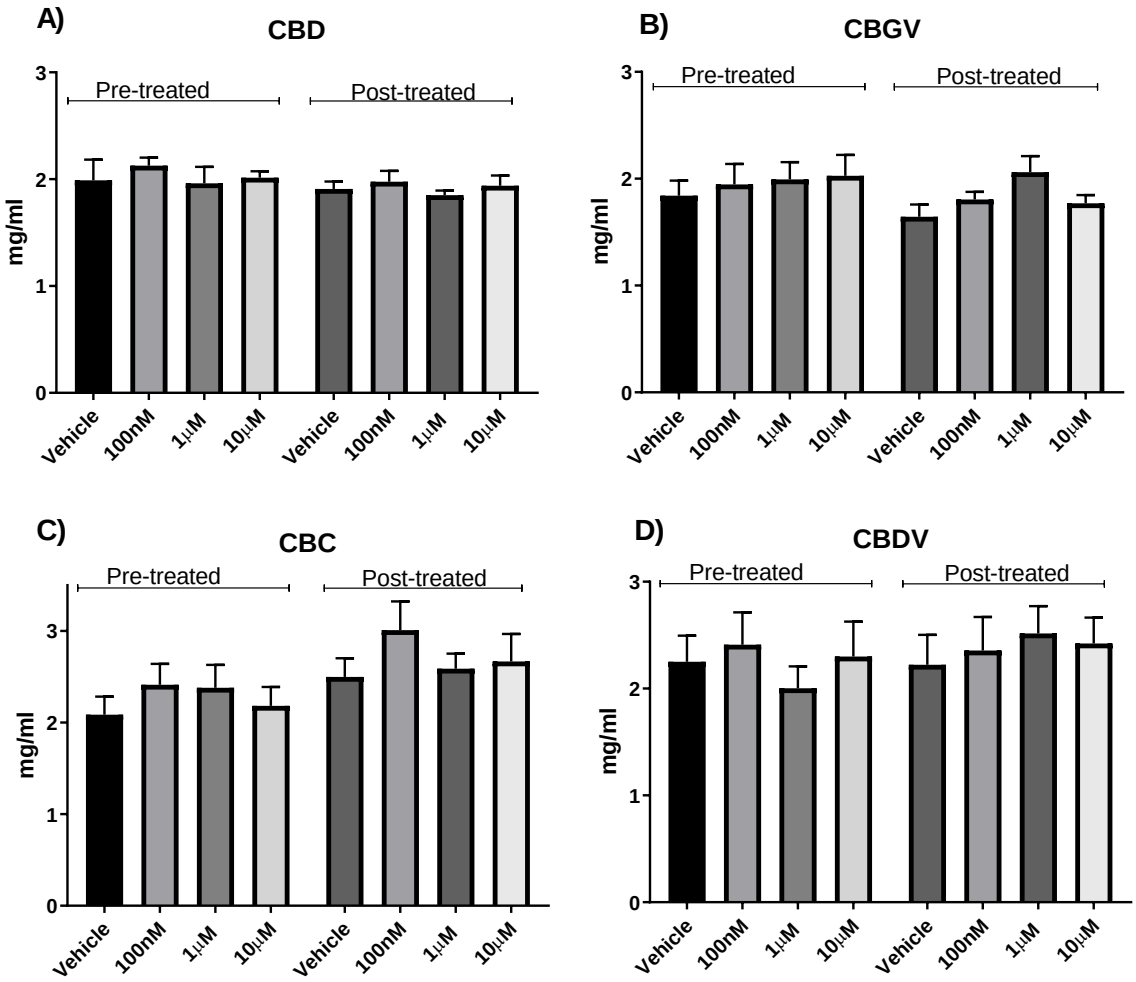


Figure 4.16 The effect of phytocannabinoid treatment on total protein levels/well 144 h following 8 h OGD in fully confluent astrocytes. Data are represented as mean ± SEM (n=9-12, from two separate experiments). The Shapiro-Wilk test determined that the data were normally distributed. Data were analysed using a two-way repeated measures ANOVA and Tukey's post-hoc. *p<0.05 as indicated by connecting lines.

4.3.4 Cell damage (LDH)

OGD protocol

Immediately following 8 h OGD, a significant increase in LDH secretion was seen, indicating cell damage. There was also a period of secondary damage that would arise later; however, not all cells followed the same temporal pattern, and the magnitude of secondary damage varied between cells (figure 4.17A-D).

CBD

Pre-administration of CBD 10 μM was able to reduce the acute damage caused by OGD at the 8 h time point by 48.23% ±30.3 ($p<0.05$) when compared to vehicle treated cells (figure 4.17A). At the 112 h time point, CBD reduced the release of LDH in a concentration- dependent manner, by a mean percentage difference of; 100 nM = 67.48% ±13 ($p = 0.001$), 1 μM = 85.23% ±8.4 ($p < 0.0001$), and 10μM = 102.8% ±7.5 ($p < 0.0001$) relative to vehicle control (figure 4.17A). Post-treatment with CBD reduced of LDH levels at 40 h by 41% ±9 ($p<0.05$) at 1 μM and by 47% ±6 ($p<0.05$) at 10 μM (figure 4.17B).

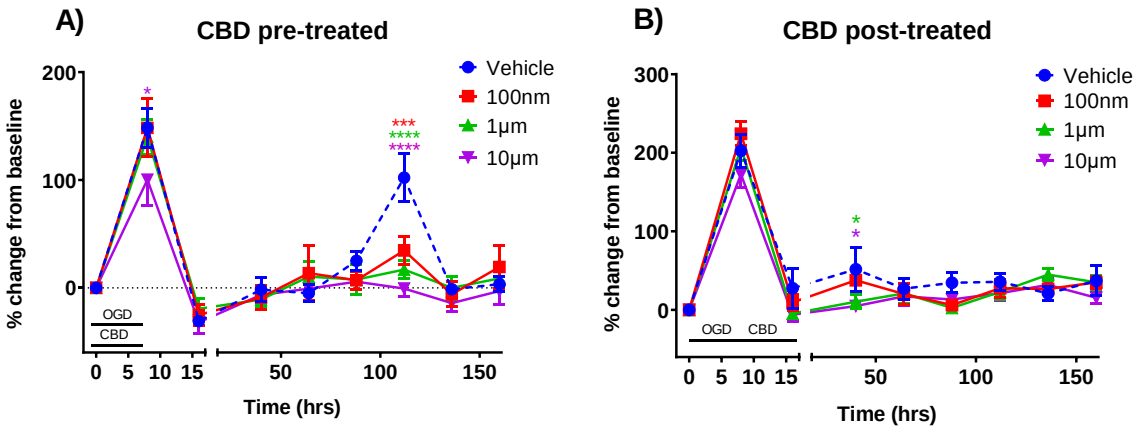


Figure 4.17 The effect of CBD treatment on LDH levels over time in fully confluent astrocytes, represented as percentage change from baseline for pre-treated (A) or post-treated (B) cells after an 8-hour OGD protocol. The Shapiro-Wilk test determined that the data were normally distributed. Data are presented as mean ± SEM and analysed using two-way repeated measures ANOVA and Dunnett's post-hoc comparison to vehicle. CBD pre-treated (vehicle N=9, CBD N=10), CBD post-treated (Vehicle N=12, CBD N=12) from 3 separate experiments. *p<0.05, ***p<0.001, ****p<0.0001 vs their respective vehicle.

CBGV

CBGV administered before initiating the 8 h OGD protocol reduced the initial increase of LDH in a concentration-dependent manner, with a percentage mean difference from vehicle of 59.29% ±16 ($p<0.001$) at 1 μM, and by 130.5% ±20 ($p<0.0001$) at 10 μM relative to vehicle (figure 4.18A). Where secondary damage was induced, the pre-administration of CBGV offset these increases at the 112 h time point; all concentrations of prophylactic CBGV used reduced the release of LDH by a mean difference of 69% ±12 ($p<0.0001$) at 100 nM, 63% ±15 ($p<0.0001$) at 1 μM, and 57% ±16 ($p<0.001$) at 10 μM relative to vehicle (figure 4.18A).

Post-treatment with CBGV following 8 h OGD protocol reduced LDH concentrations at 40 h by 39% ±4 ($p<0.05$) at 100 nM, and by 43% ±4.7 ($p<0.05$) at 10 µM relative to vehicle (figure 4.18B). At 88 h CBGV 1 µM attenuated LDH release by 39% ±7.3 ($p<0.05$) relative to vehicle. At 112 h CBGV reduced LDH release in concentration dependent manner, producing a 43% ±10.2 ($p<0.05$) decrease at 100 nM, 59% ±4.6 ($p<0.001$) decrease at 1 µM, and 60% ±9.7 ($p<0.001$) decrease at 10 µM relative to vehicle (figure 4.18B).

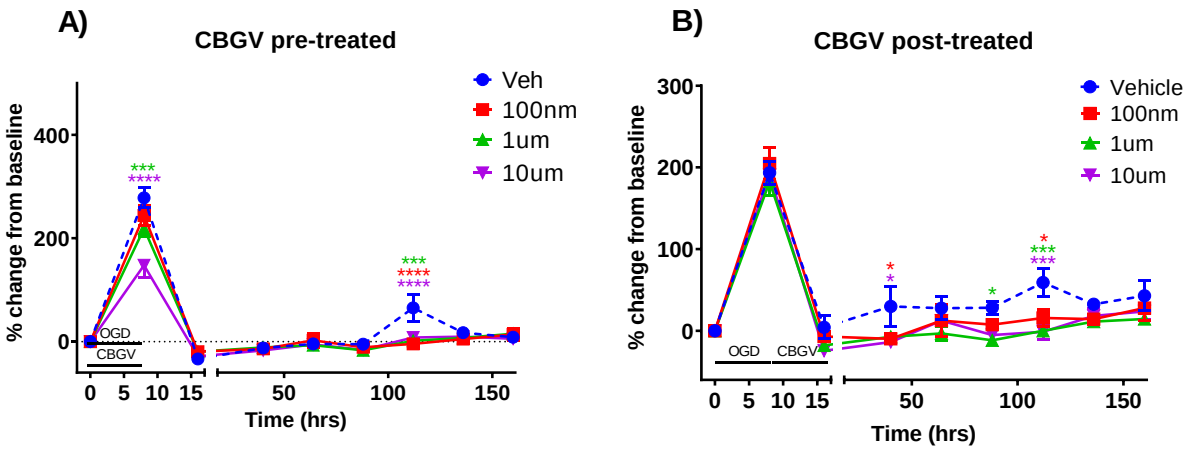


Figure 4.18 The effect of CBD treatment on LDH levels over time in fully confluent astrocytes, represented as percentage change from baseline for pre-treated (A) or post-treated (B) cells after an 8-hour OGD protocol. The Shapiro-Wilk test determined that the data were normally distributed. Data are presented as mean ± SEM and analysed using a two-way repeated measures ANOVA and Dunnett's post-hoc comparison to vehicle. CBD pre-treated (vehicle N=9, CBD N=10), CBD post-treated (Vehicle N=12, CBD N=12) from three separate experiments. *p<0.05, ***p<0.001, ****p<0.0001 vs their respective vehicle.

CBC

Pre-administration and post-administration of CBC did not affect LDH levels at any time points tested (figure 4.19A-B).

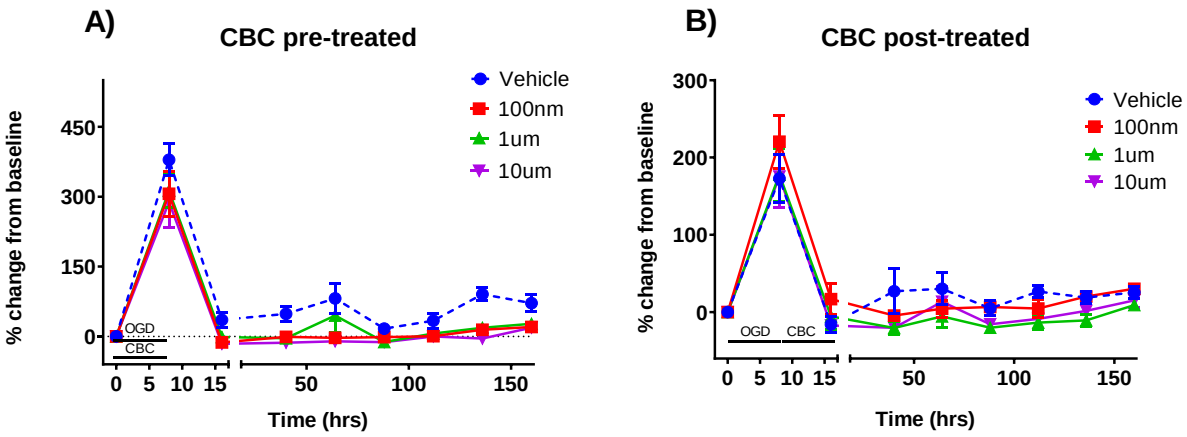


Figure 4.19 The effect of CBC treatment on LDH levels over time in fully confluent astrocytes, represented as percentage change from baseline for pre-treated (A) or post-treated (B) cells after an 8-hour OGD protocol. The Shapiro-Wilk test determined that the data were normally distributed. Data are presented as mean ± SEM and analysed using a two-way repeated measures ANOVA and Dunnett's post-hoc comparison to vehicle. CBC pre-treated (vehicle N=12, CBC N=12), CBC post-treated (Vehicle N=12, CBC N=9) from three separate experiments. *p<0.05, **p<0.01, ***p<0.001, ****p<0.0001 vs vehicle.

CBDV

CBDV 100nM given prior to the OGD significantly increased LDH release at the 8 h timepoint 142.2% ±49 ($p<0.0001$) (figure 4.20A). CBDV applied immediately following the 8 h OGD did not affect LDH concentration (figure 4.20B).

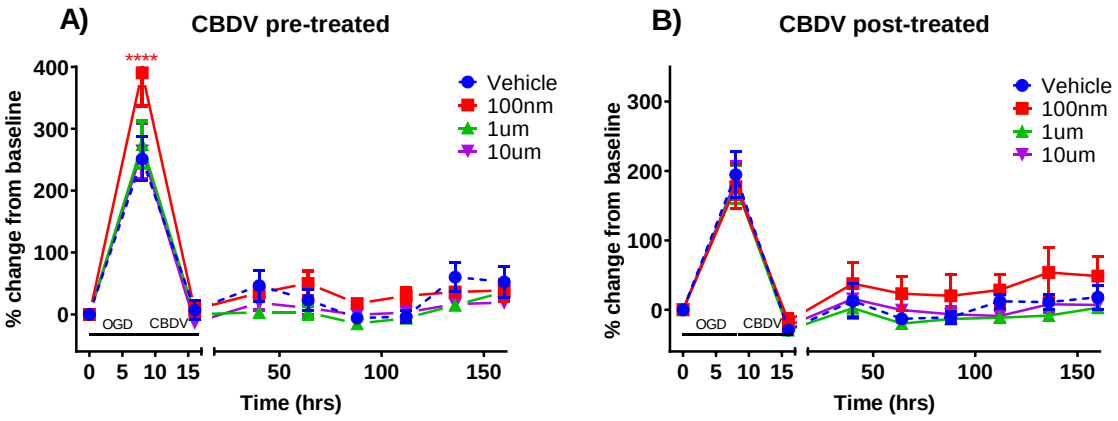


Figure 4.20 The effect of CBDV treatment on LDH levels over time in fully confluent astrocytes, represented as percentage change from baseline for pre-treated (A) or post-treated (B) cells after an 8 h OGD protocol. The Shapiro-Wilk test determined that the data were normally distributed. Data are presented as mean ± SEM and analysed using a two-way repeated measures ANOVA and Dunnett's post-hoc comparison to vehicle. CBDV pre-treated (vehicle N=12, CBC N=12), CBC post-treated (Vehicle N=12, CBC N=9) from three separate experiments. *p<0.05, **p<0.01, ***p<0.001, ****p<0.0001 vs vehicle.

4.3.5 Inflammation (IL-6)

OGD protocol

8 h OGD caused a significant increase in IL-6 post-OGD at 8 h by 400% ±98 ($p<0.01$). Following this, IL-6 levels did not significantly change from baseline during the reperfusion period (figure 4.21). Therefore, only the ischemic period was analysed (0-16h) when examining the effects of phytocannabinoids on the IL-6 response; subsequently, only cells pre-treated with phytocannabinoids could be assessed.

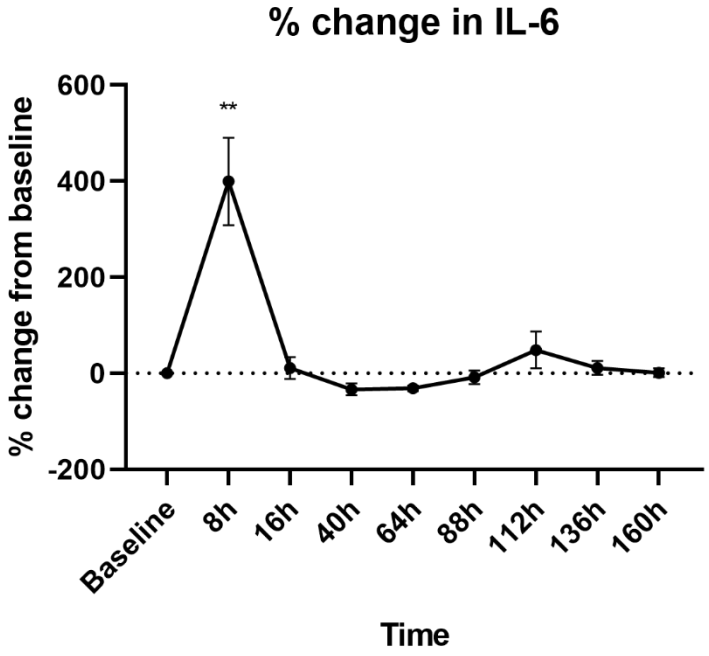


Figure 4.21 IL-6 percentage change from baseline in vehicle-treated cells (N=23, from two separate experiments). Concentrations were interpolated from a standard curve. Data are presented as mean ± SEM. Data were analysed using a repeated measures one-way ANOVA, with Dunnett's post-hoc comparison to baseline, **p<0.01.

4.3.6 The effects of CBD, CBGV, CBC, and CBDV on IL6 in astrocyte exposed to 8 h OGD

CBD, CBGV, CBC, and CBDV treatment did not affect the levels of inflammation as measured by IL-6 concentrations during the first 16 h of OGD reperfusion (figure 4.22).

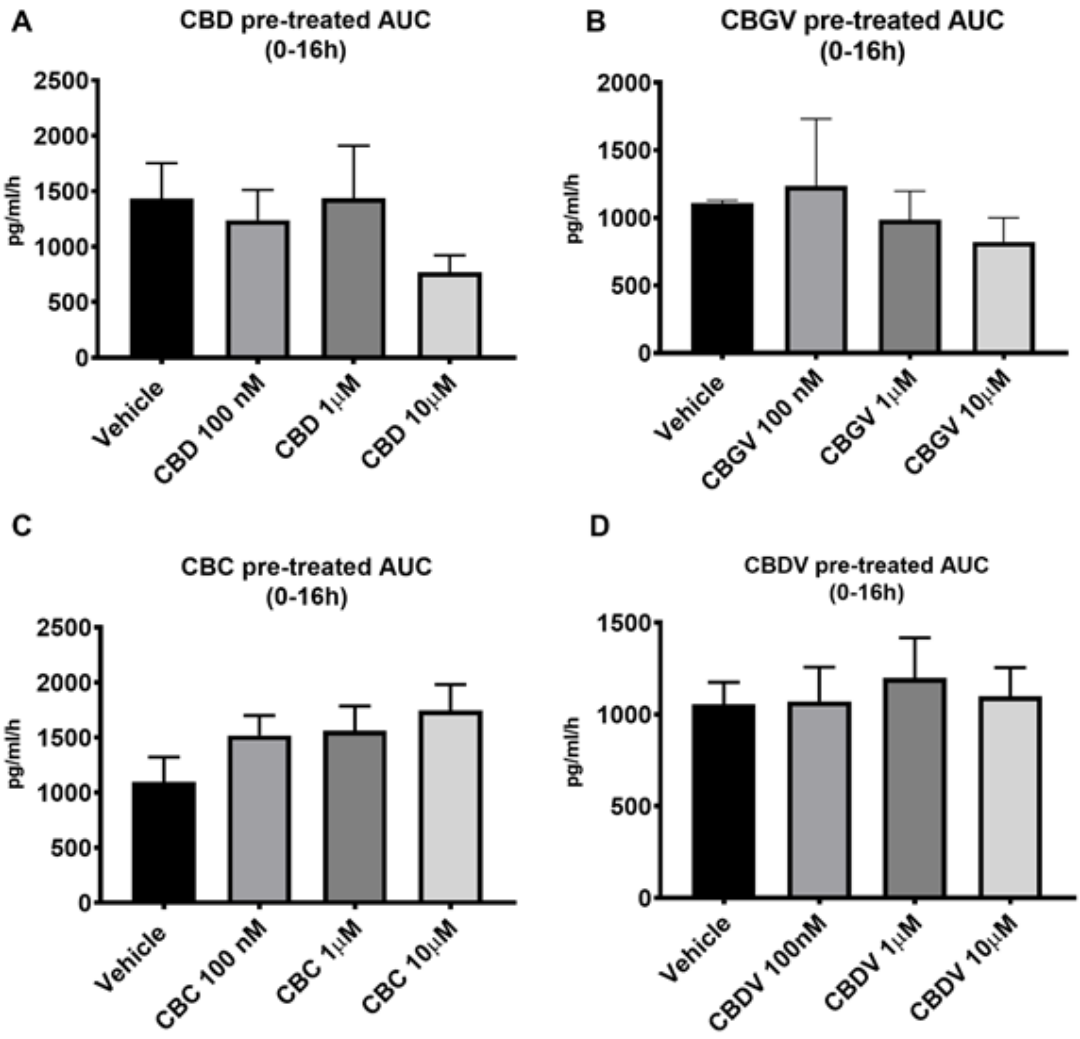


Figure 4.22 Histograms showing the effects of CBD (A), CBGV (B), CBC (C) and CBDV (D) on IL-6 area under the curve for 16 hours of reperfusion following an 8-hour OGD protocol. N= 6–9, from three separate experiments. Data are represented as mean ± SEM. Data were analysed using a one-way ANOVA for each phytocannabinoid.

Table 4.0 summarises the effects of CBD on total protein, cell damage and inflammation.

			BCA	LDH		IL-6
CBD	Pre	100 nM	NS	112 h		NS
				-68% ***		
		1 µM	NS	112 h		NS
				-85% ****		
		10 µM	NS	8 h	112 h	NS
				-48% **	-103% ****	
	Post	100 nM	NS	40 h		N/A
				NS		
		1 µM	NS	40 h		N/A
				-41% *		
		10 µM	NS	40 h		N/A
				-47% *		
CBGV	Pre	100 nM	NS	112 h		NS
				-69% ****		
		1 µM	NS	8 h	112 h	NS
				-59% ***	-63% ****	
		10 µM	NS	8 h	112 h	NS
				-131% ****	-57% ***	
		100 nM	NS	40 h	112 h	N/A

	Post			-39% *	-43% *	
		1 µM	NS	88 h	112 h	N/A
				-39% *	-59% ***	
		10 µM	NS	40 h	112 h	N/A
				-43% *	-60% ***	
			BCA	LDH		IL-6
CBC	Pre	100 nM	NS	NS		NS
		1 µM	NS	NS		NS
		10 µM	NS	NS		NS
	Post	100 nM	NS	NS		N/A
		1 µM	NS	NS		N/A
		10 µM	NS	NS		N/A
CBDV	Pre	100 nM	NS	8 h		NS
				+142% ****		
		1 µM	NS	NS		NS
		10 µM	NS	NS		NS
	Post	100 nM	NS	NS		N/A
		1 µM	NS	NS		N/A
		10 µM	NS	NS		N/A

Table 4 Summary of results from each experiment in chapter 4.

4.4 Discussion

The primary aim of this study was to investigate how the phytocannabinoids CBD, CBGV, CBC and CBDV affect astrocyte viability, inflammation and mitochondrial function following an OGD protocol. The initial experiment demonstrated that CBD, CBGV and CBC at high concentrations increased cellular damage and reduced mitochondrial complex protein I expression in a 4 h OGD protocol. The second part of the study showed parameters associated with damage increased upon extending the duration of OGD by four additional hours. Following the optimisation of a more suitable model, the second part of the study demonstrated CBD and CBGV reduced markers of cellular damage and did so to a greater extent when applied before the 8 h OGD insult was initiated.

4.4.1 The effects of CBD, CBGV, CBC and CBDV on cell death, markers of mitochondrial function and cellular metabolism in human astrocytes in normoxic and 4 h oxygen-glucose deprivation conditions

Data from these experiments suggest phytocannabinoids have different toxicity profiles in human astrocyte cells. CBD resulted in elevated levels of cell death at higher concentrations in normoxia and OGD, whereas CBC was only cytotoxic in an OGD environment and CBGV in a normoxic environment. Indeed, an *in vivo* mouse study using CBC 500 mg/kg i.p. showed toxic effects at high concentrations (Karler and Turkanis, 1978). In contrast, CBDV did not affect cellular damage in OGD or normoxic conditions.

Mitochondrial complex proteins are instrumental in driving the synthesis of ATP through the electron transport chain. The respiratory chain comprises four major protein complexes (I–IV) that generate a charge and proton gradient across the inner mitochondrial membrane that drive ATP synthesis at complex V (Rich and Maréchal, 2010). Complex I oxidizes NADH to NAD^+ and the electrons from this reaction are passed to the electron carrier ubiquinone (Sharma, Lu and Bai, 2009). This reaction is coupled to the translocation of four protons from the mitochondrial matrix into the inner mitochondrial membrane, contributing to the electrochemical gradient (Sharma, Lu and Bai, 2009). Complex II oxidises succinate to fumarate and acts as a second entry point to the ETC. When succinate oxidizes to fumarate, 2 electrons are accepted

by FAD which is then passed to ubiquinone (Paddenberg *et al.*, 2003). The products of complex I and II merge at complex III, where the electrons from carriers are passed one at time complex IV. This event also results in the release of 4 protons into the intermembrane space further contributing to the electrochemical gradient (Ahmad and Kahwaji, 2018). Complex IV, also known as cytochrome c oxidase, oxidizes cytochrome c and transfers the electrons to oxygen, the final electron carrier in aerobic cellular respiration. ATP synthase, also called complex V, uses the ETC generated proton gradient across the inner mitochondrial membrane to form ATP, completing oxidative phosphorylation (Schmidt-Rohr, 2020).

The multiplex Oxidative Phosphorylation kit (ThermoFisher, USA) kit quantifies intact mitochondrial complex proteins. The amount of protein detected can be used to infer capacity of the mitochondrial respiratory chain, as intact protein expression generally correlates well with functional output at each complex (Zheng, 2012). The 4h OGD protocol reduced the protein levels of complex I, II, III and IV, complex V was unaffected. These results indicate that the OGD period does reduce the capacity of the ETC. However, LDH levels as a marker of cell damage were not elevated by the 4 h protocol. Indicating while energy production is impaired, it is not impaired to an extent that results in cellular damage. Interestingly measurements of cellular metabolism, specifically by NAD(P)H- reductase enzymes was increased following the 4 h OGD protocol, perhaps suggesting a reduction of available NADH, as less complex I is available to utilise this electron carrier therefore reducing any competition between substrates, reflecting an increase in formazan production in the MTS assay. The function of complexes I, II, and III have been shown to be impaired in animal models of stroke, producing increased ROSs (Sims, 1991; Allen *et al.*, 1995). Like the results reflect, Complex IV's activity is not known to be impaired by hypoxia or anoxia, however its function is heavily impaired by reperfusion, which is comparable to the reintroduction of oxygen and glucose in this cellular model (Kuroda *et al.*, 1996).

Under normoxic conditions, only CBD at the highest concentration tested significantly decreased mitochondrial complex protein expression. In OGD conditions, CBDV decreased mitochondrial complex protein I. Given that a substantial portion of free radical production is made at this complex protein during aerobic metabolism, reductions in this protein could prove protective during the reperfusion period, as complex II can still support ETC function (Matsuzaki *et al.*, 2009). Under control and OGD conditions, cellular metabolism was not significantly affected by 24 h treatment with CBD, CBGV, CBC or CBDV, suggesting any changes in mitochondrial complex protein expression does not affect cellular metabolism.

4.4.2 The effects of a 4 and 8 h OGD protocol on human astrocytes

Astrocytes are known to be highly resistant to OGD conditions relative to neurons. Astrocytes have energy reserves stored as glycogen, and as a testament to their robustness, they can be cultured from a cadaver up to 24 h following death (Gibbons and Dragunow, 2010). Through a syncytium, astrocytes connected by gap junctions, can also buffer Ca^{++}, K^{+}, glucose and H_2O, reducing any molecular disturbances through spatial buffering (Takano *et al.*, 2009). Given the more robust nature of astrocytes, this experiment aimed to increase cellular damage by increasing the duration of OGD by four more hours. This was achieved by comparing a 4 and 8 h OGD protocol.

As expected, both 4 and 8 h OGD resulted in reductions in protein levels, with the 8 h OGD protocol substantially reducing protein levels more relative to the 4 h OGD.

The cytokine IL-6 was used to measure the intensity of inflammation in each of the conditions. Literature indicates IL-6 levels correlate well with the severity of damage in either imaging or clinical aspects, e.g., functional mobility and infarct volume (Rodríguez-Yáñez and Castillo, 2008; Shaafi *et al.*, 2014). Both OGD protocols caused a significant increase in IL-6 across all the time points, except 24 h in the 8 h OGD protocol. In the 4 h OGD protocol, reductions in IL-6 at later time points may be due to the resolution of inflammation. A period where pro-inflammatory signals decrease, and endogenous anti-inflammatory and pro-resolving molecules are upregulated (Fullerton and Gilroy, 2016). Unlike the 4 h OGD protocol, the 8 h OGD does not follow this pattern and shows a trend for increase. Demonstrating a failure to resolve inflammation, indicating the 8 h OGD protocol creates more chronic inflammation. Interpreting inflammatory response data requires care as an acute inflammatory response causes cell death, but in later stages, cytokines like IL-6 may help restore homeostatic function, such as neurite outgrowth (Suzuki, Tanaka and Suzuki, 2009). However, in chronic inflammation, cells cannot resolve inflammation and continue exacerbating tissue damage (Lindsberg and Grau, 2003).

Relative to normoxic conditions, both protocols caused an increase in LDH levels immediately following OGD, indicating cellular damage. This increase appears to return to baseline after 24 h reperfusion; however, LDH levels continue to rise after

48 h. The initial increases in LDH are likely caused by cell damage induced by oxygen-glucose deprivation (necrotic cell death). The gradual rise at the 48-72 h time-points could reflect cellular programmed death and damaging mechanisms induced by reperfusion, i.e. increased ROS generation. Compared to other studies using an 8 h OGD protocol, experiments showed a similar percentage increase in secreted LDH at 24 h (Sun *et al.*, 2017). Additionally, this group also showed Poly [ADP-ribose] polymerase (PARP) and Caspase-3 activity was significantly upregulated following OGD/R, indicating apoptotic mechanisms are active at later time points.

Overall, there was a significant increase in mitochondrial complex protein expression in the 4 or 8 h OGD relative to normoxic conditions. This is in contrast to the experiments carried out in the previous section, where a 4 h OGD significantly decreased all mitochondrial complex proteins. However, the previous sections experiments assessed mitochondrial complex protein levels 24 h after OGD, whereas experiments from this section assessed mitochondrial complex protein expression 72 h post-OGD. These contrasting findings between the two sections are likely a result of different temporal expression patterns following OGD. It could be, for example, at 24 h following OGD, there are decreases in mitochondrial proteins caused by cell damage. However, at later stages, cells begin to upregulate the number of mitochondria to compensate for the damage caused by OGD/reperfusion, e.g. re-establishing ionic gradients. Indeed this is in line with other literature demonstrating with reperfusion mitochondrial biogenesis peak 72 h following MCAO in rats (Xie *et al.*, 2014). The function of mitochondria at various points could be estimated using firefly luciferase, a reaction which produces increasing intensity of light with increasing concentrations of ATP (Lemasters and Hackenbrock, 1978). Alongside microscopic images one could estimate whether decreases in ATP are associated with reduced cell numbers or mitochondrial function.

Following OGD, the balance between ROS scavenging and production switches to the production side, creating an imbalance (Niizuma et al., 2009). Therefore, if mitochondrial complex proteins increase, ROS production may also increase and continue to damage cells. To investigate how mitochondrial complex proteins levels affect cellular damage, markers of lipid peroxidation could be measured at all-time points to assess whether increased mitochondrial proteins correlates with increased oxidative stress and whether this is consistent with cell death/damage markers. Indeed, in this experiment LDH increases that correlate with the time of measurement of mitochondrial complex proteins could reflect an increase in ROS generation.

In conclusion, the OGD protocol causes cell damage which can be measured over

time in the cell medium through assays such as LDH (not at 24h) and IL-6 (not immediately post-OGD). Reperfusion damage continues for several days post-OGD. Increased cellular damage may allow for a better scope to see the protective effects of phytocannabinoids in our model. As there appeared to be a trend for increased damage using the 8 h OGD protocol, subsequent experiments used the 8 h OGD protocol to monitor markers of cell damage over time for up to 144 h in the medium and cellular markers in the lysates at the 144 h time point.

4.4.3 Examination of the effects of phytocannabinoid on human astrocytes exposed to 8 h OGD using prophylactic and therapeutic strategies

This part of the study aimed to assess how phytocannabinoids, applied before or following an 8 h OGD protocol, influenced astrocyte survival and inflammation.

LDH levels in cerebral spinal fluid correlate well with the infarct size and indicate the extent of the lesion into deeper cortical regions (Lampl *et al.*, 1990). LDH measurements from this experiment showed phytocannabinoids could reduce cellular damage following 8 h OGD and tend to be more effective when administered before the insult. The inflammatory response to OGD was not affected by any phytocannabinoid. It should be noted that the effect of 10 µM CBD on LDH levels was inconsistent between different experiments. CBD resulted in a considerable elevation in LDH levels, but this was not replicated in the later experiment using similar conditions. The reasons for these contrasting results is not known; however, they could be a consequence of phenotypic changes with increasing passage number, as not all cells used were from the same passage. Of all phytocannabinoids, CBGV reduced cellular damage to the greatest extent at both the acute or secondary damaging period in human astrocytes subjected to OGD/R injury.

In contrast, CBD was more effective at a later time point and when applied before the insult. These differential effects could indicate that each phytocannabinoid is mediating its effects by unique pharmacological targets. Raising the possibility that a combination of phytocannabinoids could be used to address the multitude of molecular disturbances caused by OGD/R injury. In contrast to CBD and CBGV, CBC did not affect cellular damage in normoxic or OGD conditions. Interestingly recent research has shown CBC to be an inhibitor of the LDH enzyme, which would interfere with the results obtained by this method of LDH detection, lending a possible explanation to the lack of effect (Martin *et al.*, 2021). CBDV at the highest concentration increased cellular damage. Other studies have demonstrated a similar

effect in the same experimental set-up. However, the increased damage was at a lower concentration (100 nm vs 10 uM) and at later time-points (24 h vs 8 h) (Stone, England and O'Sullivan, 2021).

IL-6 levels in stroke patients correlate well with infarct volume and sensorimotor outcomes at later stages following a stroke. None of the phytocannabinoids used in this study affected IL-6 levels. Furthermore, IL-6 vehicle data did not follow the same pattern as in the first experiments (4 h vs 8 h OGD section). In previous experiments, IL-6 appeared to increase at later time points (48 h-72 h). In contrast, IL-6 data from these experiments seems to increase only immediately post-OGD. Thus only the effects of phytocannabinoids on the acute inflammation caused by OGD were assessed. The reasons for this are uncertain; however, like LDH results, it could be that with increasing passage numbers, cells are less able to respond to OGD damage. In contrast to other studies using the same cell type, our study could not demonstrate the anti-inflammatory effect of CBD or any other phytocannabinoid tested (Hind, England and O'Sullivan, 2016; Stone, England and O'Sullivan, 2021)

A better understanding of why all cells do not undergo the same temporal pattern of damage would allow the development of a more reliable protocol to assess phytocannabinoids in these types of models. It may also be helpful to determine whether there is any variability in the oxygen concentration achieved by the GasPak bags between plates and whether this could contribute to the different temporal patterns of damage. Alternatively, an incubator capable of controlling internal oxygen concentration could be used to determine whether any effects require a specific O_2 concentration and duration of OGD.

4.4.4 Conclusion

Overall, the data from this experiment suggest phytocannabinoids can offer protection to astrocytes damaged by OGD/R injury. CBD reduces cellular damage when given prophylactically, suggesting CBD can effectively reduce cellular damage by priming astrocytes to maintain cellular homeostasis during OGD conditions. CBGV provides the greatest extent of protection, reducing cellular damage when administered before or after OGD, indicating this phytocannabinoid addresses both the ischemic and reperfusion period of injury. CBDV appeared to increase cellular damage immediately post OGD, perhaps by reducing mitochondrial complex proteins during ischemia. The fact that the effects of phytocannabinoids varied between pre and post-administration could suggest that certain phytocannabinoids, like CBGV, have unique properties that can target molecular disturbances in both

the ischemic or reperfusion period of damage. As not all populations of astrocytes displayed the same temporal pattern of damage, some of the anti-inflammatory and neuroprotective effects could have been underestimated. Future experiments should look to elucidate the mechanism of action through which these phytocannabinoids produce their effects and assess using them in combination before moving to animal studies.

5 The pharmacological effects of plant-derived versus synthetic cannabidiol (CBD) in human cell lines

5.1 Introduction

Preclinical and early clinical phase studies also demonstrate the potential of Cannabidiol (CBD) in cancer, stroke, anxiety, and pain (Hayakawa, Mishima and Fujiwara, 2010; Devinsky *et al.*, 2014; Syed, McKeage and Scott, 2014; Blessing *et al.*, 2015; Cherniakov *et al.*, 2017; Gofshteyn *et al.*, 2017; Dumitru, Sandalcioglu and Karsak, 2018; Śledziński *et al.*, 2018), and a purified form of CBD (98%, Epidiolex®) is already licensed to treat seizures associated with Dravet Syndrome, Lennox-Gastaut syndrome and tuberous sclerosis (Freeman *et al.*, 2019). Around 65 molecular targets for CBD have been identified (Ibeas Bih *et al.*, 2015; Elsaid and Le Foll, 2020), with different targets responsible for different therapeutic effects of CBD. For example, serotonin 1A receptor (5HT1A) activation is associated with reductions in anxiety, nausea, and neuroprotective effects (Hayakawa, Mishima, Nozako, Hazekawa, *et al.*, 2007; Rock *et al.*, 2012; de Mello Schier *et al.*, 2014). Transient receptor potential cation channel subfamily V member 1 (TRPV1) interactions have been implicated in the anti-nociceptive effects of CBD (Costa *et al.*, 2004). Peroxisome proliferator-activated receptor gamma (PPARγ), cyclooxygenase-2 (COX-2) and GPR55 have been linked to the anti-cancer effects of CBD (Ramer *et al.*, 2013). Cannabinoid receptor 1 (CB_1) interactions are associated with the ability of CBD to reduce intestinal permeability (Alhamoruni *et al.*, 2012; Couch *et al.*, 2019). The polypharmacology of CBD may underpin its ability to affect many pathologies.

Over-the-counter CBD products are mainly produced from *Cannabis sativa L.* with a THC content below 0.2% (hemp). Epidiolex is made using Cannabis sativa L. with a higher THC content. CBD can also be produced synthetically through a series of chemical reactions, yielding a highly purified form of CBD (Jung *et al.*, 2019). Plant-based CBD products are either refined to produce purified CBD (97-99%), or crude extraction methods are used to yield CBD alongside other phytocannabinoids, terpenes and flavonoids, known as a ‘CBD-rich extract’.

One complication that can arise in reviewing the effectiveness of CBD medicines is this range of products that include purified isolate forms or extracts containing other chemicals. Some suggest that CBD-rich extracts are therapeutically superior because of the 'entourage' hypothesis. Scientific evidence, however, is equivocal. Gallily and colleagues showed that CBD-rich extracts were more effective than purified CBD in attenuating inflammation and hyperalgesia in rats (Gallily, Yekhtin and Ondřej Hanuš, 2015). Similarly, Pagano et al. showed that a CBD-rich extract was more beneficial in attenuating intestinal inflammation and hypermobility in mice (Pagano *et al.*, 2016).

In contrast, Scott et al. found purified CBD was more efficacious than a CBD-rich extract in glioblastoma cell lines (Scott, Dalgleish and Liu, 2014). Ligresti and colleagues also found purified CBD was more potent in reducing proliferation in some cancer cell lines, while in others, the CBD-rich extract was more potent (Ligresti *et al.*, 2006). Thus, it is not clear whether purified or CBD extracts are superior or different depending on the pathological situation in which CBD is being tested. There is also no controlled clinical trial data to support either argument.

Because of the perception that CBD extracts are superior to purified CBD, synthetic CBD products are sometimes perceived as inferior. A recent study in Germany asked 153 epileptic patients whether they prefer how their CBD is sourced. 73% favoured CBD to be sourced from a plant (von Wrede *et al.*, 2020). The main reasons were a preference for a botanical origin, a perceived lack of toxicity relative to synthetic forms, and an absence of chemical reactions in the manufacturing process. Conversely, there is also a perception that contaminations of plant-derived CBD products with pesticides, heavy metals, microbial pathogens, and carcinogenic compounds during cultivation, manufacturing, and packaging may limit the pharmaceutic use of plant-derived CBD (Montoya *et al.*, 2020). There are no head-to-head clinical studies comparing plant versus synthetic CBD. However, studies assessing the efficacy, safety and pharmacokinetic parameters of a synthetically derived CBD in drug-resistant epilepsy (Klotz *et al.*, 2019; Wheless *et al.*, 2019) found a very similar safety profile, efficacy and pharmacokinetics relative to plant-derived CBD (Devinsky, Patel, Cross, *et al.*, 2018; Devinsky, Patel, Thiele, *et al.*, 2018; Szaflarski *et al.*, 2018; Thiele *et al.*, 2018).

In light of the lack of data directly comparing purified CBD of various origins, this study aimed to establish whether the CBD source affects its pharmacological effects in human cells. It was hypothesised that there would be no difference in the effects produced between each CBD assuming a similar purity between each.

5.2 Methods

5.2.1 Materials

CBD derived from two different sources (four plant-derived and two synthetically) were obtained from six companies (see table 5). Only Logical confirmed to use a synthesis process selective for the naturally occurring (-) enantiomer of CBD. Of the plant-derived sources of CBD, manufacturers analysis demonstrated Medropharm was 98.6% CBD, 0.2% CBD C4 analogue, 0.6% Cannabidivarin (CBDV) and 0.3% Cannabigerol (CBG). Flora Fusion was 99.3% CBD and 0.2% CBDV. CBDepot was 98.7% CBD, 0.3% CBD C4 analogue and 0.6% CBDV. AlibLab was 99.4% CBD and had no data regarding any impurities. Of the synthetically produced sources of CBD, Logical was 98.9%, and THCpharm was 99.8% pure. The presence of impurities was not assessed in either synthetically produced CBD used. CBD was suspended in ethanol at 10^{-1} mol/L. For each experimental repeat, a new stock solution was made.

Antagonists of receptors that mediate the effects of CBD in cellular models were used at relevant concentrations: CB_1 receptor antagonist, AM251 (100 nM); CB_2 receptor antagonist, AM630 (100 nM); GPR18 antagonist, O-1918 (1 μM); GPR55 antagonist, CID16200 (5 μM); PPARα antagonist, GW6471 (100 nM); PPARγ antagonist, GW9662 (100 nM); TRPV1 receptor antagonist, SB-36679 (1 μM); 5HT1A antagonist, WAY-100635 (300 nM). All antagonists were from Tocris, UK. When used, antagonists were applied 20 minutes before CBD.

5.2.2 Cell culture

Cells were maintained in a humidified cell culture incubator at 37°C with 5% CO_2 and cultured to 70-80% confluence in a T75 flask. SKOV-3 (The European Collection of Authenticated Cell Cultures [ECACC, UK],p24-31) cell lines were cultured to 70-80% confluence in Roswell Park Memorial Institute (RPMI) 1640 base medium containing L-glutamine and phenol red indicator (Gibco), supplemented with 10% heat-inactivated foetal bovine serum (FBS) and 1% penicillin-streptomycin (P/S). Human brain vascular pericytes (ScienceCell, USA,p3-6) were cultured in specialised pericyte medium (2% FBS, 1% pericyte growth supplement, and 1% P/S; ScienceCell, USA). CaCo2 cells (ECACC, UK) (p37-49) were cultured in

Minimum Essential Medium Eagle (MEME) (1% P/S, 1% non-essential amino acids [NEAA] and 10% FBS).

5.2.3 Gas chromatography-mass spectrometry

Test stock solutions of each CBD compound were made up at 50 µg/ml by weight in methanol. 20 µl of 10 µg/ml D3-CBD was added to 100 µl of standard and test stock solution, mixed, and evaporated until dry under nitrogen at 30 ^{o}c. Samples and standards were derivatized to their CBD-TMS esters by adding 70 µl of acetonitrile and 70 µl of BSTFA and incubating for 90 mins at 90 ^{o}C. 0.5 µl of each sample and standard was injected into a Trace 1310-TSQ 8000 GC-MS/MS (Thermo Scientific, Hemel Hempstead, UK) in SRM mode monitoring m/z transitions 390 – 319 for unlabelled CBD and 393 – 319 for D3 labelled CBD. Concentrations of test stock solutions were calculated from the standard curve of known CBD concentrations and % recovery calculated.

5.2.4 Anti-cancer effects of CBD in SKOV-3 cells

To identify the concentration of CBD to use in SKOV-3 cells, a concentration-response curve was constructed (THCPharm, supplementary figure 1). SKOV-3 cells were seeded into 96 well plates at a density of 10,000 cells/cm^2 and left to adhere for 3 h. Media was replaced with fresh media containing either vehicle (ethanol) or CBD (10-50µM). Plates were allocated into two timepoints; 24 h and 48 h. At each time point, resazurin (Sigma-Aldrich, UK) dissolved in phosphate buffer saline (PBS) (Thermo-Fisher, UK) was added to the wells to produce an in-well concentration of 100µM and returned to the incubator for 2 h. Plates were read using a Fluoroskan Ascent microplate fluorometer (Thermoelectron Corporation) at 560 nm excitation and 590 nm emission. 10 and 50 µM were identified as sub-effective and effective concentrations for similar experiments comparing CBD sources.

In separate experiments, the cytotoxic effect of CBD was investigated using confluent SKOV-3 cells. Cells were seeded into 96-well plates and given 2 days to reach confluence. The media was aspirated and replaced with fresh media either

containing ethanol (vehicle) or CBD (10 or 50 µM) for 24 or 48 h, and resazurin metabolism was measured as before.

5.2.5 Oxygen-glucose deprivation experiments in pericytes

Human pericytes were exposed to oxygen-glucose deprivation/reperfusion (OGD/R) as a model of stroke (Hind, England and O'Sullivan, 2016; Stone, England and O'Sullivan, 2019). Cells were seeded at 20,000 cells/cm^2 in a 96-well plate. Once confluent, cells were incubated for 24 h to establish baseline samples. The media was replaced with RPMI glucose-free media (Invitrogen, USA), containing either CBD (10 or 100nM) or vehicle (ethanol) based on our unpublished work. Plates were sealed into GasPak EZ Anaerobe Pouches (Beckton Dickinson, UK) and placed into the incubator, producing anoxic conditions within 20 minutes (Hind, England and O'Sullivan, 2016). After 4 h, media was collected and replaced with complete pericyte growth medium containing either CBD (10or 100nM) or ethanol (vehicle) and returned to normoxic conditions for 20 h. Media concentrations of IL-6 (immediately post OGD and 24 h, R&D systems ELISA)) and lactate dehydrogenase (LDH, 24 h only, Abcam) were measured per the manufacturer's instructions.

5.2.6 Inflammation and permeability experiments in Caco2 cells

CaCo2 Cells (P32-45) were seeded onto the apical compartments of polycarbonate transwell inserts (12 mm diameter, 0.4 µm pore diameter; Transwell, Corning Inc., USA) at a density of 20,000 cells/cm^2 with complete medium. Cells were differentiated over 21 days into gut enterocyte-like cells. Transepithelial electrical resistance (TEER, ohms, Ω) was used to quantify barrier integrity using STX2 chopstick electrodes attached to an Ohm-meter (World precision instruments, UK) (Wells *et al.*, 1998). Wells with a resistance of over 999 Ω were used for experiments. The basolateral compartments of each well were treated with 10 ng/ml interferon-gamma (IFNγ), and 8 h later, with 10 ng/mL tumour necrosis factor-alpha (TNFα). Sixteen hours later, TEER was measured, and the wells were washed once with PBS. Fresh media containing CBD (10 µM) was applied to the apical membrane, and TEER was measured up to 72 h.

5.2.7 Data analysis

Statistical analyses were performed using GraphPad Prism 8.2.0 and assessed for Gaussian distribution before analysis. Resazurin, LDH, and IL-6 datasets were analysed using one-way ANOVA alongside Dunnett's post hoc test comparing each CBD against vehicle controls and a multiple comparison comparing each CBD at the respective concentrations and time points. CaCo2 time course data were analysed using area under the curve (AUC), quantified using the trapezoidal method and compared to vehicle using an unpaired T-test. AUC data was compared by CBD source using a one-way ANOVA multiple comparison with a Dunnett's post hoc test.

5.3 Results

5.3.1 Gas chromatography/Mass spectrometry

In general, the purity of each CBD was lower for our laboratory's measurements than the manufacturers' (table 5). The reason for this discrepancy could occur due to different measurement techniques and degradation over time. Regardless, the purity of the CBD sources was independently confirmed using our analysis. Logical CBD suffered from a poor percentage recovery in both runs. Unfortunately, this particular batch of Logical CBD used in the cellular experiments had been exhausted following these runs, so purity data could not be generated from the same batch.

	Purity							Efficacy				
Manufacturer (source)	**CBD purity (our lab)**	**CBD purity (manufacturer) GC/MS**	**CBD C4 analogue**	**CBDV**	**Delta 9 THC**	**Delta 8 THC**	**CBG**	**Proliferating Skov-3 (resazurin, 48 h, 10μM vs. veh)**	**Confluent Skov-3 (resazurin, 48 h, 50μM vs. veh)**	**Pericytes (LDH, 24 h, 100nM vs. veh)**	**Pericytes (IL-6, 24 h, 100nM vs. veh)**	**CaCo2 (TEER, mean AUC, SEM, 10μM vs. veh)**
Medropharm (Plant)	93.3% ±1 GC-MS	98.6% ±0.1 HPLC	0.2% ±0.1	0.6% ±0.1	>0.01%	>0.01%	0.3% ± 0.1	-41 ± 2 (p<0.001)	-90 ± 5 (p<0.001)	-84 ± 7.3 (p<0.001)	-106 ± 12.2 (p<0.01)	218 ± 50 (p<0.001)
Flora Fusion (Plant)	100% ±1.5 GC-MS	99.3% ±0.1 CC	ND	0.2% ±0.1	ND	ND	ND	-56 ± 5 (p<0.001)	-85.2 ± .7 (p<0.001)	-83 ± 7.5 (p<0.001)	-104 ± 12.7 (p<0.0001)	292 ± 36 (p<0.0001)
CBDepot (Plant)	97% ±0.6 GC-MS	98.7% ±0.1 HPLC	0.3% ±0.1	0.6% ±0.1	ND	ND	NA	-46 ± 5 (p<0.001)	-93.4 ± 2 (p<0.001)	-85 ± 8.6 (p<0.001)	-99 ± 11.0 (p<0.001)	200 ± 60 (p>0.01)
AILAB (Plant)	95% ±1.1 GC-MS	99.4% ±0.1 HPLC	NA	NA	NA	NA	NA	-37 ± 5 (p<0.001)	-94 ± .3 (p<0.001)	-70 ± 9.6 (p<0.01)	-111 ± 13.3 (p<0.001)	598 ± 172 (p<0.01)
Logical (synthetic)	NA	98.9% GC-MS	NA	NA	NA	NA	NA	-37 ± 4 (p<0.001)	-91 ± .2 (p<0.001)	-82 ± 10.6 (p<0.001)	-115 ± 9.4 (p<0.0001)	413 ± 106 (p<0.01)
THCPharm (synthetic)	111% ±0.06 GC-MS	99.8% GC-MS	NA	NA	NA	NA	NA	-37 ± 4 (p<0.001)	-92 ± .8 (p<0.001)	-67 ± 11.2 (p<0.0001)	-114 ± 12.1 (p<0.0001)	319 ± 72 (p<0.001)

Table 5 where appropriate data were collated between similar experiments. All data are displayed as a percentage—all data displayed as percentage change relative to vehicle (±SEM). CBD samples were compared to vehicle or each other using a one-way ANOVA alongside multiple comparisons. CBD = cannabidiol, NA = not available, ND = not detectable, CBDV = cannabidivarin, THC = delta-9-tetrahydrocannabinol, CBG = cannabigerol, GC/MS = gas chromatography/mass spectrometry, HPLC = high performance liquid chromatography, CC = convergence chromatography.

5.3.2 Anti-cancer effects of plant-derived and synthetic CBD in SKOV-3 cell line

In proliferating SKOV-3 cells, at 24 h (figure 5.1A), 10 µM Medropharm (-53% ±6), Flora Fusion (-55% ±6) and CBDepot (-59% ±6) reduced resazurin metabolism relative to vehicle control (*P*<0.0001). Logical CBD also reduced resazurin metabolism, albeit to a lesser extent (-33% ±9, *P*<0.05, figure 5.1A). At 24 h or 48 h, at 50 µM, all CBD sources produced similar reductions in resazurin metabolism compared to vehicle (*P*<0.0001, figure 5.1A-B). No statistically significant differences existed between CBD sources.

In fully confluent SKOV-3 cells, after 24 h, only 50 µM CBD reduced resazurin metabolism relative to vehicle (-55 to -74%, P<0.0001, Figure 5.1C). Similarly, after 48 h, only 50 µM CBD reduced resazurin metabolism relative to vehicle (-85 to -95%, P<0.0001, figure 5.1D). No significant differences were observed at either concentration or timepoint between CBD sources.

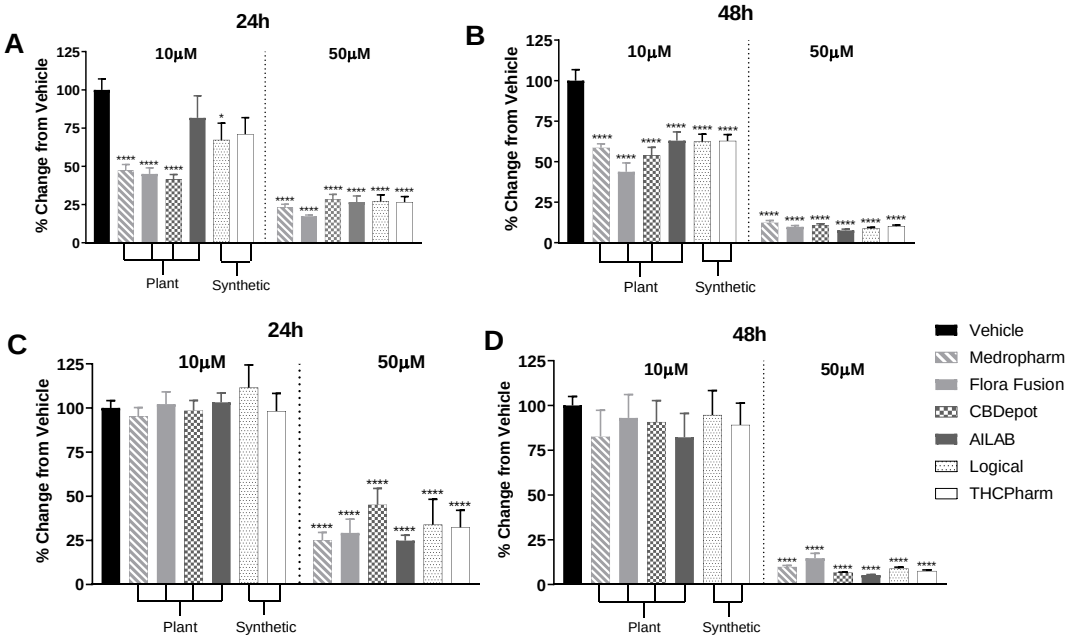


Figure 5.1 *Effects of various CBD samples on SKOV-3 cellular metabolism using resazurin assays. CBD (10 or 50 µM) was applied to proliferating SKOV-3 cells for 24 (**a**) and 48 h (**b**)* (n *= 15 from 3 separate experiments). Effects of CBD (10 and 50 µM) on confluent SKOV-3 cells applied for 24 (**c**) and 48 h (**d**)* (n *= 10 from two separate experiments). Data are displayed as mean ± SEM % change from vehicle and were compared for statistical significance against vehicle using a one-way ANOVA. *p ≤ 0.05; ****p ≤ 0.0001. CBD, cannabidiol.*

None of the selected antagonists (to 5-HT_{1A}, CB_1, CB_2, GPR18, GPR55, PPARα, PPARγ, and TRPV1 receptors) inhibited the reduction in metabolism associated with CBD (Figure 5.2).

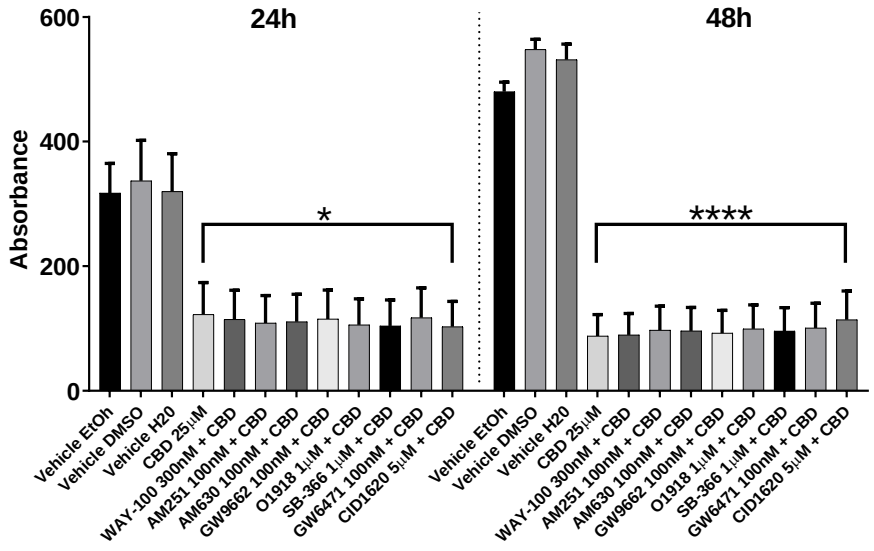


Figure 5.2 Effects of CBD (THC Pharm) 25 μM on proliferating SKOV-3 cells after 24 or 48 h in the presence of WAY-100635, AM251, AM630, GW9662, O1918, SB366791 GW6471, or CID16020046 (n = 7 from two separate experiments). Data are displayed as mean ± SEM absorbance, and CBD + antagonist data were compared against CBD 25 μM alone using a one-way ANOVA. *p ≤ 0.05; ****p ≤ 0.0001. CBD, cannabidiol.

5.3.3 The effects of CBD in pericytes exposed to OGD

IL-6 content immediately post-OGD was 225% ±63 (P<0.05, Figure 5.3A) higher than in normoxic control cells, and at 24 h was 184% ±26 higher (P<0.01, Figure 5.3B). At 24 h, LDH activity in media was 118% ± 18 higher than normoxic control cells (P<0.01, Figure 5.3C).

IL-6 secretion immediately post-OGD was not significantly raised in the presence of any CBD at 10 nM or 100 nM (Figure 5.3A). IL-6 secretion at 24 h following OGD was also not significantly raised relative to the normoxic control in the presence of CBD (100 nM). No statistical differences were present between CBD sources at their equivalent concentrations and time points.

LDH activity was also not significantly raised above normoxic control in the presence of CBD (24h, Figure 3C). At 100 nM, Medropharm (-91% ±18, p<0.05), Flora Fusion (-96% ±9, p<0.01)), CBDepot (-104% ±19, p<0.05) and THCPharm (-

73% ±18, p<0.05) also significantly reduced LDH activity relative to the OGD vehicle.

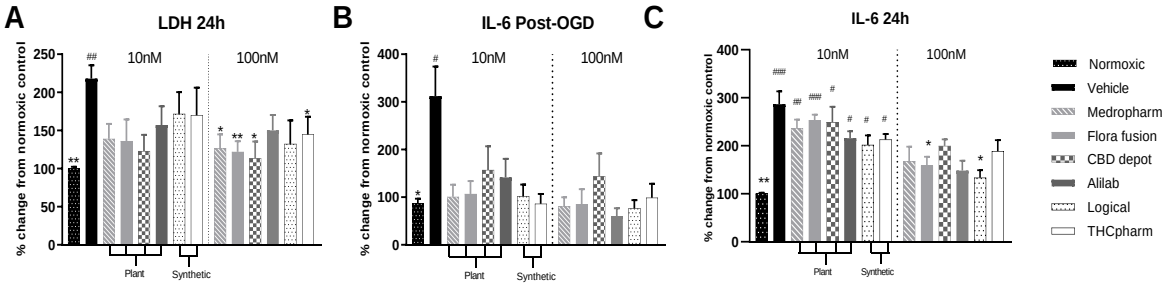


Figure 5.3 Effects of CBD in pericytes (p4–6) exposed to 4-h OGD. **a** Effect of CBD (10 or 100 nM) on LDH concentrations 24 h following initiation of OGD (n = 6, from two separate experiments). Effect of various CBD samples (10 or 100 nM) on media IL-6 concentrations immediately after OGD (**b**), or 24 h following the initiation of OGD (**c**) (n = 6, from 2 separate experiments). Data are displayed as mean ± SEM % change from normoxic control and were compared for statistical significance against the normoxic control (#) or OGD vehicle (*) using a one-way ANOVA. *p ≤ 0.05, **p ≤ 0.01, and ***p ≤ 0.001. CBD, cannabidiol; OGD, oxygen-glucose deprivation.

CBD 100 nM was co-applied with the 5HT1A antagonist WAY-100635 (Hind, England and O'Sullivan, 2016). As before, IL-6 secretion was blunted by CBD (figure 5.4A, 50-63% relative to vehicle). However, in the presence of WAY-100635, this effect was reduced such that an increase in IL-6 secretion was observed (figure 4A). There was no pronounced effect of WAY-100635 on LDH activity (figure 5.4B).

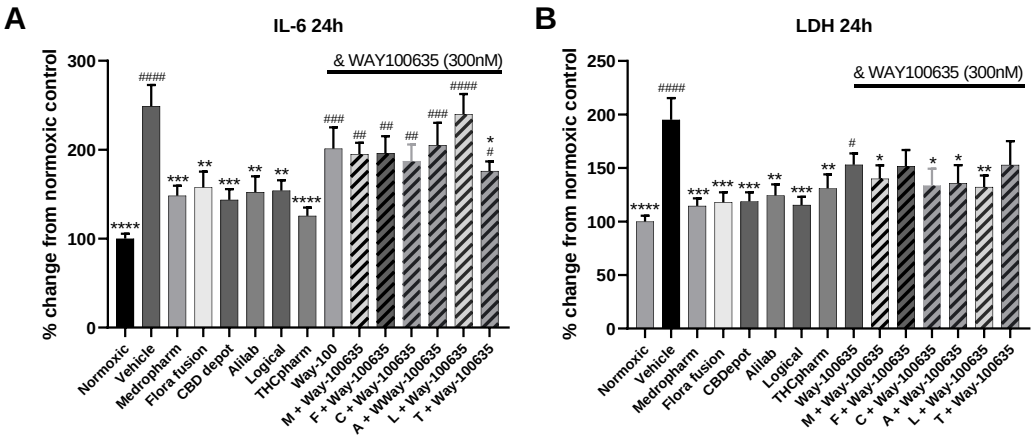


Figure 5.4 Effects of natural and synthetic CBD (100 nM) on LDH and IL-6 concentrations in pericytes exposed to 4 h OGD in the presence or absence of the 5HT1A antagonist WAY-100635 (300 nM). **a** IL-6 concentrations 24 h following the initiation of OGD (n = 11–13, from three separate experiments). **b** LDH concentrations in media from 24 h following initiation of OGD (n = 12–13, from 3 separate experiments). Data are expressed as mean ± SEM % change from normoxic and were compared to normoxic control (#) or OGD vehicle (*) using a one-way ANOVA with a multiple comparison. *p ≤ 0.05, **p ≤ 0.01, ***p ≤ 0.001, and ****p ≤ 0.0001. M, Medropharm; F, Flora Fusion; C, CBDepot; A, Ai Lab; L, Logical; T, THC Pharm; CBD, cannabidiol; OGD, oxygen-glucose deprivation.

5.3.4 CBD effects on CaCo2 barrier integrity following inflammation

Following an inflammatory protocol, barrier resistance was reduced by ~30%, indicating increased permeability (Alhamoruni *et al.*, 2012). When analysed as the total effect over time (AUC) (%·min^{-1}), all CBD products increased TEER following inflammation relative to their vehicle control (Figure 5.5B-F, and Table 1 for pooled data). No statistical differences were present between CBD sources in their ability to restore intestinal permeability.

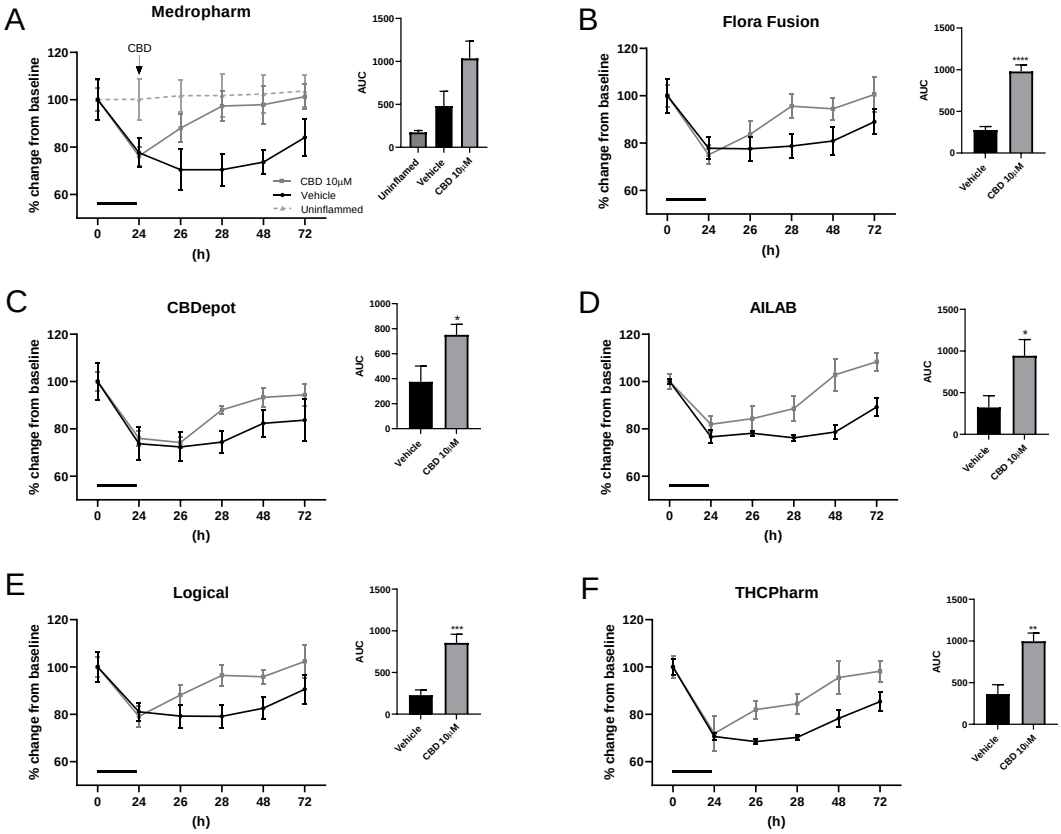


Figure 5.5 Effects of natural (**a–d**) and synthetic CBD (**e**, **f**) on intestinal permeability following a 24 h inflammatory protocol (IFNγ and TNFα, shown as the solid bar) in differentiated Caco-2 cells. Data are displayed as mean ± SEM % change from baseline inserts (n = 5–6, from three separate experiments). Time course data are displayed as AUC and analyzed using a one-way ANOVA. CBD samples were compared to vehicle or each other using a multiple comparison *p ≤ 0.05, **p ≤ 0.01, and ***p ≤ 0.001. AUC, area under the curve; CBD, cannabidiol.

As before (Figure 5.5), when CBD was administered alone, it successfully increased the recovery of TEER values following a 24 h inflammatory protocol. However, this effect was inhibited when CBD was co-administered with AM251 (1µM) (Figure 5.6).

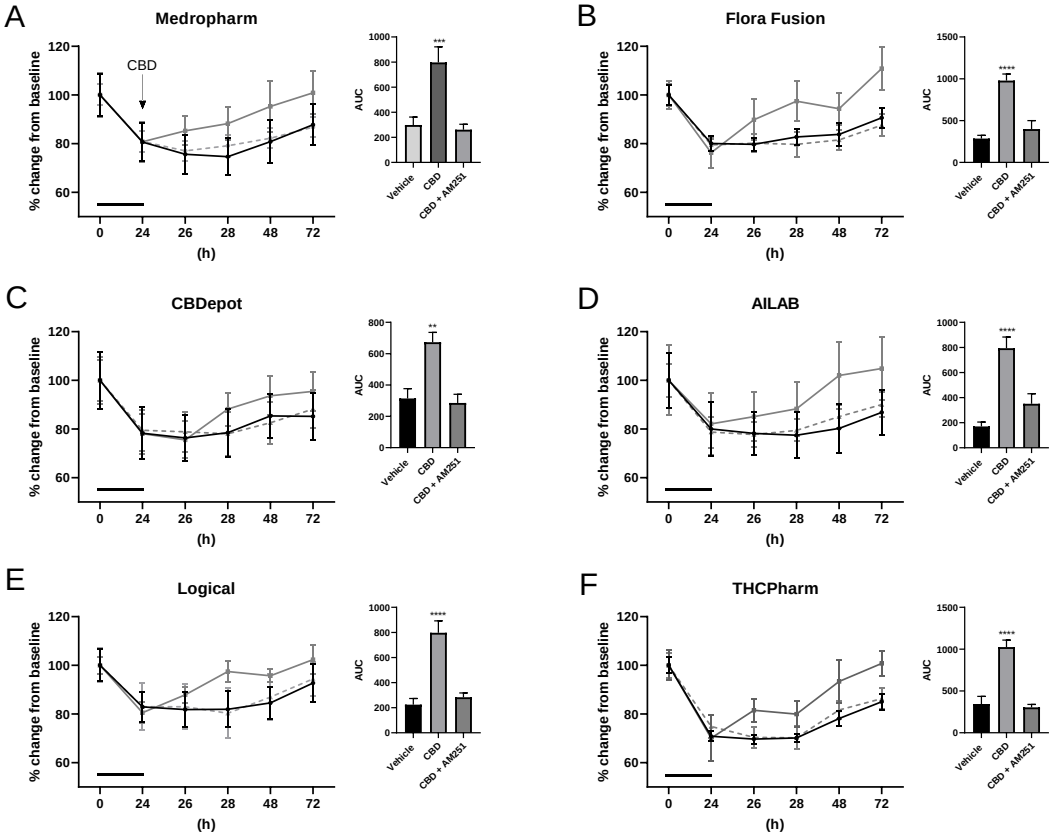


Figure 5.6 Effects of natural (**a–d**) and synthetic (**e**, **f**) CBD on intestinal permeability following a 24-h inflammatory protocol (IFNγ and TNFα, shown as the solid bar) in differentiated Caco-2 cells in the presence or absence of the CB_1 receptor antagonist AM251 (---). Time course data are displayed as AUC and analyzed using a one-way ANOVA. CBD samples were compared to vehicle or each other using a multiple comparison **p ≤ 0.01, ***p ≤ 0.001, and ****p ≤ 0.0001. AUC, area under the curve; CBD, cannabidiol.

5.4 **Discussion**

This study aimed to investigate whether CBD derived from different sources (natural or synthetic) would behave similarly in three human cell disease models. Across all experiments, each CBD tested at their respective concentrations and time-points produced very similar effects. While some minor variability existed in the magnitude of effect and percentage of purity, none of these differences manifested in one particular source of CBD being superior. This data supports our hypothesis that there is no pharmacological difference between synthetic and plant-derived CBD *in vitro*.

CBD has anti-proliferative (Ligresti *et al.*, 2006; De Petrocellis *et al.*, 2013) and anti-apoptotic features in multiple cancer cell lines (Ramer *et al.*, 2013). Therefore experiments investigated the effects of CBD in the ovarian cancer cell line SKOV-3 to see whether the CBD source influenced results. 10 µM CBD reduced cell viability in proliferating cells, and 50 µM CBD was cytotoxic in proliferating and confluent cells. The effects of CBD were consistently greater at 48h. None of the purified CBD sources differed in their efficacy across concentrations or time-points, suggesting that it's anti-proliferative/cytotoxic effects remain the same in the SKOV-3 cell line regardless of how CBD is sourced. Since the effect of CBD were not attenuated by the range of antagonists used and the high concentration of CBD required, this is likely a non-receptor mediated mechanism, for example, on mitochondria membrane potential or ROS generation (Massi *et al.*, 2013), which should be investigated in future experiments.

CBD possesses several properties that could be useful in treating ischemia and reperfusion injuries, including modulation of intracellular calcium (Ryan, Alison J. Drysdale, *et al.*, 2009), attenuating BBB permeability (Hind, England and O'Sullivan, 2016), improving glucose metabolism and optimising energy production (Sun *et al.*, 2017) and as an anti-oxidant molecule (Hampson *et al.*, 1998). The present experiments aimed to investigate the effects of different sources of CBD on cell damage in pericytes exposed to OGD and reperfusion. All CBD sources prevented OGD-induced increases in IL-6 and LDH, and the anti-inflammatory effect of CBD was partially reduced by 5HT1A antagonism, as previously observed (Mishima *et al.*, 2005; Hind, England and O'Sullivan, 2016). This suggests that synthetic and plant-derived CBD can activate 5HT1A, the molecular target underpinning many the therapeutic effects produced by CBD, including neuroprotection, anti-nausea, and anti-inflammatory (Mishima *et al.*, 2005; Bolognini *et al.*, 2013; Ward *et al.*, 2014). This is the first time the protective properties of CBD have been shown in pericytes exposed to OGD/R injury.

As previously shown (Alhamoruni *et al.*, 2012), CaCo2 barrier integrity could be restored by administering CBD to the apical compartment of transwell inserts following a 24 h inflammatory protocol. Further work demonstrated that these effects of CBD extend to human colon explants exposed to inflammation (Couch *et al.*, 2019). In both studies, the ability of CBD to restore barrier integrity was inhibited by CB_1 antagonism (Alhamoruni *et al.*, 2012; Couch *et al.*, 2019). Recently Couch and colleagues showed that CBD (600mg) was protective against aspirin-induced permeability increases in healthy volunteers *in vivo* (Couch *et al.*, 2019). In this

current set of experiments, all of the CBDs tested restored barrier integrity of differentiated CaCo2 cells following inflammation to a similar extent. The effects on barrier integrity were attenuated by antagonism of the CB_1 receptor for all CBD sources. These results suggest plant-derived and synthetic CBD have similar pharmacological effects in a cellular model of the acutely inflamed small intestine.

One caveat to consider is that plant-derived CBD can have other phytocannabinoids present, albeit in small amounts (see Table 1). However, the concentration of these compounds would be moderate with high concentrations of CBD. For example, the most abundant contaminant was CBDV (0.6%). At 50µM, the corresponding concentration of CBDV would be ~300nM. CBDVs pharmacology is not well characterised, but binding assays demonstrated a K_i of 14.7µM at CB_1 and 570nM at CB_2 (Rosenthaler *et al.*, 2014). It is therefore unlikely that the small concentrations of CBDV or other phytochemicals influenced our results at a pharmacodynamic level. Whether there are pharmacokinetic interactions between these chemicals *in vivo* remains to be tested.

This study demonstrates for the first time that the anti-cancer, neuroprotective and intestinal barrier protective properties of purified CBD are similar regardless of the source from which CBD is derived. From a pharmacological perspective. Where a molecular target is implicated (i.e. 5HT1A in stroke and CB_1 in gut permeability), the effects of CBD were similar. This suggests that any beneficial effects achieved in a clinical setting for purified CBD are likely to be similar at a pharmacodynamic level. Based on this analysis, the economic, environmental impact, purity, reliability and consistency of supply of CBD sources and the ultimate pharmaceutical form and formulation should all be considered above the starting source of the CBD in the development of new CBD medicines.

6 The effects of CBD and TMP coadministration in human cell lines

6.1 Introduction

Cannabidiol (CBD) has shown anti-cancer effects in several cancer cell lines and protective effects in cerebral ischemic-reperfusion injury models. CBDs effects in cancer include the modulation of cell proliferation, programmed cell death, migratory and invasive capacity (Seltzer *et al.*, 2020). In cellular models of oxygen-glucose deprivation/ reperfusion (OGD/R), CBD has been shown to possess several protective effects with the potential to treat stroke (Hayakawa, Mishima and Fujiwara, 2010).

Given the surmounting pre-clinical evidence of CBD in these diseases, one of the major hurdles preventing CBD from moving from bench to bedside is its inherent poor bioavailability. (Huestis, 2007; Martin *et al.*, 2018; Millar *et al.*, 2020). Due to the highly lipophilic nature of CBD (Odi *et al.*, 2020), when delivered orally in solution, CBD can precipitate in the gastrointestinal (GI) tract—resulting in an elimination rate faster than the rate of absorption (Chan and Stewart, 1996). Highly lipophilic drugs also utilise lymphatic transport to gain entry into general circulation, resulting in pk profiles that are sensitive to fed/fasted states, delayed onset of effect, and erratic inter-patient pharmacokinetics (Yáñez *et al.*, 2011). The oral bioavailability of CBD is estimated at 6%; however, little data exists in this area (Millar *et al.*, 2018).

One technique successfully used to increase the bioavailability of a drug is co-crystal formation. Pharmaceutical co-crystals are crystalline solids that complex two or more molecules together by non-covalent bonds at stoichiometric ratios (Miroshnyk, Mirza and Sandler, 2009). In this respect, if the physicochemical properties of CBD were modified to provide more suitable characteristics for drugs absorption, CBD may display less inter/intra-subject variability and improved bioavailability. For example, the drug 6-mercaptopurine (6-MP) falls into the BCS class II of drugs and possess low oral bioavailability (about 16%) limited by its poorly aqueous solubility. Co-crystal formation of 6-MP with isonicotinamide showed 169% higher oral bioavailability in rats relative to 6-MP alone, suggesting the drug

was more readily dissolved in the gut (Wang *et al.*, 2015). However, this co-crystal uses a pharmacologically inert co-former, and in some instances, co-crystals have been developed as multi-drug complexes in the hope of achieving therapeutic benefits through synergistic action. E-58425 is an example of such a drug, a co-crystal comprising two pharmacologically active molecules, celecoxib, and tramadol at a 1:1 ratio. A phase II clinical trial established that the co-crystal possessed superior efficacy and safety relative to the placebo control or tramadol alone in postoperative dental pain (EudraCT, 2013).

Tetramethylpyrazine (TMP) is an alkaloid extracted from Chuanxiong (*Ligusticum wallichii*) and is used clinically in China to treat cardiovascular disease (Chen *et al.*, 2019). Current pharmacological evidence indicates TMP possess several properties that would be useful in treating and preventing ischemic/reperfusion injury. Using a rat MCAO model of ischemic stroke, Liao and colleagues demonstrated that intraperitoneally administered TMP (5-40mg/kg) reduced infarct volume by 3-22% with a linear dose-response relationship. Furthermore, TMP at 20mg/kg was shown to reduce brain oedema by -4% 3days following 90min MCAO (Liao *et al.*, 2004). In another rat MCAO study, Chang and colleagues demonstrated that TMP (20mg/kg) could reduce the activation of caspase-3 and reduce the expression of TNF-α (Chang *et al.*, 2007). Finally, Lin and colleagues showed that TMP aided in post-stroke functional recovery 14-days following MCAO in rats (Lin *et al.*, 2015). TMPs effects in cancer are less well explored; however, some *in vitro* studies exist. Cao and colleagues using flow cytometry demonstrated that TMP at 100μM could induce apoptosis in Human HCC HepG2 cells. Also demonstrating that this effect extended to an *in vivo* mouse xenograft tumour model (Cao *et al.*, 2015). Zheng and colleagues showed TMP at 100mg/kg/day for 30 days reduced *in vivo* metastatic growth of A549 cells in the nude mouse metastatic model, and this effect was associated with reduced expression of cyclooxygenase-2 (COX-2) and activity of matrix metalloproteinase-2 (MMP-2) (Zheng *et al.*, 2012). Finally, Zhou and colleagues using a scratch wound assay, demonstrated that TMP at high concentrations (50-200μM) could drastically reduce the migratory capacity of the prostate cancer cell line PC-3, and this effect was correlated with reduced expression of forkhead box M1 (FOXM1) gene (Zhou *et al.*, 2017).

Modifications to the molecular structure of TMP are well documented. It is estimated that over 300 TMP derivatives have been synthesised (Zhao, Liu and Chen, 2016). Given the well-practised nature of developing new chemical entities using TMP, Artelo Biosciences have developed a co-crystal complex using CBD and TMP. The

co-crystal allows for a patentable matter, reduces the likelihood of polymorphisms and may offer improved physicochemical and pharmacological characteristics.

To successfully develop a co-crystal, one must consider any pharmacological interactions between the two drugs. Thus these experiments aimed to examine the individual pharmacological properties of CBD and TMP in 2 human cellular models of disease (cancer and stroke) and assess whether co-application of these molecules at a 1:1 ratio produces synergistic, additive, neutral or compromised efficacy. Given some of the overlapping pharmacology, it was hypothesised TMP would work synergistically or additively with CBD by decreasing cellular viability in cancer cells and reducing markers of inflammation and cell death in cellular models of stroke.

6.2 Methods

6.2.1 General methods

Drugs

Cannabidiol was supplied by THC pharm GmbH (Germany). TMP was supplied by Sigma Aldrich (UK). Drugs were dissolved in ethanol as CBD, TMP or CBD and TMP at equimolar concentrations and stored in -20^{o}C as stock concentrations of 10^{-1}.

Cells

All cells were maintained in a humidified cell culture incubator at 37^{o}C with 5% CO_2 and grown to 70-80% in a T75 flask before seeding into plates. CaCo2 cells (The European Collection of Authenticated Cell Cultures [ECACC, UK]) were cultured using Minimum Essential Medium Eagle (MEME), supplemented with 1% penicillin-streptomycin (P/S), 1% non-essential amino acids (NEAA) and 10% heat-inactivated foetal bovine serum (FBS). DU-145 cells (ECACC, UK) (p11-35) were cultured using Roswell Park Memorial Institute (RPMI) 1640 base medium containing L-glutamine and phenol red indicator (Gibco). Cell medium was supplemented with 10% heat-inactivated FBS and 1% P/S. SKOV-3 cells (The European Collection of Authenticated Cell Cultures [ECACC, UK]) were cultured using RPMI 1640 base medium containing L-glutamine and phenol red indicator

(Gibco). Cell medium was supplemented with 10% heat-inactivated FBS and 1% P/S. Human astrocytes (ScienCell, USA) were cultured in a specialised commercial medium (2% FBS, 1% astrocyte growth supplement and 1% P/S). Human brain vascular pericytes (ScienCell, USA) were cultured in a specialised commercial Pericyte medium (2% FBS, 1% pericyte growth supplement, and 1% P/S).

6.2.2 Experimental procedures

Cancer cell line experiments

Proliferating studies

CaCo2 (p47-49), DU-145 (p11-14) and SKOV-3 (p34-37) cells were seeded in 96 well plates at 10,000 cells per well. Cells were given three hours to adhere to wells, at which point CBD, TMP or CBD + TMP was applied at 1, 5, 10, 15, 20, 25 or 30 µM. Resazurin (100µM) was then added to wells 24 or 48h following the application of drugs. The cellular metabolism of resazurin to resorufin was measured as a marker of cell viability by measuring absorbance at 530nm and 590nm following 1hr of exposure of resazurin at 100µM.

Fully confluent studies

CaCo2 (p49-50), DU-145 (p12-13) and SKOV-3 (p36-37) cells were seeded in 96 well plates at 10,000 cells per well. Cells were given 24h to reach confluence, confirmed by light microscopy. At which point CBD, TMP or CBD + TMP was applied at 1, 5, 10, 15, 20, 25, 30 µM. Resazurin was then added to wells at 48 or 72h following the application of drugs and absorbance measured.

To assess moderate concentration over moderate exposure times, CaCo2 (p45-47), DU-145 (p35-38) and SKOV-3 (p23-24) cells were seeded in 6 well plates at 100,000 cells per well. Cells were given 48h to reach confluence, confirmed by light microscopy. At which point, cells were treated with 10 µM, 15 µM or 20 µM of drugs every three days until the end of the experiment. 144h following the initial application of the drugs, cell viability was measured using resazurin assay, and images were taken using light microscopy. Before light microscopy, cells were washed with phosphate-based buffer (ph7.4) to remove cellular debris.

To assess low concentrations over prolonged exposure times, CaCo2 (p36), DU-145 (p12-13) and SKOV-3 (p21-27) cells were seeded in 96 well plates at 10,000 cells per well. Cells were given 24h to reach confluence, confirmed by light microscopy. At which point, cells were treated with 100 nm, 1 µM or 5 µM of drugs at two-day intervals for ten days. Following ten days of drug exposure, cell viability was measured using a resazurin assay.

Scratch wound assays

To assess the migratory capacity of each cell type and the effect CBD, TMP or CBD and TMP in combination have on this parameter. DU-145 (p27-28) and SKOV3 (p27) cells were seeded into six-well plates at a density of 800,000 cells per/well. At 90% confluence, cells were serum-starved (1% FBS) for one day before performing the scratch wound. The cell monolayer was scratched with a p200 pipet tip in a straight line, using a sterile plate lid to guide the scratching motion. 1ml of PBS was used to remove cellular debris and smooth the edge of the scratch. PBS was then aspirated and replaced with 5ml of the respective medium. CaCo2 cells did not possess enough migratory capacity to be used in this assay.

Oxygen glucose deprivation/reperfusion experiments

Human brain astrocytes (p2-6) and human brain pericytes (p3-6) were exposed to oxygen-glucose deprivation/reperfusion (OGD/R) conditions for 8 and 4h respectively as a cellular model of stroke (Hind, England and O'Sullivan, 2016; Stone, England and O'Sullivan, 2019). Cells were seeded at a density of 10,000 cells/cm^2 in a 96 well cell culture plate. Once confluent, spent media was aspirated, and cells were washed in 100µl of PBS, which was aspirated and replaced with RPMI glucose-free media (Invitrogen, USA), containing either CBD, TMP, CBD+TMP (1µM or 10µM, astrocytes) (10nm or 100nm, pericytes) or vehicle (ethanol) based on published and unpublished work by our laboratory (Hind, England and O'Sullivan, 2016). Immediately following the addition of glucose-free media, plates were sealed into GasPak EZ Anaerobe Pouches (Beckton Dickinson, UK) and placed into the incubator, producing anoxic conditions within 20 minutes (Hind, England and O'Sullivan, 2016). Following OGD, media was collected and replaced with their respective growth medium containing either CBD, TMP,

CBD+TMP or vehicle and returned to normoxic conditions (5% CO_2, 95% air, reperfusion period) for a further 24h (astrocytes) or 20h (pericytes). At that point, the final media samples were collected, and a resazurin assay was performed to assess cell viability. An IL-6 (at 24h only) duoset ELISA (R&D systems), and a lactate dehydrogenase (LDH) activity assay (Abcam, US) was performed on media samples (immediately post-OGD and 24h) as per the manufacturer's instructions to assess inflammation and cellular damage, respectively.

Data analysis

All statistical analysis was conducted using GraphPad Prism 7. ImageJ was used to quantify the area of scratch wound assays. All data were presented as mean percentage change from vehicle ±SEM, or mean percentage change from normoxic ±SEM in OGD experiments. One-way ANOVA using multiple comparison was used to detect significant differences between vehicle, normoxic and drugs.

6.3 Results

6.3.1 Effects of CBD and TMP in proliferating cancer cell lines

In all cell lines tested (CaCo2, DU-145 and SKOV-3), CBD possessed a linear concentration-response relationship that was potentiated over time (figure 6.1A-C).

At 24 h, CBD in CaCo2 and DU-145 cells did not produce a large enough effect to predict an IC_{50} value; however, in SKOV-3 cells (figure 6.1C), CBD produced an IC_{50} of 17.5 µM ±1.

At 48 h, the IC_{50} for CBD in CaCo2 cells (Figure 6.1A) was 18.5 µM ±1.2, 9.5 µM ±0.2 in DU-145 cells (figure 6.1B) and 11 µM ±0.4 in SKOV-3 cells (Figure 6.1C). In all the cell lines, TMP did not produce a linear concentration-response relationship. However, TMP decreased cellular viability relative to vehicle at 48 h by 60-70% in CaCo2 cells (Figure 6.1A), 36-61% in DU-145 cells (Figure 6.1B) and 40-45% in SKOV-3 cells (Figure 6.1C). At 48 h, CBD + TMP produced a classic inhibitor response curve in DU-145 (Figure 6.1B) and SKOV-3 cells (Figure 6.1C), with an IC_{50} of 3.5 µM ±0.2 and 2.5 µM ±1 respectively. In CaCo2 cells (Figure 6.1A), CBD+TMP did not produce a classic inhibitor response curve with increasing concentrations, and reductions in cell viability ranged from 54-68% ($p<0.0001$, at all concentrations).

When comparing the IC_{50} of CBD vs. CBD+TMP, The IC_{50} value of CBD was lowered by inclusion of TMP by -6 µM ±1.3 ($p<0.001$) in DU-145 cells (Figure 6.1B) and by 8.9 µM ± 1.1 ($p<0.0001$) in SKOV-3 cells (Figure 6.1C) at 48h. No other significant differences existed between the IC_{50} of CBD and CBD+TMP at any other time points, in any cell type.

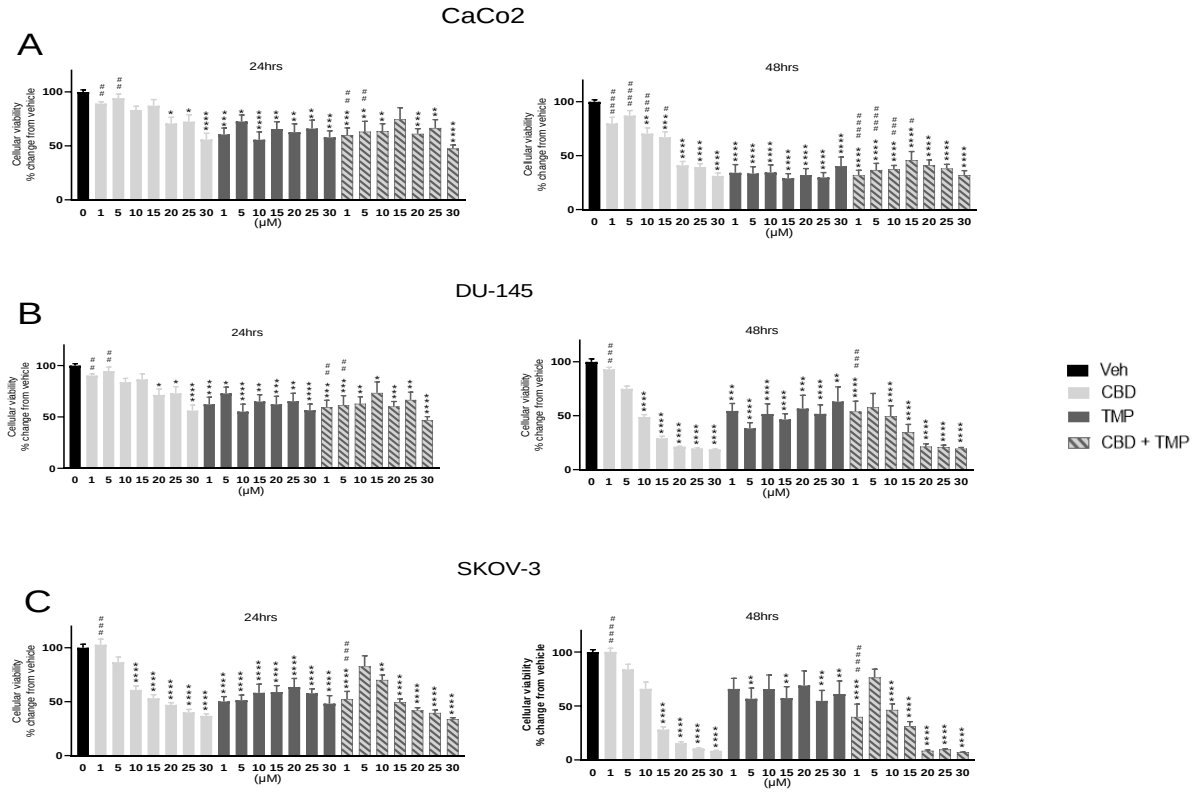


Figure 6.1 The effects of CBD, TMP and CBD + TMP (1-30 μM) on cellular viability in proliferating cancer cell lines using resazurin assays. A) Effects of CBD, TMP and CBD + TMP on proliferating CaCo2 cells (p49-50) 48 and 72 h following drug application. B) Effects of CBD, TMP and CBD + TMP on proliferating DU-145 cells (p12-13) 48 and 72 h following drug application. C) Effects of CBD, TMP and CBD + TMP on proliferating SKOV-3 cells (p36-37) 48 and 72h following drug application. In all cell types n= 8, from two separate experiments. Data are presented as percentage change from vehicle S.E.M and was compared for statistical significance against vehicle (*) or between CBD and CBD + TMP (#) at their respective concentrations and time-points using a one way ANOVA.*/# P ≤ 0.05, **/## P ≤ 0.01, ***/### P ≤ 0.001, ****/#### P ≤ 0.0001.

6.3.2 Effects of CBD and TMP in fully confluent cancer cell lines

In CaCo2 cells (figure 6.2A), at 48 h, CBD caused a statistically significant increase in cellular viability relative to vehicle, by 16% ±2 ($p<0.05$) at 5 μM, 21% ±3 ($p<0.01$) at 15 μM, 21% ±3 ($p<0.0001$) at 20 μM, 30% ±3 ($p<0.01$) at 25 μM and 33% ±5 ($p<0.0001$) at 30 μM. However, at 72 h, this increase was no longer present, and none of the concentrations of CBD statistically differed from vehicle. TMP had no significant effect on CaCo2 cell viability at any time point relative to vehicle. At 48 h, CBD+TMP produced a significant increase in cell viability by 17% ±4 ($p<0.05$) at 15 μM, 37% ±3 ($p<0.0001$) at 20 μM, 37% ±4 ($p<0.0001$) at 25 μM and 46% ±5 ($p<0.0001$) at 30 μM relative to vehicle. At 72 h, these increases were no longer apparent, and CBD+TMP at all concentrations no longer statistically differed from

vehicle. When compared against each other at their respective concentrations, there were no statistical differences between CBD and CBD+TMP.

In DU-145 cells (figure 6.2B), at 48 h, CBD caused a statistically significant decrease in cellular viability by -11% ±2 ($p<0.01$) at 5µM, -10% ±3 ($p<0.05$) at 15 µM, and -12% ±3 ($p<0.001$) at 20 µM. TMP produced a significant decrease in cell viability at three concentrations; -9% ±1 ($p<0.05$) at 5 µM, -10% ±3 ($p<0.05$) at 10 µM, and -9% ±2 ($p<0.05$) at 20 µM. CBD+TMP caused a significant decrease in cellular metabolism by 9% ±2 ($p<0.05$) at 5 µM and 11% ±3 ($p<0.01$) at 10 µM. At 72 h, in DU145 cells CBD+TMP at 30 µM produced a significant decrease in cell viability, by -16% ±3 ($p<0.01$). When compared against each other at their respective concentrations, there was no statistically significant differences between CBD and CBD+TMP.

At 48 h, in SKOV-3 (Figure 6.2C) cells, only TMP produced a significant decrease in cellular viability. By -33% ±11 ($p<0.05$) at 1 µM and -29% ±12 ($p<0.05$) at 5 µM. At 72 h, in SKOV-3 cells, CBD 30 µM reduced cellular viability by -42% ±7 ($p<0.0001$) relative to vehicle. CBD+TMP reduced cellular viability relative to vehicle at two concentrations: by -35% ±7 ($p<0.0001$) at 20 µM and by -20% ±5 ($p<0.05$) at 30 µM. When compared against each other at their respective concentrations, the inclusion of TMP alongside CBD increased the ability of CBD 20 µM to decrease cell viability by 21% ±6 ($p<0.01$). However, at 30 µM, CBD alongside TMP attenuated CBDs ability to decrease cell viability by -22% ±7 ($p<0.01$). At all other concentrations, no statistical differences existed between CBD and CBD+TMP at their respective concentrations.

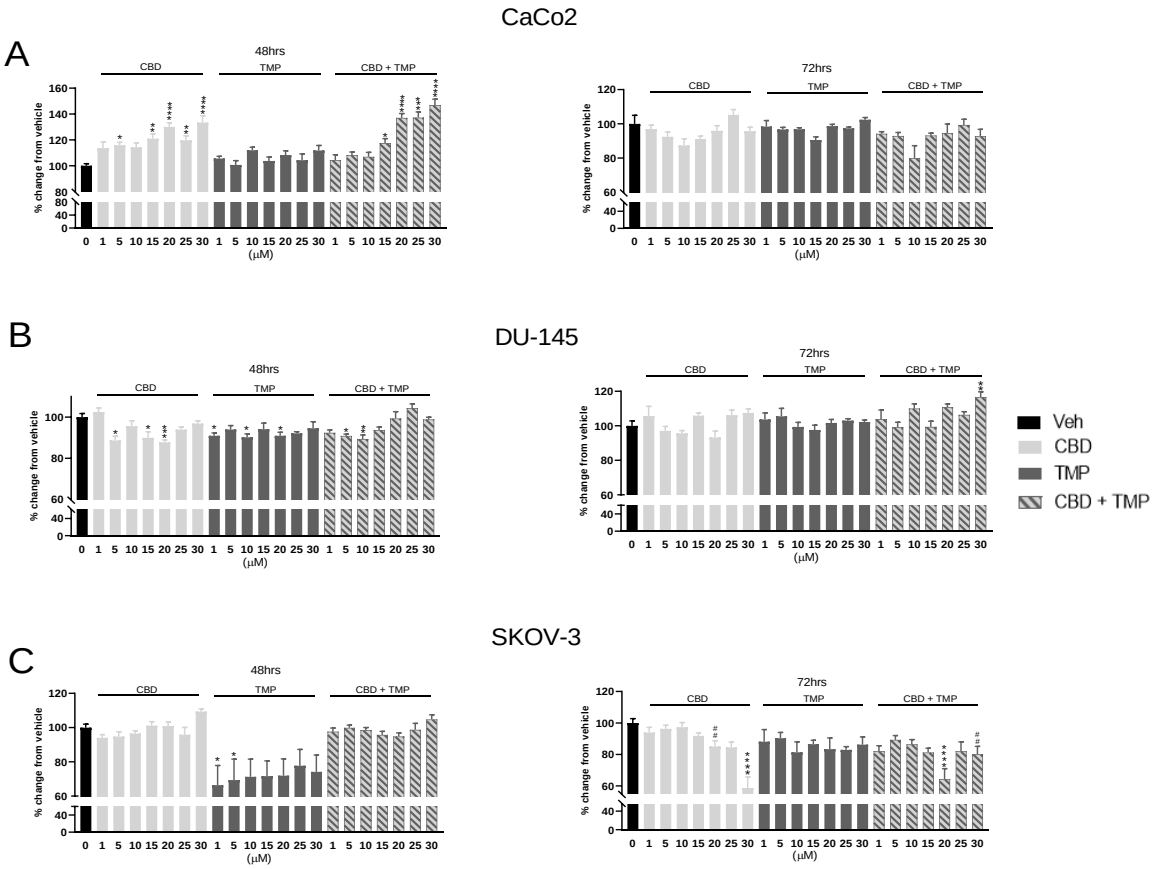


Figure 6.2 The effects of CBD, TMP and CBD + TMP (1-30 μM) on cellular viability in fully confluent cancer cell lines using resazurin assays. A) Effects of CBD, TMP and CBD + TMP on fully confluent CaCo2 cells (p49-50) 48 and 72 h following drug application. B) Effects of CBD, TMP and CBD + TMP on fully confluent DU-145 cells (p12-13) 48 and 72h following drug application. C) Effects of CBD, TMP and CBD + TMP on fully confluent SKOV-3 cells (p36-37) 48 and 72 h following drug application. In all cell types n= 8, from two separate experiments. Data are presented as percentage change from vehicle S.E.M and was compared for statistical significance against vehicle (*) or between CBD and CBD + TMP at their respective concentrations and time-points (#) using a one way ANOVA.*/# P ≤ 0.05, **/## P ≤ 0.01, ***/### P ≤ 0.001, ****/#### P ≤ 0.0001.

6.3.3 Effects of CBD and TMP in fully confluent cancer cell lines over moderate exposure times (144h)

In CaCo2 cells (figure 6.3A, see supplementary figure 1 for images) at 144 h, CBD produced a decrease in cellular viability relative to vehicle by -29% ±6 ($p<0.01$) at 15 μM and -25% ±5 ($p<0.05$) at 20 μM. TMP had no significant effect on cellular viability relative to vehicle at any of the concentrations tested. CBD+TMP at 20 μM by -27% ±7 ($p<0.05$). No significant differences existed between CBD and CBD+TMP at their respective concentrations.

In DU-145 cells (figure 6.3B, see supplementary figure 2 for images) at 144 h CBD produced a decrease in cellular viability relative to vehicle by -15% ±0.6 ($p<0.0001$)

at 10 µM, -26% ±0.7 (p<0.0001) at 15 µM, and -32% ±0.3 (p<0.0001) at 20 µM. At 144 h, TMP produced an increase in cellular viability relative to vehicle by 7% ±1.4 (p<0.01) at 15 µM, and 5% ±0.5 (p<0.05) at 20µM. At 144 h, CBD+TMP reduced cellular viability relative to vehicle by -13% ±0.5 (p<0.0001) at 10µM, -31% ±0.4 (p<0.0001) at 15µM, and -34% ±0.6 (p<0.0001) at 20µM. When compared against each other at their respective concentrations, the inclusion of TMP alongside CBD increased the ability of CBD 15 µM to decrease cell viability by 5% ±1.8 (p<0.05). No other significant differences were present between CBD and CBD+TMP at their respective concentrations.

In SKOV-3 cells (figure 6.3C, see supplementary figure 3) at 144 h CBD produced a decrease in cellular viability relative to vehicle by -49% ±0.7 (p<0.001) at 15 µM and -89% ±0.3 (p<0.0001) at 20 µM. TMP had no statistically significant effect on cell viability relative to vehicle. CBD+TMP reduced cellular viability relative to vehicle by -31% ±1.4 (p<0.05) at 10 µM, -76% ±0.5 (p<0.0001) at 15 µM and -90% ±0.5 (p<0.0001) at 15 µM. When compared against each other at their respective concentrations, the inclusion of TMP alongside CBD increased the ability of CBD 15 µM to decrease cell viability by 27% ±8 (p<0.05). No other significant differences were present between CBD and CBD+TMP at their respective concentrations.

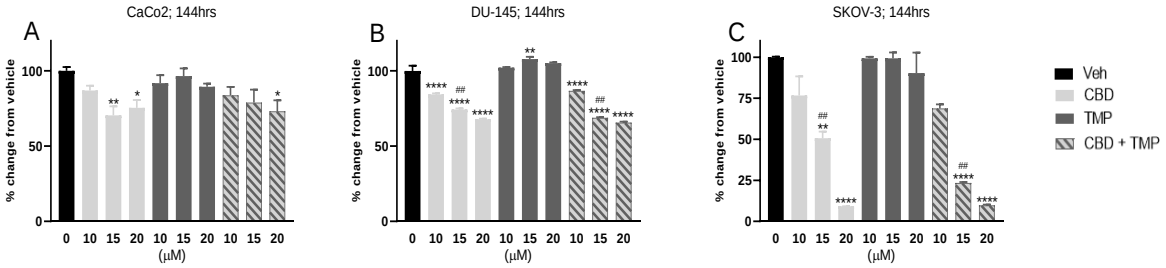


Figure 6.3 The effects of CBD, TMP and CBD + TMP (10,15 and 20 µM) on cellular viability using moderate concentrations over moderate exposure times in three fully confluent cancer cell lines using resazurin assays. Fresh media containing drugs or vehicle was applied at 0h and then again at 72 h. A) The effects of CBD, TMP and CBD + TMP in fully confluent CaCo2 (p45-47) cells 144h following the initial application of drugs. B) The effects of CBD, TMP and CBD + TMP in fully confluent DU-145 (p35-38) cells 144 h following the initial application of drugs. C) The effects of CBD, TMP and CBD + TMP in fully confluent SKOV-3 (p23-24) cells 144 h following the initial application of drugs. In all cell types n=6, from two separate experiments. Data are presented as percentage change from vehicle S.E.M and was compared for statistical significance against vehicle (*) or between CBD and CBD + TMP at their respective concentrations and time-points (#) using a one way ANOVA.*/# P ≤ 0.05, **/## P ≤ 0.01, ***/### P ≤ 0.001, ****/#### P ≤ 0.0001.

6.3.4 Effects of CBD and TMP in fully confluent cancer cell lines over prolonged exposure times (240h)

To assess the possibility that lower concentrations may prove cytotoxic if exposure times were increased, the cellular viability at 240 h following exposure to the drugs at 48 h intervals was assessed. In all cell lines, none of the compounds tested, at any of the concentrations (100 nM, 1 µM and 5 µM), produced statistically detectable differences relative to vehicle (figure 6.4A-C).

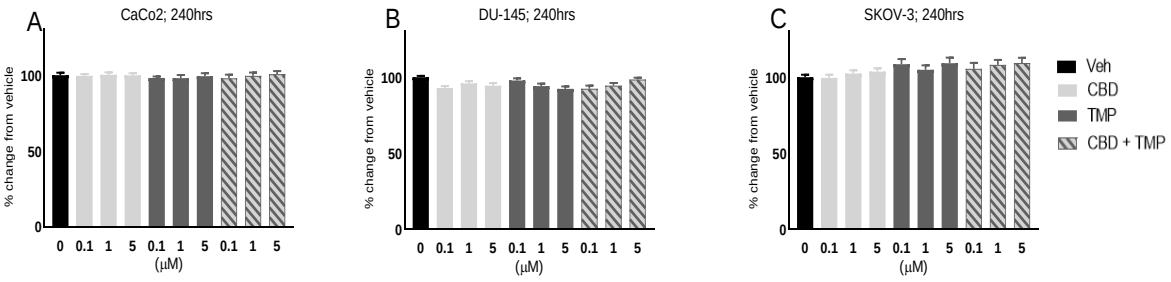


Figure 6.4 The effects of CBD, TMP and CBD + TMP (100nM, 1µM and 5µM) on cellular viability using low concentrations over extended exposure times in three fully confluent cancer cell lines using resazurin assays. Fresh media containing drugs or vehicle was applied at 0h and then every 48h until 240h. A) The effects of CBD, TMP and CBD + TMP in fully confluent CaCo2 (p21-27) cells 240h following the initial application of drugs. B) The effects of CBD, TMP and CBD + TMP in fully confluent DU-145 (p12-13) cells 240h following the initial application of drugs. C) The effects of CBD, TMP and CBD + TMP in fully confluent SKOV-3 (p36) cells 240h following the initial application of drugs. In all cell types n=8, from two separate experiments. Data are presented as percentage change from vehicle S.E.M and was compared for statistical significance against vehicle (*) or between CBD and CBD + TMP at their respective concentrations and time-points (#) using a one way ANOVA.*/# P ≤ 0.05, **/## P ≤ 0.01, ***/### P ≤ 0.001, ****/#### P ≤ 0.0001.

6.3.5 Effects of CBD and TMP on scratch wound closure in cancer cell lines

In DU-145 cells at 24 h (figure 6.5A), the vehicle wound had closed by 69% ±2. CBD at 10 µM reduced the rate of wound closure by -42% ±3 ($p<0.0001$) and by -62% ±1 ($p<0.0001$) at 20 µM. TMP had no significant effect on the rate of wound closure relative to vehicle. CBD+TMP at 10 µM reduced the rate of wound closure by -37% ±3 ($p<0.0001$) and by -50% ±4 ($p<0.0001$) at 20 µM. When compared against each other at their respective concentrations, the inclusion of TMP alongside CBD decreased the ability of CBD 20 µM to reduce the rate of wound closure relative to vehicle by 13% ±4 ($p<0.01$). No other significant differences were present between CBD and CBD+TMP at their respective concentrations.

In DU-145 cells at 48 h (figure 6.5B), the vehicle wound had closed by 100% ± 0. CBD at 10 µM reduced the rate of wound closure by -47% ±4 ($p<0.0001$) and by -74% ±3 ($p<0.0001$) at 20 µM. TMP had no significant effect on the rate of wound closure relative to vehicle. CBD+TMP at 10 µM reduced the rate of wound closure by -44% ±2 ($p<0.0001$) and by -52% ±2 ($p<0.0001$) at 20 µM. When compared against each other at their respective concentrations, the inclusion of TMP alongside CBD decreased the ability of CBD 20 µM to reduce the rate of wound closure relative to vehicle by 23% ±4 ($p<0.01$). No other significant differences were present between CBD and CBD+TMP at their respective concentrations.

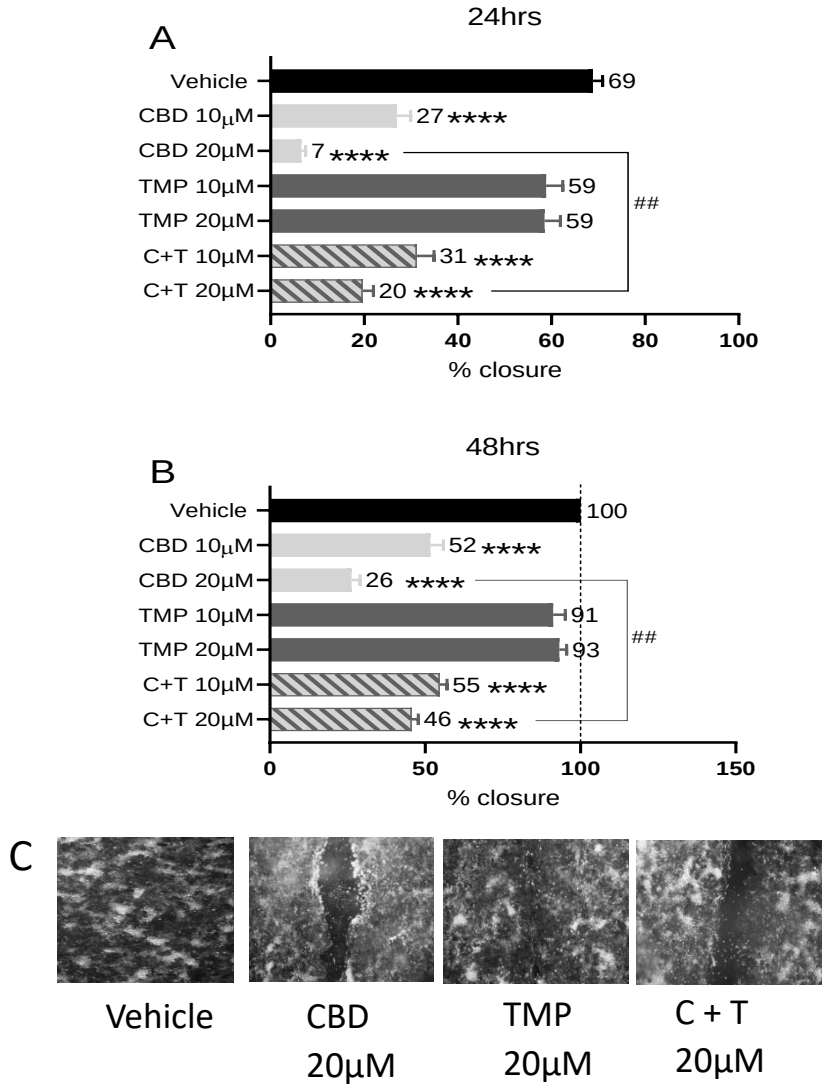


Figure 6.5 The effects of CBD, TMP and CBD + TMP (10 or 20 µM) on serum-starved DU-145 cells (p27-28) in a scratch wound assay. Effects of CBD, TMP and CBD + TMP on wound closure rate at A) 24 h or B) 48 h. In all experiments n= 6, from two separate experiments. C) Light microscope images 48h following scratch wound procedure correspond with figure 6.5B**.** Data are presented as mean percentage closure from baseline S.E.M and was compared for statistical significance against vehicle or between CBD and CBD + TMP at their respective concentrations and time-points using a one way ANOVA.* P ≤ 0.05, ** P ≤ 0.01, *** P ≤ 0.001, **** P ≤ 0.0001.

In SKOV-3 cells at 24 h (figure 6.6A), the vehicle wound had closed by 55% ±4. None of the drugs tested statistically affected the rate of wound closure at this time point.

In SKOV-3 cells at 48 h (figure 6.6B), the vehicle wound had closed by 100% ±0. CBD at 10 µM reduced the rate of wound closure by -29% ±2 ($p<0.0001$) and by -68% ±3 ($p<0.0001$) at 20 µM. TMP had no significant effect on the rate of wound closure relative to vehicle. CBD+TMP at 10 µM reduced the rate of wound closure by -31% ±6 ($p<0.0001$) and by -40% ±3 ($p<0.0001$) at 20 µM. When compared against each other at their respective concentrations, the inclusion of TMP alongside CBD decreased the ability of CBD 20 µM to reduce the rate of wound closure relative to vehicle by 28% ±4 ($p<0.0001$). No other significant differences were present between CBD and CBD+TMP at their respective concentrations.

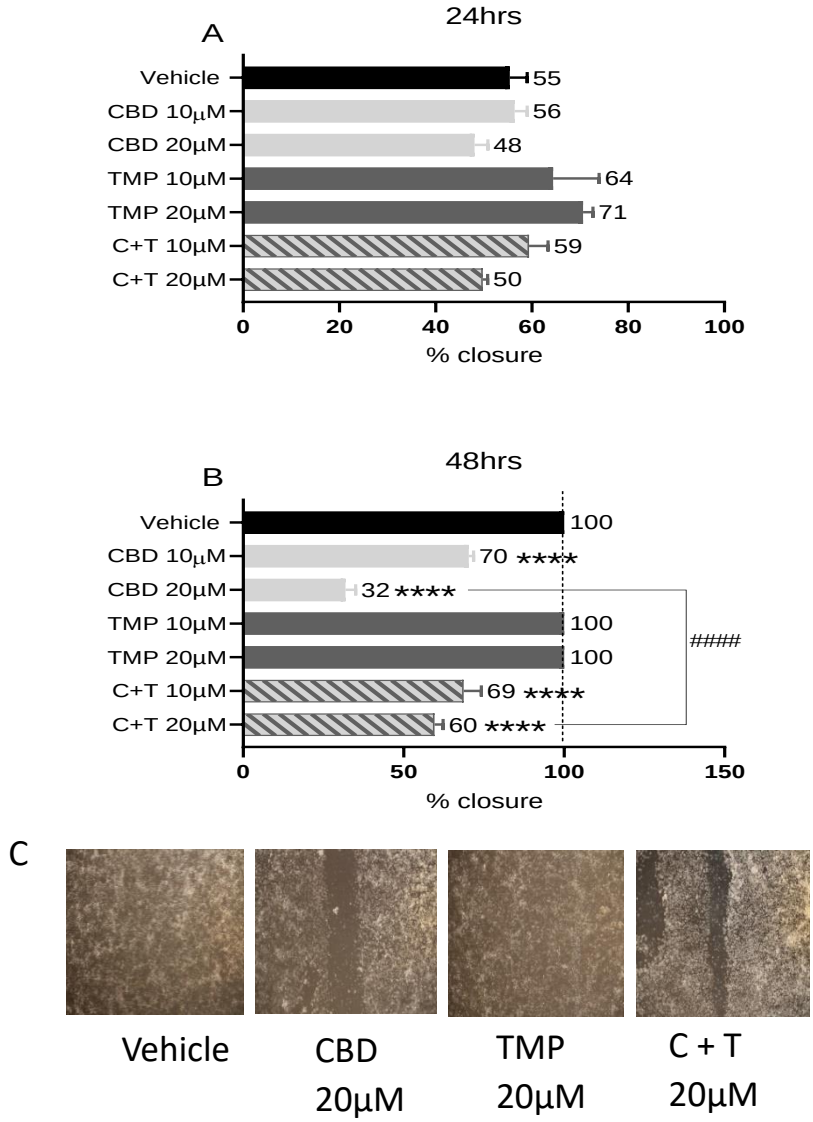


Figure 6.6 The effects of CBD, TMP and CBD + TMP (10 or 20 μM) on serum-starved SKOV-3 cells (p27) in a scratch wound assay. CBD, TMP and CBD + TMP effects on wound closure rate at A) 24h or B) 48h. In all experiments n= 6, from two separate experiments. C) Light microscope images 48 h following scratch wound procedure correspond with figure 6.6B**.** Data are presented as mean percentage closure from baseline S.E.M and was compared for statistical significance against vehicle or between CBD and CBD + TMP at their respective concentrations and time-points using a one way ANOVA.* P ≤ 0.05, ** P ≤ 0.01, *** P ≤ 0.001, **** P ≤ 0.0001.

6.3.6 Effects of CBD and TMP on resazurin metabolism in Astrocytes 32h following the initiation of OGD/R

No significant differences existed between vehicle and normoxic control (figure 6.7A). CBD 10 μM reduced the metabolism of resazurin by 12% ±2 ($p<0.05$) relative to vehicle. TMP 10 μM reduced the metabolism of resazurin by 26% ±3 ($p<0.0001$) relative to vehicle. CBD + TMP reduced the metabolism of resazurin by 23% ±3 ($p<0.0001$) at 1 μM and by 29% ±2 ($p<0.0001$) at 10 μM relative to vehicle. When compared against each other at their respective concentrations, the inclusion of

TMP alongside CBD decreased the metabolism of resazurin by 21% ±4 ($p<0.0001$) at 1 µM and by 17% ±4 ($p<0.001$) at 10 µM. No other significant differences were present between CBD and CBD+TMP at their respective concentrations.

6.3.7 Effects of CBD and TMP on IL-6 and LDH concentrations in Astrocytes exposed to OGD/R

32h following the initiation of OGD, no significant difference was present between vehicle and normoxic control (figure 6.7B).

At 1 µM, CBD reduced IL-6 media concentrations by -59% ±2 ($p<0.0001$) relative to vehicle. TMP 1µM reduced IL-6 media concentration by -39% ±4 ($p<0.001$) relative to vehicle. CBD + TMP at 1 µM reduced IL-6 media concentrations by -40% ±4 ($p<0.001$) relative to vehicle. CBD 10 µM increased IL-6 media concentrations by 28% ±10 ($p<0.01$) relative to vehicle. TMP 10 µM reduced IL-6 media content by -47% ±4 ($p<0.0001$) relative to vehicle. CBD+TMP at 10 µM had no statistically significant effect on IL-6 media concentration relative to vehicle. When compared against each other at their respective concentrations, the inclusion of TMP alongside CBD at 10 µM attenuated the ability of CBD to increase IL-6 media concentrations by -28% ±8 ($p<0.01$) at 10 µM. No other significant differences were present between CBD and CBD+TMP at their respective concentrations (figure 6.7B).

LDH content immediately post-OGD was 120% ±8 ($p<0.0001$) (Figure 6.7C) higher in vehicle + OGD than in normoxic control and at 32 h, was 1% ±26 (NS) higher in vehicle + OGD than in normoxic control (Figure 6.7D).

Immediately post-OGD (figure 6.7C), CBD 10 µM reduced LDH concentrations in cell media by -73% ±10 ($p<0.01$) relative to vehicle. At this time point, no other significant differences were present between any drugs and vehicle. When compared against each other at their respective concentrations, the inclusion of TMP alongside CBD at 10 µM attenuated the ability of CBD to reduce LDH cell media concentrations by -66% ±20 ($p<0.01$) at 10 µM. No other significant differences were present between CBD and CBD+TMP at their respective concentrations.

32 h following the initiation of OGD (figure 6.7D), none of the drugs tested at 1 µM produced any significant effect relative to vehicle. At the same time point, CBD 10 µM had no significant effect on LDH media concentration relative to vehicle. TMP 10 µM decreased LDH media concentration by -23% ±3 ($p<0.05$) relative to vehicle.

CBD+TMP 10 µM increased LDH media concentrations relative to vehicle by 20% ±6 ($p<0.05$). No significant differences were present between CBD and CBD+TMP at their respective concentrations.

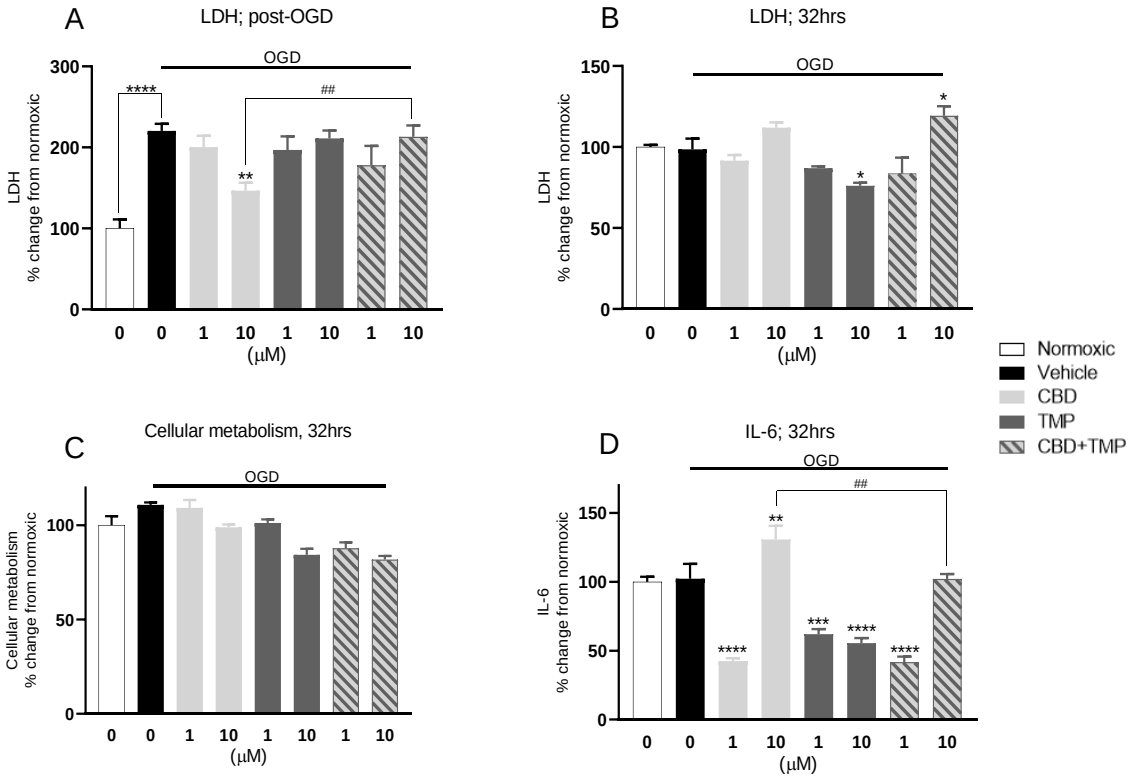


Figure 6.7 The effects of CBD, TMP and CBD + TMP (1 or 10 µM) in astrocytes exposed to 8 h OGD and 24 h reperfusion. Drugs were applied immediately before and after OGD. The effects of CBD, TMP and CBD + TMP on LDH media concentrations A) immediately post-OGD (8 h) and B) 32 h following the initiation of OGD. C) The effect of CBD, TMP and CBD + TMP on cellular viability 32 h following the initiation of OGD using resazurin assays. D) The effects of CBD, TMP and CBD + TMP on IL-6 media concentrations 32 h following the initiation of OGD. In all assays n= 6-8, from two separate experiments. Data are presented as percentage change from normoxic S.E.M and was compared for statistical significance against vehicle (*) or between CBD and CBD + TMP at their respective concentrations and time-points (#) using a one way ANOVA.*/# P ≤ 0.05, **/## P ≤ 0.01, ***/### P ≤ 0.001, ****/#### P ≤ 0.0001.

6.3.8 Effects of CBD and TMP on resazurin metabolism in Pericytes 24h following the initiation of OGD/R

24 h following the initiation of OGD (figure 6.8A), the metabolism of resazurin was 67% ±5 ($p<0.0001$) higher in vehicle relative to normoxic control.

CBD at any of the concentrations tested had no statistically significant effect on the metabolism of resazurin relative to vehicle. TMP reduced the metabolism of

resazurin by -22% ±4 ($p<0.05$) at 100 nM and -22% ±3 ($p<0.05$) at 1 µM relative to vehicle. CBD+TMP reduced the metabolism of resazurin by -25% ±4 ($p<0.01$) at 100 nM and by -19% ±2 ($p<0.05$) at 1 µM. When compared against each other at their respective concentrations, no other significant differences were present between CBD and CBD+TMP (figure 8A).

6.3.9 Effects of CBD and TMP on IL-6 and LDH concentrations in Pericytes exposed to OGD/R

24 h following the initiation of OGD IL-6 media concentrations were 182% ±23 ($p<0.0001$) higher in vehicle than normoxic control (figure 6.8B).

CBD at 1 µM reduced IL-6 media content by 104% ±24 ($p<0.05$) relative to vehicle. TMP had no significant effect on IL-6 media content relative to vehicle. CBD+TMP 100 nM reduced IL-6 media content by 108% ±28 ($p<0.05$) relative to vehicle control. When compared against each other at their respective concentrations, no significant differences were present between CBD and CBD+TMP (figure 6.8B).

LDH media content immediately post-OGD was 207% ±24 ($p<0.0001$) (figure 6.8C) higher in vehicle than normoxic control and at 24 h, was 116% ±7 ($p<0.0001$) higher in vehicle than in normoxic control (figure 6.8D).

Immediately post-OGD (figure 6.8C), CBD or TMP had no significant effect on LDH concentrations relative to vehicle. CBD+TMP reduced LDH concentration by 101% ±38 ($p<0.05$) at 100 nM and by 118% ±28 ($p<0.05$) at 1 µM. When compared against each other at their respective concentrations, no other significant differences were present between CBD and CBD+TMP.

24 h following the initiation of OGD (figure 6.8D) CBD reduced LDH media concentrations by 76% ±12 ($p<0.0001$) at 100 nM and by 112% ±9 ($p<0.0001$) at 1 µM. TMP reduced LDH media concentrations by 77% ±21 ($p<0.0001$) at 100 nM and 73% ±12 ($p<0.0001$) at 1 µM. CBD+TMP reduced LDH media concentrations by 79% ±5 ($p<0.0001$) at 100 nM and 89% ±6 ($p<0.0001$) at 1 µM. When compared against each other at their respective concentrations no other significant differences were present between CBD and CBD+TMP.

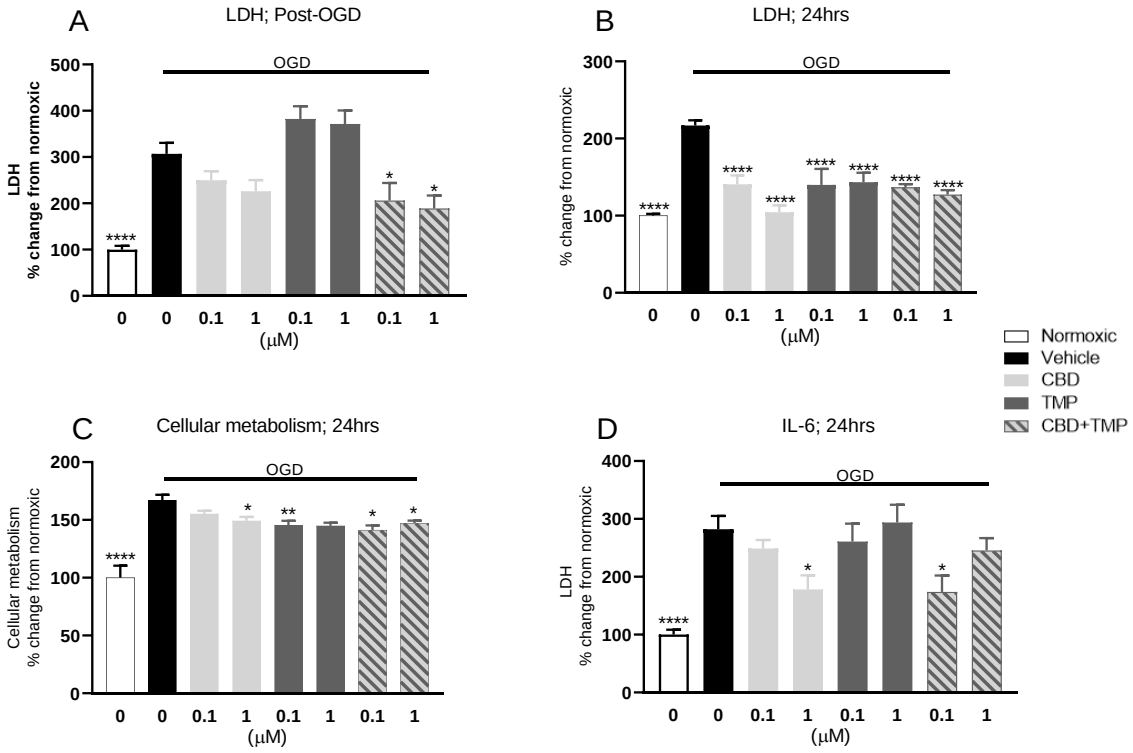


Figure 6.8 The effects of CBD, TMP and CBD + TMP (100 nM or 1 μM) in Pericytes exposed to 4 h OGD and 20 h reperfusion. Drugs were applied immediately before and after OGD. The effects of CBD, TMP and CBD + TMP on LDH media concentrations A) immediately post-OGD (4 h) and) 24 h following the initiation of OGD. C) The effect of CBD, TMP and CBD + TMP on cellular viability 24 h following the initiation of OGD using resazurin assays. D) The effects of CBD, TMP and CBD + TMP on IL-6 media concentrations 24 h following the initiation of OGD. In all assays n= 6, from two separate experiments. Data are presented as percentage change from normoxic S.E.M and was compared for statistical significance against vehicle (*) or between CBD and CBD + TMP at their respective concentrations and time-points (#) using a one way ANOVA.*/# P ≤ 0.05, **/## P ≤ 0.01, ***/### P ≤ 0.001, ****/#### P ≤ 0.0001.

6.4 **Discussion**

In this study, the efficacy and pharmacology of these CBD and TMP applied independently or together at 1:1 ratios in cellular models of cancer and stroke. The effects of the two drugs on proliferative capacity, viability, and migration in CaCo2, DU-145, and SKOV3 cell lines. As well as assessing their effects on markers of cellular damage and inflammation in astrocyte or pericyte models of ischemic reperfusion injury.

Our results demonstrate in proliferating cancer cell lines, co-application of CBD and TMP at a 1:1 ratio relative to CBD alone was more efficacious at reducing cellular proliferation at the lower concentrations tested. However, this effect was absent at the higher concentrations tested, demonstrating that after a specific increase in concentration, the inclusion of TMP no longer increases the anti-proliferative effect of CBD. In scratch wound assays assessing migration of cancer cells, co-application of CBD and TMP reduced the anti-migratory effects of CBD. Indicating the mechanisms of action of each drug need to be investigated to understand these contrasting effects on proliferation and migration. In astrocytes exposed to OGD/R injury, the combination of CBD and TMP improved the ability of CBD to increase cell viability immediately post-OGD. However, this effect did not persist at the later timepoint. CBD alongside TMP at the later timepoint prevented the increase in IL-6 caused by CBD applied alone. In pericytes exposed to OGD/R injury, TMP delivered alongside CBD did not affect endpoints tested relative to CBD alone.

In cancer cell line experiments, CBD alone produced anti-proliferative and anti-migratory effects in line with current literature (Pisanti *et al.*, 2009). Anti-proliferative effects in prostate and ovarian cancer cell lines have been associated with inhibition of GPR55. Antagonism at this receptor prevents the endogenous ligand, lysophosphatidylinositol (LPI), from activating the receptor and the mobilization of Ca^{++} that subsequently activates ERK downstream pathways promoting cell proliferation (Pĩeiro, Maffucci and Falasca, 2011). In the colorectal cancer cell lines, Aviello and colleagues showed that 10 µM CBD possessed anti-proliferative effects associated with interactions with CB1, TRPV1 and PPARγ receptors (Aviello *et al.*, 2012). Out of the three cancer cell lines tested, the anti-proliferative effects of CBD were most significant in the SKOV-3 cell line, and the IC_{50} values obtained were similar to those found in other studies (Fraguas-Sánchez *et al.*, 2020).

In contrast, the anti-migratory effects of CBD were greatest in the DU-145 cell line. The anti-migratory properties of CBD in cancer cell lines have been associated with the inhibition of Epidermal growth factor (EGF) signalling pathways and subsequent inhibition of NF-kB signalling (Elbaz *et al.*, 2015). NF-kB signalling plays a significant role in the migration of cancer cells. NF-kB induces the expression of C-X-C chemokine receptor type 4 (CXCR-4), which upon activation by its endogenous ligand, stromal cell-derived factor 1 alpha (SDF-1alpha), promotes cancer cell migration (Helbig *et al.*, 2003). Therefore, the reduction in migration seen in this study by CBD could result from modulating NF-kB signalling and should be probed in future studies using these cell lines.

TMP also produced anti-proliferative and migratory effects, albeit to a lesser extent than CBD. Notably, the effects of TMP on proliferation and migration were not linear with increasing concentration. There is little literature on the effects of TMP cancer. However, one study was able to demonstrate anti-migratory effects of TMP in the SKOV-3 cell line and correlating this effect with decreased production of IL-8 (Yin *et al.*, 2011). Unfortunately, the lowest concentration of TMP used in this experiment was relatively high, 183µM, thus reducing the translation value of this study. In this same study, whilst the authors demonstrated anti-migratory effects of TMP, they failed to see anti-proliferative effects. Elsewhere, Zhou and colleagues demonstrated that TMP at 3.6µM could reduce cell proliferation in the PC-3 prostate cancer cell line, which correlated with a reduced expression of Forkhead box protein M1 (FOXM1) (Zhou *et al.*, 2017). These conflicting results highlight the need for a mechanism of action studies across a broad range of cancer cell lines using appropriate concentrations to ensure any effects are not off-target, leading to unwanted side effects at a clinical level.

In all the proliferating cancer cell line experiments, TMP delivered alongside CBD increased the potency of CBD, and this effect persisted at all timepoints. This effect was absent in fully confluent cells, indicating this additive effect may only be possible at the early stages of the cell growth cycle. Indeed, previous studies have shown CBD can halt the growth cycle at the G_0–G_1 stage by attenuating CDK2 and cyclin E expression (Zhang *et al.*, 2019). Interestingly higher concentrations of both drugs have been shown to possess cytotoxic effects (Yin *et al.*, 2011; Zhang *et al.*, 2019). Suggesting with higher concentrations, this additive effect may extend to cytotoxic effects in confluent cancer cells and not just anti-proliferative effects. Indeed, when exposure times to the drugs were increased using moderate concentrations, TMP alongside CBD in DU-145 and SKOV-3 increased the cytotoxic

effect of CBD. However, at lower concentrations with prolonged exposure times, none of the drugs had any effect. Indicating micro molar concentrations are required for cytotoxic effects irrespective of increasing exposure times. To further understand the nature of this effect, future studies should repeat these experiments alongside flow cytometry using annexin V staining to assess whether a particular stage of the cell growth cycle correlates with the additive effect.

Both drugs have been shown to reduce cellular migration, reducing the probability of cancers metastasising to other parts of the body (Yin *et al.*, 2011; Go *et al.*, 2020). Unlike the previous endpoints, TMP attenuated the ability of CBD to reduce the migration of cancer cells. Although both drugs have been shown to possess anti-migratory properties, competition for the same molecular target could reduce the efficacy of the other drug, especially if CBD is more potent at the molecular target that mediates this effect.

Given the surmounting pre-clinical evidence and earlier meta-analysis conducted showing CBD is neuroprotective and reduces infarct volume in animal models of cerebral ischemic reperfusion injury, the effects of co-application of TMP alongside CBD affected the efficacy of CBD in a cellular model of ischemic reperfusion injury. CBD has already been shown to reduce IL-6 in cellular OGD/R models (Hind, England and O'Sullivan, 2016). This inflammatory marker correlates well with worse infarct volume and post-stroke recovery following cerebral ischemic reperfusion injury (Smith *et al.*, 2004). LDH is an enzyme exclusively expressed in the cytosol of cells, and its presence outside of the cell indicates a compromised cell membrane. Likewise, the presence of this enzyme in the cerebral spinal fluid (CSF) and the blood of stroke patients correlates well with the severity of the stroke (Lampl *et al.*, 1990).

CBD alone reduced cellular damage and the inflammatory response in both astrocytes and pericytes. However, CBD also raised IL-6 in astrocytes at a higher concentration; this is typical of CBD pharmacology and often displays a bell-shaped concentration-response curve in other studies. (Gallily, Yekhtin and Ondřej Hanuš, 2015). Multiple mechanisms exist through which CBD could produce protective effects in an ischemia-reperfusion insult. Hampson and colleagues showed CBD produced anti-oxidant activity against glutamate-induced excitotoxicity in rat cortical neurons, with a potency comparable to Butylated hydroxytoluene (BHT) (Hampson *et al.*, 1998). Ryan and colleagues showed CBD prevented increases in intracellular Ca^{++} in isolated rat hippocampal neurons exposed to high extracellular K^{+} by

modulating the mitochondrial Na^{+}-Ca^{++} exchanger (NCX) (Ryan, Alison J. Drysdale, *et al.*, 2009). Sun and colleagues showed CBD increased basal mitochondrial respiration, ATP linked oxygen consumption rate and spare respiratory capacity (Sun *et al.*, 2017). Hind and colleagues showed CBD protected the integrity of the blood-brain barrier (BBB) following OGD/R in a co-culture model of the BBB (Hind, England and O'Sullivan, 2016). CBD has also been shown to influence aquaporin 4 (AQP4) expression in inflamed bowel tissue, which may have implications in modulating cerebral oedema in both the early (cytotoxic swelling) and late (vasogenic swelling) (Couch *et al.*, 2019). More clinically relevant evidence comes from a series of *in vivo* studies assessing the effects of CBD in animal models of stroke. Two separate labs have generated most of the data in this area. They have shown CBD can reduce infarct volume when given before, during and after MCAO in rats (Khaksar and Bigdeli, 2016, 2017a, 2017b, 2017c) and mice (Hayakawa *et al.*, 2004, 2008, 2009; Mishima *et al.*, 2005; Hayakawa, Mishima, Nozako, Hazekawa, *et al.*, 2007; Hayakawa, Mishima, Nozako, Ogata, *et al.*, 2007; Hayakawa, Mishima and Fujiwara, 2010). Additionally, Mishima and colleagues showed that in mice, this effect was mediated by the serotonin 1A (5-$HT1_A$) receptor (Mishima *et al.*, 2005).

TMP reduced both cellular damage and the inflammatory response in astrocytes exposed to OGD/R. In pericytes, TMP only reduced cellular damage, with no apparent effect on the inflammatory response. There is minor literature on the effects of TMP in cerebral ischemic-reperfusion injury. However, Shao and colleagues showed that TMP protects neurons from OGD in a cellular model (Shao *et al.*, 2017). This protective effect was possibly mediated by preventing decreases in Transient receptor potential cation channel (TRPC6) associated with OGD injury. Another study also showed that TMP increases glutamate uptake by inhibiting synthesis and secretion; this attenuates glutamate excitotoxicity (Fu et al., 2008). In more clinically relevant models, 20 mg/kg TMP delivered intraperitoneally 4 h following MCAO reduced infarct volume and neurological deficits (Zhu *et al.*, 2009). Another study demonstrated that TMP attenuates apoptosis and neuronal loss in another rat model of cerebral ischemic reperfusion injury. The authors also showed that TMP reduced the activation of microglia cells, the production of Monocyte chemotactic protein-1 (MCP-1), and subsequently reduced the invasion of inflammatory cells to the site of damage (Liao *et al.*, 2004).

In Astrocytes, the combination of CBD and TMP produced a similar decrease in IL-6 compared to CBD alone. At higher concentrations where CBD caused an increase

in IL-6, the inclusion of TMP prevented this. Indicating co-application of the two drugs produces a neutral effect or reduces the probability of off-target side effects, which may have implications for overcoming the bell-shaped dose-response curve encountered in CBD pharmacology. When looking at markers of cell damage, TMP reduced the ability of CBD to protect against cellular damage caused by the OGD/R protocol. In astrocytes, these data indicate that the combination of CBD and TMP maintains the ability of CBD to reduce inflammation and cellular damage. In the pericyte model of cerebral ischemic reperfusion injury, CBD and TMP applied in combination did not affect efficacy relative to CBD alone, suggesting in this model, combining the two drugs produced a neutral effect and did not reduce or increase their efficacy.

In cancer cell line experiments, TMP applied alongside CBD at the same concentration possessed additive or neutral effects; only the anti-migratory effects of CBD were attenuated by co-application of CBD and TMP. In ODG/R experiments, the results were less promising, and only neutral or inhibitory effects were observed when CBD and TMP were co-applied. These effects of CBD and TMP at equimolar concentrations indicate that in cancer cell lines, TMP and CBD could be a viable option for development of a co-crystal. The nature of the TMP molecule allows it to be easily linked with other reactive groups through the generation of several intermediate molecules 2-bromomethyl-3,5,6-trimethylpyrazine (TMP-Br), 3,5,6-trimethylpyrazine-2-yl (TMP-OH), 3,5,6-trimethylpyrazine-2-carboxylic acid (TMP-COOH), and 2,5-dimethylol-3,6-dimethylpyrazine (OH-TMP-OH)groups (Xu *et al.*, 2015). Further experiments should assess the effects different ratios of the two drugs could have on efficacy, as synergistic effects could be amplified by adjusting the ratio of CBD to TMP. Likewise, where adverse effects on efficacy were observed, different ratios have the potential to prevent this. Investigation into the mechanisms of action responsible for the effects in these models would also help understand why additive, neutral or inhibitory effects happen in distinct endpoints and help identify models where a synergistic effect could manifest.

These results demonstrate that CBD and TMP applied at equimolar concentrations possess efficacy in models of cancer. Future studies should investigate these same models, using CBD and TMP in the co-crystal form, rather than co-application. Furthermore, Absorption, Distribution, Metabolism, and Excretion (ADME) studies are required to understand where and how the co-crystal will be broken down into its individual constituents. As the co-crystal might exert pharmacological effects in its co-crystal form before being broke down into its separate constituents, CBD and

TMP. Early studies using an *in vitro* approach should establish how gastrointestinal fluids affect the co-crystal and determine where the co-crystal will be separated. In conditions like colorectal cancer, the co-crystal may reach the target tissue intact and possess different pharmacology; therefore, ADME studies will help better prepare for *in vivo* studies.

7 Grand discussion

By the age of 55, the chances of experiencing a stroke increase two-fold and another two-fold every ten years following (Feigin *et al.*, 2014). Indeed, 75% of strokes occur in people 65 and over and are more common amongst the male gender (Yousufuddin and Young, 2019). The occurrence of stroke has been projected to increase by 34% in Europe, which will almost treble the socio-economic burden on society, currently placed at £25.6 billion per year in the UK (King *et al.*, 2020). These statistics demonstrate the need for a new generation of treatments that not only target the acute stage of stroke but assist in post-stroke functional recovery.

Molecular disturbances associated with stroke such as; excitotoxicity, chronic inflammation and disruption of the BBB can be modulated by the endocannabinoid system (Marsicano *et al.*, 2003; Hossmann, 2006; Hind *et al.*, 2015; Katchan, David and Shoenfeld, 2016). This raises the possibility that exogenous molecules' that modulate the endocannabinoid system may provide a novel treatment for stroke. This thesis aimed to assess the use of phytocannabinoids in stroke using meta-analysis, *in vivo* and cellular models. As well as contributing towards the development of a co-crystal by assessing whether the source of CBD affects its pharmacological activity and the efficacy of its constituents together and independently in cellular models of disease.

Chapter two of this thesis assessed the use of CBD as a treatment for *in vivo* models of stroke by collating all available data of cerebral focal ischemic studies in animals. The meta-analysis identified that CBD could reduce infarct volume in both mice and rats subjected to MCAO through two different routes of administration (iv and icv). Unfortunately, only one study used within the meta-analysis assessed the delivery of CBD following the insult, which is a more clinically relevant scenario. This single study demonstrated CBD could reduce infarct volume when delivered therapeutically; however, the 95% confidence intervals covered a wide range, indicating the actual accuracy of this effect is poorly estimated.

Studies within the meta-analysis also assessed how CBD treatment affected neurological and sensorimotor outcomes. Treatment with CBD led to early neurological improvement at 24 h, but with no significant benefit seen in the later measurements at 336 h. Only one study observed neurological outcomes at later time points, and given the subjective nature of measuring neurological scores, more studies would be needed to validate these results (Hayakawa *et al.*, 2009). However, more animals were used when evaluating sensorimotor coordination using rota-rod tests (Hayakawa, Mishima, Nozako, Hazekawa, *et al.*, 2007; Hayakawa *et al.*, 2008, 2009). These observations conducted in mice showed CBD did not affect rota-rod scores in the early 24-hour groups but improved the time spent on the rota-rod in the 72 h and 336 h groups. Ultimately, the lack of studies from different laboratories hinders the results' power. Eggers statics highlighted this and indicated it was likely that significant publication bias was present. A small body of evidence is generally less precise than if more studies existed, meaning any justification to perform clinical trials will rely on more positive results from *in vivo* studies.

STAIR guidelines dictate (Albers *et al.*, 2011), the *in vivo* models should also demonstrate the efficacy of CBD in permanent models of occlusion, including female animals, follow sensorimotor outcomes at early and late time points and use sample size calculations. Furthermore, studies should consider assessing repeat dosing using clinically relevant time-points (post-stroke) and routes of administration (oral).

The third chapter aimed to demonstrate the efficacy of CBD in a permanent model of MCAO. This study showed that without adequate reperfusion, CBD and CBDA applied 20 minutes intravenously following permanent occlusion of the MCA has no effect on infarct volume. This negative result could stem from the fact higher doses of a drug are needed to produce effects in permanent models of ischemic reperfusion injury, primarily where iv routes of administration are used (Sydserff *et al.*, 2000; Lyden *et al.*, 2002). Furthermore, the protective effects of CBDA were expected to manifest at lower doses. The 5HT1A receptor mediates the protective effects of both phytocannabinoids used in this model, and CBDA is more potent at this receptor (Bolognini *et al.*, 2013). However, one study demonstrated that acidic cannabinoids are far less able to cross the BBB when delivered through oral and intraperitoneal routes of administration in mice (Anderson, Low, *et al.*, 2019).

Despite the negative results of chapter three, it is worth considering that pharmaceutical companies have patented several drugs that target the endocannabinoid system to treat stroke. A clinical trial assessing the use of THC and CBD for post-stroke spasticity has been undertaken; however, the results have not been published (Marinelli *et al.*, 2017). Over 20 MAGL inhibitors have been patented in neurodegenerative diseases that may translate for stroke (Choi, Mou and Silva, 2019; Bononi *et al.*, 2021). The invested interest of pharmaceutical companies in using phytocannabinoids to treat stroke indicates that a great deal of pre-clinical research has been undertaken. However, the results of these studies are not publically available. Given the lack of data on using other phytocannabinoids for stroke, a cellular model was used in the next chapter to identify other phytocannabinoids that may have therapeutic potential.

The fourth chapter explored the effects of several phytocannabinoids in astrocytes exposed to OGD/R injury, specifically assessing how the time of administration affects efficacy. The results suggested that phytocannabinoids can offer protection to astrocytes damaged by OGD/R injury. CBD effectively reduces cellular damage when given prophylactically, suggesting CBD can effectively reduce cellular damage by priming astrocytes to maintain cellular homeostasis during OGD conditions, which could identify reasons for the negative results seen in chapter 3. Of all phytocannabinoids tested in this model, CBGV provided the greatest extent of protection. Effectively reducing cellular damage when administered before or after OGD, indicating this phytocannabinoid addresses both the ischemic and reperfusion period of injury. CBDV appeared to increase cellular damage immediately post OGD, perhaps by reducing mitochondrial complex proteins during ischemia, meaning less ATP is available for cells. The effects of phytocannabinoids varied between pre and post-administration; this could suggest that certain phytocannabinoids, like CBGV, have unique properties that can target molecular disturbances in both the ischemic or reperfusion period of damage. As not all populations of astrocytes displayed the same temporal pattern of damage, some of the anti-inflammatory and neuroprotective effects of other phytocannabinoids could have been underestimated. This could be due to different oxygen concentrations being achieved using anoxic scavenging bags; future experiments could use an incubator capable of controlling oxygen concentrations to investigate whether a specific oxygen concentration is required. Future experiments should look to elucidate the mechanism of action through which these phytocannabinoids produce their effects and assess using them in combination before moving to animal studies.

Although the potential of other phytocannabinoids was demonstrated in chapter four, one of the principal problems that arise when using phytocannabinoids is their undesirable physicochemical properties. This study aimed to demonstrate that no matter the source of CBD (synthetic vs natural), the pharmacological effects would remain the same. This would enable the strategic development of a co-crystal without consideration of the source of CBD. Chapter five demonstrated for the first time that the anti-cancer, neuroprotective and intestinal barrier protective properties of purified CBD are similar regardless of the source from which CBD is derived. From a pharmacological perspective, where a molecular target is implicated (i.e. 5HT1A in stroke and CB_1 in gut permeability), the effects of CBD were similar. This suggests that any beneficial effects achieved in a clinical setting for purified CBD are likely to be similar at a pharmacodynamic level. Based on this analysis, the economic, environmental impact, purity, reliability and consistency of supply of CBD sources and the ultimate pharmaceutical form and formulation should all be considered above the starting source of the CBD in the development of new CBD medicines. One limitation of this study is the inability to rule out the influence polymorphism would have on the development of the co-crystal. Polymorphs possess the same molecular structure; however, they can form different crystalline structures at the polymer level. It is well documented the effects polymorphism can have on drug development. For example, the development of ritonavir, an anti-viral drug used to treat HIV, was based on the only known crystal form (Findlay, 2007). However, as a marketed drug, the large production scale produced a new and significantly less-soluble polymorph, which precipitated out of solution. Upon assessing the dissolution properties of the drug, the capsule failed to present the same properties as the original form. Subsequent studies showed that the new form exhibited reduced solubility in hydroalcoholic solutions than the original form (Bučar, Lancaster and Bernstein, 2015). Outside of the physicochemical properties changing, this also has consequences for patents of matter, as the original patent does not grant exclusivity to both forms. These observations indicate that polymorphisms could exist due to deriving CBD from different sources or the isolation process.

Following the indication from chapter five that CBD derived from natural or synthetic sources possess the same pharmacology. Chapter six aimed to assess the efficacy of CBD and TMP applied at a 1:1 ratio compared to the effects of CBD or TMP alone in three human cellular models of disease. Our results demonstrate that in

proliferating cancer cell lines, co-application of CBD and TMP at a 1:1 ratio relative to CBD alone was more efficacious at reducing cellular proliferation at the lower concentrations tested. However, this effect was absent at the higher concentrations tested, demonstrating that after a specific increase in concentration, the inclusion of TMP no longer increases the anti-proliferative effect of CBD. In scratch wound assays assessing migration of cancer cells, co-application of CBD and TMP reduced the anti-migratory effects relative to CBD alone. However it is difficult to discern whether these effects manifest as a result of anti-proliferative or anti-migratory effects. Indicating the mechanisms of action of each drug need to be investigated using endpoints that explicitly examine proliferation and migration. Flow cytometery could aid in answering this question, by assessing how the combination each drug effects the growth cycle of each cell. For example most cells analysed were found to be in the resting-no dividing stage of the growth cycle, it would likely indicate these effects are produced by anti-proliferative mechanisms.

In astrocytes exposed to OGD/R injury, the combination of CBD and TMP improved the ability of CBD to increase cell viability immediately post-OGD. However, this effect did not persist at the later timepoint. CBD alongside TMP at the later timepoint prevented the increase in IL-6 caused by CBD applied alone. In pericytes exposed to OGD/R injury, TMP delivered alongside CBD did not affect CBDs effects in any of the endpoints tested.

These results indicate that CBD and TMP are viable options for a co-crystal with the proper investigation of Absorption, Distribution, Metabolism, and Excretion (ADME) parameters. Early studies using an *in vitro* approach should establish how gastrointestinal fluids affect the co-crystal and determine where the co-crystal will be separated. In conditions like colorectal cancer, the co-crystal may reach the target tissue intact and possess different pharmacology; therefore, *in vitro* ADME studies will help better prepare for *in vivo* studies.

To conclude, this thesis demonstrates that phytocannabinoids have the potential in treating cerebral ischemic reperfusion injury. With a robust development plan, the formation of a co-crystal offers a potential strategy to overcome the inherent poor physicochemical properties of CBD and potentially other phytocannabinoids.

8 Bibliography

Abbott, N. J., Rönnbäck, L. and Hansson, E. (2006) 'Astrocyte-endothelial interactions at the blood-brain barrier', *Nature Reviews Neuroscience*, 7(1), pp. 41–53. doi: 10.1038/nrn1824.

Adamson, J., Beswick, A. and Ebrahim, S. (2004) 'Is stroke the most common cause of disability?', *Journal of Stroke and Cerebrovascular Diseases*, 13(4), pp. 171–177. doi: 10.1016/j.jstrokecerebrovasdis.2004.06.003.

Adibhatla, R. M. and Hatcher, J. F. (2008) 'Tissue plasminogen activator (tPA) and matrix metalloproteinases in the pathogenesis of stroke: therapeutic strategies.', *CNS & neurological disorders drug targets*, 7(3), pp. 243–53.

Aguiar, A. J. *et al.* (1967) 'Effect of polymorphism on the absorption of chloramphenicol from chloramphenicol palmitate', *Journal of Pharmaceutical Sciences*. John Wiley & Sons, Ltd, 56(7), pp. 847–853. doi: 10.1002/jps.2600560712.

Ahmad, M. and Kahwaji, C. I. (2018) 'Biochemistry, Electron Transport Chain', *StatPearls*. StatPearls Publishing. Available at: http://www.ncbi.nlm.nih.gov/pubmed/30252361 (Accessed: 21 May 2022).

Albers, G. W. *et al.* (2011) 'Stroke treatment academic industry roundtable (STAIR) recommendations for maximizing the use of intravenous thrombolytics and expanding treatment options with intra-arterial and neuroprotective therapies', *Stroke*, pp. 2645–2650. doi: 10.1161/STROKEAHA.111.618850.

Alberts *et al.* (2002) *Molecular biology of the cell*. 4th Editio. Garland Science. doi: 10.1091/mbc.E14-10-1437.

Alexander, S. (2012) 'So what do we call GPR18 now?', *British Journal of Pharmacology*. Wiley-Blackwell, 165(8), p. 2411. doi: 10.1111/J.1476-5381.2011.01731.X.

Alhamoruni, A. *et al.* (2012) 'Cannabinoids mediate opposing effects on inflammation-induced intestinal permeability', *British Journal of Pharmacology*. John Wiley & Sons, Ltd (10.1111), 165(8), pp. 2598–2610. doi: 10.1111/j.1476-5381.2011.01589.x.

Allen, K. L. *et al.* (1995) 'Changes of respiratory chain activity in mitochondrial and synaptosomal fractions isolated from the gerbil brain after graded ischaemia', *Journal of Neurochemistry*. Blackwell Publishing Ltd, 64(5), pp. 2222–2229. doi: 10.1046/j.1471-4159.1995.64052222.x.

Ameri, A. (1999) 'The effects of cannabinoids on the brain', *Progress in Neurobiology*, 58(4), pp. 315–348. doi: 10.1016/S0301-0082(98)00087-2.

Anavi-Goffer, S. *et al.* (2012) 'Modulation of L-α-lysophosphatidylinositol/GPR55 mitogen-activated protein kinase (MAPK) signaling by cannabinoids', *Journal of Biological Chemistry*. J Biol Chem, 287(1), pp. 91–104. doi: 10.1074/jbc.M111.296020.

Anderson, L. L., Absalom, N. L., *et al.* (2019) 'Coadministered cannabidiol and clobazam: Preclinical evidence for both pharmacodynamic and pharmacokinetic interactions', *Epilepsia*. Blackwell Publishing Inc., 60(11), pp. 2224–2234. doi: 10.1111/epi.16355.

Anderson, L. L., Low, I. K., *et al.* (2019) 'Pharmacokinetics of Phytocannabinoid Acids and

Anticonvulsant Effect of Cannabidiolic Acid in a Mouse Model of Dravet Syndrome', *Journal of Natural Products*. J Nat Prod, 82(11), pp. 3047–3055. doi: 10.1021/acs.jnatprod.9b00600.

Argaw, A. T. *et al.* (2012a) 'Astrocyte-derived VEGF-A drives blood-brain barrier disruption in CNS inflammatory disease', *Journal of Clinical Investigation*. Eur Neurol, 122(7), pp. 2454–2468. doi: 10.1172/JCI60842.

Argaw, A. T. *et al.* (2012b) 'Astrocyte-derived VEGF-A drives blood-brain barrier disruption in CNS inflammatory disease', *Journal of Clinical Investigation*. American Society for Clinical Investigation, 122(7), pp. 2454–2468. doi: 10.1172/JCI60842.

Armstrong, E. H. *et al.* (2014) 'Structural basis for ligand regulation of the fatty acidbinding protein 5, peroxisome proliferator-activated receptor β/δ (FABP5-PPARβ/ δ) signaling pathway', *Journal of Biological Chemistry*. J Biol Chem, 289(21), pp. 14941–14954. doi: 10.1074/jbc.M113.514646.

Armulik, A. *et al.* (2010) 'Pericytes regulate the blood-brain barrier', *Nature*. Nature Publishing Group, 468(7323), pp. 557–561. doi: 10.1038/nature09522.

Ashton, J. C. *et al.* (2006) 'Expression of the cannabinoid CB2 receptor in the rat cerebellum: An immunohistochemical study', *Neuroscience Letters*, 396, pp. 113–116. doi: 10.1016/j.neulet.2005.11.038.

Astrup, J. *et al.* (1977) 'Cortical Evoked Potential and Extracellular K + and H + at Critical Levels of Brain Ischemia', *Stroke*, 8(1), pp. 51–57. doi: 10.1161/01.STR.8.1.51.

Atwood, B. K. *et al.* (2012) 'Functional Selectivity in CB2 Cannabinoid Receptor Signaling and Regulation: Implications for the Therapeutic Potential of CB2 Ligands', *Molecular Pharmacology*, 81(2), pp. 250–263. doi: 10.1124/mol.111.074013.

Auwerx, J. *et al.* (1999) 'A unified nomenclature system for the nuclear receptor superfamily', *Cell*. Cell, 97(2), pp. 161–163. doi: 10.1016/S0092-8674(00)80726-6.

Aviello, G. *et al.* (2012) 'Chemopreventive effect of the non-psychotropic phytocannabinoid cannabidiol on experimental colon cancer', *Journal of Molecular Medicine*, 90(8), pp. 925–934. doi: 10.1007/s00109-011-0856-x.

Baker, K. *et al.* (1998) 'Synthetic combined superoxide dismutase/catalase mimetics are protective as a delayed treatment in a rat stroke model: a key role for reactive oxygen species in ischemic brain injury.', *The Journal of pharmacology and experimental therapeutics*, 284(1), pp. 215–221.

Ballabh, P., Braun, A. and Nedergaard, M. (2004) 'The blood-brain barrier: An overview: Structure, regulation, and clinical implications', *Neurobiology of Disease*, 16(1), pp. 1–13. doi: 10.1016/j.nbd.2003.12.016.

Beal, C. C. (2010) 'Gender and stroke symptoms: a review of the current literature.', *The Journal of neuroscience nursing : journal of the American Association of Neuroscience Nurses*, 42(2), pp. 80–7. doi: 10.1097/JNN.0b013e3181ce5c70.

Becerra-Calixto, A. and Cardona-Gómez, G. P. (2017) 'The Role of Astrocytes in Neuroprotection after Brain Stroke: Potential in Cell Therapy.', *Frontiers in molecular neuroscience*. Frontiers Media SA, 10, p. 88. doi: 10.3389/fnmol.2017.00088.

Beetsch, J. W. *et al.* (1998) 'Xanthine oxidase-derived superoxide causes reoxygenation injury of ischemic cerebral endothelial cells.', *Brain research*, 786(1–2), pp. 89–95.

Beppu, K. *et al.* (2014) 'Optogenetic countering of glial acidosis suppresses glial glutamate

release and ischemic brain damage', *Neuron*. Elsevier, 81(2), pp. 314–320. doi: 10.1016/j.neuron.2013.11.011.

Birnbaum, A. K. *et al.* (2019) 'Food effect on pharmacokinetics of cannabidiol oral capsules in adult patients with refractory epilepsy', *Epilepsia*. Blackwell Publishing Inc., 60(8), pp. 1586–1592. doi: 10.1111/epi.16093.

Bisogno, T. *et al.* (2003) 'Cloning of the first sn1-DAG lipases points to the spatial and temporal regulation of endocannabinoid signaling in the brain', *Journal of Cell Biology*. J Cell Biol, 163(3), pp. 463–468. doi: 10.1083/jcb.200305129.

Blessing, E. M. *et al.* (2015) 'Cannabidiol as a Potential Treatment for Anxiety Disorders', *Neurotherapeutics*, 12(4), pp. 825–836. doi: 10.1007/s13311-015-0387-1.

Bodor, A. L. *et al.* (2005) 'Endocannabinoid Signaling in Rat Somatosensory Cortex: Laminar Differences and Involvement of Specific Interneuron Types', *Journal of Neuroscience*, 25(29), pp. 6845–6856. doi: 10.1523/JNEUROSCI.0442-05.2005.

Bolognini, D. *et al.* (2013) 'Cannabidiolic acid prevents vomiting in *Suncus murinus* and nausea-induced behaviour in rats by enhancing 5-HT $_{1A}$ receptor activation', *British Journal of Pharmacology*. John Wiley & Sons, Ltd, 168(6), pp. 1456–1470. doi: 10.1111/bph.12043.

Boneva, N. B. *et al.* (2010) 'Differential expression of FABP 3, 5, 7 in infantile and adult monkey cerebellum', *Neuroscience Research*. Neurosci Res, 68(2), pp. 94–102. doi: 10.1016/j.neures.2010.07.2028.

Bonkowski, D. *et al.* (2011) 'The CNS microvascular pericyte: Pericyte-astrocyte crosstalk in the regulation of tissue survival', *Fluids and Barriers of the CNS*. BioMed Central, p. 8. doi: 10.1186/2045-8118-8-8.

Bononi, G. *et al.* (2021) 'An updated patent review of monoacylglycerol lipase (MAGL) inhibitors (2018-present)', *Expert Opinion on Therapeutic Patents*. Expert Opin Ther Pat, pp. 153–168. doi: 10.1080/13543776.2021.1841166.

Bouaboula, M. *et al.* (2005) 'Anandamide induced PPARγ transcriptional activation and 3T3-L1 preadipocyte differentiation', *European Journal of Pharmacology*. Elsevier, 517(3), pp. 174–181. doi: 10.1016/j.ejphar.2005.05.032.

Boveris, A. and Chance, B. (1973) 'The Mitochondrial Generation of Hydrogen Peroxide GENERAL PROPERTIES AND EFFECT OF HYPERBARIC OXYGEN', *Biochem. J*, 134, pp. 707–716.

Bowler, E. and Oltean, S. (2019) 'Alternative splicing in angiogenesis', *International Journal of Molecular Sciences*. Multidisciplinary Digital Publishing Institute (MDPI). doi: 10.3390/ijms20092067.

Bretón, R. R., César, J. and Rodríguez, G. (2012) 'Excitotoxicity and Oxidative Stress in Acute Ischemic Stroke', *Acute Ischemic Stroke*, 3, pp. 30–58. doi: 10.5772/1438.

Britch, S. C., Babalonis, S. and Walsh, S. L. (2021) 'Cannabidiol: pharmacology and therapeutic targets', *Psychopharmacology*. Psychopharmacology (Berl), 238(1), pp. 9–28. doi: 10.1007/s00213-020-05712-8.

Brown, A. M. (2004) 'Brain glycogen re-awakened.', *Journal of neurochemistry*, 89(3), pp. 537–52. doi: 10.1111/j.1471-4159.2004.02421.x.

Brown, D. C. and Iadarola, M. J. (2015) 'TRPV1 Agonist Cytotoxicity for Chronic Pain Relief: From Mechanistic Understanding to Clinical Application', *TRP Channels as Therapeutic*

Targets: From Basic Science to Clinical Use. Academic Press, pp. 99–118. doi: 10.1016/B978-0-12-420024-1.00006-0.

Brusco, A. *et al.* (2008) 'Postsynaptic localization of CB2 cannabinoid receptors in the rat hippocampus', *Synapse*, 62(12), pp. 944–949. doi: 10.1002/syn.20569.

Bučar, D. K., Lancaster, R. W. and Bernstein, J. (2015) 'Disappearing Polymorphs Revisited', *Angewandte Chemie - International Edition*. John Wiley & Sons, Ltd, 54(24), pp. 6972–6993. doi: 10.1002/anie.201410356.

Buciuc, M., Conte, G. M. and Scharf, E. L. (2021) 'Endocannabinoid Response in Acute Ischemic Stroke: Elevated 2-Arachidonoylglycerol', *Stroke*. Cold Spring Harbor Laboratory Press, pp. E131–E132. doi: 10.1161/STROKEAHA.121.034131.

Burstein, S. (2015) 'Cannabidiol (CBD) and its analogs: a review of their effects on inflammation', *Bioorganic & Medicinal Chemistry*, 23(7), pp. 1377–1385. doi: 10.1016/j.bmc.2015.01.059.

Bushong, E. a *et al.* (2002) 'Protoplasmic astrocytes in CA1 stratum radiatum occupy separate anatomical domains.', *The Journal of neuroscience : the official journal of the Society for Neuroscience*, 22(1), pp. 183–192. doi: 22/1/183 [pii].

Campbell, B. C. V. *et al.* (2013) 'Failure of collateral blood flow is associated with infarct growth in ischemic stroke', *Journal of Cerebral Blood Flow and Metabolism*. SAGE Publications, 33(8), pp. 1168–1172. doi: 10.1038/jcbfm.2013.77.

Cao, J. *et al.* (2015) 'Tetramethylpyrazine (TMP) exerts antitumor effects by inducing apoptosis and autophagy in hepatocellular carcinoma', *International Immunopharmacology*. Elsevier, 26(1), pp. 212–220. doi: 10.1016/j.intimp.2015.03.028.

Cao, Z., Balasubramanian, A. and Marrelli, S. P. (2014) 'Pharmacologically induced hypothermia via TRPV1 channel agonism provides neuroprotection following ischemic stroke when initiated 90 min after reperfusion', *American Journal of Physiology - Regulatory, Integrative and Comparative Physiology*. American Physiological Society, 306(2), p. R149. doi: 10.1152/AJPREGU.00329.2013.

Casals, J. B. *et al.* (2011) 'The Use of Animal Models for Stroke Research: A Review', *Comparative Medicine*. American Association for Laboratory Animal Science, 61(4), p. 305. Available at: /pmc/articles/PMC3155396/ (Accessed: 14 July 2021).

Cavuoto, P. *et al.* (2007) 'The expression of receptors for endocannabinoids in human and rodent skeletal muscle', *Biochemical and Biophysical Research Communications*, 364(1), pp. 105–110. doi: 10.1016/j.bbrc.2007.09.099.

Celsi, F. *et al.* (2009) 'Mitochondria, calcium and cell death: A deadly triad in neurodegeneration', *Biochimica et Biophysica Acta (BBA) - Bioenergetics*. Elsevier, 1787(5), pp. 335–344. doi: 10.1016/J.BBABIO.2009.02.021.

Chalothorn, D. *et al.* (2009) 'Chloride intracellular channel-4 Is a determinant of native collateral formation in skeletal muscle and brain', *Circulation Research*. NIH Public Access, 105(1), pp. 89–98. doi: 10.1161/CIRCRESAHA.109.197145.

Chan, O. H. and Stewart, B. H. (1996) 'Physicochemical and drug-delivery considerations for oral drug bioavailability', *Drug Discovery Today*. Elsevier Ltd, pp. 461–473. doi: 10.1016/1359-6446(96)10039-8.

Chang, Y. *et al.* (2007) 'Tetramethylpyrazine suppresses HIF-1α, TNF-α, and activated

caspase-3 expression in middle cerebral artery occlusion-induced brain ischemia in rats', *Acta Pharmacologica Sinica*. Acta Pharmacol Sin, 28(3), pp. 327–333. doi: 10.1111/j.1745-7254.2007.00514.x.

Chao, C. C., Molitor, T. W. and Hu, S. (1993) 'Neuroprotective role of IL-4 against activated microglia.', *Journal of immunology (Baltimore, Md. : 1950)*, 151(3), pp. 1473–81.

Chapin, J. C. and Hajjar, K. A. (2015) 'Fibrinolysis and the control of blood coagulation', *Blood Reviews*. Churchill Livingstone, 29(1), pp. 17–24. doi: 10.1016/j.blre.2014.09.003.

Chen, Y. *et al.* (2019) 'Efficacy and safety of tetramethylpyrazine phosphate on pulmonary hypertension: Study protocol for a randomized controlled study', *Trials*. BioMed Central, 20(1), pp. 1–8. doi: 10.1186/s13063-019-3770-0.

Chen, Y. and Swanson, R. A. (2003) 'Astrocytes and Brain Injury', *Journal of Cerebral Blood Flow & Metabolism*, 23(2), pp. 137–149. doi: 10.1097/01.WCB.0000044631.80210.3C.

Cherniakov, I. *et al.* (2017) 'The effect of Pro NanoLipospheres (PNL) formulation containing natural absorption enhancers on the oral bioavailability of delta-9-tetrahydrocannabinol (THC) and cannabidiol (CBD) in a rat model', *European Journal of Pharmaceutical Sciences*. Elsevier, 109(May 2018), pp. 21–30. doi: 10.1016/j.ejps.2017.07.003.

Childs, S. L. *et al.* (2004) 'Crystal engineering approach to forming cocrystals of amine hydrochlorides with organic acids. Molecular complexes of fluoxetine hydrochloride with benzoic, succinic, and fumaric acids', *Journal of the American Chemical Society*. American Chemical Society, 126(41), pp. 13335–13342. doi: 10.1021/ja048114o.

Choi, S. H., Mou, Y. and Silva, A. C. (2019) 'Cannabis and Cannabinoid Biology in Stroke: Controversies, Risks, and Promises', *Stroke*. Lippincott Williams & Wilkins Hagerstown, MD, pp. 2640–2645. doi: 10.1161/STROKEAHA.118.023587.

Chong, J. Y. and Sacco, R. L. (2005) 'Risk Factors for Stroke, Assessing Risk, and the Mass and High-Risk Approaches for Stroke Prevention', *CONTINUUM: Lifelong Learning in Neurology*, 11, pp. 18–34. doi: 10.1212/01.CON.0000293708.61582.f4.

Clayton, J. A., Chalothorn, D. and Faber, J. E. (2008) 'Vascular endothelial growth factor-a specifies formation of native collaterals and regulates collateral growth in ischemia', *Circulation Research*. NIH Public Access, 103(9), pp. 1027–1036. doi: 10.1161/CIRCRESAHA.108.181115.

Codolo, G. *et al.* (2013) 'Triggering of Inflammasome by Aggregated α–Synuclein, an Inflammatory Response in Synucleinopathies', *PLoS ONE*. Edited by R. L. Mosley. Public Library of Science, 8(1), p. e55375. doi: 10.1371/journal.pone.0055375.

Corbett, G. T., Gonzalez, F. J. and Pahan, K. (2015) 'Activation of peroxisome proliferator-activated receptor α stimulates ADAM10-mediated proteolysis of APP', *Proceedings of the National Academy of Sciences of the United States of America*. Proc Natl Acad Sci U S A, 112(27), pp. 8445–8450. doi: 10.1073/pnas.1504890112.

Corrales, P., Vidal-Puig, A. and Medina-Gómez, G. (2018) 'PPARS and metabolic disorders associated with challenged adipose tissue plasticity', *International Journal of Molecular Sciences*. Multidisciplinary Digital Publishing Institute (MDPI). doi: 10.3390/ijms19072124.

Correale, J. and Villa, A. (2009) 'Cellular elements of the blood-brain barrier', *Neurochemical Research*, pp. 2067–2077. doi: 10.1007/s11064-009-0081-y.

Costa, B. *et al.* (2004) 'Vanilloid TRPV1 receptor mediates the antihyperalgesic effect of the

nonpsychoactive cannabinoid, cannabidiol, in a rat model of acute inflammation.', *British journal of pharmacology*. Wiley-Blackwell, 143(2), pp. 247–50. doi: 10.1038/sj.bjp.0705920.

Cota, D. *et al.* (2003) 'The endogenous cannabinoid system affects energy balance via central orexigenic drive and peripheral lipogenesis.', *The Journal of clinical investigation*. American Society for Clinical Investigation, 112(3), pp. 423–31. doi: 10.1172/JCI17725.

Cota, D. (2007) 'CB1 receptors: emerging evidence for central and peripheral mechanisms that regulate energy balance, metabolism, and cardiovascular health', *Diabetes/Metabolism Research and Reviews*. John Wiley & Sons, Ltd., 23(7), pp. 507–517. doi: 10.1002/dmrr.764.

Couch, D. G. *et al.* (2019) 'Palmitoylethanolamide and Cannabidiol Prevent Inflammation-induced Hyperpermeability of the Human Gut In Vitro and In Vivo—A Randomized, Placebo-controlled, Double-blind Controlled Trial', *Inflammatory Bowel Diseases*. Oxford Academic, 25(6), pp. 1006–1018. doi: 10.1093/ibd/izz017.

Coyle, J. T. and Puttfarcken, P. (1993) 'Oxidative stress, glutamate, and neurodegenerative disorders.', *Science (New York, N.Y.)*, 262(5134), pp. 689–95. doi: 10.1126/science.7901908.

Craft, R. M., Marusich, J. A. and Wiley, J. L. (2013) 'Sex differences in cannabinoid pharmacology: A reflection of differences in the endocannabinoid system?', in *Life Sciences*. NIH Public Access, pp. 476–481. doi: 10.1016/j.lfs.2012.06.009.

Croci, T. *et al.* (1998) 'In vitro functional evidence of neuronal cannabinoid CB1 receptors in human ileum.', *British journal of pharmacology*. Wiley-Blackwell, 125(7), pp. 1393–5. doi: 10.1038/sj.bjp.0702190.

Csáki, K. F. (2011) 'Synthetic surfactant food additives can cause intestinal barrier dysfunction', *Medical Hypotheses*. Churchill Livingstone, 76(5), pp. 676–681. doi: 10.1016/j.mehy.2011.01.030.

Cunningham, L. A., Wetzel, M. and Rosenberg, G. A. (2005) 'Multiple roles for MMPs and TIMPs in cerebral ischemia', *Glia*, 50(4), pp. 329–339. doi: 10.1002/glia.20169.

David, J. C. *et al.* (1996) 'AMPA receptor activation is rapidly toxic to cortical astrocytes when desensitization is blocked.', *The Journal of neuroscience : the official journal of the Society for Neuroscience*, 16(1), pp. 200–9.

David, S. and Kroner, A. (2011) 'Repertoire of microglial and macrophage responses after spinal cord injury', *Nature Reviews Neuroscience*, 12(7), pp. 388–399. doi: 10.1038/nrn3053.

Deguchi, K. *et al.* (2014) 'Pericyte protection by edaravone after tissue plasminogen activator treatment in rat cerebral ischemia', *Journal of Neuroscience Research*. Wiley-Blackwell, 92(11), pp. 1509–1519. doi: 10.1002/jnr.23420.

Deiana, S. *et al.* (2012) 'Plasma and brain pharmacokinetic profile of cannabidiol (CBD), cannabidivarine (CBDV), Δ9-tetrahydrocannabivarin (THCV) and cannabigerol (CBG) in rats and mice following oral and intraperitoneal administration and CBD action on obsessive–compulsive behavi', *Psychopharmacology*. Springer-Verlag, 219(3), pp. 859–873. doi: 10.1007/s00213-011-2415-0.

Deitmer, J. W. and Rose, C. R. (1996) 'pH regulation and proton signalling by glial cells.', *Progress in neurobiology*, 48(2), pp. 73–103.

Deutsch, D. G. and Chin, S. A. (1993) 'Enzymatic synthesis and degradation of anandamide,

a cannabinoid receptor agonist.', *Biochemical pharmacology*, 46(5), pp. 791–6.

Devane, W. A. *et al.* (1992) 'Isolation and structure of a brain constituent that binds to the cannabinoid receptor', *Science*. American Association for the Advancement of Science, 258(5090), pp. 1946–1949. doi: 10.1126/science.1470919.

Devinsky, O. *et al.* (2014) 'Cannabidiol: Pharmacology and potential therapeutic role in epilepsy and other neuropsychiatric disorders', *Epilepsia*. Wiley/Blackwell (10.1111), 55(6), pp. 791–802. doi: 10.1111/epi.12631.

Devinsky, O., Patel, A. D., Cross, J. H., *et al.* (2018) 'Effect of Cannabidiol on Drop Seizures in the Lennox–Gastaut Syndrome', *New England Journal of Medicine*. Massachussetts Medical Society, 378(20), pp. 1888–1897. doi: 10.1056/NEJMoa1714631.

Devinsky, O., Patel, A. D., Thiele, E. A., *et al.* (2018) 'Randomized, dose-ranging safety trial of cannabidiol in Dravet syndrome', *Neurology*. NLM (Medline), 90(14), pp. e1204–e1211. doi: 10.1212/WNL.0000000000005254.

Ding, S. (2014) 'Ca2+ Signaling in Astrocytes and its Role in Ischemic Stroke', in, pp. 189–211. doi: 10.1007/978-3-319-08894-5_10.

Dodson, R. F. *et al.* (1977) 'Acute tissue response to cerebral ischemia in the gerbil. An ultrastructural study.', *Journal of the neurological sciences*, 33(1–2), pp. 161–70.

Doyle, K. P., Simon, R. P. and Stenzel-Poore, M. P. (2008) 'Mechanisms of ischemic brain damage', *Neuropharmacology*. NIH Public Access, 55(3), pp. 310–318. doi: 10.1016/j.neuropharm.2008.01.005.Neuropharmacology.

Du, Q. *et al.* (2019) 'The Role of Transient Receptor Potential Vanilloid 1 in Common Diseases of the Digestive Tract and the Cardiovascular and Respiratory System', *Frontiers in Physiology*. Frontiers, 10, p. 1064. doi: 10.3389/FPHYS.2019.01064.

Dumitru, C. A., Sandalcioglu, I. E. and Karsak, M. (2018) 'Cannabinoids in Glioblastoma Therapy: New Applications for Old Drugs', *Frontiers in Molecular Neuroscience*, 11, p. 159. doi: 10.3389/fnmol.2018.00159.

Eddleston, M. P. Mucke, L. (1993) 'Molecular profile of reactive astrocytes - implications for their role in neurologic disease.', *Neuroscience*, 54(1), pp. 15–36.

Edvinsson, L. and Krause, D. (2002) *Cerebral Blood Flow and Metabolism.* Lippincott Williams & Wilkins.

Elbaz, M. *et al.* (2015) 'Modulation of the tumor microenvironment and inhibition of EGF/EGFR pathway: Novel anti-tumor mechanisms of Cannabidiol in breast cancer', *Molecular Oncology*. Elsevier, 9(4), pp. 906–919. doi: 10.1016/j.molonc.2014.12.010.

Elbegdorj, O., Westkaemper, R. B. and Zhang, Y. (2013) 'A homology modeling study toward the understanding of three-dimensional structure and putative pharmacological profile of the G-protein coupled receptor GPR55', *Journal of Molecular Graphics and Modelling*. J Mol Graph Model, 39, pp. 50–60. doi: 10.1016/j.jmgm.2012.10.005.

Elphick, M. R. and Egertová, M. (2005) 'The phylogenetic distribution and evolutionary origins of endocannabinoid signalling.', *Handbook of experimental pharmacology*, (168), pp. 283–97.

Elsaid, S. and Le Foll, B. (2020) 'The complexity of pharmacology of cannabidiol (CBD) and its implications in the treatment of brain disorders', *Neuropsychopharmacology*. Springer Nature, pp. 229–230. doi: 10.1038/s41386-019-0518-1.

Eltzschig, H. K. and Eckle, T. (2011) 'Ischemia and reperfusion-from mechanism to translation', *Nature Medicine*. NIH Public Access, pp. 1391–1401. doi: 10.1038/nm.2507.

England, T. J. *et al.* (2015) 'Cannabinoids in experimental stroke: A systematic review and meta-analysis', *Journal of Perinatology*. Nature Publishing Group, pp. 348–358. doi: 10.1038/jcbfm.2014.218.

EudraCT (2013) *EudraCT Number 2013-000059-42 - Clinical trial results - EU Clinical Trials Register*. Available at: https://www.clinicaltrialsregister.eu/ctr-search/trial/2011-002778-21/results (Accessed: 6 October 2020).

Feige, J. N. *et al.* (2006) 'From molecular action to physiological outputs: Peroxisome proliferator-activated receptors are nuclear receptors at the crossroads of key cellular functions', *Progress in Lipid Research*. Prog Lipid Res, pp. 120–159. doi: 10.1016/j.plipres.2005.12.002.

Feigin, V. L. *et al.* (2014) 'Global and regional burden of stroke during 1990-2010: Findings from the Global Burden of Disease Study 2010', *The Lancet*. Lancet Publishing Group, 383(9913), pp. 245–255. doi: 10.1016/S0140-6736(13)61953-4.

Fernandes, A., Miller-Fleming, L. and Pais, T. F. (2014) 'Microglia and inflammation: conspiracy, controversy or control?', *Cellular and Molecular Life Sciences*. Springer Basel, 71(20), pp. 3969–3985. doi: 10.1007/s00018-014-1670-8.

Findlay, V. J. (2007) 'Ritonavir', *xPharm: The Comprehensive Pharmacology Reference*. Elsevier, pp. 1–6. doi: 10.1016/B978-008055232-3.62543-7.

Finkbeiner, S. (1992) 'Calcium waves in astrocytes-filling in the gaps', *Neuron*, 8(6), pp. 1101–1108. doi: 10.1016/0896-6273(92)90131-V.

Flores-Sanchez, I. J. and Verpoorte, R. (2008) 'Secondary metabolism in cannabis', in *Phytochemistry Reviews*. Springer, pp. 615–639. doi: 10.1007/s11101-008-9094-4.

de Fonseca, F. R. *et al.* (2005) 'The endocannabinoid system: Physiology and pharmacology', *Alcohol and Alcoholism*, 40(1), pp. 2–14. doi: 10.1093/alcalc/agh110.

Fowler, C. J. (2012) 'Anandamide uptake explained?', *Trends in Pharmacological Sciences*. Elsevier Current Trends, 33(4), pp. 181–185. doi: 10.1016/j.tips.2012.01.001.

Fraguas-Sánchez, A. I. *et al.* (2020) 'Enhancing ovarian cancer conventional chemotherapy through the combination with cannabidiol loaded microparticles', *European Journal of Pharmaceutics and Biopharmaceutics*. Elsevier B.V., 154, pp. 246–258. doi: 10.1016/j.ejpb.2020.07.008.

Franco, V. *et al.* (2020) 'The Interplay Between Liver First-Pass Effect and Lymphatic Absorption of Cannabidiol and Its Implications for Cannabidiol Oral Formulations', *Clinical Pharmacokinetics*. Adis, 59(12), pp. 1493–1500. doi: 10.1007/s40262-020-00931-w.

Franco, V. and Perucca, E. (2019) 'Pharmacological and Therapeutic Properties of Cannabidiol for Epilepsy', *Drugs*. Springer International Publishing, pp. 1435–1454. doi: 10.1007/s40265-019-01171-4.

Freeman, T. P. *et al.* (2019) 'Medicinal use of cannabis based products and cannabinoids', *BMJ (Online)*. BMJ Publishing Group, 365. doi: 10.1136/bmj.l1141.

Freilich, R. W., Woodbury, M. E. and Ikezu, T. (2013) 'Integrated expression profiles of mRNA and miRNA in polarized primary murine microglia', *PLoS ONE*. Edited by J. El Khoury. Public Library of Science, 8(11), p. e79416. doi: 10.1371/journal.pone.0079416.

Friedman, J. R. and Nunnari, J. (2014) 'Mitochondrial form and function', *Nature*. Nature Publishing Group, pp. 335–343. doi: 10.1038/nature12985.

Fujimoto, M. *et al.* (2008) 'Tissue inhibitor of metalloproteinases protect blood-brain barrier disruption in focal cerebral ischemia', *Journal of Cerebral Blood Flow and Metabolism*. J Cereb Blood Flow Metab, 28(10), pp. 1674–1685. doi: 10.1038/jcbfm.2008.59.

Fullerton, J. N. and Gilroy, D. W. (2016) 'Resolution of inflammation: A new therapeutic frontier', *Nature Reviews Drug Discovery*. Nature Publishing Group, pp. 551–567. doi: 10.1038/nrd.2016.39.

Furman, J. L. and Norris, C. M. (2014) 'Calcineurin and glial signaling: neuroinflammation and beyond.', *Journal of neuroinflammation*. BioMed Central, 11(1), p. 158. doi: 10.1186/s12974-014-0158-7.

Gallily, R., Yekhtin, Z. and Ondřej Hanuš, L. (2015) 'Overcoming the Bell-Shaped Dose-Response of Cannabidiol by Using Cannabis Extract Enriched in Cannabidiol', *Pharmacology & Pharmacy*, 6, pp. 75–85. doi: 10.4236/pp.2015.62010.

Gerriets, T. *et al.* (2004) 'Noninvasive Quantification of Brain Edema and the Space-Occupying Effect in Rat Stroke Models Using Magnetic Resonance Imaging', *Stroke*. Lippincott Williams & Wilkins, 35(2), pp. 566–571. doi: 10.1161/01.STR.0000113692.38574.57.

Gibbons, H. M. and Dragunow, M. (2010) 'Adult human brain cell culture for neuroscience research', *International Journal of Biochemistry and Cell Biology*. Int J Biochem Cell Biol, pp. 844–856. doi: 10.1016/j.biocel.2009.12.002.

Giffard, R. G. *et al.* (1990) 'Acidosis reduces NMDA receptor activation, glutamate neurotoxicity, and oxygen-glucose deprivation neuronal injury in cortical cultures', *Brain Research*, 506(2), pp. 339–342. doi: 10.1016/0006-8993(90)91276-M.

Giffard, R. G. *et al.* (2000) *The Electrogenic Sodium Bicarbonate Cotransporter: Developmental Expression in Rat Brain and Possible Role in Acid Vulnerability*.

Giffard, R. G., Monyer, H. and Choi, D. W. (1990) 'Selective vulnerability of cultured cortical glia to injury by extracellular acidosis.', *Brain research*, 530(1), pp. 138–41.

Glass, M., Dragunow, M. and Faull, R. L. (1997) 'Cannabinoid receptors in the human brain: a detailed anatomical and quantitative autoradiographic study in the fetal, neonatal and adult human brain.', *Neuroscience*, 77(2), pp. 299–318.

Glass, M. and Felder, C. C. (1997) 'Concurrent stimulation of cannabinoid CB1 and dopamine D2 receptors augments cAMP accumulation in striatal neurons: evidence for a Gs linkage to the CB1 receptor.', *The Journal of neuroscience : the official journal of the Society for Neuroscience*, 17(14), pp. 5327–33.

Glass, M. and Northup, J. K. (1999) 'Agonist selective regulation of G proteins by cannabinoid CB(1) and CB(2) receptors.', *Molecular pharmacology*, 56(6), pp. 1362–9.

Go, Y. Y. *et al.* (2020) 'Cannabidiol enhances cytotoxicity of anti-cancer drugs in human head and neck squamous cell carcinoma', *Scientific Reports*. Nature Research, 10(1), pp. 1–11. doi: 10.1038/s41598-020-77674-y.

Gofshteyn, J. S. *et al.* (2017) 'Cannabidiol as a Potential Treatment for Febrile Infection-Related Epilepsy Syndrome (FIRES) in the Acute and Chronic Phases', *Journal of Child*

Neurology, 32(1), pp. 35–40. doi: 10.1177/0883073816669450.

Gong, J.-P. *et al.* (2006) 'Cannabinoid CB2 receptors: Immunohistochemical localization in rat brain', *Brain Research*, 1071(1), pp. 10–23. doi: 10.1016/j.brainres.2005.11.035.

Goritz, C. *et al.* (2011) 'A Pericyte Origin of Spinal Cord Scar Tissue', *Science*, 333(6039), pp. 238–242. doi: 10.1126/science.1203165.

Gourdin, M. and Dubois, P. (2013) 'Impact of Ischemia on Cellular Metabolism', in *Artery Bypass*. InTech. doi: 10.5772/54509.

Graeber, M. B. and Streit, W. J. (2010) 'Microglia: Biology and pathology', *Acta Neuropathologica*. Springer-Verlag, 119(1), pp. 89–105. doi: 10.1007/s00401-009-0622-0.

Greco, R. *et al.* (2020) 'Characterization of CB2 Receptor Expression in Peripheral Blood Monocytes of Acute Ischemic Stroke Patients', *Translational Stroke Research 2020 12:4*. Springer, 12(4), pp. 550–558. doi: 10.1007/S12975-020-00851-8.

Greenwood, J. *et al.* (2011) 'Review: Leucocyte-endothelial cell crosstalk at the blood-brain barrier: A prerequisite for successful immune cell entry to the brain', *Neuropathology and Applied Neurobiology*, 37(1), pp. 24–39. doi: 10.1111/j.1365-2990.2010.01140.x.

Gülck, T. and Møller, B. L. (2020) 'Phytocannabinoids: Origins and Biosynthesis', *Trends in Plant Science*. Elsevier Ltd. doi: 10.1016/j.tplants.2020.05.005.

Guo, Q. *et al.* (2021) 'Fatty acid-binding proteins aggravate cerebral ischemia-reperfusion injury in mice', *Biomedicines*. Multidisciplinary Digital Publishing Institute (MDPI), 9(5). doi: 10.3390/biomedicines9050529.

Gupta, S., Kesarla, R. and Omri, A. (2013) 'Formulation Strategies to Improve the Bioavailability of Poorly Absorbed Drugs with Special Emphasis on Self-Emulsifying Systems', *ISRN Pharmaceutics*. Hindawi Limited, 2013, pp. 1–16. doi: 10.1155/2013/848043.

Guy, G. W. and Robson, P. J. (2003a) 'A phase I, double blind, three-way crossover study to assess the pharmacokinetic profile of Cannabis Based Medicine Extract (CBME) administered sublingually in variant cannabinoid ratios in normal healthy male volunteers (GWPK0215)', *Journal of Cannabis Therapeutics*, 3(4), pp. 121–152. doi: 10.1300/J175v03n04_02.

Guy, G. W. and Robson, P. J. (2003b) 'A phase I, open label, four-way crossover study to compare the pharmacokinetic profiles of a single dose of 20 mg of a Cannabis Based Medicine Extract (CBME) administered on 3 different areas of the Buccal Mucosa and to investigate the pharmacokinetics of CBME per oral in healthy male and female volunteers (GWPK0112)', *Journal of Cannabis Therapeutics*. Taylor & Francis Group , 3(4), pp. 79–120. doi: 10.1300/J175v03n04_01.

Haj-Dahmane, S. *et al.* (2018) 'Fatty-acid-binding protein 5 controls retrograde endocannabinoid signaling at central glutamate synapses', *Proceedings of the National Academy of Sciences of the United States of America*. National Academy of Sciences, 115(13), pp. 3482–3487. doi: 10.1073/pnas.1721339115.

Hakkoum, D., Stoppini, L. and Muller, D. (2007) 'Interleukin-6 promotes sprouting and functional recovery in lesioned organotypic hippocampal slice cultures', *Journal of Neurochemistry*. Blackwell Publishing Ltd, 100(3), pp. 747–757. doi: 10.1111/j.1471-4159.2006.04257.x.

Halestrap, A. P. *et al.* (1997) 'Cyclosporin A binding to mitochondrial cyclophilin inhibits the permeability transition pore and protects hearts from ischaemia/reperfusion injury.', *Molecular and cellular biochemistry*, 174(1–2), pp. 167–72.

Hall, C. N. *et al.* (2014) 'Capillary pericytes regulate cerebral blood flow in health and disease', *Nature*. Europe PMC Funders, 508(1), pp. 55–60. doi: 10.1038/nature13165.

Hampson, A. J. *et al.* (1998) 'Cannabidiol and (-)Delta9-tetrahydrocannabinol are neuroprotective antioxidants.', *Proceedings of the National Academy of Sciences of the United States of America*. National Academy of Sciences, 95(14), pp. 8268–73. doi: 10.1073/pnas.95.14.8268.

Hampson, A. J. *et al.* (2000) 'Neuroprotective antioxidants from marijuana', *Annals of the New York Academy of Sciences*, 899(1), pp. 274–282. doi: 10.1111/j.1749-6632.2000.tb06193.x.

Han, L. *et al.* (2016) 'Lymphatic transport of orally administered probucol-loaded mPEG-DSPE micelles', *Drug Delivery*. Drug Deliv, 23(6), pp. 1955–1961. doi: 10.3109/10717544.2015.1028600.

Hanisch, U.-K. and Kettenmann, H. (2007) 'Microglia: active sensor and versatile effector cells in the normal and pathologic brain', *Nature Neuroscience*, 10(11), pp. 1387–1394. doi: 10.1038/nn1997.

Hatano, S. (1976) 'Experience from a multicentre stroke register: a preliminary report', *Bulletin of the World Health Organization*. World Health Organization, 54(5), pp. 541–553.

Hayakawa, K. *et al.* (2004) *Cannabidiol prevents infarction via the non-CB1 cannabinoid receptor mechanism*, *NeuroReport*. doi: 10.1097/00001756-200410250-00016.

Hayakawa, K., Mishima, K., Nozako, M., Hazekawa, M., *et al.* (2007) 'Delayed treatment with cannabidiol has a cerebroprotective action via a cannabinoid receptor-independent myeloperoxidase-inhibiting mechanism', *Journal of Neurochemistry*. Wiley/Blackwell (10.1111), 102(5), pp. 1488–1496. doi: 10.1111/j.1471-4159.2007.04565.x.

Hayakawa, K., Mishima, K., Nozako, M., Ogata, A., *et al.* (2007) 'Repeated treatment with cannabidiol but not Δ9-tetrahydrocannabinol has a neuroprotective effect without the development of tolerance', *Neuropharmacology*. Pergamon, 52(4), pp. 1079–1087. doi: 10.1016/j.neuropharm.2006.11.005.

Hayakawa, K. *et al.* (2008) 'Cannabidiol prevents a post-ischemic injury progressively induced by cerebral ischemia via a high-mobility group box1-inhibiting mechanism', *Neuropharmacology*. Pergamon, 55(8), pp. 1280–1286. doi: 10.1016/J.NEUROPHARM.2008.06.040.

Hayakawa, K. *et al.* (2009) 'Therapeutic time window of cannabidiol treatment on delayed ischemic damage via high-mobility group box1-inhibiting mechanism.', *Biological & pharmaceutical bulletin*, 32(9), pp. 1538–44. doi: 10.1248/bpb.32.1538.

Hayakawa, K., Mishima, K. and Fujiwara, M. (2010) 'Therapeutic potential of non-psychotropic cannabidiol in ischemic stroke', *Pharmaceuticals*. Molecular Diversity Preservation International, pp. 2197–2212. doi: 10.3390/ph3072197.

Heiss, W.-D. (2014) 'Radionuclide Imaging in Ischemic Stroke', *Journal of Nuclear Medicine*. Society of Nuclear Medicine, 55(11), pp. 1831–1841. doi: 10.2967/jnumed.114.145003.

Helbig, G. *et al.* (2003) 'NF-κB promotes breast cancer cell migration and metastasis by

inducing the expression of the chemokine receptor CXCR4', *Journal of Biological Chemistry*. J Biol Chem, 278(24), pp. 21631–21638. doi: 10.1074/jbc.M300609200.

Hellriegel, E. T., Bjornsson, T. D. and Hauck, W. W. (1996) 'Interpatient variability in bioavailability is related to the extent of absorption: Implications for bioavailability and bioequivalence studies', *Clinical Pharmacology and Therapeutics*. Clin Pharmacol Ther, pp. 601–607. doi: 10.1016/S0009-9236(96)90208-8.

Herkenham, M. *et al.* (1990) 'Cannabinoid receptor localization in brain', *Proceedings of the National Academy of Sciences USA*, 87(5), pp. 1932–1936. doi: 10.1073/pnas.87.5.1932.

Herkenham, M. *et al.* (1991) 'Characterization and localization of cannabinoid receptors in rat brain: a quantitative in vitro autoradiographic study.', *The Journal of neuroscience : the official journal of the Society for Neuroscience*, 11(2), pp. 563–83.

Hickey, M. B. *et al.* (2007) 'Performance comparison of a co-crystal of carbamazepine with marketed product', *European Journal of Pharmaceutics and Biopharmaceutics*. Eur J Pharm Biopharm, 67(1), pp. 112–119. doi: 10.1016/j.ejpb.2006.12.016.

Hill, J. K. *et al.* (1999) 'Temporal modulation of cytokine expression following focal cerebral ischemia in mice.', *Brain research*, 820(1–2), pp. 45–54. doi: 10.1016/s0006-8993(98)01140-8.

Hillard, C. J. (2000) 'Biochemistry and pharmacology of the endocannabinoids arachidonylethanolamide and 2-arachidonylglycerol', *Prostaglandins and Other Lipid Mediators*. Prostaglandins Other Lipid Mediat, 61(1–2), pp. 3–18. doi: 10.1016/S0090-6980(00)00051-4.

Hillard, C. J. (2008) 'Role of cannabinoids and endocannabinoids in cerebral ischemia.', *Current pharmaceutical design*, 14(23), pp. 2347–61. doi: 10.2174/138161208785740054.

Hind, W. H. *et al.* (2015) 'Endocannabinoids modulate human blood-brain barrier permeability in vitro', *British Journal of Pharmacology*. Br J Pharmacol, 172(12), pp. 3015–3027. doi: 10.1111/bph.13106.

Hind, W. H., England, T. J. and O'Sullivan, S. E. (2016) 'Cannabidiol protects an in vitro model of the blood-brain barrier from oxygen-glucose deprivation via PPARγ and 5-HT1A receptors.', *British journal of pharmacology*. Wiley-Blackwell, 173(5), pp. 815–25. doi: 10.1111/bph.13368.

Ho, B. Y. *et al.* (1999) 'Coupling of the expressed cannabinoid CB1 and CB2 receptors to phospholipase C and G protein-coupled inwardly rectifying K+ channels.', *Receptors & channels*, 6(5), pp. 363–374.

Hooijmans, C. R. *et al.* (2014) 'SYRCLE's risk of bias tool for animal studies', *BMC Medical Research Methodology*, 14(1), p. 43. doi: 10.1186/1471-2288-14-43.

Hörter, D. and Dressman, J. B. (2001) 'Influence of physicochemical properties on dissolution of drugs in the gastrointestinal tractac', *Advanced Drug Delivery Reviews*. Adv Drug Deliv Rev, 46(1–3), pp. 75–87. doi: 10.1016/S0169-409X(00)00130-7.

Hossmann, K. -A (1994) 'Viability thresholds and the penumbra of focal ischemia', *Annals of Neurology*, 36(4), pp. 557–565. doi: 10.1002/ana.410360404.

Hossmann, K. A. (2006) 'Pathophysiology and therapy of experimental stroke', *Cellular and Molecular Neurobiology*. Cell Mol Neurobiol, 26(7–8), pp. 1057–1083. doi: 10.1007/s10571-006-9008-1.

Howlett, A. C. (2005) 'Cannabinoid receptor signaling', *Handbook of Experimental Pharmacology*, 168(168), pp. 53–79. doi: 10.1007/3-540-26573-2-2.

Howlett, A. C. and Fleming, R. M. (1984) 'Cannabinoid inhibition of adenylate cyclase. Pharmacology of the response in neuroblastoma cell membranes.', *Molecular pharmacology*, 26(3), pp. 532–8.

Howlett, A. C., Qualy, J. M. and Khachatrian, L. L. (1986) 'Involvement of Gi in the inhibition of adenylate cyclase by cannabimimetic drugs.', *Molecular pharmacology*, 29(3), pp. 307–13.

Huang, J., Upadhyay, U. M. and Tamargo, R. J. (2006) 'Inflammation in stroke and focal cerebral ischemia', *Surgical Neurology*. Elsevier, 66(3), pp. 232–245. doi: 10.1016/j.surneu.2005.12.028.

Huestis, M. A. (2007) *Human cannabinoid pharmacokinetics*, *Chemistry and Biodiversity*. NIH Public Access. doi: 10.1002/cbdv.200790152.

Iannotti, F. A. *et al.* (2014) 'Nonpsychotropic plant cannabinoids, Cannabidivarin (CBDV) and Cannabidiol (CBD), activate and desensitize Transient Receptor Potential Vanilloid 1 (TRPV1) channels in vitro: Potential for the treatment of neuronal hyperexcitability', *ACS Chemical Neuroscience*. American Chemical Society, 5(11), pp. 1131–1141. doi: 10.1021/cn5000524.

Ibeas Bih, C. *et al.* (2015) 'Molecular Targets of Cannabidiol in Neurological Disorders', *Neurotherapeutics*. Springer US, 12(4), pp. 699–730. doi: 10.1007/s13311-015-0377-3.

Ibsen, M. S., Connor, M. and Glass, M. (2017) 'Cannabinoid CB1 and CB2 Receptor Signaling and Bias', *Cannabis and Cannabinoid Research*, 2(1), pp. 48–60. doi: 10.1089/can.2016.0037.

Ingels, F. *et al.* (2004) 'Effect of simulated intestinal fluid on drug permeability estimation across Caco-2 monolayers', *International Journal of Pharmaceutics*. Int J Pharm, 274(1–2), pp. 221–232. doi: 10.1016/j.ijpharm.2004.01.014.

Itin, C. *et al.* (2020) 'Prolonged oral transmucosal delivery of highly lipophilic drug cannabidiol', *International Journal of Pharmaceutics*. Elsevier B.V., 581, p. 119276. doi: 10.1016/j.ijpharm.2020.119276.

Itin, C., Domb, A. J. and Hoffman, A. (2019) 'A meta-opinion: cannabinoids delivered to oral mucosa by a spray for systemic absorption are rather ingested into gastro-intestinal tract: the influences of fed / fasting states', *Expert Opinion on Drug Delivery*. Taylor and Francis Ltd, 16(10), pp. 1031–1035. doi: 10.1080/17425247.2019.1653852.

Izzo, A. A. *et al.* (2009) *Non-psychotropic plant cannabinoids: new therapeutic opportunities from an ancient herb*, *Trends in Pharmacological Sciences*. doi: 10.1016/j.tips.2009.07.006.

Izzo, A. A. *et al.* (2012) 'Inhibitory effect of cannabichromene, a major non-psychotropic cannabinoid extracted from Cannabis sativa, on inflammation-induced hypermotility in mice', *British Journal of Pharmacology*. Wiley-Blackwell, 166(4), pp. 1444–1460. doi: 10.1111/j.1476-5381.2012.01879.x.

Janani, C. and Ranjitha Kumari, B. D. (2015) 'PPAR gamma gene - A review', *Diabetes and Metabolic Syndrome: Clinical Research and Reviews*. Diabetes Metab Syndr, pp. 46–50. doi: 10.1016/j.dsx.2014.09.015.

Jia, Y. *et al.* (2016) 'Tetramethylpyrazine inhibits tumor growth of lung cancer through

disrupting angiogenesis via BMP/Smad/Id-1 signaling', *International Journal of Oncology*. Int J Oncol, 48(5), pp. 2079–2086. doi: 10.3892/ijo.2016.3443.

Jiang, X. and Wang, X. (2004) 'CYTOCHROME C-MEDIATED APOPTOSIS'. doi: 10.1146/annurev.biochem.73.011303.073706.

Jilani, T. N. and Siddiqui, A. H. (2021) *Tissue Plasminogen Activator*, *StatPearls*. StatPearls Publishing. Available at: http://www.ncbi.nlm.nih.gov/pubmed/29939694 (Accessed: 24 June 2021).

John, G. R., Lee, S. C. and Brosnan, C. F. (2003) 'Cytokines: Powerful Regulators of Glial Cell Activation', *The Neuroscientist*, 9(1), pp. 10–22. doi: 10.1177/1073858402239587.

Johns, D. G. *et al.* (2007) 'The novel endocannabinoid receptor GPR55 is activated by atypical cannabinoids but does not mediate their vasodilator effects', *British Journal of Pharmacology*. Wiley-Blackwell, 152(5), p. 825. doi: 10.1038/SJ.BJP.0707419.

Johnson, A. C. and Greenwood-Van Meerveld, B. (2016) 'The Pharmacology of Visceral Pain', *Advances in Pharmacology*. Academic Press, 75, pp. 273–301. doi: 10.1016/BS.APHA.2015.11.002.

Jung, B. *et al.* (2019) 'Synthetic Strategies for (−)-Cannabidiol and Its Structural Analogs', *Chemistry – An Asian Journal*, 14(21), pp. 3749–3762. doi: 10.1002/asia.201901179.

Kamouchi, M. *et al.* (2004) 'Calcium influx pathways in rat CNS pericytes', *Molecular Brain Research*. Brain Res Mol Brain Res, 126(2), pp. 114–120. doi: 10.1016/j.molbrainres.2004.03.008.

Katchan, V., David, P. and Shoenfeld, Y. (2016) 'Cannabinoids and autoimmune diseases: A systematic review', *Autoimmunity Reviews*. Autoimmun Rev, pp. 513–528. doi: 10.1016/j.autrev.2016.02.008.

Katona, I. *et al.* (2006) 'Molecular composition of the endocannabinoid system at glutamatergic synapses.', *The Journal of neuroscience : the official journal of the Society for Neuroscience*. NIH Public Access, 26(21), pp. 5628–37. doi: 10.1523/JNEUROSCI.0309-06.2006.

Kelly-Hayes, M. *et al.* (2003) 'The influence of gender and age on disability following ischemic stroke: The Framingham study', *Journal of Stroke and Cerebrovascular Diseases*, 12(3), pp. 119–126. doi: 10.1016/S1052-3057(03)00042-9.

Kendall, D. A. and Yudowski, G. A. (2017) 'Cannabinoid receptors in the central nervous system: Their signaling and roles in disease', *Frontiers in Cellular Neuroscience*. Frontiers Media SA, 10, p. 294. doi: 10.3389/fncel.2016.00294.

Khaksar, s and Bigdeli, M. (2016) 'Protective Effect of Different Doses of Cannabidiol on Blood-Brain Barrier Permeability and Damages Resulting from Cerebral Ischemia Model in Rats', *ZUMS Journal*. ZUMS Journal, 24(106), pp. 63–78. Available at: http://zums.ac.ir/journal/browse.php?a_id=3694&sid=1&slc_lang=en (Accessed: 25 November 2018).

Khaksar, S. and Bigdeli, M. R. (2017a) 'Anti-excitotoxic effects of cannabidiol are partly mediated by enhancement of NCX2 and NCX3 expression in animal model of cerebral ischemia', *European Journal of Pharmacology*. Elsevier, 794, pp. 270–279. doi: 10.1016/J.EJPHAR.2016.11.011.

Khaksar, S. and Bigdeli, M. R. (2017b) 'Correlation Between Cannabidiol-Induced Reduction

of Infarct Volume and Inflammatory Factors Expression in Ischemic Stroke Model.', *Basic and clinical neuroscience*. Iranian Neuroscience Society, 8(2), pp. 139–146. doi: 10.18869/nirp.bcn.8.2.139.

Khaksar, S. and Bigdeli, M. R. (2017c) 'Intra-cerebral cannabidiol infusion-induced neuroprotection is partly associated with the TNF-α/TNFR1/NF-κB pathway in transient focal cerebral ischaemia', *Brain Injury*. Taylor & Francis, 31(13–14), pp. 1932–1943. doi: 10.1080/02699052.2017.1358397.

Khoshnam, S. E. *et al.* (2017) 'Pathogenic mechanisms following ischemic stroke', *Neurological Sciences*, pp. 1167–1186. doi: 10.1007/s10072-017-2938-1.

King, D. *et al.* (2020) 'The future incidence, prevalence and costs of stroke in the UK', *Age and Ageing*. Oxford Academic, 49(2), pp. 277–282. doi: 10.1093/AGEING/AFZ163.

Klatzo, I. (1967) 'Neuropathological Aspects of Brain Edema', *Journal of Neuropathology and Experimental Neurology*, 26(1), pp. 1–14. doi: 10.1097/00005072-196701000-00001.

Klotz, K. A. *et al.* (2019) 'Efficacy and Tolerance of Synthetic Cannabidiol for Treatment of Drug Resistant Epilepsy', *Frontiers in Neurology*, 10. doi: 10.3389/fneur.2019.01313.

Koehler, R. C., Roman, R. J. and Harder, D. R. (2009) 'Astrocytes and the regulation of cerebral blood flow', *Trends in Neurosciences*, pp. 160–169. doi: 10.1016/j.tins.2008.11.005.

Kohno, M. *et al.* (2006) 'Identification of N-arachidonylglycine as the endogenous ligand for orphan G-protein-coupled receptor GPR18', *Biochemical and Biophysical Research Communications*, 347(3), pp. 827–832. doi: 10.1016/j.bbrc.2006.06.175.

Kuffler, S. W., Nicholls, J. G. and Orkand, R. K. (1966) 'Physiological properties of glial cells in the central nervous system of amphibia.', *Journal of neurophysiology*, 29(4), pp. 768–787. doi: 10.1152/jn.1966.29.4.768.

Kuida, K. (2000) 'Caspase-9', *International Journal of Biochemistry and Cell Biology*. Elsevier Ltd, 32(2), pp. 121–124. doi: 10.1016/S1357-2725(99)00024-2.

Kurabayashi, M. *et al.* (2005) '2-Arachidonoylglycerol increases in ischemia-reperfusion injury of the rat liver', *Journal of Investigative Surgery*. Taylor & Francis, 18(1), pp. 25–31. doi: 10.1080/08941930590905189.

Kuroda, S. *et al.* (1996) 'Secondary bioenergetic failure after transient focal ischaemia is due to mitochondrial injury', *Acta physiologica Scandinavica*. Acta Physiol Scand, 156(2), pp. 149–150. doi: 10.1046/J.1365-201X.1996.449170000.X.

L, C.-B. *et al.* (2014) 'Activation of GPR18 by cannabinoid compounds: a tale of biased agonism', *British journal of pharmacology*. Br J Pharmacol, 171(16), pp. 3908–3917. doi: 10.1111/BPH.12746.

Lakhan, S. E. *et al.* (2013) 'Matrix metalloproteinases and blood-brain barrier disruption in acute ischemic stroke', *Frontiers in Neurology*. Frontiers Media SA, 4 APR. doi: 10.3389/fneur.2013.00032.

Lampl, Y. *et al.* (1990) 'Cerebrospinal fluid lactate dehydrogenase levels in early stroke and transient ischemic attacks', *Stroke*, 21(6), pp. 854–857. doi: 10.1161/01.STR.21.6.854.

Lane, J. R. *et al.* (2010) 'The endocannabinoid 2-arachidonylglycerol is a negative allosteric modulator of the human A3 adenosine receptor', *Biochemical Pharmacology*. Elsevier, 79(1), pp. 48–56. doi: 10.1016/J.BCP.2009.07.024.

Laprairie, R. B. *et al.* (2015) 'Cannabidiol is a negative allosteric modulator of the cannabinoid CB1 receptor', *British Journal of Pharmacology*. Wiley/Blackwell (10.1111), 172(20), pp. 4790–4805. doi: 10.1111/bph.13250.

Lara-Ochoa, F. and Espinosa-Pérez, G. (2007) 'Cocrystals definitions', *Supramolecular Chemistry*. Taylor & Francis Group, 19(8), pp. 553–557. doi: 10.1080/10610270701501652.

Lauckner, J. E. *et al.* (2008) 'GPR55 is a cannabinoid receptor that increases intracellular calcium and inhibits M current', *Proceedings of the National Academy of Sciences of the United States of America*. Proc Natl Acad Sci U S A, 105(7), pp. 2699–2704. doi: 10.1073/pnas.0711278105.

Lavine, S. D., Hofman, F. M. and Zlokovic, B. V. (1998) 'Circulating Antibody against Tumor Necrosis Factor–Alpha Protects Rat Brain from Reperfusion Injury', *Journal of Cerebral Blood Flow & Metabolism*, 18(1), pp. 52–58. doi: 10.1097/00004647-199801000-00005.

Lemasters, J. J. and Hackenbrock, C. R. (1978) 'Firefly Luciferase Assay for ATP Production by Mitochondria', *Methods in Enzymology*. Academic Press, 57(C), pp. 36–50. doi: 10.1016/0076-6879(78)57006-7.

Lennmyr, F. *et al.* (1998) 'Expression of vascular endothelial growth factor (VEGF) and its receptors (Flt-1 and Flk-1) following permanent and transient occlusion of the middle cerebral artery in the rat', *Journal of Neuropathology and Experimental Neurology*, 57(9), pp. 874–882. doi: 10.1097/00005072-199809000-00009.

Li, H. *et al.* (1998) 'Cleavage of BID by caspase 8 mediates the mitochondrial damage in the Fas pathway of apoptosis.', *Cell*, 94(4), pp. 491–501.

Liao, S. L. *et al.* (2004) 'Tetramethylpyrazine reduces ischemic brain injury in rats', *Neuroscience Letters*, 372(1–2), pp. 40–45. doi: 10.1016/j.neulet.2004.09.013.

Liesz, A. *et al.* (2009) 'Regulatory T cells are key cerebroprotective immunomodulators in acute experimental stroke', *Nature Medicine*, 15(2), pp. 192–199. doi: 10.1038/nm.1927.

Ligresti, A. *et al.* (2006) 'Antitumor activity of plant cannabinoids with emphasis on the effect of cannabidiol on human breast carcinoma', *Journal of Pharmacology and Experimental Therapeutics*. J Pharmacol Exp Ther, 318(3), pp. 1375–1387. doi: 10.1124/jpet.106.105247.

Lin, B. (2009) 'Integrating Comprehensive and Alternative Medicine into stroke. Herbal Treatment of Ischemia', in *Complementary and Alternative Therapies and the Aging Population*. Academic Press, pp. 229–274. doi: 10.1016/B978-0-12-374228-5.00012-3.

Lin, J.-B. *et al.* (2015) 'Effects of Tetramethylpyrazine on Functional Recovery and Neuronal Dendritic Plasticity after Experimental Stroke'. doi: 10.1155/2015/394926.

Lindsberg, P. J. and Grau, A. J. (2003) 'Inflammation and Infections as Risk Factors for Ischemic Stroke', *Stroke*. Lippincott Williams & Wilkins, 34(10), pp. 2518–2532. doi: 10.1161/01.STR.0000089015.51603.CC.

Lipton, S. (2004) 'Failures and successes of NMDA receptor antagonists: molecular basis for the use of open-channel blockers like memantine in the treatment of acute and chronic neurologic insults.', *NeuroRx : the journal of the American Society for Experimental NeuroTherapeutics*. Am. Soc. for Experimental NeuroTherapeutics, 1(1), pp. 101–10. doi: 10.1602/neurorx.1.1.101.

Lukas, G., Brindle, S. D. and Greengard, P. (1971) 'The route of absorption of

intraperitoneally administered compounds.', *Journal of Pharmacology and Experimental Therapeutics*, 178(3), pp. 562–564.

Lukaszevicz, A.-C. *et al.* (2002) 'High Sensitivity of Protoplasmic Cortical Astroglia to Focal Ischemia', *Journal of Cerebral Blood Flow & Metabolism*, 22(3), pp. 289–298. doi: 10.1097/00004647-200203000-00006.

Luo, R. *et al.* (2020) 'Activation of PPARA-mediated autophagy reduces Alzheimer disease-like pathology and cognitive decline in a murine model', *Autophagy*. Autophagy, 16(1), pp. 52–69. doi: 10.1080/15548627.2019.1596488.

Lyden, P. *et al.* (2002) 'Clomethiazole acute stroke study in ischemic stroke (CLASS-I): Final results', *Stroke*. Stroke, 33(1), pp. 122–128. doi: 10.1161/hs0102.101478.

Mackie, K. (2005) 'Distribution of cannabinoid receptors in the central and peripheral nervous system.', *Handbook of experimental pharmacology*, (168), pp. 299–325.

MacVicar, B. A. and Newman, E. A. (2015) 'Astrocyte regulation of blood flow in the brain.', *Cold Spring Harbor perspectives in biology*. Cold Spring Harbor Laboratory Press, 7(5). doi: 10.1101/cshperspect.a020388.

Malemud, C. J. (2006) 'Matrix metalloproteinases (MMPs) in health and disease: An overview', *Frontiers in Bioscience*. Front Biosci, 11(2 P.1591-2006), pp. 1696–1701. doi: 10.2741/1915.

Mancini, I. *et al.* (2009) 'Constitutive activity of cannabinoid-2 (CB 2) receptors plays an essential role in the protean agonism of (+)AM1241 and L768242', *British Journal of Pharmacology*, 158(1), pp. 382–391. doi: 10.1111/j.1476-5381.2009.00154.x.

Manley, G. T. *et al.* (2004) 'New insights into water transport and edema in the central nervous system from phenotype analysis of aquaporin-4 null mice', *Neuroscience*, 129(4), pp. 981–989. doi: 10.1016/j.neuroscience.2004.06.088.

Manley, G. T. *et al.* (2009) 'Role of aquaporin-4 in cerebral edema and stroke', *Handbook of Experimental Pharmacology*, 190, pp. 159–170. doi: 10.1007/978-3-540-79885-9_7.

Marinelli, L. *et al.* (2017) 'A randomised controlled cross-over double-blind pilot study protocol on THC:CBD oromucosal spray efficacy as an add-on therapy for post-stroke spasticity', *BMJ Open*. BMJ Publishing Group, 7(9). doi: 10.1136/bmjopen-2017-016843.

Marler, J. R. (1995) 'NINDS-TPA, 1995, TISSUE PLASMINOGEN ACTIVATOR FOR ACUTE ISCHEMIC STROKE', *New England Journal of Medicine*. N Engl J Med, 333(24), pp. 1581–1588. doi: 10.1056/NEJM199512143332401.

Marsicano, G. *et al.* (2003) 'CB1 cannabinoid receptors and on-demand defense against excitotoxicity', *Science*. American Association for the Advancement of Science, 302(5642), pp. 84–88. doi: 10.1126/science.1088208.

Martin, G. *et al.* (1997) 'Coordinate regulation of the expression of the fatty acid transport protein and acyl-CoA synthetase genes by PPARα and PPARγ activators', *Journal of Biological Chemistry*. J Biol Chem, 272(45), pp. 28210–28217. doi: 10.1074/jbc.272.45.28210.

Martin, J. H. *et al.* (2018) 'Exogenous Cannabinoid Efficacy: Merely a Pharmacokinetic Interaction?', *Clinical Pharmacokinetics*. Springer International Publishing, 57(5), pp. 539–545. doi: 10.1007/s40262-017-0599-0.

Martin, L. J. *et al.* (2021) 'Cannabichromene and Δ9-Tetrahydrocannabinolic Acid Identified

as Lactate Dehydrogenase-A Inhibitors by in Silico and in Vitro Screening', *Journal of Natural Products*. J Nat Prod, 84(5), pp. 1469–1477. doi: 10.1021/acs.jnatprod.0c01281.

Di Marzo, V. *et al.* (1994) 'Formation and inactivation of endogenous cannabinoid anandamide in central neurons', *Nature*. Nature Publishing Group, 372(6507), pp. 686–691. doi: 10.1038/372686a0.

Di Marzo, V., Bisogno, T. and De Petrocellis, L. (2005) 'The biosynthesis, fate and pharmacological properties of endocannabinoids', in *Handbook of Experimental Pharmacology*. Springer, Berlin, Heidelberg, pp. 147–185. doi: 10.1007/3-540-26573-2-5.

Di Marzo, V. and Fontana, A. (1995) 'Anandamide, an endogenous cannabinomimetic eicosanoid: "Killing two birds with one stone"', *Prostaglandins, Leukotrienes and Essential Fatty Acids*, 53(1), pp. 1–11. doi: 10.1016/0952-3278(95)90077-2.

Massi, P. *et al.* (2013) 'Cannabidiol as potential anticancer drug', *British Journal of Clinical Pharmacology*. Wiley-Blackwell, 75(2), pp. 303–312. doi: 10.1111/j.1365-2125.2012.04298.x.

Matsuzaki, S. *et al.* (2009) 'Regulated Production of Free Radicals by the Mitochondrial Electron Transport Chain: Cardiac Ischemic Preconditioning', *Advanced drug delivery reviews*. NIH Public Access, 61(14), p. 1324. doi: 10.1016/J.ADDR.2009.05.008.

Matute, C. *et al.* (2002) 'Excitotoxicity in glial cells', *European Journal of Pharmacology*, pp. 239–246. doi: 10.1016/S0014-2999(02)01847-2.

McAllister, S. D. *et al.* (1999) 'Cannabinoid receptors can activate and inhibit G protein-coupled inwardly rectifying potassium channels in a xenopus oocyte expression system.', *The Journal of pharmacology and experimental therapeutics*, 291(2), pp. 618–26.

McKemy, D. D. (2007) 'TRPM8: The Cold and Menthol Receptor', *TRP Ion Channel Function in Sensory Transduction and Cellular Signaling Cascades*. CRC Press/Taylor & Francis, pp. 199–210. Available at: https://www.ncbi.nlm.nih.gov/books/NBK5238/ (Accessed: 13 July 2021).

McPartland, J. M. *et al.* (2015) 'Are cannabidiol and Δ9-tetrahydrocannabivarin negative modulators of the endocannabinoid system? A systematic review', *British Journal of Pharmacology*. John Wiley & Sons, Ltd, pp. 737–753. doi: 10.1111/bph.12944.

McVey, D. C. *et al.* (2003) 'Endocannabinoids induce ileitis in rats via the capsaicin receptor (VR1)', *Journal of Pharmacology and Experimental Therapeutics*. J Pharmacol Exp Ther, 304(2), pp. 713–722. doi: 10.1124/jpet.102.043893.

Mechoulam, R. *et al.* (1995) 'Identification of an endogenous 2-monoglyceride, present in canine gut, that binds to cannabinoid receptors', *Biochemical Pharmacology*, 50(1), pp. 83–90. doi: 10.1016/0006-2952(95)00109-D.

Mehta, S. L., Manhas, N. and Raghubir, R. (2007) 'Molecular targets in cerebral ischemia for developing novel therapeutics', *Brain Research Reviews*, 54(1), pp. 34–66. doi: 10.1016/j.brainresrev.2006.11.003.

De Meijer, E. P. M., Hammond, K. M. and Micheler, M. (2009) 'The inheritance of chemical phenotype in Cannabis sativa L. (III): Variation in cannabichromene proportion', *Euphytica*. Springer, 165(2), pp. 293–311. doi: 10.1007/s10681-008-9787-1.

de Mello Schier, A. R. *et al.* (2014) 'Antidepressant-like and anxiolytic-like effects of cannabidiol: a chemical compound of Cannabis sativa.', *CNS & neurological disorders drug*

targets, 13(6), pp. 953–60. Available at: http://www.ncbi.nlm.nih.gov/pubmed/24923339 (Accessed: 29 May 2019).

Memezawa, H., Smith, M. L. and Siesjo, B. K. (1992) 'Penumbral tissues salvaged by reperfusion following middle cerebral artery occlusion in rats', *Stroke*, 23(4), pp. 552–559. doi: 10.1161/01.STR.23.4.552.

Metodiewa, D. and Kośka, C. (2000) 'Reactive oxygen species and reactive nitrogen species: relevance to cyto(neuro)toxic events and neurologic disorders. An overview.', *Neurotoxicity research*, 1(3), pp. 197–233. doi: 10.1007/BF03033290.

Michinaga, S. and Koyama, Y. (2015) 'Pathogenesis of brain edema and investigation into anti-edema drugs', *International Journal of Molecular Sciences*. MDPI AG, pp. 9949–9975. doi: 10.3390/ijms16059949.

Millar, S. A. *et al.* (2018) *A systematic review on the pharmacokinetics of cannabidiol in humans*, *Frontiers in Pharmacology*. Frontiers Media S.A. doi: 10.3389/fphar.2018.01365.

Millar, S. A. *et al.* (2020) 'Towards Better Delivery of Cannabidiol (CBD)', *Pharmaceuticals*. MDPI AG, 13(9), p. 219. doi: 10.3390/ph13090219.

Miroshnyk, I., Mirza, S. and Sandler, N. (2009) 'Pharmaceutical co-crystals - An opportunity for drug product enhancement', *Expert Opinion on Drug Delivery*, pp. 333–341. doi: 10.1517/17425240902828304.

Mishima, K. *et al.* (2005) 'Cannabidiol prevents cerebral infarction via a serotonergic 5-hydroxytryptamine1A receptor-dependent mechanism', *Stroke*, 36(5), pp. 1071–1076. doi: 10.1161/01.STR.0000163083.59201.34.

Mizui, T., Kinouchi, H. and Chan, P. H. (1992) 'Depletion of brain glutathione by buthionine sulfoximine enhances cerebral ischemic injury in rats.', *The American journal of physiology*, 262(2 Pt 2), pp. H313-7.

Montagne, M. (2004) 'Book Review: The Medicinal Uses of Cannabis and Cannabinoids', *Annals of Pharmacotherapy*, 38(12), pp. 2180–2180. doi: 10.1345/aph.1e471.

Montoya, Z. *et al.* (2020) 'Cannabis Contaminants Limit Pharmacological Use of Cannabidiol', *Frontiers in Pharmacology*. Frontiers Media S.A., p. 1439. doi: 10.3389/fphar.2020.571832.

Morales, P. *et al.* (2020) 'Therapeutic Exploitation of GPR18: Beyond the Cannabinoids?', *Journal of Medicinal Chemistry*. American Chemical Society, pp. 14216–14227. doi: 10.1021/acs.jmedchem.0c00926.

Morales, P., Hurst, D. P. and Reggio, P. H. (2017) 'Molecular Targets of the Phytocannabinoids: A Complex Picture', *Progress in the chemistry of organic natural products*. NIH Public Access, pp. 103–131. doi: 10.1007/978-3-319-45541-9_4.

Morales, P., Reggio, P. H. and Jagerovic, N. (2017) 'An overview on medicinal chemistry of synthetic and natural derivatives of cannabidiol', *Frontiers in Pharmacology*. Frontiers, 8(JUN), p. 422. doi: 10.3389/fphar.2017.00422.

Moretti, R. *et al.* (2015) 'Blood-brain barrier dysfunction in disorders of the developing brain', *Frontiers in Neuroscience*. Frontiers, 9(FEB), p. 40. doi: 10.3389/fnins.2015.00040.

Morgan, C. J. A. *et al.* (2018) 'Individual and combined effects of acute delta-9-tetrahydrocannabinol and cannabidiol on psychotomimetic symptoms and memory function', *Translational Psychiatry*, 8(1), p. 181. doi: 10.1038/s41398-018-0191-x.

Mori, E. *et al.* (1992) 'Inhibition of polymorphonuclear leukocyte adherence suppresses no-reflow after focal cerebral ischemia in baboons.', *Stroke*. American Heart Association, Inc., 23(5), pp. 712–8. doi: 10.1161/01.STR.23.5.712.

Mori, M. A. *et al.* (2017) 'Cannabidiol reduces neuroinflammation and promotes neuroplasticity and functional recovery after brain ischemia', *Progress in Neuro-Psychopharmacology and Biological Psychiatry*. Elsevier, 75, pp. 94–105. doi: 10.1016/J.PNPBP.2016.11.005.

Morrison, G. *et al.* (2019) 'A Phase 1, Open-Label, Pharmacokinetic Trial to Investigate Possible Drug-Drug Interactions Between Clobazam, Stiripentol, or Valproate and Cannabidiol in Healthy Subjects', *Clinical Pharmacology in Drug Development*. Blackwell Publishing Ltd, 8(8), pp. 1009–1031. doi: 10.1002/cpdd.665.

Muller, C. *et al.* (2020) 'A Closer Look at Anandamide Interaction With TRPV1', *Frontiers in Molecular Biosciences*. Frontiers, 7, p. 144. doi: 10.3389/FMOLB.2020.00144.

Muller, C., Morales, P. and Reggio, P. H. (2018) 'Cannabinoid Ligands Targeting TRP Channels.', *Frontiers in molecular neuroscience*. Frontiers Media SA, 11, p. 487. doi: 10.3389/fnmol.2018.00487.

Munro, S., Thomas, K. L. and Abu-Shaar, M. (1993) 'Molecular characterization of a peripheral receptor for cannabinoids', *Nature*, 365(6441), pp. 61–65. doi: 10.1038/365061a0.

Muoio, V., Persson, P. B. and Sendeski, M. M. (2014) 'The neurovascular unit - concept review', *Acta Physiologica*, pp. 790–798. doi: 10.1111/apha.12250.

N, C. *et al.* (2015) 'Identification of resolvin D2 receptor mediating resolution of infections and organ protection', *The Journal of experimental medicine*. J Exp Med, 212(8), pp. 1203–1217. doi: 10.1084/JEM.20150225.

Naccarato, M. *et al.* (2010) 'Possible Anandamide and Palmitoylethanolamide involvement in human stroke', *Lipids in Health and Disease 2010 9:1*. BioMed Central, 9(1), pp. 1–6. doi: 10.1186/1476-511X-9-47.

Nadal, X. *et al.* (2017) 'Tetrahydrocannabinolic acid is a potent PPARγ agonist with neuroprotective activity', *British Journal of Pharmacology*. Wiley-Blackwell, 174(23), pp. 4263–4276. doi: 10.1111/bph.14019.

Näveri, L., Näveri, H. and Härkönen, M. (2001) 'Myocardial Energy Metabolism', *Annales Chirurgiae et Gynaecologiae*. Academic Press, 76(1), pp. 543–569. doi: 10.1016/B978-012656975-9/50034-1.

Nie, J. and Lewis, D. L. (2001) 'Structural domains of the CB1 cannabinoid receptor that contribute to constitutive activity and G-protein sequestration.', *The Journal of neuroscience : the official journal of the Society for Neuroscience*, 21(22), pp. 8758–8764.

Nielsen, S. *et al.* (1997) 'Specialized membrane domains for water transport in glial cells: high-resolution immunogold cytochemistry of aquaporin-4 in rat brain.', *The Journal of neuroscience : the official journal of the Society for Neuroscience*, 17(1), pp. 171–80.

Nilius, B. and Owsianik, G. (2011) 'The transient receptor potential family of ion channels', *Genome Biology*. BioMed Central, 12(3), p. 218. doi: 10.1186/GB-2011-12-3-218.

Nishimura, A. *et al.* (2016) 'Detrimental role of pericyte Nox4 in the acute phase of brain ischemia', *Journal of Cerebral Blood Flow and Metabolism*. SAGE Publications, 36(6), pp.

1143–1154. doi: 10.1177/0271678X15606456.

Nishino, T. (1994) 'The conversion of xanthine dehydrogenase to xanthine oxidase and the role of the enzyme in reperfusion injury', *Journal of Biochemistry*. Oxford University Press, pp. 1–6. doi: 10.1093/oxfordjournals.jbchem.a124480.

Nomura, D. K. *et al.* (2011) 'Endocannabinoid hydrolysis generates brain prostaglandins that promote neuroinflammation', *Science*. Science, 334(6057), pp. 809–813. doi: 10.1126/science.1209200.

Norenberg, M. D., Rama Rao, K. V and Jayakumar, A. R. (2005) 'Mechanisms of ammonia-induced astrocyte swelling', in *Metabolic Brain Disease*, pp. 303–318. doi: 10.1007/s11011-005-7911-7.

Nyíri, G. *et al.* (2005) 'CB1 cannabinoid receptors are enriched in the perisynaptic annulus and on preterminal segments of hippocampal GABAergic axons', *Neuroscience*, 136(3), pp. 811–822. doi: 10.1016/j.neuroscience.2005.01.026.

O'Donnell, J. C., Jackson, J. G. and Robinson, M. B. (2016) 'Transient Oxygen/Glucose Deprivation Causes a Delayed Loss of Mitochondria and Increases Spontaneous Calcium Signaling in Astrocytic Processes.', *The Journal of neuroscience : the official journal of the Society for Neuroscience*. Society for Neuroscience, 36(27), pp. 7109–27. doi: 10.1523/JNEUROSCI.4518-15.2016.

O'Sullivan, S. E. (2016) 'An update on PPAR activation by cannabinoids', *British Journal of Pharmacology*. Wiley-Blackwell, pp. 1899–1910. doi: 10.1111/bph.13497.

Odi, R. *et al.* (2020) 'A perspective on the physicochemical and biopharmaceutic properties of marketed antiseizure drugs—From phenobarbital to cenobamate and beyond', *Epilepsia*. Blackwell Publishing Inc., p. epi.16597. doi: 10.1111/epi.16597.

Ohlsson, A. *et al.* (1986) 'Single-dose kinetics of deuterium-labelled cannabidiol in man after smoking and intravenous administration', *Biological Mass Spectrometry*. Biomed Environ Mass Spectrom, 13(2), pp. 77–83. doi: 10.1002/bms.1200130206.

Okamoto, Y. *et al.* (2004) 'Molecular Characterization of a Phospholipase D Generating Anandamide and Its Congeners', *Journal of Biological Chemistry*, 279(7), pp. 5298–5305. doi: 10.1074/jbc.M306642200.

Okazaki, H. *et al.* (2011) 'Early Holocene coastal environment change inferred from deposits at Okinoshima archeological site, Boso Peninsula, central Japan', *Quaternary International*. Pergamon, 230(1–2), pp. 87–94. doi: 10.1016/J.QUAINT.2009.11.002.

Olney, J. W. (1969) 'Brain lesions, obesity, and other disturbances in mice treated with monosodium glutamate.', *Science*, 164(880), pp. 719–721. doi: 10.1126/science.164.3880.719.

Ooboshi, H. *et al.* (2005) 'Postischemic Gene Transfer of Interleukin-10 Protects Against Both Focal and Global Brain Ischemia', *Circulation*, 111(7), pp. 913–919. doi: 10.1161/01.CIR.0000155622.68580.DC.

Osei-Hyiaman, D. *et al.* (2005) 'Endocannabinoid activation at hepatic CB1 receptors stimulates fatty acid synthesis and contributes to diet-induced obesity.', *The Journal of clinical investigation*. American Society for Clinical Investigation, 115(5), pp. 1298–305. doi: 10.1172/JCI23057.

Paciaroni, M., Caso, V. and Agnelli, G. (2009) 'The concept of ischemic penumbra in acute

stroke and therapeutic opportunities', *European Neurology*. Karger Publishers, pp. 321–330. doi: 10.1159/000210544.

Paddenberg, R. *et al.* (2003) 'Essential role of complex II of the respiratory chain in hypoxia-induced ROS generation in the pulmonary vasculature', *American Journal of Physiology - Lung Cellular and Molecular Physiology*. Am J Physiol Lung Cell Mol Physiol, 284(5 28-5). doi: 10.1152/ajplung.00149.2002.

Pagano, E. *et al.* (2016) 'An Orally Active Cannabis Extract with High Content in Cannabidiol attenuates Chemically-induced Intestinal Inflammation and Hypermotility in the Mouse.', *Frontiers in pharmacology*. Frontiers Media SA, 7, p. 341. doi: 10.3389/fphar.2016.00341.

Pagano, E. *et al.* (2019) 'The non-euphoric phytocannabinoid cannabidivarin counteracts intestinal inflammation in mice and cytokine expression in biopsies from UC pediatric patients', *Pharmacological Research*. Academic Press, 149. doi: 10.1016/j.phrs.2019.104464.

Papadopoulos, M. C. *et al.* (2004) 'Aquaporin-4 facilitates reabsorption of excess fluid in vasogenic brain edema', *The FASEB Journal*, 18(11), pp. 1291–3. doi: 10.1096/fj.04-1723fje.

Pardridge, W. M. (2011) 'Drug transport in brain via the cerebrospinal fluid', *Fluids and Barriers of the CNS*. doi: 10.1186/2045-8118-8-7.

Parmentier-Batteur, S. *et al.* (2002) 'Increased Severity of Stroke in CB1 Cannabinoid Receptor Knock-Out Mice', *The Journal of Neuroscience* , 22(22), pp. 9771–9775.

Paschen, W., Oláh, L. and Mies, G. (2002) 'Effect of Transient Focal Ischemia of Mouse Brain on Energy State and NAD Levels', *Journal of Neurochemistry*. Blackwell Science Ltd., 75(4), pp. 1675–1680. doi: 10.1046/j.1471-4159.2000.0751675.x.

Pazos, M. R. *et al.* (2013) 'Mechanisms of cannabidiol neuroprotection in hypoxic–ischemic newborn pigs: Role of 5HT1A and CB2 receptors', *Neuropharmacology*. Pergamon, 71, pp. 282–291. doi: 10.1016/J.NEUROPHARM.2013.03.027.

Pekny, M. and Nilsson, M. (2005) 'Astrocyte activation and reactive gliosis', *Glia*, 50(4), pp. 427–434. doi: 10.1002/glia.20207.

Pekny, M. and Pekna, M. (2014) 'Astrocyte Reactivity and Reactive Astrogliosis: Costs and Benefits', *Physiological Reviews*, 94(4), pp. 1077–1098. doi: 10.1152/physrev.00041.2013.

Pekny, M., Wilhelmsson, U. and Pekna, M. (2014) 'The dual role of astrocyte activation and reactive gliosis', *Neuroscience Letters*. Elsevier, 565, pp. 30–38. doi: 10.1016/J.NEULET.2013.12.071.

Perea, G., Navarrete, M. and Araque, A. (2009) 'Tripartite synapses: astrocytes process and control synaptic information', *Trends in Neurosciences*. Elsevier Current Trends, 32(8), pp. 421–431. doi: 10.1016/J.TINS.2009.05.001.

Peres, F. F. *et al.* (2018) 'Cannabidiol as a Promising Strategy to Treat and Prevent Movement Disorders?', *Frontiers in Pharmacology*. Frontiers, 0(MAY), p. 482. doi: 10.3389/FPHAR.2018.00482.

Pertwee, R. G. (1997) 'Pharmacology of cannabinoid CB1 and CB2 receptors', *Pharmacology and Therapeutics*, 74(2), pp. 129–180. doi: 10.1016/S0163-7258(97)82001-3.

Pertwee, R. G. (2006) 'The pharmacology of cannabinoid receptors and their ligands: an overview', *International Journal of Obesity*, 30, pp. S13–S18. doi: 10.1038/sj.ijo.0803272.

Pertwee, R. G. (2008) 'The diverse CB1 and CB2 receptor pharmacology of three plant cannabinoids: Δ9-tetrahydrocannabinol, cannabidiol and Δ9-tetrahydrocannabivarin', *British Journal of Pharmacology*. Wiley-Blackwell, 153(2), p. 199. doi: 10.1038/SJ.BJP.0707442.

Petrocellis, L. De *et al.* (2008) 'Plant-Derived Cannabinoids Modulate the Activity of Transient Receptor Potential Channels of Ankyrin Type-1 and Melastatin Type-8', *Journal of Pharmacology and Experimental Therapeutics*. American Society for Pharmacology and Experimental Therapeutics, 325(3), pp. 1007–1015. doi: 10.1124/JPET.107.134809.

De Petrocellis, L. *et al.* (2011) 'Effects of cannabinoids and cannabinoid-enriched Cannabis extracts on TRP channels and endocannabinoid metabolic enzymes', *British Journal of Pharmacology*. Wiley-Blackwell, 163(7), pp. 1479–1494. doi: 10.1111/j.1476-5381.2010.01166.x.

De Petrocellis, L. *et al.* (2013) 'Non-THC cannabinoids inhibit prostate carcinoma growth in vitro and in vivo: Pro-apoptotic effects and underlying mechanisms', *British Journal of Pharmacology*. Wiley-Blackwell, 168(1), pp. 79–102. doi: 10.1111/j.1476-5381.2012.02027.x.

De Petrocellis, L. and Di Marzo, V. (2010) 'Non-CB1, Non-CB2 receptors for endocannabinoids, plant cannabinoids, and synthetic cannabimimetics: Focus on G-protein-coupled receptors and transient receptor potential channels', *Journal of Neuroimmune Pharmacology*, pp. 103–121. doi: 10.1007/s11481-009-9177-z.

Pĩeiro, R., Maffucci, T. and Falasca, M. (2011) 'The putative cannabinoid receptor GPR55 defines a novel autocrine loop in cancer cell proliferation', *Oncogene*. Nature Publishing Group, 30(2), pp. 142–152. doi: 10.1038/onc.2010.417.

Pisanti, S. *et al.* (2009) 'Use of cannabinoid receptor agonists in cancer therapy as palliative and curative agents', *Best Practice and Research: Clinical Endocrinology and Metabolism*. Best Pract Res Clin Endocrinol Metab, pp. 117–131. doi: 10.1016/j.beem.2009.02.001.

Porter, A. G. and Jänicke, R. U. (1999) 'Emerging roles of caspase-3 in apoptosis', *Cell Death and Differentiation*, pp. 99–104. doi: 10.1038/sj.cdd.4400476.

Porter, C. J. H., Trevaskis, N. L. and Charman, W. N. (2007) *Lipids and lipid-based formulations: Optimizing the oral delivery of lipophilic drugs*, *Nature Reviews Drug Discovery*. Nature Publishing Group. doi: 10.1038/nrd2197.

Prieto, M. and Alonso, G. (1999) 'Differential Sensitivity of Cultured Tanycytes and Astrocytes to Hydrogen Peroxide Toxicity', *Experimental Neurology*, 155(1), pp. 118–127. doi: 10.1006/exnr.1998.6970.

Ramer, R. *et al.* (2013) 'COX-2 and PPAR- Confer Cannabidiol-Induced Apoptosis of Human Lung Cancer Cells', *Molecular Cancer Therapeutics*. American Association for Cancer Research, 12(1), pp. 69–82. doi: 10.1158/1535-7163.MCT-12-0335.

Ramirez, S. H. *et al.* (2012) 'Activation of cannabinoid receptor 2 attenuates leukocyte-endothelial cell interactions and blood-brain barrier dysfunction under inflammatory conditions', *Journal of Neuroscience*. J Neurosci, 32(12), pp. 4004–4016. doi: 10.1523/JNEUROSCI.4628-11.2012.

Rana, S. *et al.* (2017) 'Interfacial engineering of nanoparticles for cancer therapeutics', in *Nanostructures for Cancer Therapy*. Elsevier, pp. 177–209. doi: 10.1016/B978-0-323-46144-3.00007-6.

Rao, V. L. *et al.* (2001) 'Antisense knockdown of the glial glutamate transporter GLT-1, but not the neuronal glutamate transporter EAAC1, exacerbates transient focal cerebral ischemia-induced neuronal damage in rat brain.', *The Journal of neuroscience : the official journal of the Society for Neuroscience*. Society for Neuroscience, 21(6), pp. 1876–83.

Reichenbach, Z. W. *et al.* (2016) 'The CB1 antagonist, SR141716A, is protective in permanent photothrombotic cerebral ischemia', *Neuroscience Letters*. NIH Public Access, 630, pp. 9–15. doi: 10.1016/j.neulet.2016.07.041.

Rempel, V. *et al.* (2013) 'Antagonists for the Orphan G-Protein-Coupled Receptor GPR55 Based on a Coumarin Scaffold', *Journal of Medicinal Chemistry*. American Chemical Society, 56(11), pp. 4798–4810. doi: 10.1021/JM4005175.

Rich, P. R. and Maréchal, A. (2010) 'The mitochondrial respiratory chain', *Essays in Biochemistry*. Portland Press, 47, pp. 1–23. doi: 10.1042/BSE0470001.

Rivers-Auty, J. R., Smith, P. F. and Ashton, J. C. (2014) 'The cannabinoid CB2 receptor agonist GW405833 does not ameliorate brain damage induced by hypoxia-ischemia in rats', *Neuroscience Letters*. Elsevier Ireland Ltd, 569, pp. 104–109. doi: 10.1016/j.neulet.2014.03.077.

Rock, E. M. *et al.* (2012) 'Cannabidiol, a nonpsychotropic component of cannabis, attenuates vomiting and nausea-like behaviour via indirect agonism of 5-HT 1A somatodendritic autoreceptors in the dorsal raphe nucleus', *British Journal of Pharmacology*. Br J Pharmacol, 165(8), pp. 2620–2634. doi: 10.1111/j.1476-5381.2011.01621.x.

Rockwell, C. E. *et al.* (2006) 'Interleukin-2 suppression by 2-arachidonyl glycerol is mediated through peroxisome proliferator-activated receptor γ independently of cannabinoid receptors 1 and 2', *Molecular Pharmacology*. Mol Pharmacol, 70(1), pp. 101–111. doi: 10.1124/mol.105.019117.

Rodríguez-Muñoz, M. *et al.* (2018) 'Cannabidiol enhances morphine antinociception, diminishes NMDA-mediated seizures and reduces stroke damage via the sigma 1 receptor 11 Medical and Health Sciences 1109 Neurosciences 11 Medical and Health Sciences 1115 Pharmacology and Pharmaceutical Scien', *Molecular Brain*. BioMed Central Ltd., 11(1), p. 51. doi: 10.1186/s13041-018-0395-2.

Rodríguez-Yáñez, M. and Castillo, J. (2008) 'Role of inflammatory markers in brain ischemia', *Current Opinion in Neurology*. Curr Opin Neurol, 21(3), pp. 353–357. doi: 10.1097/WCO.0b013e3282ffafbf.

Romano, M. R. and Lograno, M. D. (2012) 'Involvement of the peroxisome proliferator-activated receptor (PPAR) alpha in vascular response of endocannabinoids in the bovine ophthalmic artery', *European Journal of Pharmacology*. Eur J Pharmacol, 683(1–3), pp. 197–203. doi: 10.1016/j.ejphar.2012.02.049.

Romera, C. *et al.* (2007) 'Ischemic preconditioning reveals that GLT1/EAAT2 glutamate transporter is a novel PPARγ target gene involved in neuroprotection', *Journal of Cerebral Blood Flow and Metabolism*. J Cereb Blood Flow Metab, 27(7), pp. 1327–1338. doi: 10.1038/sj.jcbfm.9600438.

Rosenberg, P. A. and Aizenman, E. (1989) 'Hundred-fold increase in neuronal vulnerability to glutamate toxicity in astrocyte-poor cultures of rat cerebral cortex', *Neuroscience Letters*, 103(2), pp. 162–168. doi: 10.1016/0304-3940(89)90569-7.

Rosenthaler, S. *et al.* (2014) 'Differences in receptor binding affinity of several phytocannabinoids do not explain their effects on neural cell cultures', *Neurotoxicology and Teratology*. Pergamon, 46, pp. 49–56. doi: 10.1016/J.NTT.2014.09.003.

Ross, R. A. (2003) 'Anandamide and vanilloid TRPV1 receptors', *British Journal of Pharmacology*. Wiley-Blackwell, 140(5), pp. 790–801. doi: 10.1038/sj.bjp.0705467.

Ross, R. A. (2009) 'The enigmatic pharmacology of GPR55', *Trends in Pharmacological Sciences*, 30(3), pp. 156–163. doi: 10.1016/J.TIPS.2008.12.004.

Rossi, D. J., Brady, J. D. and Mohr, C. (2007) 'Astrocyte metabolism and signaling during brain ischemia', *NATURE NEUROSCIENCE*, 10(11), pp. 3–7. doi: 10.1038/nn2004.

Rossi, D. J., Oshima, T. and Attwell, D. (2000) 'Glutamate release in severe brain ischaemia is mainly by reversed uptake', *Nature*, 403(January), pp. 316–321. doi: 10.1038/35002090.

Roth, J. M. (2011) 'Recombinant Tissue Plasminogen Activator for the Treatment of Acute Ischemic Stroke', *Baylor University Medical Center Proceedings*. Informa UK Limited, 24(3), pp. 257–259. doi: 10.1080/08998280.2011.11928729.

Rothstein, J. D. *et al.* (1996) 'Knockout of Glutamate Transporters Reveals a Major Role for Astroglial Transport in Excitotoxicity and Clearance of Glutamate', *Neuron*, 16(1), pp. 675–686.

Ryan, D., Drysdale, Alison J., *et al.* (2009) 'Cannabidiol targets mitochondria to regulate intracellular ca2+ levels', *Journal of Neuroscience*, 29(7), pp. 2053–2063. doi: 10.1523/JNEUROSCI.4212-08.2009.

Ryan, D., Drysdale, Alison J, *et al.* (2009) 'Cellular/Molecular Cannabidiol Targets Mitochondria to Regulate Intracellular Ca 2ε Levels'. doi: 10.1523/JNEUROSCI.4212-08.2009.

Ryberg, E. *et al.* (2007) 'The orphan receptor GPR55 is a novel cannabinoid receptor', *British Journal of Pharmacology*. Br J Pharmacol, 152(7), pp. 1092–1101. doi: 10.1038/sj.bjp.0707460.

Saeed, S. A. *et al.* (2007) 'Some new prospects in the understanding of the molecular basis of the pathogenesis of stroke', *Experimental Brain Research*, 182(1), pp. 1–10. doi: 10.1007/s00221-007-1050-9.

Saka, R. O., McGuire, A. and Wolfe, C. DA (2005) 'Economic burden of stroke in England', *National Audit Office*, pp. 1–29.

Sattler, R. and Tymianski, M. (2000) 'Molecular mechanisms of calcium-dependent excitotoxicity.', *Journal of molecular medicine (Berlin, Germany)*, 78(1), pp. 3–13.

Sawzdargo, M. *et al.* (1999) 'Identification and cloning of three novel human G protein-coupled receptor genes GPR52, GPR53 and GPR55: GPR55 is extensively expressed in human brain', *Molecular Brain Research*. Brain Res Mol Brain Res, 64(2), pp. 193–198. doi: 10.1016/S0169-328X(98)00277-0.

Scemes, E. and Giaume, C. (2006) 'Astrocyte calcium waves: What they are and what they do', *Glia*. NIH Public Access, 54(7), pp. 716–725. doi: 10.1002/glia.20374.

Scheiber, I. F., Mercer, J. F. B. and Dringen, R. (2014) 'Metabolism and functions of copper in brain', *Progress in Neurobiology*. Pergamon, 116(6), pp. 33–57. doi: 10.1016/j.pneurobio.2014.01.002.

Schinzel, A. C. *et al.* (2005) 'Cyclophilin D is a component of mitochondrial permeability transition and mediates neuronal cell death after focal cerebral ischemia', *Proceedings of the National Academy of Sciences*, 102(34), pp. 12005–12010. doi: 10.1073/pnas.0505294102.

Schmidt-Rohr, K. (2020) 'Oxygen Is the High-Energy Molecule Powering Complex Multicellular Life: Fundamental Corrections to Traditional Bioenergetics', *ACS Omega*. American Chemical Society, 5(5), pp. 2221–2233. doi: 10.1021/acsomega.9b03352.

Schousboe, A. *et al.* (2014) 'Glutamate Metabolism in the Brain Focusing on Astrocytes', in *Advances in neurobiology*. NIH Public Access, pp. 13–30. doi: 10.1007/978-3-319-08894-5_2.

Schurman, L. D. *et al.* (2019) 'Molecular Mechanism and Cannabinoid Pharmacology', *Handbook of Experimental Pharmacology*. Springer, Cham, 258, pp. 323–353. doi: 10.1007/164_2019_298.

Scott, K. A., Dalgleish, A. G. and Liu, W. M. (2014) 'The Combination of Cannabidiol and 9-Tetrahydrocannabinol Enhances the Anticancer Effects of Radiation in an Orthotopic Murine Glioma Model', *Molecular Cancer Therapeutics*, 13(12), pp. 2955–2967. doi: 10.1158/1535-7163.MCT-14-0402.

Seltzer, E. S. *et al.* (2020) 'Cannabidiol (Cbd) as a promising anti-cancer drug', *Cancers*. MDPI AG, pp. 1–26. doi: 10.3390/cancers12113203.

Shaafi, S. *et al.* (2014) 'Interleukin-6, a reliable prognostic factor for ischemic stroke', *Iranian Journal of Neurology*. Tehran University of Medical Sciences, 13(2), p. 70. Available at: /pmc/articles/PMC4187333/ (Accessed: 27 August 2021).

Shao, Z. *et al.* (2017) 'Tetramethylpyrazine Protects Neurons from Oxygen-Glucose Deprivation-Induced Death.', *Medical science monitor : international medical journal of experimental and clinical research*. International Scientific Information, Inc., 23, pp. 5277–5282. doi: 10.12659/MSM.904554.

Sharma, L. K., Lu, J. and Bai, Y. (2009) 'Mitochondrial Respiratory Complex I: Structure, Function and Implication in Human Diseases', *Current medicinal chemistry*. NIH Public Access, 16(10), p. 1266. doi: 10.2174/092986709787846578.

Shearer, J. A., Coker, S. J. and Carswell, H. V. O. (2018) 'Detrimental effects of 2-arachidonoylglycerol on whole blood platelet aggregation and on cerebral blood flow after a focal ischemic insult in rats', *American Journal of Physiology - Heart and Circulatory Physiology*. Am J Physiol Heart Circ Physiol, 314(5), pp. H967–H977. doi: 10.1152/ajpheart.00299.2017.

Shuaib, A. (2006) 'Neuroprotection – STAIR-Way to the Future?', *Cerebrovascular Diseases*. Karger Publishers, 22(1), pp. 10–17. doi: 10.1159/000092328.

Sibson, N. R. *et al.* (1998) 'Stoichiometric coupling of brain glucose metabolism and glutamatergic neuronal activity', *Neurobiology*, 95, pp. 316–321.

Siddiqui, Y. D. *et al.* (2019) 'Resolvin D2 Induces Resolution of Periapical Inflammation and Promotes Healing of Periapical Lesions in Rat Periapical Periodontitis', *Frontiers in Immunology*. Frontiers Media SA, 10(FEB), p. 307. doi: 10.3389/FIMMU.2019.00307.

Sido, J. M., Nagarkatti, P. S. and Nagarkatti, M. (2015) 'Role of Endocannabinoid Activation of Peripheral CB1 Receptors in the Regulation of Autoimmune Disease', *International Reviews of Immunology*. NIH Public Access, pp. 403–414. doi:

10.3109/08830185.2014.921165.

Da Silva, V. K. *et al.* (2014) 'Cannabidiol normalizes caspase 3, synaptophysin, and mitochondrial fission protein DNM1L expression levels in rats with brain iron overload: Implications for neuroprotection', *Molecular Neurobiology*. Humana Press Inc., pp. 222–233. doi: 10.1007/s12035-013-8514-7.

Silver, I. A., Deas, J. and Erecińska, M. (1997) 'Ion homeostasis in brain cells: Differences in intracellular ion responses to energy limitation between cultured neurons and glial cells', *Neuroscience*, 78(2), pp. 589–601. doi: 10.1016/S0306-4522(96)00600-8.

Silvestro, S. *et al.* (2019) 'Use of cannabidiol in the treatment of epilepsy: Efficacy and security in clinical trials', *Molecules*. MDPI AG. doi: 10.3390/molecules24081459.

Simard, J. M. *et al.* (2007) 'Brain oedema in focal ischaemia: molecular pathophysiology and theoretical implications', *Lancet Neurology*. NIH Public Access, pp. 258–268. doi: 10.1016/S1474-4422(07)70055-8.

Simi, A. *et al.* (2007) 'Interleukin-1 and inflammatory neurodegeneration', *Biochemical Society Transactions*, 35(5), pp. 1122–1126. doi: 10.1042/BST0351122.

Sims, N. R. (1991) 'Selective impairment of respiration in mitochondria isolated from brain subregions following transient forebrain ischemia in the rat', *Journal of neurochemistry*. J Neurochem, 56(6), pp. 1836–1844. doi: 10.1111/J.1471-4159.1991.TB03438.X.

Sims, N. R. and Anderson, M. F. (2002) 'Mitochondrial contributions to tissue damage in stroke', *Neurochemistry International*, 40, pp. 511–526.

Sims, N. R. and Muyderman, H. (2009) 'Mitochondria, oxidative metabolism and cell death in stroke', *BBA - Molecular Basis of Disease*, 1802, pp. 80–91. doi: 10.1016/j.bbadis.2009.09.003.

Śledziński, P. *et al.* (2018) 'The current state and future perspectives of cannabinoids in cancer biology.', *Cancer medicine*. Wiley-Blackwell, 7(3), pp. 765–775. doi: 10.1002/cam4.1312.

Smith, C. J. *et al.* (2004) 'Peak plasma interleukin-6 and other peripheral markers of inflammation in the first week of ischaemic stroke correlate with brain infarct volume, stroke severity and long-term outcome', *BMC Neurology*. BioMed Central, 4(1), pp. 1–8. doi: 10.1186/1471-2377-4-2.

Sofroniew, M. V. (2009) 'Molecular dissection of reactive astrogliosis and glial scar formation', *Trends in Neurosciences*. NIH Public Access, 32(12), pp. 638–647. doi: 10.1016/j.tins.2009.08.002.

Sofroniew, M. V. and Vinters, H. V. (2010) 'Astrocytes: Biology and pathology', *Acta Neuropathologica*, pp. 7–35. doi: 10.1007/s00401-009-0619-8.

Stella, N. (2010) 'Cannabinoid and cannabinoid-like receptors in microglia, astrocytes, and astrocytomas', *Glia*. NIH Public Access, 58(9), pp. 1017–1030. doi: 10.1002/glia.20983.

Stempel, A. V. *et al.* (2016) 'Cannabinoid Type 2 Receptors Mediate a Cell Type-Specific Plasticity in the Hippocampus.', *Neuron*. NIH Public Access, 90(4), pp. 795–809. doi: 10.1016/j.neuron.2016.03.034.

Stienstra, R. *et al.* (2007) 'PPARs, obesity, and inflammation', *PPAR Research*. Hindawi Limited. doi: 10.1155/2007/95974.

Stone, N. L., England, T. J. and O'Sullivan, S. E. (2019) 'A Novel Transwell Blood Brain Barrier Model Using Primary Human Cells', *Frontiers in Cellular Neuroscience*. Frontiers Media S.A., 13, p. 230. doi: 10.3389/fncel.2019.00230.

Stone, N. L., England, T. J. and O'Sullivan, S. E. (2021) 'Protective Effects of Cannabidivarin and Cannabigerol on Cells of the Blood–Brain Barrier Under Ischemic Conditions', *Cannabis and Cannabinoid Research*. doi: 10.1089/can.2020.0159.

Stott, C. G. *et al.* (2013) 'A phase i study to assess the effect of food on the single dose bioavailability of the THC/CBD oromucosal spray', *European Journal of Clinical Pharmacology*. Eur J Clin Pharmacol, 69(4), pp. 825–834. doi: 10.1007/s00228-012-1393-4.

Stout, S. M. and Cimino, N. M. (2014) 'Exogenous cannabinoids as substrates, inhibitors, and inducers of human drug metabolizing enzymes: A systematic review', *Drug Metabolism Reviews*. Taylor & Francis, 46(1), pp. 86–95. doi: 10.3109/03602532.2013.849268.

Südhof, T. C. (2012) 'Calcium control of neurotransmitter release', *Cold Spring Harbor Perspectives in Biology*. Cold Spring Harbor Laboratory Press, 4(1), p. a011353. doi: 10.1101/cshperspect.a011353.

Sugiura, T. *et al.* (1995) '2-arachidonoylglycerol: A possible endogenous cannabinoid receptor ligand in brain', *Biochemical and Biophysical Research Communications*. Biochem Biophys Res Commun, 215(1), pp. 89–97. doi: 10.1006/bbrc.1995.2437.

Sugiura, T. and Waku, K. (2000) '2-Arachidonoylglycerol and the cannabinoid receptors', *Chemistry and Physics of Lipids*, 108(1–2), pp. 89–106. doi: 10.1016/S0009-3084(00)00189-4.

Suh, S. W. *et al.* (2003) 'Hypoglycemic neuronal death and cognitive impairment are prevented by poly(ADP-ribose) polymerase inhibitors administered after hypoglycemia.', *The Journal of neuroscience : the official journal of the Society for Neuroscience*, 23(33), pp. 10681–90.

Sun, S. *et al.* (2017) 'Cannabidiol attenuates OGD/R-induced damage by enhancing mitochondrial bioenergetics and modulating glucose metabolism via pentose-phosphate pathway in hippocampal neurons.', *Redox biology*. Elsevier, 11, pp. 577–585. doi: 10.1016/j.redox.2016.12.029.

Suzuki, S., Tanaka, K. and Suzuki, N. (2009) 'Ambivalent aspects of interleukin-6 in cerebral ischemia: Inflammatory versus neurotrophic aspects', *Journal of Cerebral Blood Flow and Metabolism*. SAGE PublicationsSage UK: London, England, pp. 464–479. doi: 10.1038/jcbfm.2008.141.

Swanson, R. A., Farrell, K. and Stein, B. A. (1997) 'Astrocyte energetics, function, and death under conditions of incomplete ischemia: a mechanism of glial death in the penumbra.', *Glia*, 21(1), pp. 142–53.

Swanson, R., Ying, W. and Kauppinen, T. (2004) 'Astrocyte Influences on Ischemic Neuronal Death', *Current Molecular Medicine*, 4(2), pp. 193–205. doi: 10.2174/1566524043479185.

Sweeney, M. D., Ayyadurai, S. and Zlokovic, B. V (2016) 'Pericytes of the neurovascular unit: Key functions and signaling pathways', *Nature Neuroscience*. Nature Publishing Group, pp. 771–783. doi: 10.1038/nn.4288.

Sydserff, S. G. *et al.* (2000) 'Clomethiazole is neuroprotective in models of global and focal cerebral ischemia when infused at doses producing clinically relevant plasma concentrations', *Brain Research*. Brain Res, 862(1–2), pp. 59–62. doi: 10.1016/S0006-

8993(00)02071-0.

Sydserff, S. G. *et al.* (2002) 'Effect of NXY-059 on infarct volume after transient or permanent middle cerebral artery occlusion in the rat; studies on dose, plasma concentration and therapeutic time window', *British Journal of Pharmacology*. Wiley-Blackwell, 135(1), pp. 103–112. doi: 10.1038/sj.bjp.0704449.

Syed, Y. Y., McKeage, K. and Scott, L. J. (2014) 'Delta-9-Tetrahydrocannabinol/Cannabidiol (Sativex®): A Review of Its Use in Patients with Moderate to Severe Spasticity Due to Multiple Sclerosis', *Drugs*, 74(5), pp. 563–578. doi: 10.1007/s40265-014-0197-5.

Szaflarski, J. P. *et al.* (2018) 'Long-term safety and treatment effects of cannabidiol in children and adults with treatment-resistant epilepsies: Expanded access program results', *Epilepsia*. Blackwell Publishing Inc., 59(8), pp. 1540–1548. doi: 10.1111/epi.14477.

Takano, T. *et al.* (2009) 'Astrocytes and ischemic injury', *Stroke; a journal of cerebral circulation*. NIH Public Access, 40(3 Suppl), p. S8. doi: 10.1161/STROKEAHA.108.533166.

Takeda, S. *et al.* (2014) 'Down-regulation of cyclooxygenase-2 (cox-2) by cannabidiolic acid in human breast cancer cells', *Journal of Toxicological Sciences*. J Toxicol Sci, 39(5), pp. 711–716. doi: 10.2131/jts.39.711.

Takenouchi, R. *et al.* (2012) 'N-arachidonoyl glycine induces macrophage apoptosis via GPR18', *Biochemical and Biophysical Research Communications*. Academic Press, 418(2), pp. 366–371. doi: 10.1016/J.BBRC.2012.01.027.

Tang, L., Khan, S. U. and Muhammad, N. A. (2001) 'Evaluation and selection of bio-relevant dissolution media for a poorly water-soluble new chemical entity', *Pharmaceutical Development and Technology*, 6(4), pp. 531–540. doi: 10.1081/PDT-120000291.

Tarkowski, E. *et al.* (1995) 'Early intrathecal production of interleukin-6 predicts the size of brain lesion in stroke.', *Stroke*, 26(8), pp. 1393–8.

Taylor, L. *et al.* (2019) 'A Phase 1, Open-Label, Parallel-Group, Single-Dose Trial of the Pharmacokinetics and Safety of Cannabidiol (CBD) in Subjects With Mild to Severe Hepatic Impairment', *Journal of Clinical Pharmacology*. Blackwell Publishing Inc., 59(8), pp. 1110–1119. doi: 10.1002/jcph.1412.

Tejima, E. *et al.* (2009) 'Neuroprotective effects of overexpressing tissue inhibitor of metalloproteinase TIMP-1', *Journal of Neurotrauma*. Mary Ann Liebert, Inc., 26(11), pp. 1935–1941. doi: 10.1089/neu.2009.0959.

Theparambil, S. M. *et al.* (2020) 'Astrocytes regulate brain extracellular pH via a neuronal activity-dependent bicarbonate shuttle', *Nature Communications*. Nature Publishing Group, 11(1), pp. 1–15. doi: 10.1038/s41467-020-18756-3.

Thiele, E. A. *et al.* (2018) 'Cannabidiol in patients with seizures associated with Lennox-Gastaut syndrome (GWPCARE4): a randomised, double-blind, placebo-controlled phase 3 trial', *The Lancet*. Elsevier, 391(10125), pp. 1085–1096. doi: 10.1016/S0140-6736(18)30136-3.

Thomas, B. F., Compton, D. R. and Martin, B. R. (1990) 'Characterization of the lipophilicity of natural and synthetic analogs of delta 9-tetrahydrocannabinol and its relationship to pharmacological potency.', *Journal of Pharmacology and Experimental Therapeutics*, 255(2).

Traynelis, S. F. and Cull-Candy, S. G. (1990) 'Proton inhibition of N-methyl-D-aspartate

receptors in cerebellar neurons', *Nature*. Nature, 345(6273), pp. 347–350. doi: 10.1038/345347a0.

Tsou, K. *et al.* (1998) 'Immunohistochemical distribution of cannabinoid CB1 receptors in the rat central nervous system.', *Neuroscience*, 83(2), pp. 393–411.

Turcotte, C. *et al.* (2016) 'The CB2 receptor and its role as a regulator of inflammation', *Cellular and Molecular Life Sciences*. Springer, 73(23), p. 4449. doi: 10.1007/S00018-016-2300-4.

Ulrich Dirnagl, C. I. and M. A. M. (1999) 'Pathobiology of ischaemic stroke: an integrated view', *TINS*, 22(9).

Vay, L., Gu, C. and McNaughton, P. A. (2012) 'The thermo-TRP ion channel family: Properties and therapeutic implications', *British Journal of Pharmacology*. Br J Pharmacol, 165(4), pp. 787–801. doi: 10.1111/j.1476-5381.2011.01601.x.

Veldhuis, W. B. *et al.* (2003) 'In vivo excitotoxicity induced by ouabain, a Na+/K+-ATPase inhibitor', *Journal of Cerebral Blood Flow and Metabolism*. SAGE PublicationsSage UK: London, England, 23(1), pp. 62–74. doi: 10.1097/01.WCB.0000039287.37737.50.

Victor Nadler, J. (2010) 'Plasticity of glutamate synaptic mechanisms', *Epilepsia*, 51(SUPPL. 5), p. 17. doi: 10.1111/j.1528-1167.2010.02803.x.

Wang, J. R. *et al.* (2015) 'Improving the dissolution and bioavailability of 6-mercaptopurine via co-crystallization with isonicotinamide', *Bioorganic and Medicinal Chemistry Letters*. Elsevier Ltd, 25(5), pp. 1036–1039. doi: 10.1016/j.bmcl.2015.01.022.

Wang, J. and Ueda, N. (2009) 'Biology of endocannabinoid synthesis system', *Prostaglandins and Other Lipid Mediators*. Elsevier, 89(3–4), pp. 112–119. doi: 10.1016/j.prostaglandins.2008.12.002.

Wang, X. *et al.* (1995) 'Expression of Interleukin-6, c-Fos , and zif268 mRNAs in Rat Ischemic Cortex', *Journal of Cerebral Blood Flow & Metabolism*, 15(1), pp. 166–171. doi: 10.1038/jcbfm.1995.18.

Wanner, I. B. *et al.* (2013) 'Glial Scar Borders Are Formed by Newly Proliferated, Elongated Astrocytes That Interact to Corral Inflammatory and Fibrotic Cells via STAT3-Dependent Mechanisms after Spinal Cord Injury', *Journal of Neuroscience*, 33(31), pp. 12870–12886. doi: 10.1523/JNEUROSCI.2121-13.2013.

Ward, S. J. *et al.* (2014) 'Cannabidiol inhibits paclitaxel-induced neuropathic pain through 5-HT 1A receptors without diminishing nervous system function or chemotherapy efficacy', *British Journal of Pharmacology*. Br J Pharmacol, 171(3), pp. 636–645. doi: 10.1111/bph.12439.

Ward, S. J. *et al.* (2018) 'Surprising outcomes in cannabinoid CB1/CB2 receptor double knockout mice in two models of ischemia', *Life sciences*. NIH Public Access, 195, p. 1. doi: 10.1016/J.LFS.2017.12.030.

Warden, A. *et al.* (2016) 'Localization of PPAR isotypes in the adult mouse and human brain', *Scientific Reports*. Nature Publishing Group, 6. doi: 10.1038/SREP27618.

Watanabe, K. *et al.* (1996) 'Inhibition of anandamide amidase activity in mouse brain microsomes by cannabinoids', *Biological and Pharmaceutical Bulletin*. Biol Pharm Bull, 19(8), pp. 1109–1111. doi: 10.1248/bpb.19.1109.

Waxman, E. A. and Lynch, D. R. (2005) 'N-methyl-D-aspartate receptor subtypes: Multiple

roles in excitotoxicity and neurological disease', *Neuroscientist*, pp. 37–49. doi: 10.1177/1073858404269012.

Wells, C. L. *et al.* (1998) 'Cytochalasin-induced actin disruption of polarized enterocytes can augment internalization of bacteria.', *Infection and immunity*, 66(6), pp. 2410–9. Available at: http://www.ncbi.nlm.nih.gov/pubmed/9596696 (Accessed: 11 November 2019).

Welsh, F. A., Marcy, V. R. and Sims, R. E. (1991) 'NADH Fluorescence and Regional Energy Metabolites during Focal Ischemia and Reperfusion of Rat Brain', *Journal of Cerebral Blood Flow & Metabolism*, 11(3), pp. 459–465. doi: 10.1038/jcbfm.1991.88.

Whalley, B. J. *et al.* (2018) 'A role of GPR55 in the antiepileptic properties of cannabidiol (CBD) (P2.277)', *Neurology*, 90(15 Supplement), p. P2.277.

Wheless, J. W. *et al.* (2019) 'Pharmacokinetics and Tolerability of Multiple Doses of Pharmaceutical-Grade Synthetic Cannabidiol in Pediatric Patients with Treatment-Resistant Epilepsy', *CNS Drugs*. Springer International Publishing, 33(6), pp. 593–604. doi: 10.1007/s40263-019-00624-4.

Wilhelmsson, U. *et al.* (2006) 'Redefining the concept of reactive astrocytes as cells that remain within their unique domains upon reaction to injury.', *Proceedings of the National Academy of Sciences of the United States of America*. National Academy of Sciences, 103(46), pp. 17513–8. doi: 10.1073/pnas.0602841103.

Wilson, R. I. and Nicoll, R. A. (2001) 'Endogenous cannabinoids mediate retrograde signalling at hippocampal synapses.', *Nature*. Nature Publishing Group, 410(6828), pp. 588–592. doi: 10.1038/35069076.

Wójtowicz, S. *et al.* (2020) 'The Novel Role of PPAR Alpha in the Brain: Promising Target in Therapy of Alzheimer's Disease and Other Neurodegenerative Disorders', *Neurochemical Research 2020 45:5*. Springer, 45(5), pp. 972–988. doi: 10.1007/S11064-020-02993-5.

Wolburg, H. and Lippoldt, A. (2002) 'Tight junctions of the blood-brain barrier: Development, composition and regulation', *Vascular Pharmacology*, 38(6), pp. 323–337. doi: 10.1016/S1537-1891(02)00200-8.

Wood, T. B., Spivey, W. T. N. and Easterfield, T. H. (1896) 'XL. - Charas. The resin of Indian hemp', *Journal of the Chemical Society, Transactions*. The Royal Society of Chemistry, pp. 539–546. doi: 10.1039/CT8966900539.

Wotherspoon, G. *et al.* (2005) 'Peripheral nerve injury induces cannabinoid receptor 2 protein expression in rat sensory neurons', *Neuroscience*, 135(1), pp. 235–245. doi: 10.1016/j.neuroscience.2005.06.009.

von Wrede, R. *et al.* (2020) 'Plant derived versus synthetic cannabidiol: Wishes and commitment of epilepsy patients', *Seizure*. W.B. Saunders Ltd, 80, pp. 92–95. doi: 10.1016/j.seizure.2020.06.012.

Wright, K. L., Duncan, M. and Sharkey, K. A. (2008) 'Cannabinoid 2 receptors in the gastrointestinal tract: a regulatory system in states of inflammation', *British Journal of Pharmacology*, 153(2), pp. 263–270. doi: 10.1038/sj.bjp.0707486.

Wu, C. Y. and Benet, L. Z. (2005) 'Predicting drug disposition via application of BCS: Transport/absorption/ elimination interplay and development of a biopharmaceutics drug disposition classification system', *Pharmaceutical Research*. Springer, pp. 11–23. doi: 10.1007/s11095-004-9004-4.

Xi, Z.-X. *et al.* (2011) 'Brain cannabinoid CB2 receptors modulate cocaine's actions in mice', *Nature Neuroscience*. NIH Public Access, 14(9), pp. 1160–1166. doi: 10.1038/nn.2874.

Xie, Y. *et al.* (2014) 'Reperfusion promotes mitochondrial biogenesis following focal cerebral ischemia in rats', *PLoS ONE*. Public Library of Science, 9(3), p. e92443. doi: 10.1371/journal.pone.0092443.

Xiong, W. *et al.* (2017) 'Inhibitory effects of tetramethylpyrazine on pain transmission of trigeminal neuralgia in CCI-ION rats', *Brain Research Bulletin*. Brain Res Bull, 134, pp. 72–78. doi: 10.1016/j.brainresbull.2017.07.005.

Xu, K. *et al.* (2015) 'An overview on structural modifications of ligustrazine and biological evaluation of its synthetic derivatives', *Research on Chemical Intermediates*. Kluwer Academic Publishers, 41(3), pp. 1385–1411. doi: 10.1007/s11164-013-1281-2.

Yáñez, J. A. *et al.* (2011) 'Intestinal lymphatic transport for drug delivery', *Advanced Drug Delivery Reviews*, pp. 923–942. doi: 10.1016/j.addr.2011.05.019.

Yemisci, M. *et al.* (2009) 'Pericyte contraction induced by oxidative-nitrative stress impairs capillary reflow despite successful opening of an occluded cerebral artery', *Nature Medicine*. Nat Med, 15(9), pp. 1031–1037. doi: 10.1038/nm.2022.

Yin, J. *et al.* (2011) 'Tetramethylpyrazine inhibits migration of SKOV3 human ovarian carcinoma cells and decreases the expression of interleukin-8 via the ERK1 / 2 , p38 and AP-1 signaling pathways', pp. 671–679. doi: 10.3892/or.2011.1334.

Yoshimoto, T. and Siesjö, B. K. (1999) 'Posttreatment with the immunosuppressant cyclosporin A in transient focal ischemia', *Brain Research*, 839(2), pp. 283–291. doi: 10.1016/S0006-8993(99)01733-3.

Yousufuddin, M. and Young, N. (2019) 'Aging and ischemic stroke', *Aging*. Impact Journals, LLC, 11(9), pp. 2542–2544. doi: 10.18632/aging.101931.

Yrjänheikki, J. *et al.* (1998) 'Tetracyclines inhibit microglial activation and are neuroprotective in global brain ischemia.', *Proceedings of the National Academy of Sciences of the United States of America*. National Academy of Sciences, 95(26), pp. 15769–74.

Yu, S. *et al.* (2014) 'Fatty acid-binding protein 5 (fabp5) regulates cognitive function both by decreasing anandamide levels and by activating the nuclear receptor peroxisome proliferatoractivated receptor α/β (pparα/β) in the brain', *Journal of Biological Chemistry*. American Society for Biochemistry and Molecular Biology, 289(18), pp. 12748–12758. doi: 10.1074/jbc.M114.559062.

Zagzoog, A. *et al.* (2020) 'In vitro and in vivo pharmacological activity of minor cannabinoids isolated from Cannabis sativa', *Scientific Reports*. Nature Publishing Group, 10(1), p. 20405. doi: 10.1038/s41598-020-77175-y.

Zaremba, J., Skrobanski, P. and Losy, J. (2001) 'Tumour necrosis factor-alpha is increased in the cerebrospinal fluid and serum of ischaemic stroke patients and correlates with the volume of evolving brain infarct.', *Biomedicine & pharmacotherapy = Biomedecine & pharmacotherapie*, 55(5), pp. 258–63.

Zauner, A. *et al.* (2002) 'Brain oxygenation and energy metabolism: part I-biological function and pathophysiology.', *Neurosurgery*, 51(2), pp. 289–301; discussion 302.

Zechariah, A. *et al.* (2013) 'Vascular endothelial growth factor promotes pericyte coverage of brain capillaries, improves cerebral blood flow during subsequent focal cerebral

ischemia, and preserves the metabolic penumbra', *Stroke*. Stroke, 44(6), pp. 1690–1697. doi: 10.1161/STROKEAHA.111.000240.

Zendulka, O. *et al.* (2016) 'Cannabinoids and Cytochrome P450 Interactions', *Current Drug Metabolism*. Bentham Science Publishers Ltd., 17(3), pp. 206–226. doi: 10.2174/1389200217666151210142051.

Zgair, A. *et al.* (2016) 'Dietary fats and pharmaceutical lipid excipients increase systemic exposure to orally administered cannabis and cannabis-based medicines', *American Journal of Translational Research*. E-Century Publishing Corporation, 8(8), pp. 3448–3459. Available at: www.ajtr.org (Accessed: 21 August 2020).

Zhang, H. *et al.* (2010) 'Wide genetic variation in the native pial collateral circulation is a major determinant of variation in severity of stroke', *Journal of Cerebral Blood Flow and Metabolism*. SAGE Publications, 30(5), pp. 923–934. doi: 10.1038/jcbfm.2010.10.

Zhang, M. *et al.* (2007) 'Cannabinoid CB2 receptor activation decreases cerebral infarction in a mouse focal ischemia/reperfusion model', *Journal of Cerebral Blood Flow and Metabolism*. J Cereb Blood Flow Metab, 27(7), pp. 1387–1396. doi: 10.1038/sj.jcbfm.9600447.

Zhang, X. *et al.* (2019) 'Cannabidiol induces cell cycle arrest and cell apoptosis in human gastric cancer SGC-7901 cells', *Biomolecules*. MDPI AG, 9(8). doi: 10.3390/biom9080302.

Zhang, Z. G. *et al.* (2000) 'VEGF enhances angiogenesis and promotes blood-brain barrier leakage in the ischemic brain', *Journal of Clinical Investigation*. American Society for Clinical Investigation, 106(7), pp. 829–838. doi: 10.1172/JCI9369.

Zhao, Y., Liu, Y. and Chen, K. (2016) 'Mechanisms and Clinical Application of Tetramethylpyrazine (an Interesting Natural Compound Isolated from Ligusticum Wallichii): Current Status and Perspective', *Oxidative Medicine and Cellular Longevity*. Hindawi Limited. doi: 10.1155/2016/2124638.

Zheng, C. Y. *et al.* (2012) 'Inhibition of cyclooxygenase-2 by tetramethylpyrazine and its effects on A549 cell invasion and metastasis', *International Journal of Oncology*, 40(6), pp. 2029–2037. doi: 10.3892/ijo.2012.1375.

Zheng, W. (2012) 'Multiplex Detection of Oxidative Phosphorylation (OXPHOS) as a Mechanistic Indicator for Mitochondrial Health and Toxicity', *White paper*.

Zhou, Y. *et al.* (2017) 'Tetramethylpyrazine inhibits prostate cancer progression by downregulation of forkhead box M1', *Oncology Reports*. Spandidos Publications, 38(2), pp. 837–842. doi: 10.3892/or.2017.5768.

Zhu, X. L. *et al.* (2009) 'Therapeutic time window and mechanism of tetramethylpyrazine on transient focal cerebral ischemia/reperfusion injury in rats', *Neuroscience Letters*. Elsevier, 449(1), pp. 24–27. doi: 10.1016/j.neulet.2008.09.007.

Zlokovic, B. V. (2008) 'The Blood-Brain Barrier in Health and Chronic Neurodegenerative Disorders', *Neuron*. Neuron, pp. 178–201. doi: 10.1016/j.neuron.2008.01.003.

Zoppi, S. *et al.* (2011) 'Regulatory role of cannabinoid receptor 1 in stress-induced excitotoxicity and neuroinflammation', *Neuropsychopharmacology*. Nature Publishing Group, 36(4), pp. 805–818. doi: 10.1038/npp.2010.214.

Zou, H. *et al.* (1997) 'Apaf-1, a human protein homologous to C. elegans CED-4, participates in cytochrome c-dependent activation of caspase-3.', *Cell*, 90(3), pp. 405–13.

Zygmunt, P. M. *et al.* (1999) 'Vanilloid receptors on sensory nerves mediate the vasodilator action of anandamide', *Nature 1999 400:6743*. Nature Publishing Group, 400(6743), pp. 452–457. doi: 10.1038/22761.

9 Appendices

Study	Origin of lab	Animal species used	Model used	Total dose of CBD (mg/kg)	ROA	Time of administration relative to insult	Unit of infarct volume	Time of assessment after occlusion	Other assessment	Time of other assessment relative to insult	Quality of study score	Risk of bias score
Hayakawa et al., 2004											5	4
Experiment 1	Osaka (Japan)	ddY Mice	MCAO - T - 4h	6	IP	Pre (3mg/kg), 3h (3mg/kg)	mm^3	24h				
Mishima et al., 2005											5	5
Experiment 1	Fukuoka (Japan)	ddY Mice	MCAO - T - 4h	0.2	IP	Pre-onset (0.1mg/kg) + 3h post (0.1mg/kg)	mm^3	24h				
Experiment 2	Fukuoka (Japan)	ddY Mice	MCAO - T - 4h	2	IP	Pre-onset (1mg/kg) + 3h post (1mg/kg)	mm^3	24h				
Experiment 3	Fukuoka (Japan)	ddY Mice	MCAO - T - 4h	6	IP	Pre-onset (3mg/kg) + 3h post (3mg/kg)	mm^3	24h				
Experiment 4	Fukuoka (Japan)	ddY Mice	MCAO - T - 4h	20	IP	Pre-onset (10mg/kg) + 3h post (10mg/kg)	mm^3	24h				
Hayakawa et al., 2007a											5	4
Experiment 1	Osaka (Japan)	ddY Mice	MCAO - T - 4h	0.2	IP	Pre-onset (0.1 mg/kg) and 3h post (0.1mg/kg)	mm^3	24h				
Experiment 2	Osaka (Japan)	ddY Mice	MCAO - T - 4h	2	IP	Pre-onset (1 mg/kg) and 3h post (1mg/kg)	mm^3	24h				
Experiment 3	Osaka (Japan)	ddY Mice	MCAO - T - 4h	6	IP	Pre-onset (3 mg/kg) and 3h post (3 mg/kg)	mm^3	24h				
Experiment 7	Osaka (Japan)	ddY Mice	MCAO - T - 4h	6	IP	Pre-onset (3mg/kg) and 3h post (3mg/kg)	mm^3	24h and 72h				
Experiment 9	Osaka (Japan)	ddY Mice	MCAO - T - 4h	6	IP	Pre-onset (3mg/kg) and 3h post (3mg/kg)	mm^3	24h and 72h				
Experiment 10	Osaka (Japan)	ddY Mice	MCAO - T - 4h	3	IP	Pre-onset	mm^3	24h	Rota-rod test	24h and 72h		
Experiment 11	Osaka (Japan)	ddY Mice	MCAO - T - 4h	3	IP	3h post	mm^3	24h				
Experiment 12	Osaka (Japan)	ddY Mice	MCAO - T - 4h	3	IP	4h post	mm^3	24h				
Experiment 13	Osaka (Japan)	ddY Mice	MCAO - T - 4h	3	IP	5h post	mm^3	24h				
Experiment 14	Osaka (Japan)	ddY Mice	MCAO - T - 4h	3	IP	6h post	mm^3	24h				
Hayakawa et al., 2007b											5	5

Experiment 1	Fukuoka (Japan)	ddY Mice	MCAO - T - 4h	0.2	IP	Pre-onset (0.1 mg/kg) and 3h post (0.1mg/kg)	mm^3	24h				
Experiment 2	Fukuoka (Japan)	ddY Mice	MCAO - T - 4h	2	IP	Pre-onset (1 mg/kg) and 3h post (1mg/kg)	mm^3	24h				
Experiment 3	Fukuoka (Japan)	ddY Mice	MCAO - T - 4h	6	IP	Pre-onset (3 mg/kg) and 3h post (3 mg/kg)	mm^3	24h				
Hayakawa et al., 2008											5	5
Experiment 1	Fukuoka (Japan)	ddY Mice	MCAO - T - 4h	0.2	IP	Pre-onset (0.1 mg/kg) and 3h post (0.1mg/kg)	mm^3	24h				
Experiment 2	Fukuoka (Japan)	ddY Mice	MCAO - T - 4h	2	IP	Pre-onset (1 mg/kg) and 3h post (1mg/kg)	mm^3	24h				
Experiment 3	Fukuoka (Japan)	ddY Mice	MCAO - T - 4h	6	IP	Pre-onset (3 mg/kg) and 3h post (3 mg/kg)	mm^3	24h				
Experiment4	Fukuoka (Japan)	ddY Mice	MCAO - T - 4h	6	IP	Pre-onset (3 mg/kg) and 3h post (3 mg/kg)	n/a	24h	Neurological score, rota rod test	24h		
Experiment5	Fukuoka (Japan)	ddY Mice	MCAO - T - 4h	6	IP	Pre-onset (3 mg/kg) and 3h post (3 mg/kg)	n/a	72h	Neurological score, rota-rod test	72h		
Hayakawa et al., 2009											5	5
Experiment 1	Osaka (Japan)	ddY Mice	MCAO - T - 4h	3	IP	Daily for 14d from day 1	n/a	24h	Neurological score, rota-rod test	24h		
Experiment 2	Osaka (Japan)	ddY Mice	MCAO - T - 4h	3	IP	Daily for 12d from day 3	n/a	24h	Neurological score, rota-rod test	24h		
Experiment 3	Osaka (Japan)	ddY Mice	MCAO - T - 4h	3	IP	Daily for 10d from day 5	n/a	24h	Neurological score, rota-rod test	24h		
Experiment 4	Osaka (Japan)	ddY Mice	MCAO - T - 4h	3	IP	Daily for 14d from day 1	n/a	168h	Neurological score	24h		
Experiment 5	Osaka (Japan)	ddY Mice	MCAO - T - 4h	3	IP	Daily for 12d from day 3	n/a	168h	Neurological score	24h		
Experiment 6	Osaka (Japan)	ddY Mice	MCAO - T - 4h	3	IP	Daily for 10d from day 5	n/a	168h	Neurological score, rota-rod test			
Experiment 7	Osaka (Japan)	ddY Mice	MCAO - T - 4h	3	IP	Daily for 14d from day 1	n/a	336h	Neurological score, rota-rod test	336h		
Experiment 8	Osaka (Japan)	ddY Mice	MCAO - T - 4h	3	IP	Daily for 12d from day 3	n/a	336h	Neurological score, rota-rod test	336h		

Experiment 9	Osaka (Japan)	ddY Mice	MCAO - T - 4h	3	IP	Daily for 10d from day 5	n/a	336h	Neurological score, rota-rod test	336h		
Khaksar & Bigdeli, 2016											5	6
Experiment 1	Tehran (Iran)	Wistar rats	MCAO - T - 1h	0.00083	ICV	5d prior to occlusion (0.00005mg once a day to each rat)	mm^3	24h	Neurological score	24h		
Experiment 2	Tehran (Iran)	Wistar rats	MCAO - T - 1h	0.0017	ICV	5d prior to occlusion (0.0001mg once a day to each rat)	mm^3	24h	Neurological score	24h		
Experiment 3	Tehran (Iran)	Wistar rats	MCAO - T - 1h	0.0033	ICV	5d prior to occlusion (0.0002mg once a day to each rat)	mm^3	24h	Neurological score	24h		
Khaksar & Bigdeli, 2017a											7	7
Experiment 1	Tehran (Iran)	Wistar rats	MCAO - T - 1h	0.00083	ICV	5d prior to occlusion (0.00005mg once a day)	mm^3	24h	Neurological score	24h		
Experiment 2	Tehran (Iran)	Wistar rats	MCAO - T - 1h	0.0017	ICV	5d prior to occlusion (0.0001mg once a day)	mm^3	24h	Neurological score	24h		
Experiment 3	Tehran (Iran)	Wistar rats	MCAO - T - 1h	0.0033	ICV	5d prior to occlusion (0.0002mg once a day)	mm^3	24h	Neurological score	24h		
Khaksar & Bigdeli 2017b											6	7
Experiment 1	Tehran (Iran)	Wistar rats	MCAO - T - 1h	0.00083	ICV	Pre-onset – 30min post occlusion	mm^3	24h				
Experiment 2	Tehran (Iran)	Wistar rats	MCAO - T - 1h	0.0017	ICV	Pre-onset – 30min post occlusion	mm^3	24h				
Experiment 3	Tehran (Iran)	Wistar rats	MCAO - T - 1h	0.0033	ICV	Pre-onset – 30min post occlusion	mm^3	24h				
Khaksar & Bigdeli, 2017c											7	7
Experiment 1	Tehran (Iran)	Wistar rats	MCAO - T - 1h	0.00083	ICV	Pre-onset – 30min post occlusion	mm^3	24h	Neurological score	24h		
Experiment 2	Tehran (Iran)	Wistar rats	MCAO - T - 1h	0.0017	ICV	Pre-onset – 30min post occlusion	mm^3	24h	Neurological score	24h		
Experiment 3	Tehran (Iran)	Wistar rats	MCAO - T - 1h	0.0033	ICV	Pre-onset – 30min post occlusion	mm^3	24h	Neurological score	24h		

Supplementary table 1 Characteristics of included studies.

Study	Peer reviewed	Statement of control temperature	Random allocation	Blinded to induction of ischemia	Blind to assessment of outcome	Use of anaesthetic without intrinsic neuroprotection	Appropriate animal model	Sample size calculations	Animal welfare statement	Statement on conflicts of interest	Total score
Hayakawa et al.,2004	1	1				1	1		1		5
Mishima et al., 2005	1	1				1	1		1		5
Hayakawa et al., 2007a	1	1				1	1		1		5
Hayakawa et al., 2007b	1	1				1	1		1		5
Hayakawa et al., 2009	1					1	1		1		4
Khaksar & Bigdeli, 2016	1	1	1			1	1		1	1	5
Khaksar & Bigdeli, 2017a	1	1	1			1	1		1	1	7
Khaksar & Bigdeli, 2017b		1	1			1	1		1	1	6
Khaksar & Bigdeli, 2017c	1	1	1			1	1		1	1	7

Supplementary table 2 Assessment of study quality using CAMARADES criteria.

Types of bias	Domain	Hayakawa et al., 2004	Mishima et al., 2005	Hayakawa et al., 2007a	Hayakawa et al., 2007b	Hayakawa et al., 2008	Hayakawa et al., 2009	Khaksar & Bigdeli, 2016	Khaksar & Bigdeli, 2017a	Khaksar & Bigdeli, 2017b	Khaksar & Bigdeli, 2017c
Selection bias	Sequence generation	**0**	**0**	**0**	**1**	**0**	**0**	**1**	**1**	**1**	**1**
	Baseline characteristics	**1**	**1**	**1**	**1**	**1**	**1**	**1**	**1**	**1**	**1**
	Allocation concealment	**0**	**0**	**0**	**0**	**0**	**0**	**1**	**1**	**1**	**1**
Performance bias	Random housing	**1**	**1**	**1**	**1**	**1**	**1**	**1**	**1**	**1**	**1**
	Blinding	**0**	**0**	**0**	**0**	**0**	**0**	**0**	**0**	**0**	**0**
Detection bias	Random outcome assessment	**0**	**0**	**0**	**0**	**0**	**0**	**0**	**0**	**0**	**0**
Detection bias	Blinding	**0**	**0**	**0**	**0**	**0**	**0**	**0**	**0**	**0**	**0**
Attrition bias	Incomplete outcome data	**1**	**1**	**1**	**1**	**1**	**1**	**1**	**1**	**1**	**1**
Reporting bias	Selective reporting	**1**	**1**	**1**	**0**	**1**	**1**	**1**	**1**	**1**	**1**
Other bias	**Other sources of bias**	**0**	**1**	**0**	**1**	**1**	**1**	**0**	**1**	**1**	**1**

Supplementary table 3 SYRCLE risk of bias assessment.

Study	Blood pressure	Blood gases	Glucose	Regional CBF	Total
Hayakawa 2004	0	0	0	0	0
Mishima 2005	1	1	0	1	3
Hayakawa 2007a	1	1	1	1	4
Hayakawa 2007b	0	1	0	1	2
Hayakawa 2008	1	1	1	1	4
Hayakawa 2008	0	0	0	0	0
Khaksar 2016	0	0	0	0	0
Khaksar 2017a	0	0	0	0	0
Khaksar 2017b	0	0	0	0	0
Khaksar 2017c	0	0	0	0	0

Supplementary table 4 Summary of the types of physiological monitoring studies included.